Electronic Supplementary Material (ESI) for Inorganic Chemistry Frontiers.

Selective Buchwald-Hartwig Arylation of C-Amino-1,2,4-Triazoles and other Coordinating Aminoheterocycles Enabled by Bulky NHC Ligands and TPEDO Activator

Alexander V. Astakhov,[†] Andrey Yu. Chernenko,[†] Vadim V. Kutyrev, [†] Gleb S. Ranny, [†] Mikhail M. Minyaev,[‡] Victor M. Chernyshev,[†]* Valentine P. Ananikov[†‡]*

[†] *Platov South-Russian State Polytechnic University (NPI), Prosveschenya 132, 346428 Novocherkassk, Russian Federation*
E-mail: chern13@yandex.ru
[‡]*Zelinsky Institute of Organic Chemistry, Russian Academy of Sciences, Leninsky Prospect 47, Moscow, 119991, Russia*
E-mail: val@ioc.ac.ru

Supplementary Information

Extended experimental data

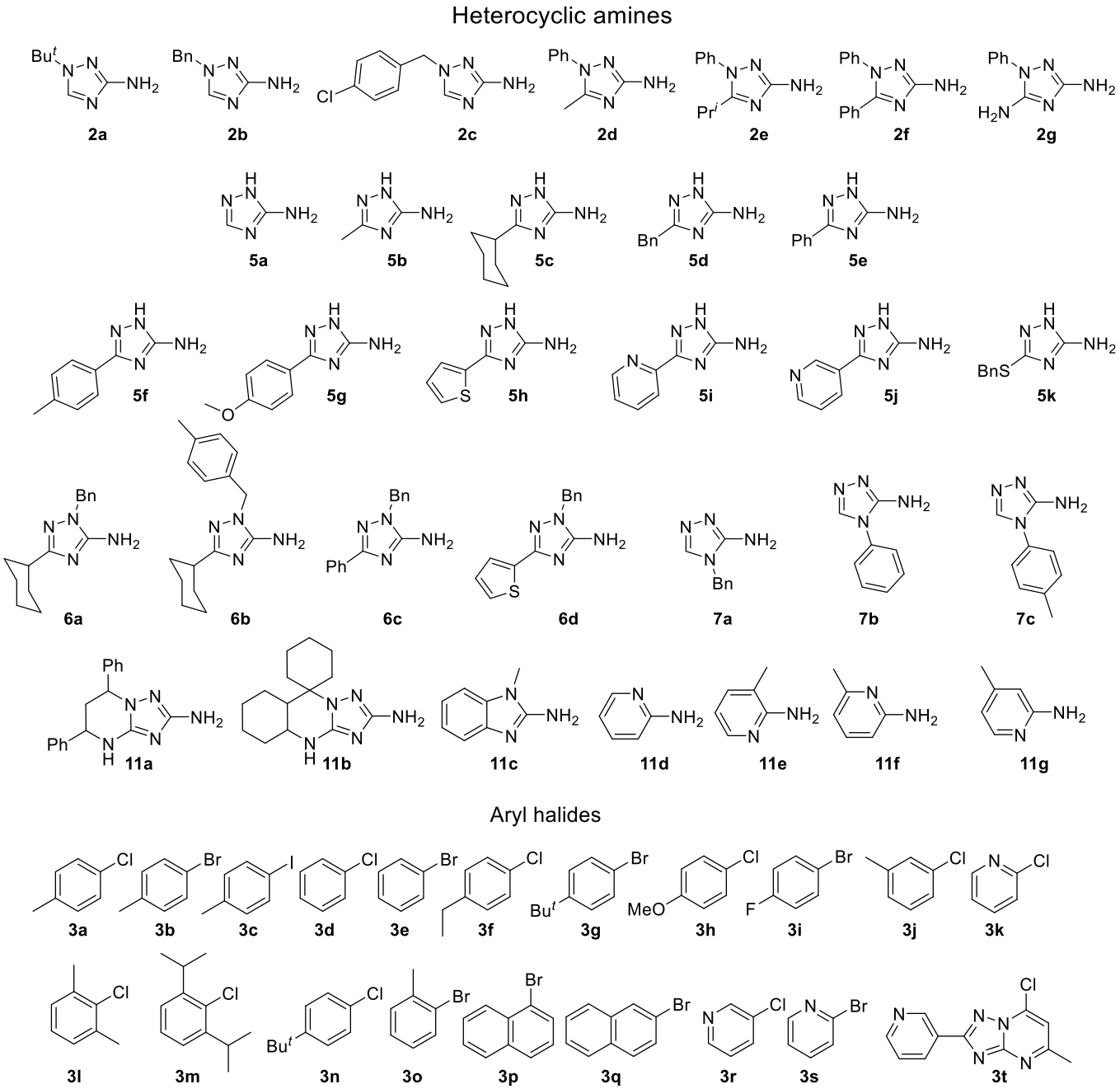

Figure S1. Overview of heterocyclic amines and (hetero)aryl halides used in the study

Scheme S1. Synthesis of compounds **1h**

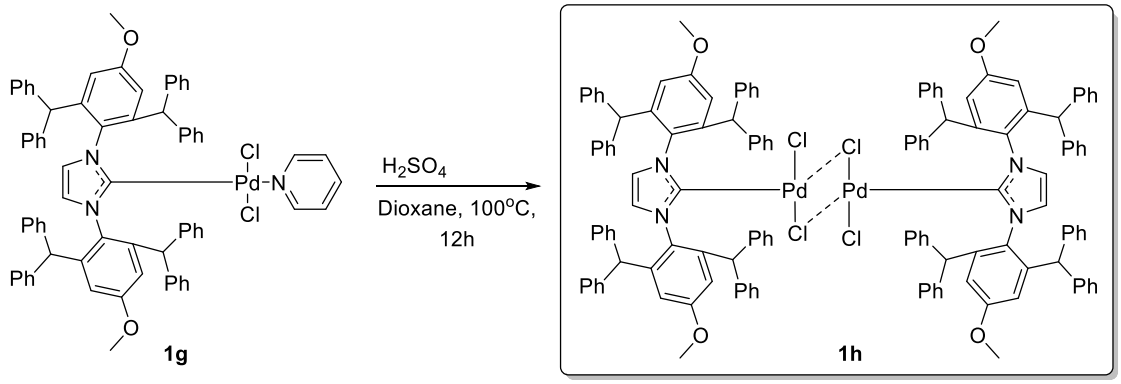

Scheme S2. Synthesis of compounds **2d-f**

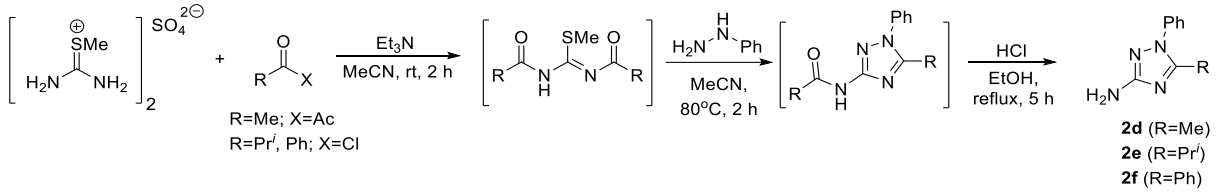

Scheme S3. Synthesis of compounds **6a-d**

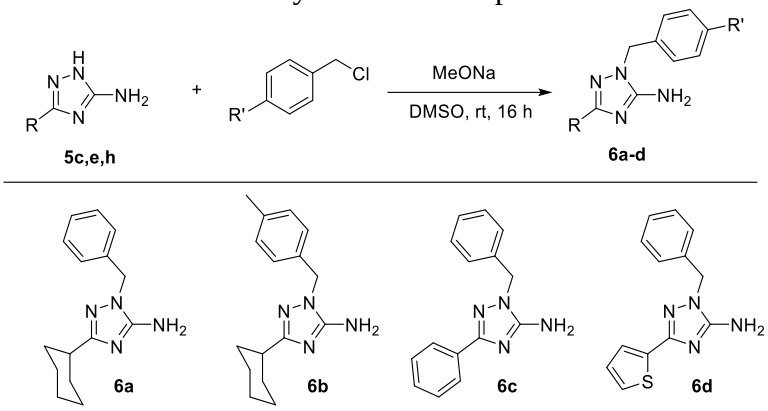

Table S1. Yields of compounds **4a** and **4a′** in the reaction of **2a** with **3a-c**[a]**c** under catalysis with various precatalysts.[a]

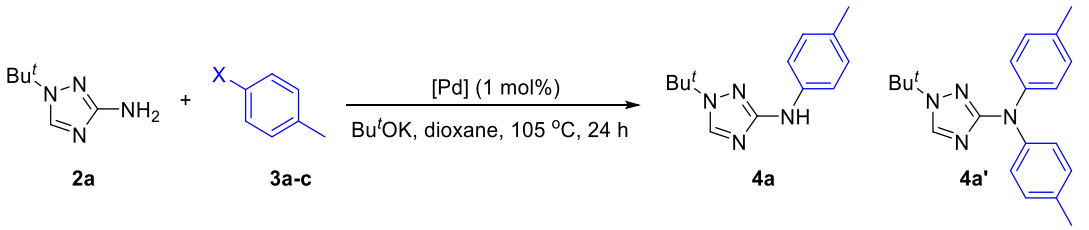

Entry	Precatalyst	[Pd] loading, mol%	Solvent	Yield **4a/4a′**, %[b]		
				3a, X=Cl	**3b**, X=Br	**3c**, X=I
1.	**1a**	1	dioxane	0	0	0
2.	**1b**	1	dioxane	0	0	0
3.	**1c**	1	dioxane	trace	2/0	3/0
4.	**1d**	1	dioxane	6/1	27/20	20/1
5.	**1e**	1	dioxane	19/1	40/19	38/2
6.	**1g**	1	dioxane	95/trace	93/4	85/4
7.	**1h**	1	dioxane	99/trace	96/3	91/5
8.	**1i**	1	dioxane	96/trace	94/4	86/3
9.	$(IPr^{OMe*})\times HCl + Pd(OAc)_2$	1	dioxane	72/trace	65/9	32/2
10.	$Pd(OAc)_2$	1	dioxane	0	0	0
11.	Py_2PdCl_2	1	dioxane	0	0	0

[a] Reaction conditions: **2a** (0.2 mmol), tolyl chloride **3a** (0.2 mmol), ButOK (0.5 mmol), palladium catalyst (2 μmol, 1 mol%), dioxane (1 mL), 105 °C, 24 h. [b] The yields of **4a** and **4a'** were determined by GC-MS.

Table S2. The effect of potential Pd(II) to Pd(0) reductants on the yield of compound **4a** under catalysis with precatalyst 1g[a]

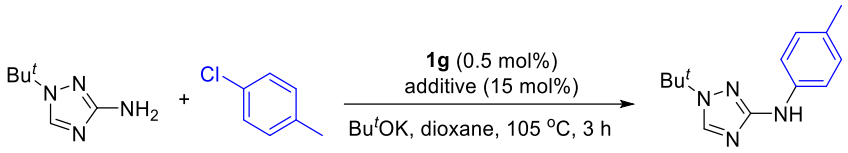

2a **3a** **4a**

Entry	Additive (15 mol%)	Yield **4a**, %[b]
1.	none	36
2.	PriOH	80
3.	$PhB(OH)_2$	66
4.	acetone	71
5.	3-pentanone	85
6.	morpholine	67
7.	propiophenone	70
8.	acetophenone	82
9.	PivOH	56
10.	TPEDO	98

[a] Reaction conditions: **2a** (0.2 mmol), tolyl chloride **3a** (0.2 mmol), ButOK (0.5 mmol), palladium catalyst (1 μmol, 0.5 mol%), additive (0.03 mmol, 15 mol%), dioxane (1 mL), 105 °C, 3 h. [b] The yields of **4a** were determined by GC-MS.

Table S3. Optimization of Pd loading at 15 mol% TPEDO loading[a]

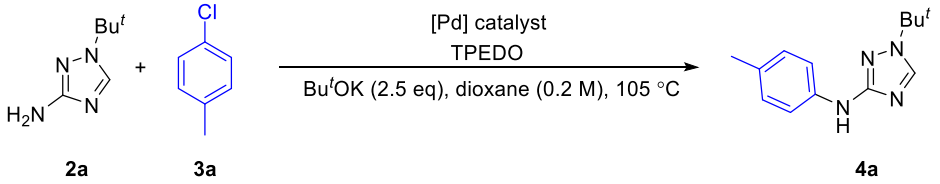

2a **3a** **4a**

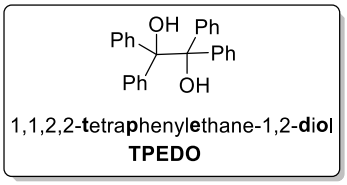

Entry	Catalyst	[Pd] loading, mol%	Additive (mol%)	Time reaction, h	Yield **4a**, %[b]
1.	$PdCl_2Py_2$	1	TPEDO (15)	24	0
2.	**1e**	1	TPEDO (15)	24	67
3.	**1e**	0.5	TPEDO (15)	24	40
4.	**1e**	0.1	TPEDO (15)	24	5
5.	**1h**	0.5	TPEDO (15)	24	99
6.	**1h**	0.3	TPEDO (15)	24	96
7.	**1h**	0.1	TPEDO (15)	24	46
8.	**1h**	0.3	none	24	85
9.	**1h**	0.1	none	24	45
10.	**1i**	0.5	TPEDO (15)	24	99
11.	**1i**	0.3	TPEDO (15)	24	89
12.	**1i**	0.1	TPEDO (15)	24	27
13.	**1i**	0.3	none	24	95
14.	**1i**	0.1	none	24	40
15.	**1g**	0.5	TPEDO (15)	24	99
16.	**1g**	0.3	TPEDO (15)	24	99
17.	**1g**	0.3	TPEDO (15)	16	**99**
18.	**1g**	0.3	TPEDO (15)	10	98
19.	**1g**	0.3	TPEDO (15)	5	95
20.	**1g**	0.2	TPEDO (15)	24	87
21.	**1g**	0.1	TPEDO (15)	24	68
22.	**1g**	0.1	none	24	50
23.	$PdCl_2Py_2$/ IPr^{OMe*}×HCl (1/1)	0.3	TPEDO (15)	16	**99**

[a] Reaction conditions: **2a** (0.2 mmol), tolyl chloride **3a** (0.2 mmol), ButOK (0.5 mmol), palladium catalyst (0.2-2 μmol, 0.1-1 mol%), TPEDO (0.03 mmol, 15 mol%), dioxane (1 mL), 105 °C, 5-24 h. [b] The yields of **4a** were determined by GC-MS.

Table S4. Optimization of TPEDO loading, base and solvent under catalysis with precatalyst 1**g**[a]

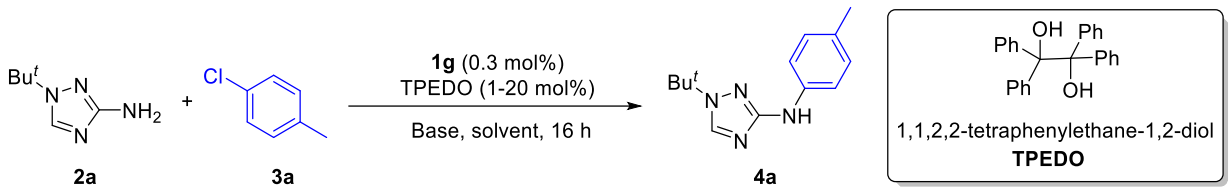

2a **3a** **4a**

Entry	Catalyst	Additive (mol%)	Solvent	Base	Temperature	Yield **4a**, %[b]
1.	**1g**	TPEDO (15)	Dioxane	t-BuOK	105	99
2.	**1g**	TPEDO (15)	Dioxane	t-BuONa	105	28
3.	**1g**	TPEDO (15)	Dioxane	t-BuOLi	105	16
4.	**1g**	TPEDO (15)	Dioxane	$CsCO_3$	105	0
5.	**1g**	TPEDO (15)	Dioxane	K_2CO_3	105	0
6.	**1g**	TPEDO (15)	Dioxane	K_3PO_4	105	0
7.	**1g**	TPEDO (15)	PhMe	t-BuOK	105	85
8.	**1g**	TPEDO (15)	DMSO	t-BuOK	105	0
9.	**1g**	TPEDO (15)	DMF	t-BuOK	105	0
10.	**1g**	TPEDO (15)	Dioxane	t-BuOK	90	trace
11.	**1g**	TPEDO (20)	Dioxane	t-BuOK	105	99
12.	**1g**	TPEDO (10)	Dioxane	t-BuOK	105	99
13.	**1g**	TPEDO (5)	Dioxane	t-BuOK	105	98
14.	**1g**	TPEDO (1)	Dioxane	t-BuOK	105	98

[a] Reaction conditions: **2a** (0.2 mmol), tolyl chloride **3a** (0.2 mmol), base (0.5 mmol), **1g** (0.6 μmol, 0.3 mol%), TPEDO (0.002-0.04 mmol, 1-20 mol%), solvent (1 mL), 70-105 °C, 16 h. [b] The yields of **4a** were determined by GC-MS.

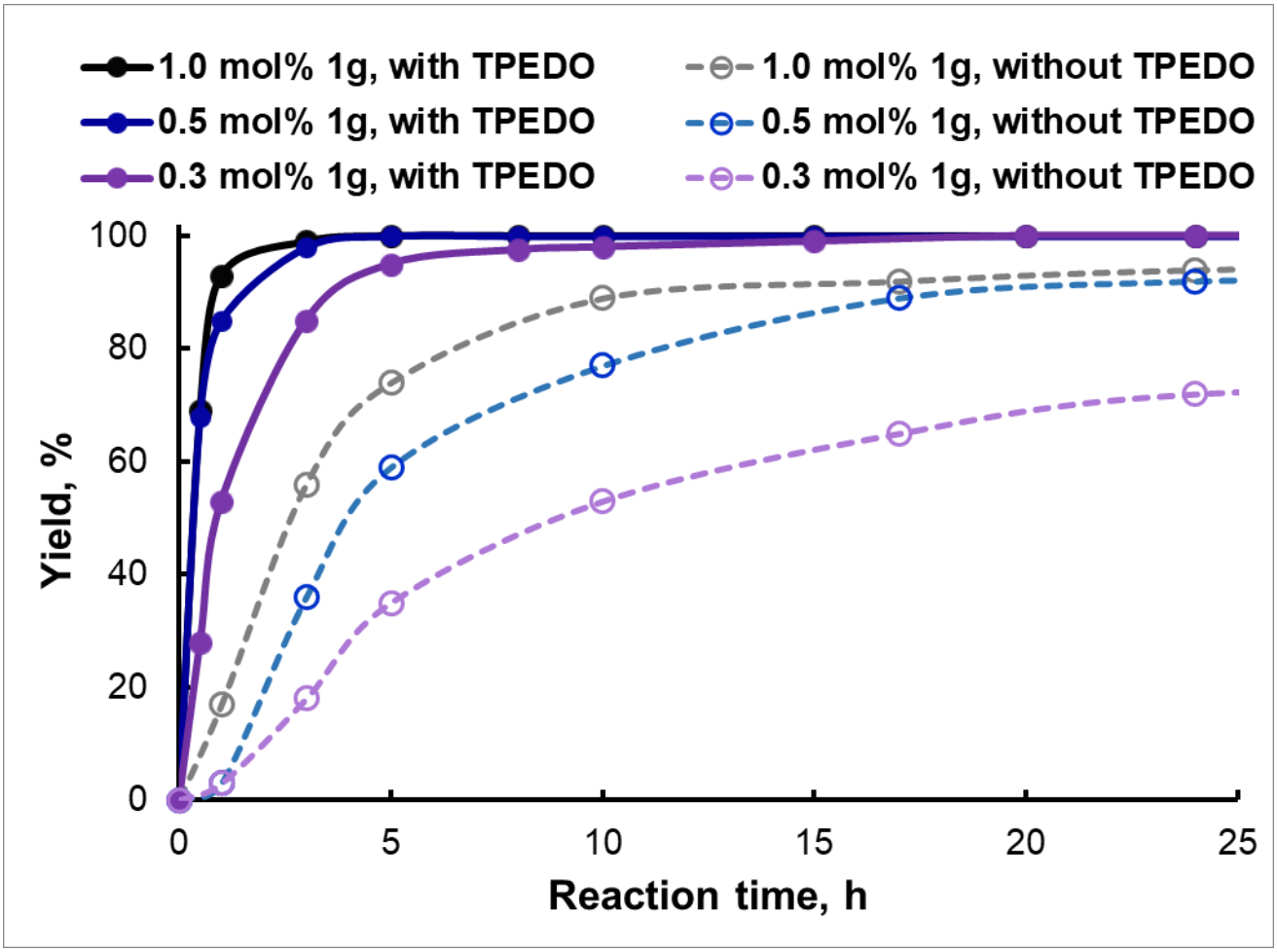

Figure S2. Kinetic curves for the formation of product **4a** upon catalysis by precatalyst **1g** in the absence and in the presence of TPEDO

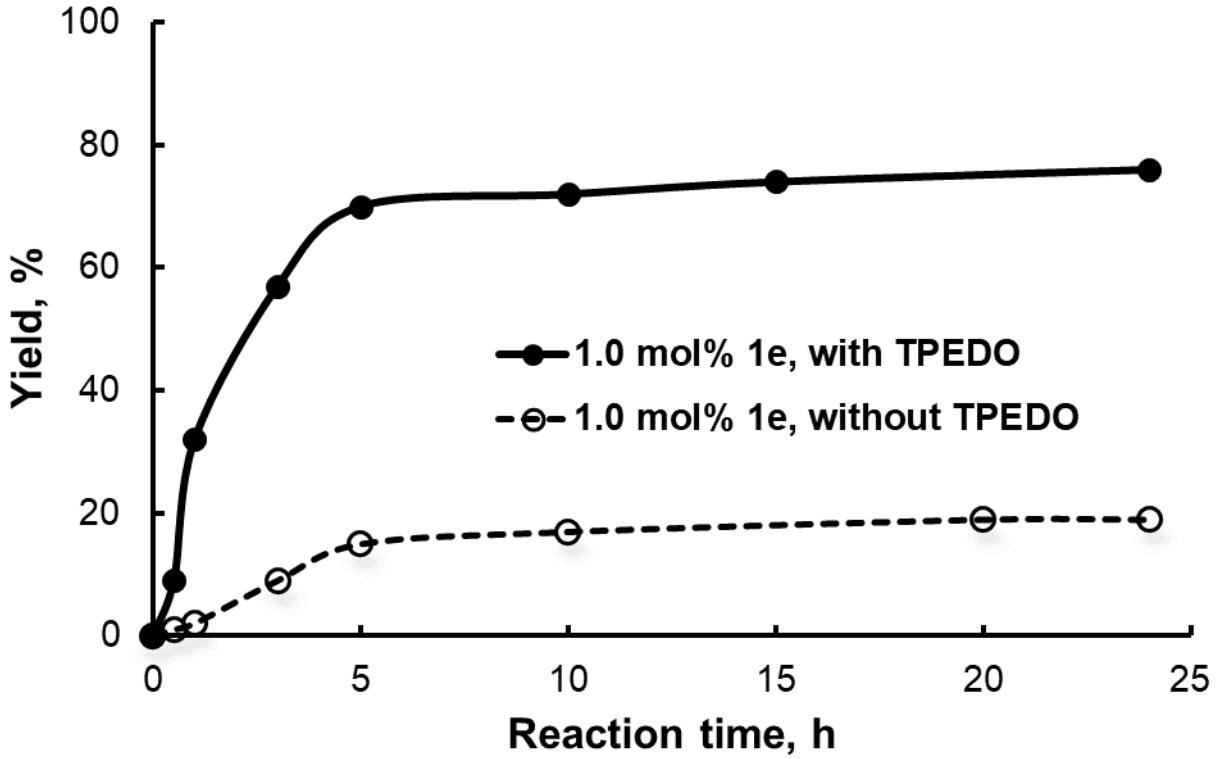

Figure S3. Kinetic curves for the formation of product **4a** upon catalysis by catalyst **1e** in the absence and presence of TPEDO

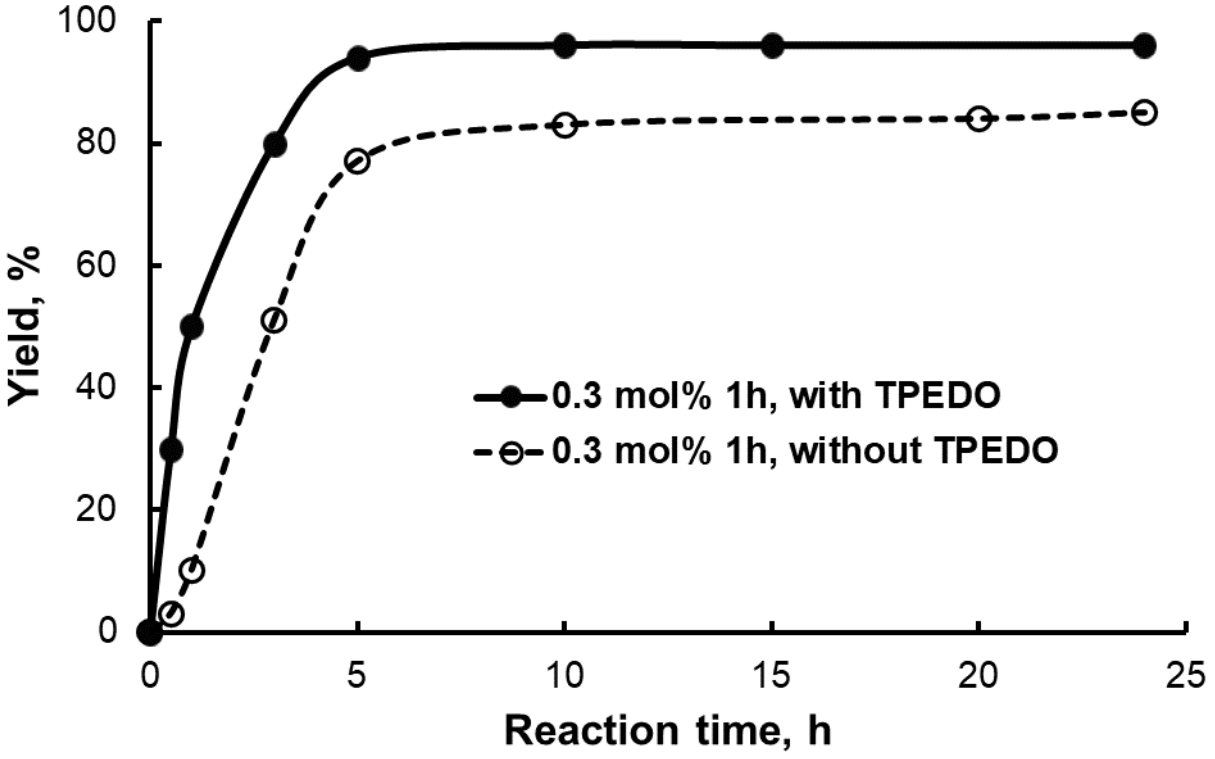

Figure S4. Kinetic curves for the formation of product **4a** upon catalysis by catalyst **1h** in the absence and presence of TPEDO

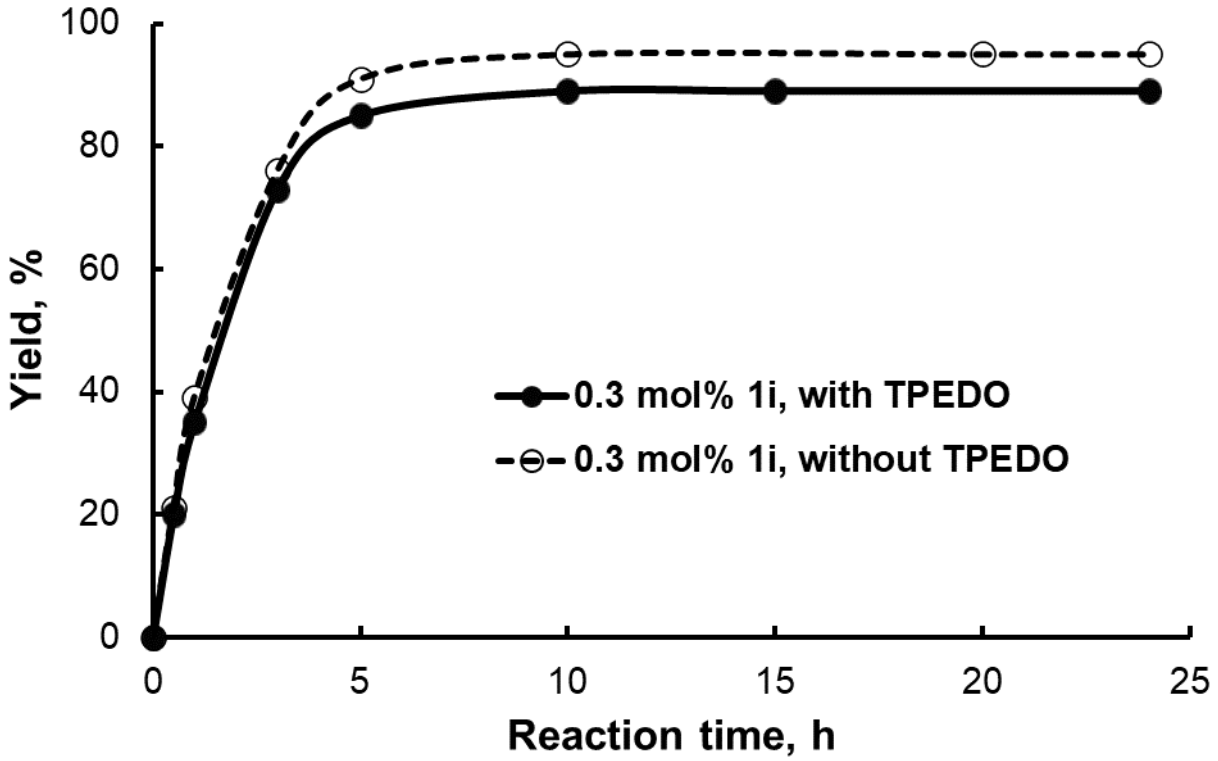

Figure S5. Kinetic curves for the formation of product **4a** upon catalysis by catalyst **1i** in the absence and presence of TPEDO

Extended DFT data

:

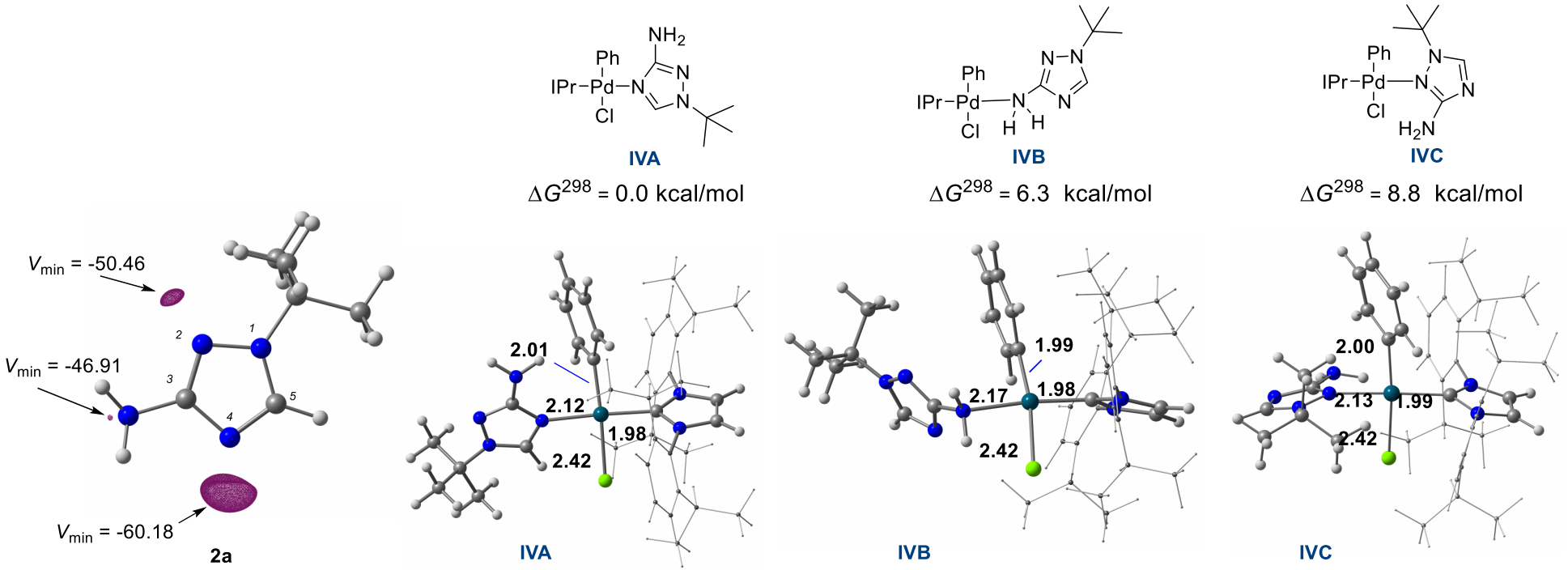

Figure S6. Molecular electrostatic potential *V* isosurface at −46.8 kcal·mol^{-1} of molecule **2a**, structures and relative Gibbs free energies of isomeric complexes **IVA**, **IVB**, **IVC**. Relative Gibbs free energy and V_{min} values were computed at the PBE1PBE/def2svp level in kcal·mol^{-1}.

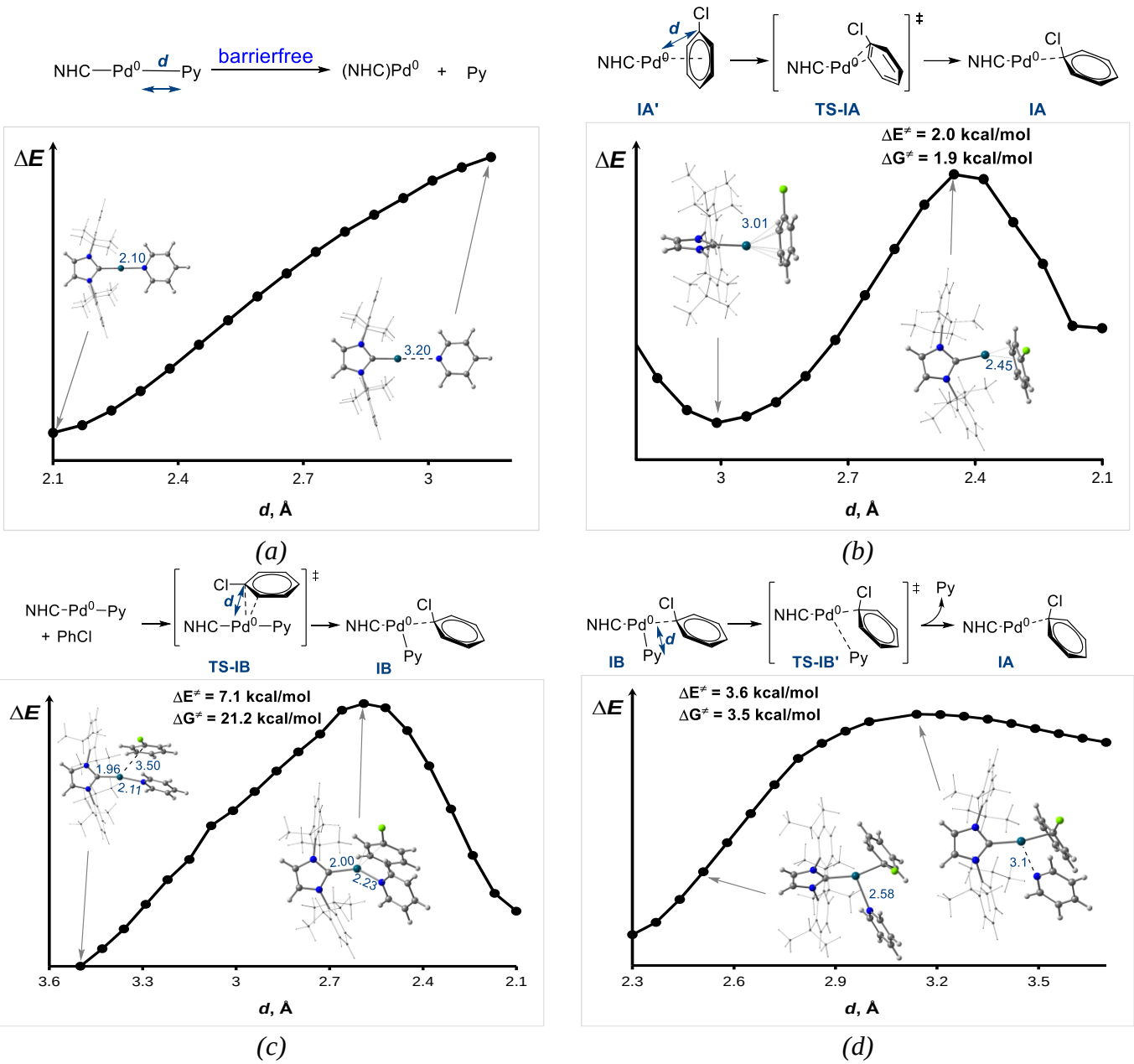

Figure S7. Potential energy profiles of alternative initial stages of the model reaction depicted in the Fig. 4: formation of (NHC)Pd^0 from (NHC)Pd^{0}Py via pyridine loosing (*a*); transformation of precoordination complex **IA′** to the intermediate **IA** (*b*); formation of the intermediate **IB** via PhCl coordination to (NHC)Pd^{0}Py (*c*); formation of **IA** from **IB** via pyridine loosing. Calculations at the PBE1PBE/def2svp level.

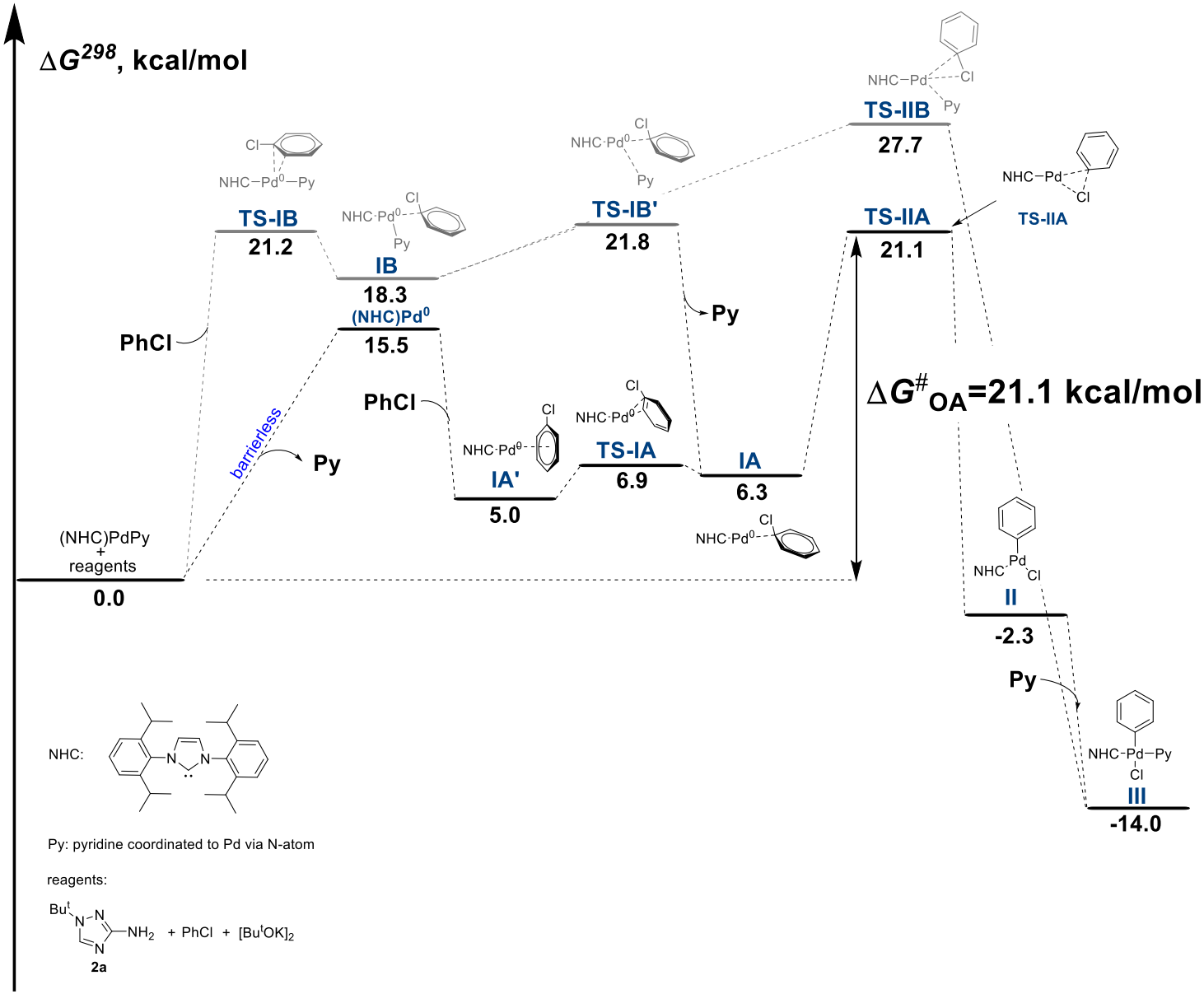

Figure S8. Relative Gibbs free energies of intermediates and transition states of the oxidative addition stage in the Pd-catalyzed Buchwald-Hartwig reaction between amino-1,2,4-triazoles and chlorobenzene computed at the PBE1PBE/def2svp level.

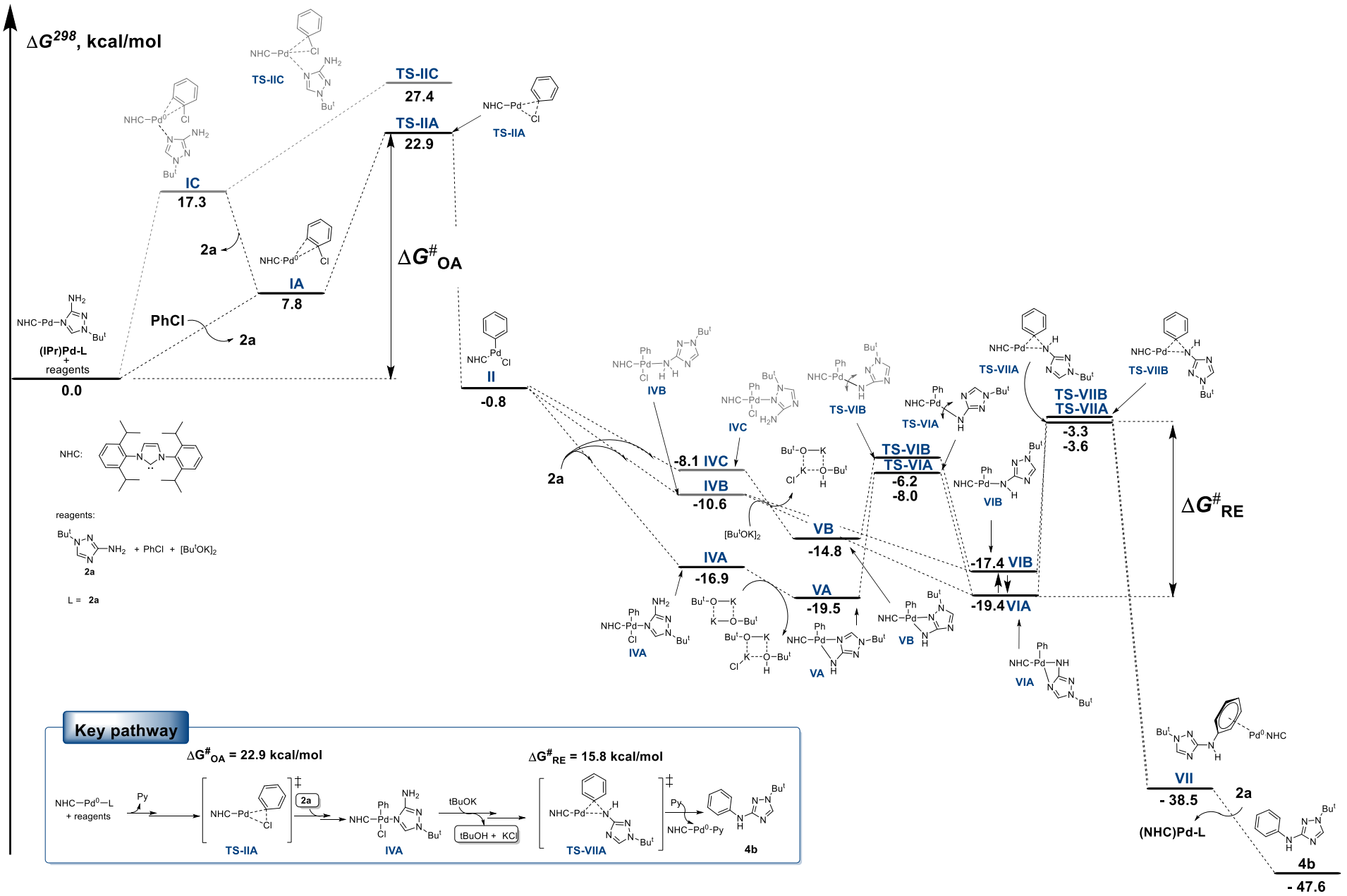

Figure S9. Relative Gibbs free energies of intermediates and transition states of the C-N coupling reaction between 3-amino-1-*tert*-butyl-1,2,4-triazole (**2a**) and chlorobenzene under catalysis with (IPr)PdL complex (L = 3-amino-1-*tert*-butyl-1,2,4-triazole). Gibbs free energy values were computed at the PBE1PBE/def2svp level.

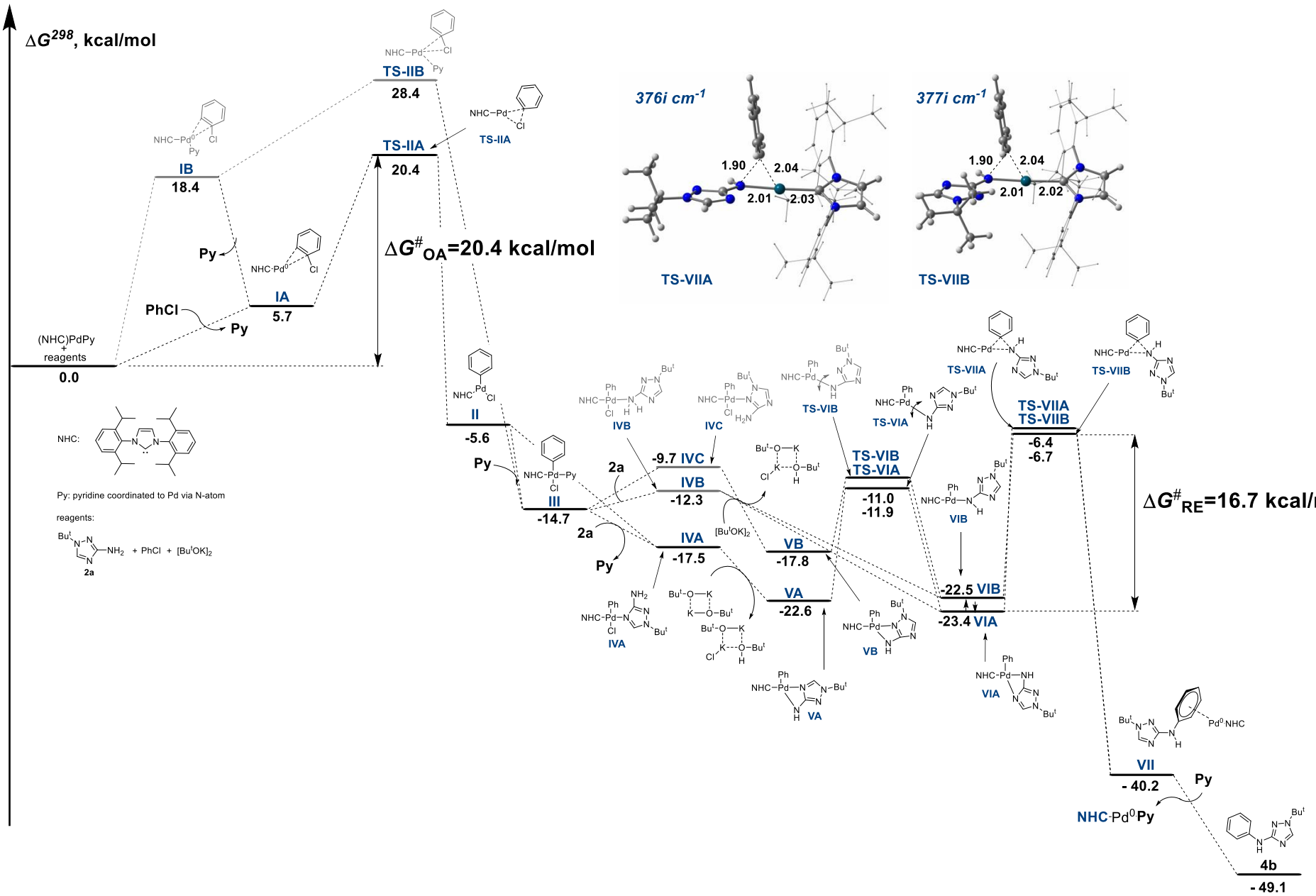

Figure S10. Relative Gibbs free energies of intermediates and transition states of the C-N coupling reaction between 3-amino-1-*tert*-butyl-1,2,4-triazole (**2a**) and chlorobenzene under catalysis with (IPr)PdPy in dioxane medium (in the IEFPCM approximation). Gibbs free energy values were computed at the PBE1PBE/def2svp level.

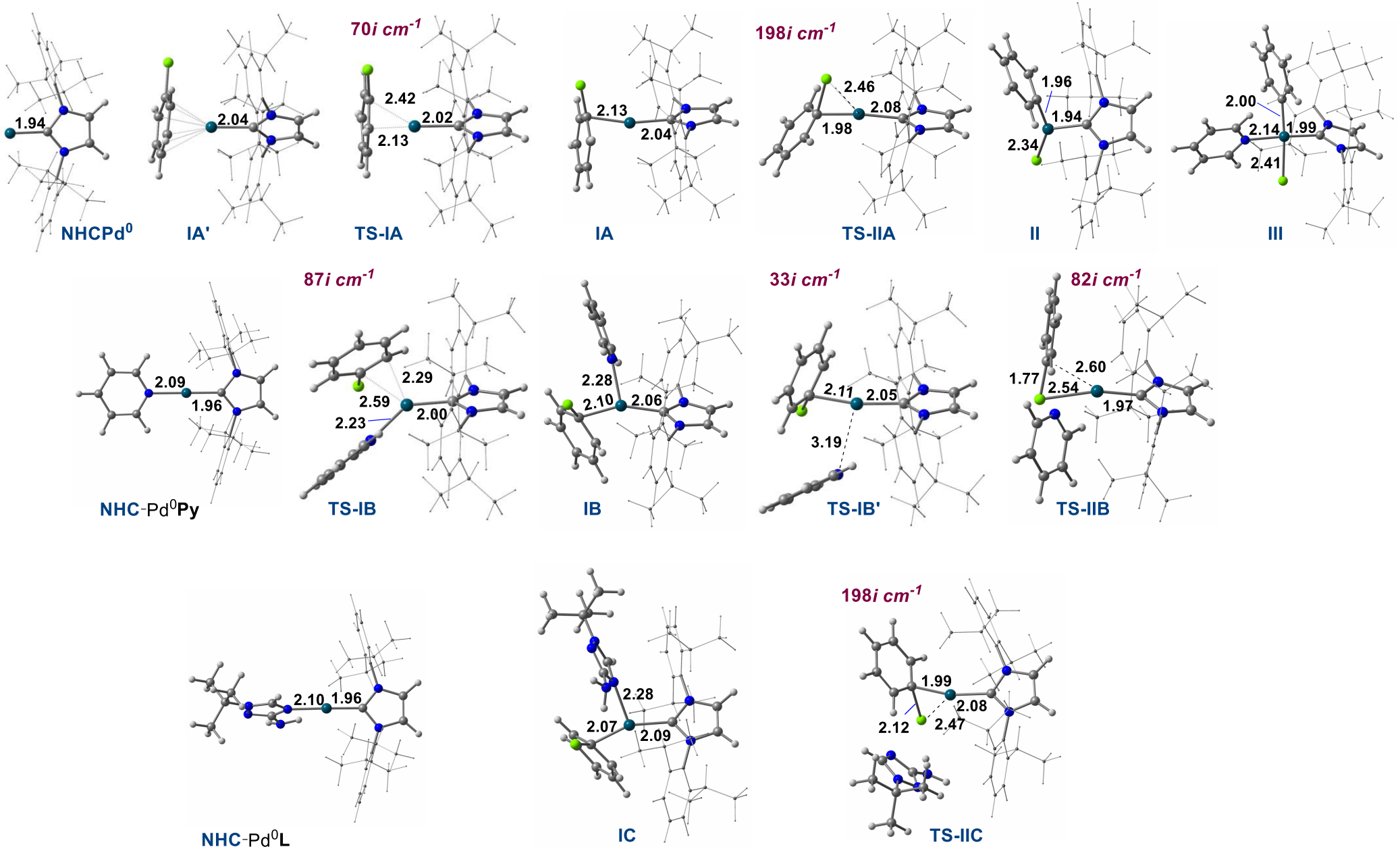

Figure S11. Optimized structures of key intermediates and transition states of the oxidative addition stage in the Pd-catalyzed Buchwald-Hartwig reaction between amino-1,2,4-triazoles and chlorobenzene computed at the PBE1PBE/def2svp level.

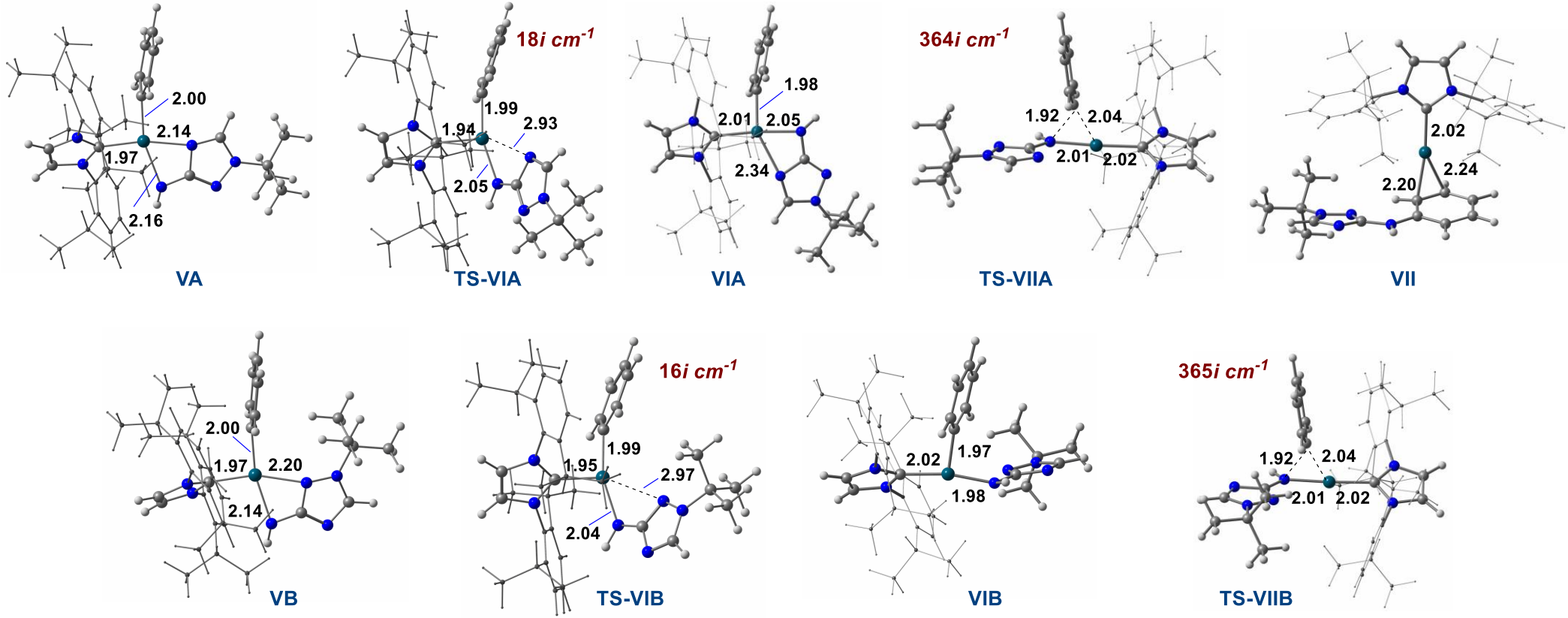

Figure S12. Optimized structures of key intermediates and transition states of the reductive elimination stage in the Pd-catalyzed Buchwald-Hartwig reaction between 3-amino-1-*tert*-butyl-1,2,4-triazole (**2a**) and chlorobenzene computed at the PBE1PBE/def2svp level.

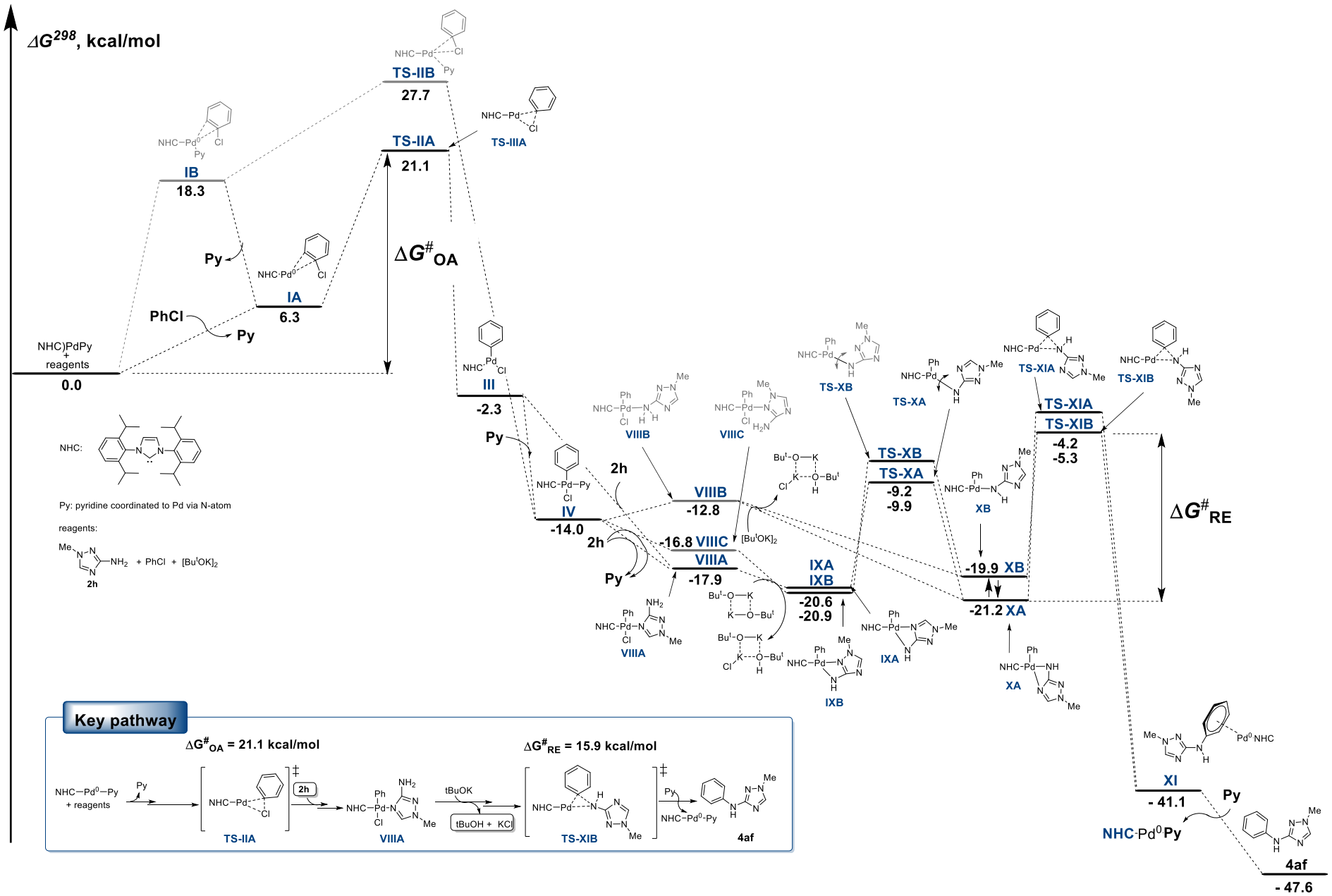

Figure S13. Relative Gibbs free energies of intermediates and transition states of the C–N coupling reaction between 3-amino-1-methyl-1,2,4-triazole (**2h**) and chlorobenzene computed at the PBE1PBE/def2svp level.

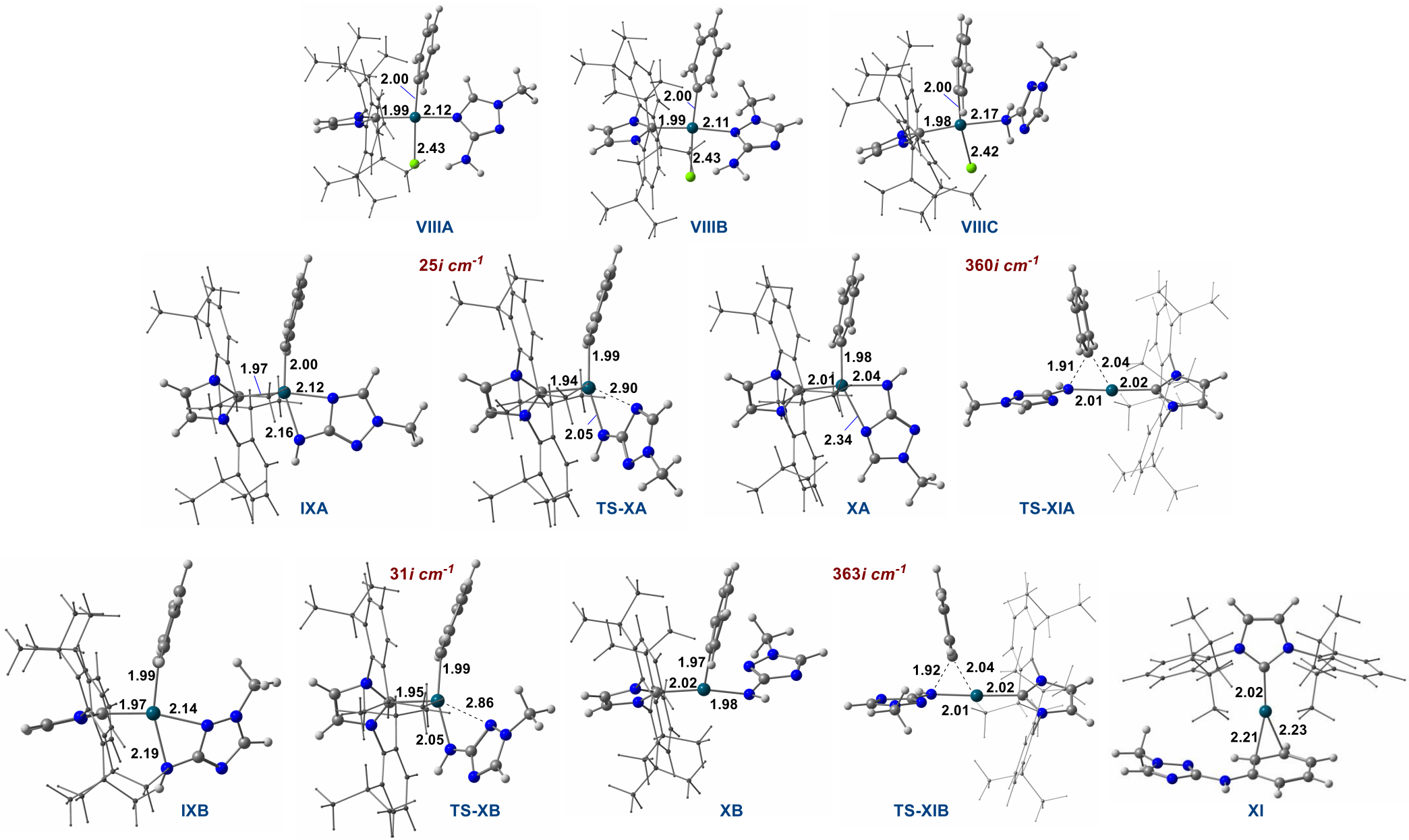

Figure S14. Optimized structures of key intermediates and transition states of the reductive elimination stage in the Pd-catalyzed Buchwald-Hartwig reaction between 3-amino-1-methyl-1,2,4-triazole (**2h**) and chlorobenzene computed at the PBE1PBE/def2svp level.

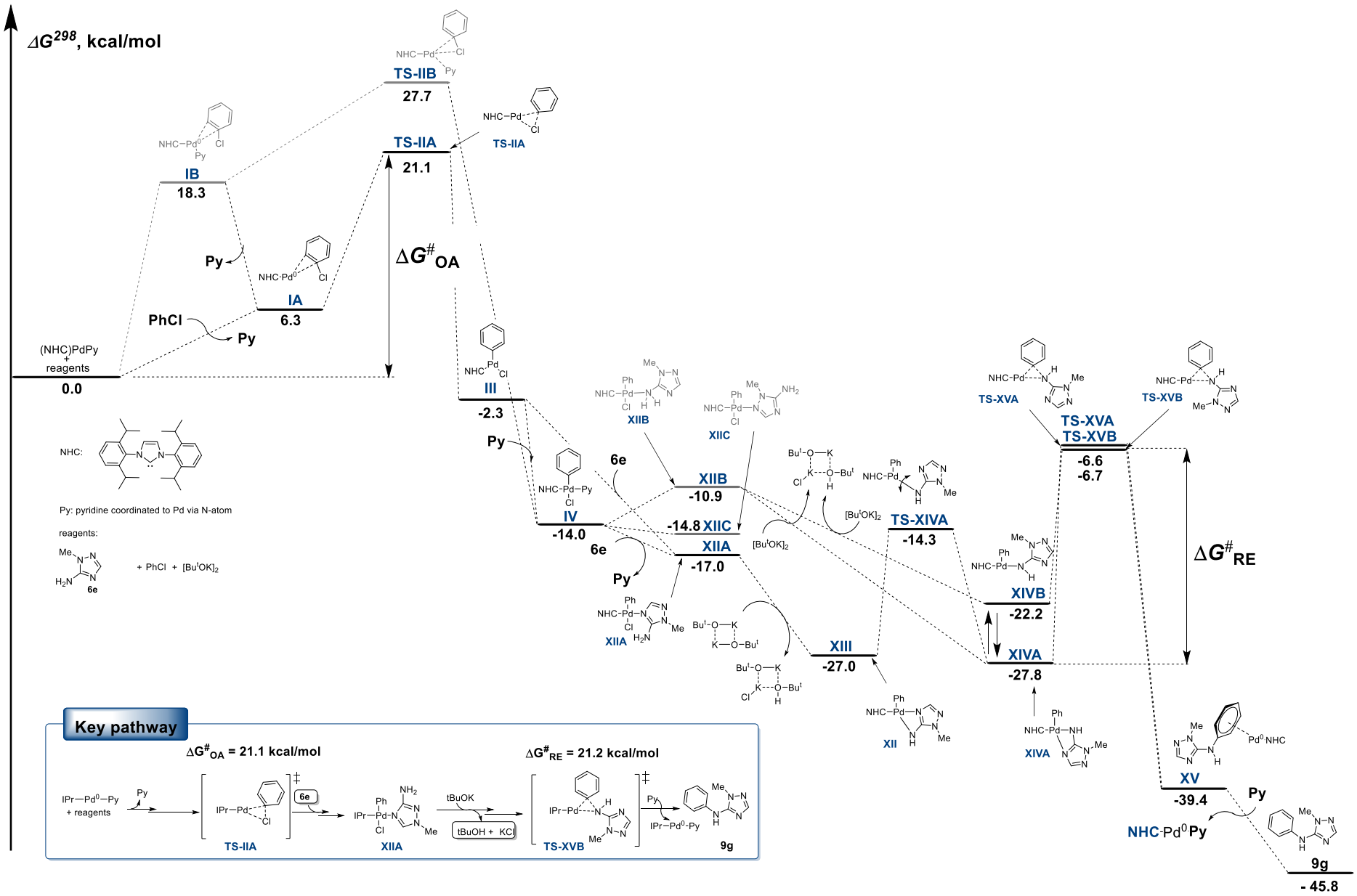

Figure S15. Relative Gibbs free energies of intermediates and transition states of the C−N coupling reaction between 5-amino-1-methyl-1,2,4-triazole (**6e)** and chlorobenzene computed at the PBE1PBE/def2svp level.

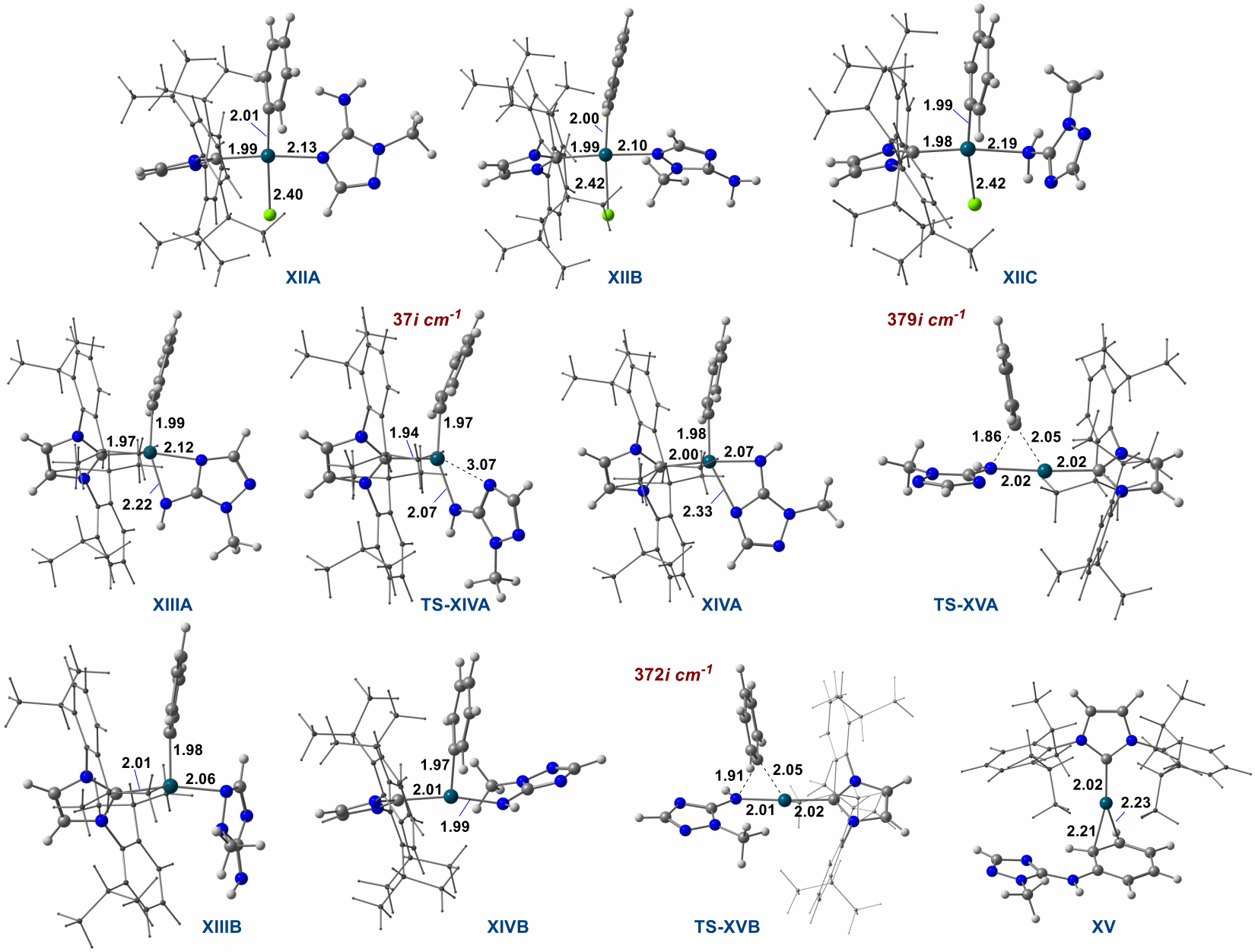

Figure S16. Optimized structures of key intermediates and transition states of the reductive elimination stages in the Pd-catalyzed Buchwald-Hartwig reaction between 5-amino-1-methyl-1,2,4-triazole (**6e)** and chlorobenzene computed at the PBE1PBE/def2svp level.

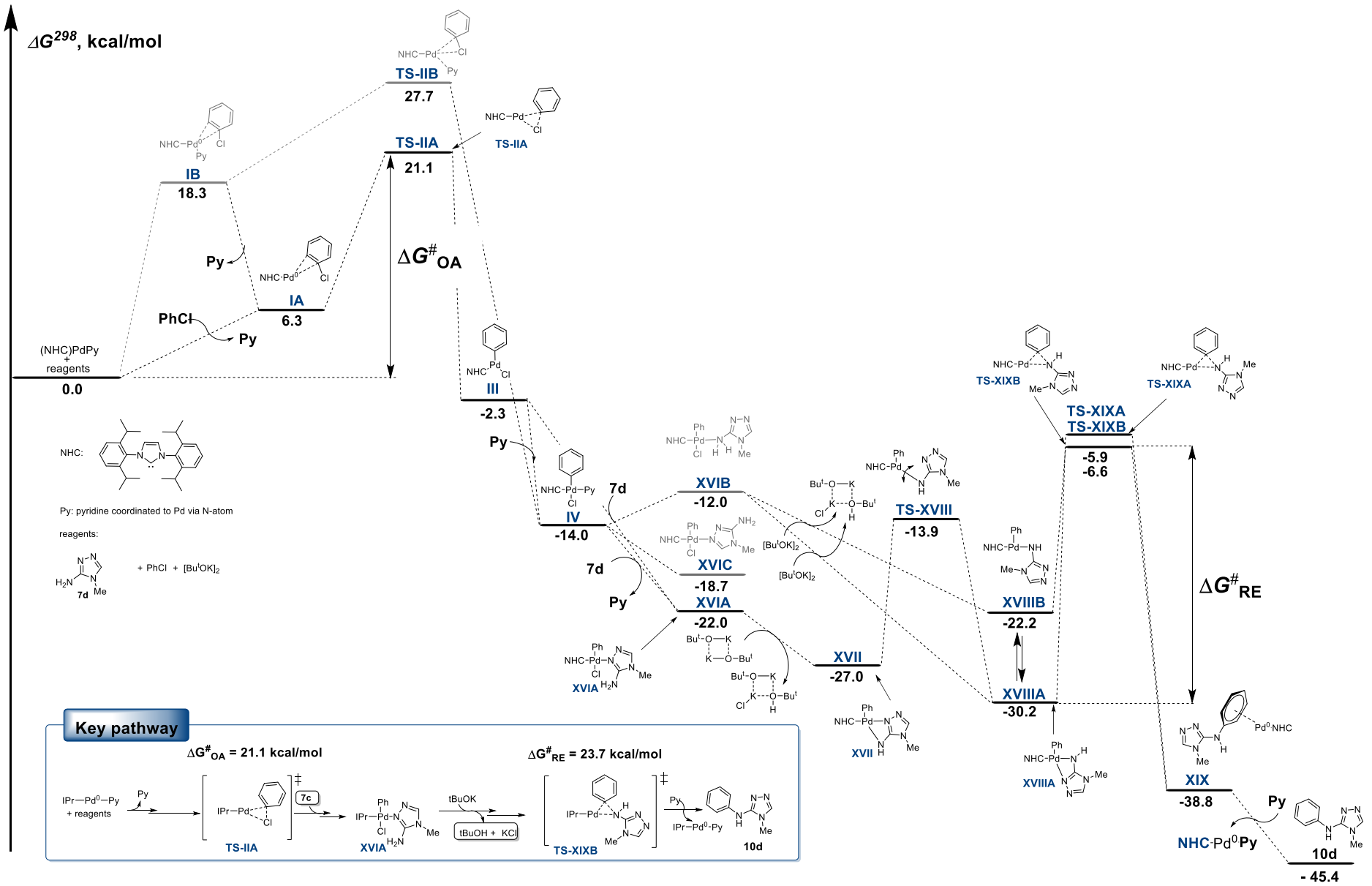

Figure S17. Relative Gibbs free energies of intermediates and transition states of the C–N coupling reaction between 3-amino-4-methyl-1,2,4-triazole (**7d)** and chlorobenzene computed at the PBE1PBE/def2svp level.

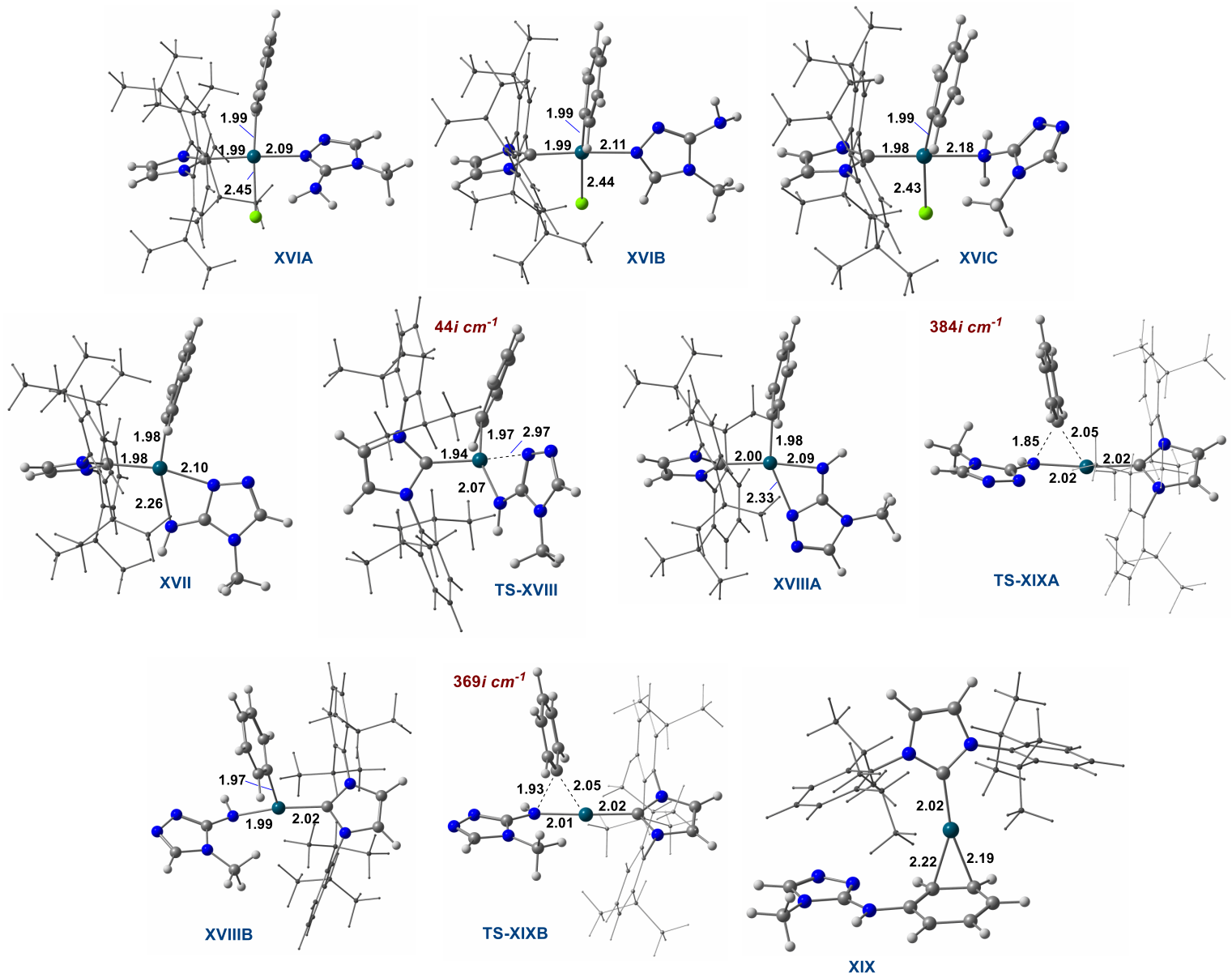

Figure S18. Optimized structures of key intermediates and transition states of the reductive elimination stage in the Pd-catalyzed Buchwald-Hartwig reaction between 3-amino-4-methyl-1,2,4-triazole (**7d)** and chlorobenzene computed at the PBE1PBE/def2svp level.

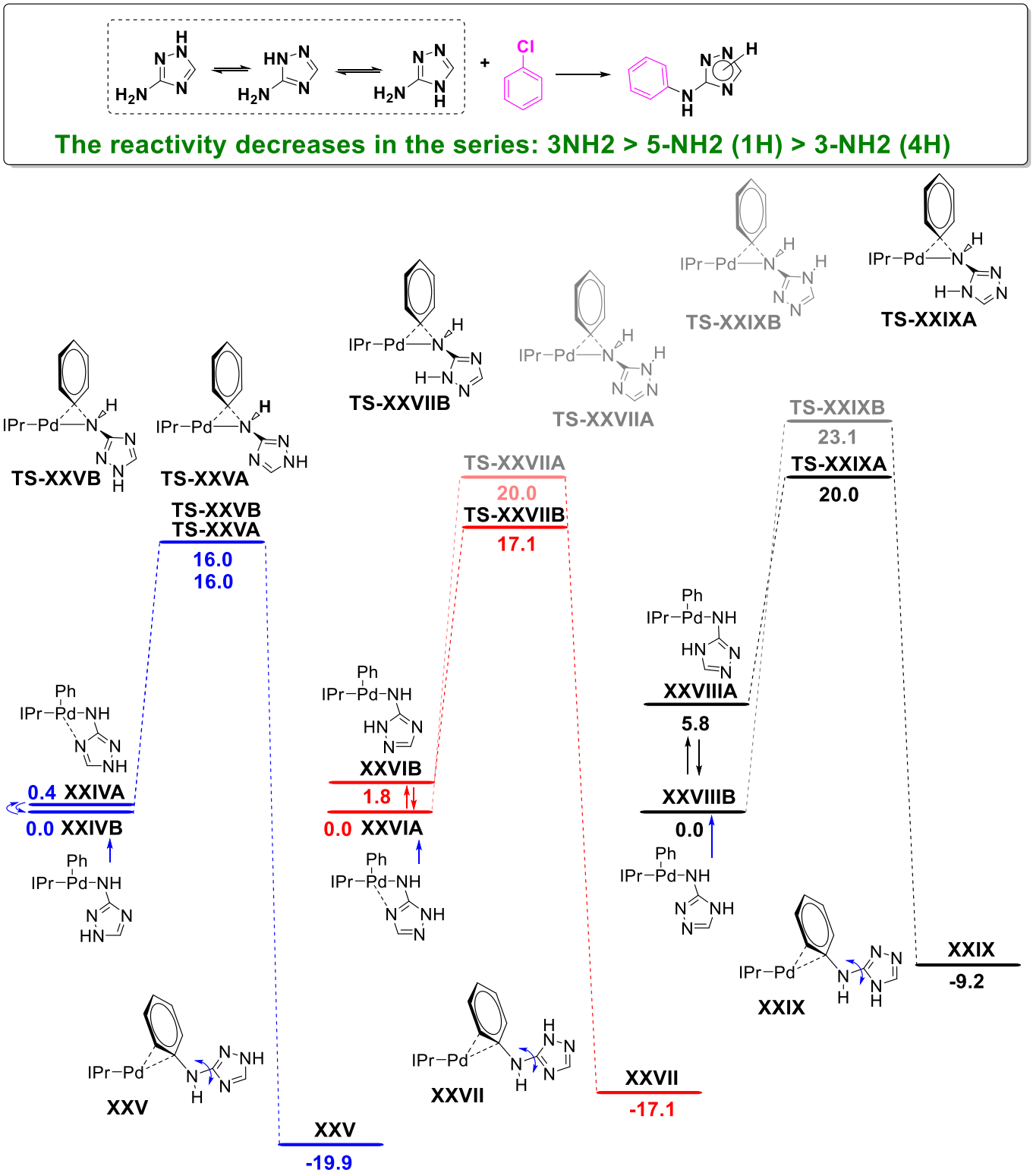

Figure S19. DFT computed relative Gibbs free energies (in kcal/mol) for the reductive elimination of various tautomeric forms in the arylation of 3-amino-1*H*-1,2,4-triazole (**5a**).

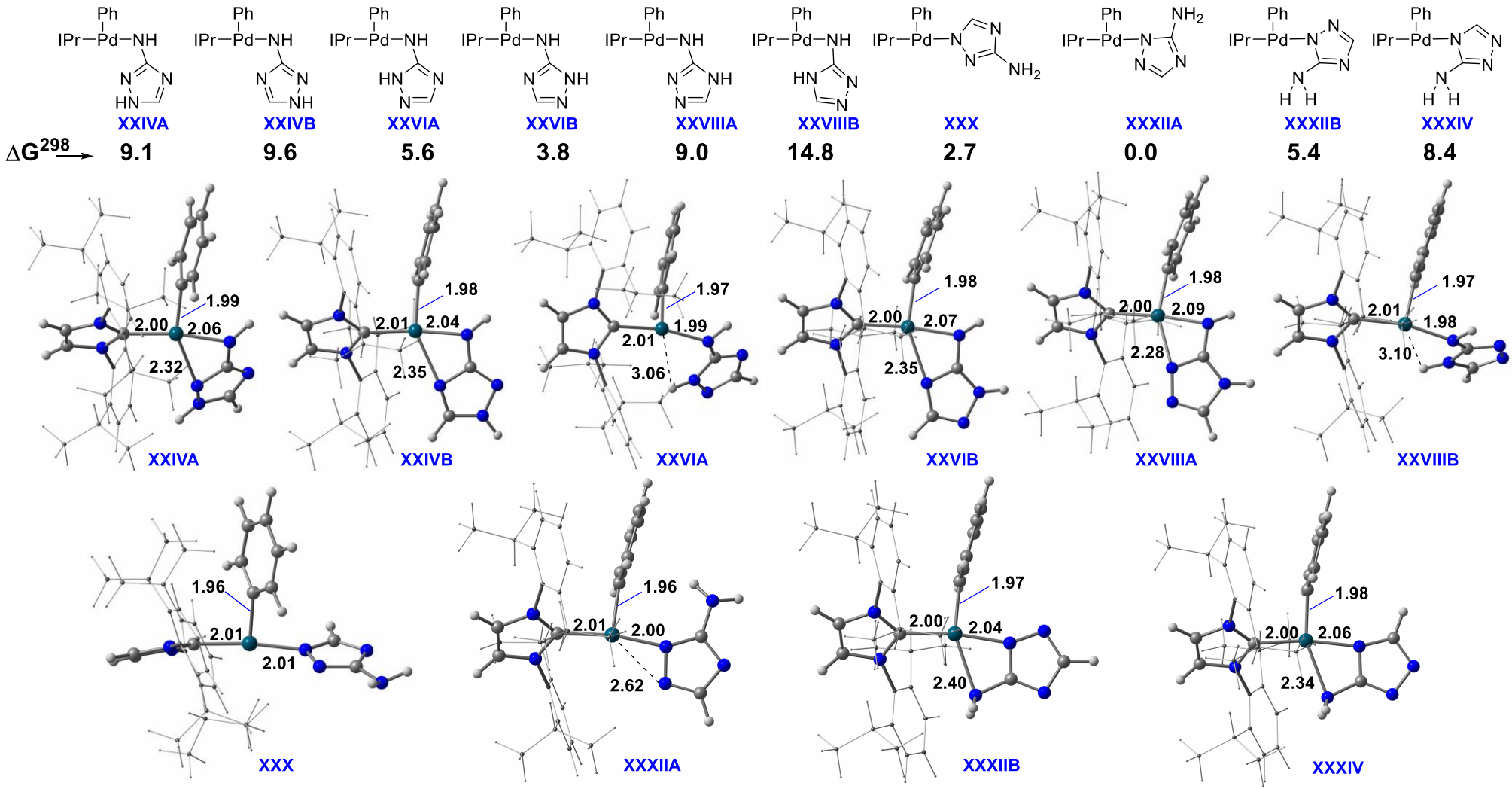

Figure S20. Structures and relative Gibbs free energies (in kcal/mol) of tautomers of key intermediates of the Pd-catalyzed Buchwald-Hartwig reaction between 3-amino-1*H*-1,2,4-triazole (**5a**) and chlorobenzene using IPr as ligand. Relative Gibbs free energy values were computed at the PBE1PBE/def2svp level.

Table S5. Calculated Relative Rate Constant (k), Activation Energies ($\Delta E^{\neq}$, kcal·mol^{-1}), Activation Enthalpies ($\Delta H^{\neq}$, kcal·mol^{-1}), Activation Gibbs Free Energies ($\Delta G^{\neq}$, kcal·mol^{-1}), Reaction Energies (ΔE, kcal·mol^{-1}), Reaction Enthalpies (ΔH, kcal·mol^{-1}) and Reaction Gibbs Free Energies (ΔG, kcal·mol^{-1}) of the reductive elimination stages in the Pd-catalyzed Buchwald-Hartwig reaction between 3(5)-amino-1(4)-R-1,2,4-triazoles and chlorobenzene [a,b]

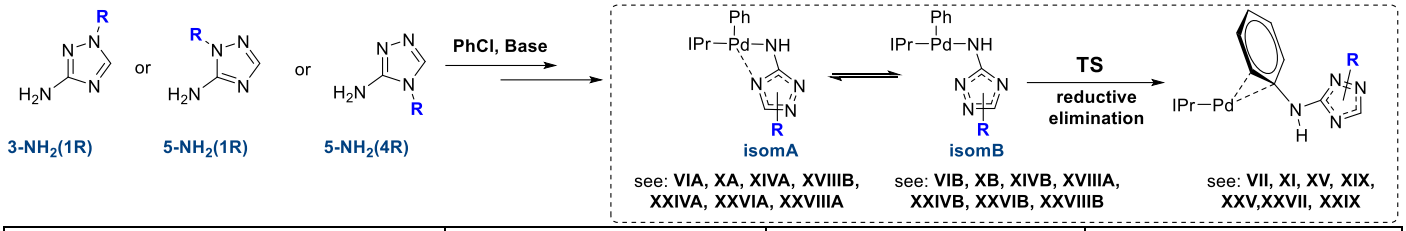

Parameter	3-NH_2(1R)	5-NH_2(1R)	3-NH_2(4R)
R = H			
$\Delta E_{isomA \rightarrow isomB}$	-0.6	+3.7	-7.1
$\Delta H_{isomA \rightarrow isomB}$	-0.7	+3.8	-7.2
$\Delta G_{isomA \rightarrow isomB}$	-0.4	+1.8	-5.8
$\Delta E^{\neq}_{RE}$	18.5	20.2	22.8
$\Delta H^{\neq}_{RE}$	17.8	19.4	22.0
$\Delta G^{\neq}_{RE}$	16.0	17.1	20.0
ΔE_{RE}	-17.8	-15.6	-8.0
ΔH_{RE}	-17.2	-15.1	-7.5
ΔG_{RE}	-19.9	-17.1	-9.2
k(max)	$1.2 \cdot 10^{1}$	1.7	$1.3 \cdot 10^{-2}$
$k_{3\text{-}NH2}/k_{5\text{-}NH2}$	-	7.1	$9.2 \cdot 10^{2}$
R = Me			
$\Delta E_{isomA \rightarrow isomB}$	+3.0	+6.3	-9.1
$\Delta H_{isomA \rightarrow isomB}$	+3.0	+6.4	-9.2
$\Delta G_{isomA \rightarrow isomB}$	+1.2	+5.6	-8.0
$\Delta E^{\neq}_{RE}$	18.1	21.8	24.6
$\Delta H^{\neq}_{RE}$	17.3	21.0	23.8
$\Delta G^{\neq}_{RE}$	15.9	21.2	23.7
ΔE_{RE}	-18.5	-10.0	-8.2
ΔH_{RE}	-17.9	-9.6	-7.7
ΔG_{RE}	-20.0	-11.6	-8.6
k(max)	$1.5 \cdot 10^{1}$	$1.9 \cdot 10^{-3}$	$2.8 \cdot 10^{-5}$
$k_{3\text{-}NH2}/k_{5\text{-}NH2}$	-	$7.5 \cdot 10^{3}$	$5.2 \cdot 10^{5}$
R = Bu^t			
$\Delta E_{isomA \rightarrow isomB}$	+4.0	+11.0	-14.1
$\Delta H_{isomA \rightarrow isomB}$	+4.0	+11.0	-14.0
$\Delta G_{isomA \rightarrow isomB}$	+2.0	+10.8	-12.7
$\Delta E^{\neq}_{RE}$	18.5	24.1	26.3
$\Delta H^{\neq}_{RE}$	17.6	23.2	25.4
$\Delta G^{\neq}_{RE}$	15.8	21.5	25.1
ΔE_{RE}	-17.5	-8.6	-5.8
ΔH_{RE}	-16.8	-8.1	-5.5
ΔG_{RE}	-19.1	-9.8	-8.7
k(max)	$1.8 \cdot 10^{1}$	$1.1 \cdot 10^{-3}$	$2.4 \cdot 10^{-6}$
$k_{3\text{-}NH2}/k_{5\text{-}NH2}$	-	$1.6 \cdot 10^{4}$	$7.2 \cdot 10^{6}$

[a] See fig. S7,S11,S13,S15,S17; [b] The relative effective rate constant of the BH reactions for 3-amino- and 5-amino-1,2,4-triazoles ($k_{3\text{-}NH2}/k_{5\text{-}NH2}$) were calculated by formula $k = \frac{k_B T}{h} e^{\frac{-\Delta G^{\neq}}{RT}}$ is rate constant at T = 298 K, where k_B is the Boltzmann constant and h is the Planck constant, $\Delta G^{\neq}$ are the Gibbs free energy of activation and R is the gas constant.

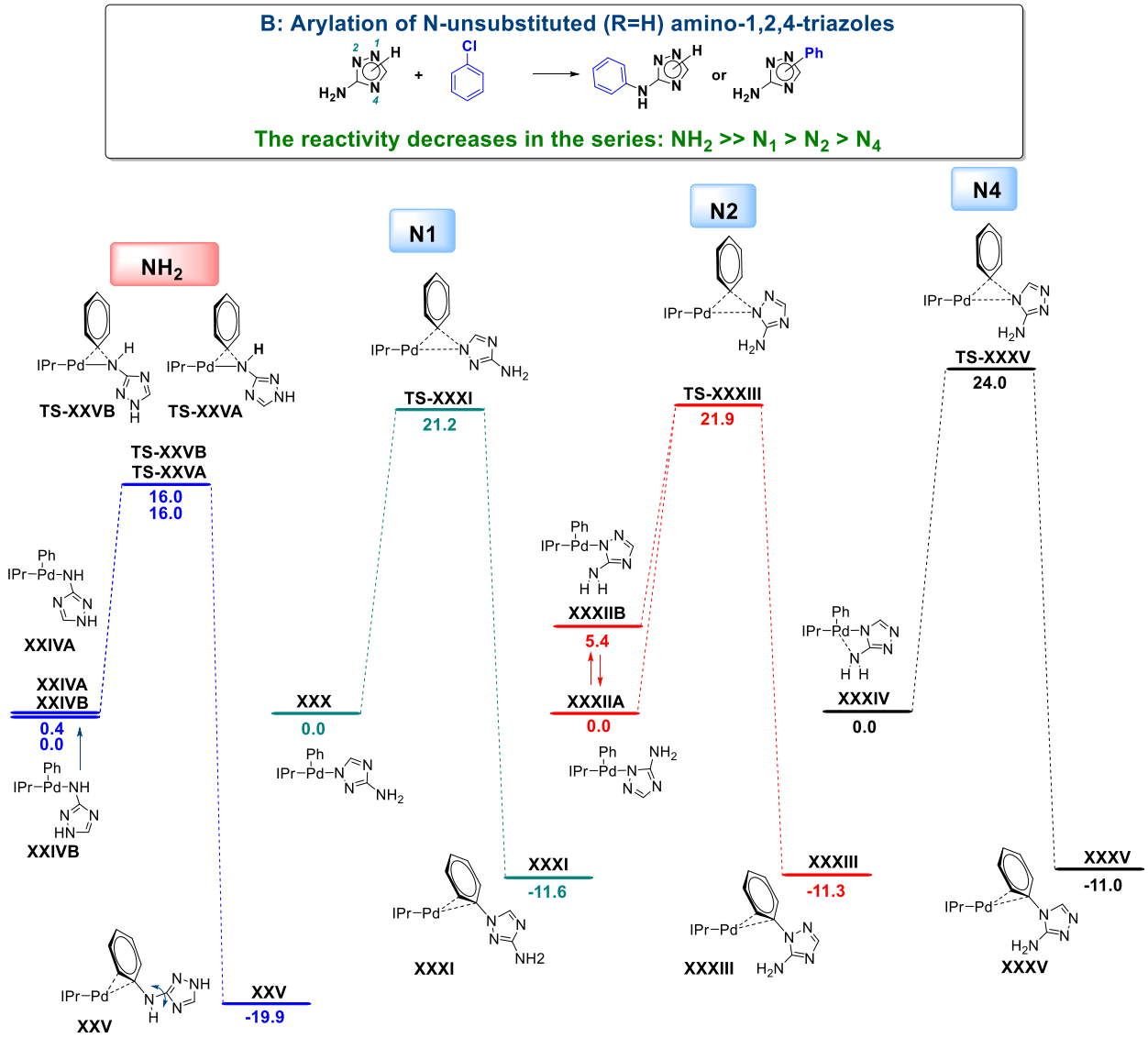

Figure S21. Relative Gibbs free energies of the reductive elimination stages leading to isomeric products in the arylation of 3-amino-1*H*-1,2,4-triazole (**5a**) with chlorobenzene computed at the PBE1PBE/def2svp level.

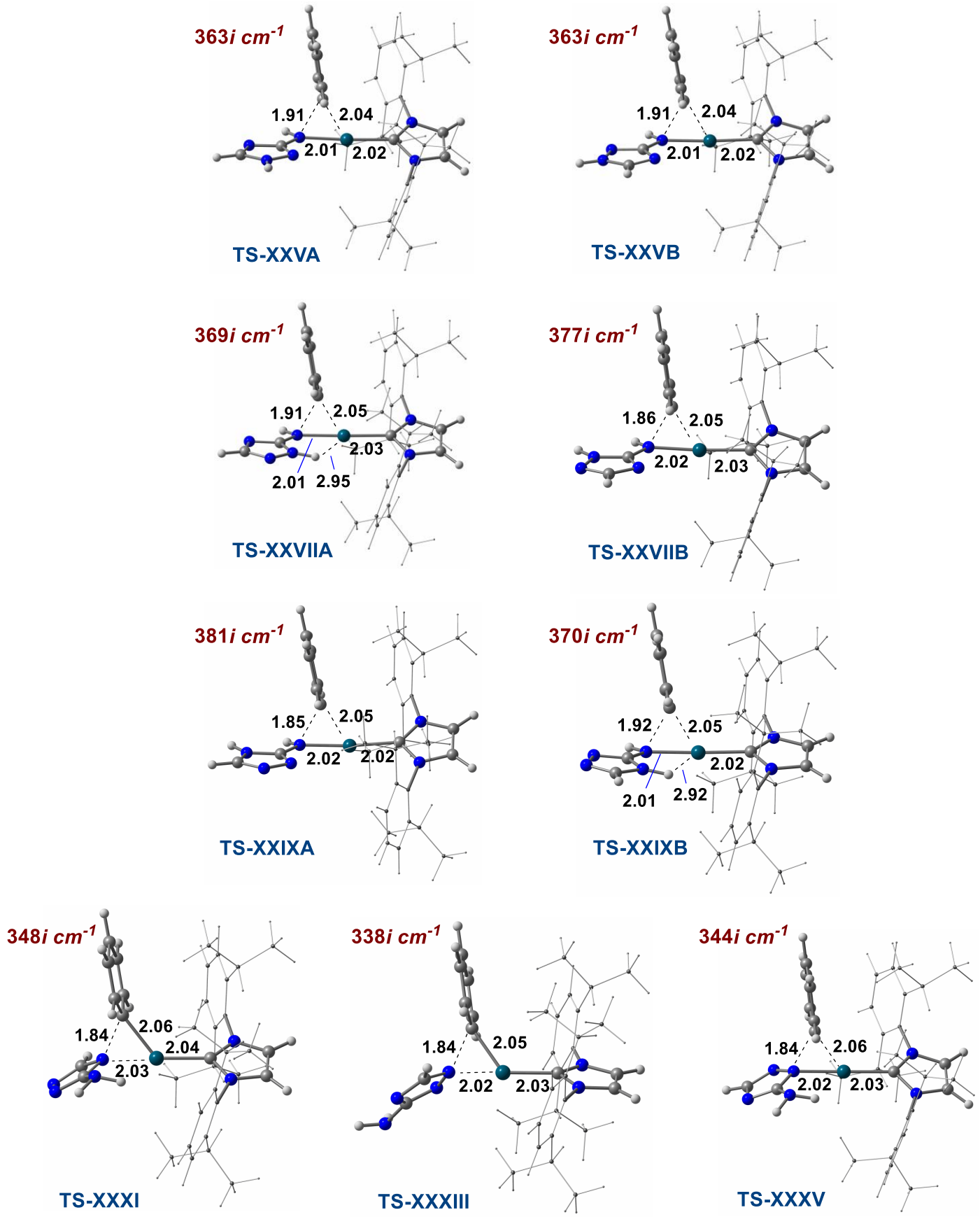

Figure S22. Structures of transition states of the reductive elimination stages in the Pd-catalyzed Buchwald-Hartwig reaction between amino-1*H*-1,2,4-triazole (**5a**) and chlorobenzene computed at the PBE1PBE/def2svp level.

X-Ray diffraction single-crystal studies

Experimental

X-ray diffraction data for **4h** and **4u** were collected at 100K on a Bruker Quest D8 diffractometer equipped with a Photon-III area-detector (shutterless φ- and ω-scan technique), using graphite-monochromatized Mo K_α-radiation. The intensity data of collected reflections were integrated with the *SAINT* program.[1] Absorption correction based on measurements of equivalent reflections was semi-empirically carried out by multi-scan methods, using SADABS.[2] The structures were solved by direct methods using SHELXT[3] and refined by the full-matrix least-squares method on refined on F^2 using SHELXL-2018.[4] Positions of all atoms were found from the electron density-difference map. Atoms were refined with individual anisotropic (non-hydrogen atoms) or isotropic (hydrogen atoms) displacement parameters.

X-ray diffraction data for **9f** were collected at 100K on a four-circle Rigaku Synergy S diffractometer equipped with a HyPix6000HE area-detector (kappa geometry, shutterless ω-scan technique), using monochromatized Cu K_α-radiation. The intensity data were integrated and corrected for absorption and decay by the CrysAlisPro program.[5] The structure was solved by direct methods using SHELXT[3] and refined by the full-matrix least-squares method on F^2 using SHELXL-2018[4] in the OLEX2 program.[6] All non-hydrogen atoms were refined with individual anisotropic displacement parameters. The position of atom H4 (at N4) was found from the electron density-difference map; the N-H distance was restrained to be 0.85(2)Å. All other hydrogen atoms were placed in ideal calculated positions (C-H distance = 0.950 Å for aromatic, 0.990 Å for methylene hydrogen atoms) and refined as riding atoms with relative isotropic displacement parameters taken as $U_{iso}(H)=1.2U_{eq}(C)$. The *Mercury* program[7] and the SHELXTL program suite[1] were used for molecular graphics.

Crystal data, data collection and structure refinement details for **4h**, **4u** and **9f** are summarized in Table S6. Crystallographic data for **4h**, **4u** and **9f** have been deposited at the Cambridge Crystallographic Data Center. CCDC 2194495 (**4h**), CCDC 2194496 (**4u**) and CCDC 2194497 (**9f**) contain the supplementary crystallographic data for this paper. These data can be obtained free of charge from the Director, CCDC, 12 Union Road, Cambridge CB2 1EZ, UK (Fax: +44 1223 336033; e-mail: deposit@ccdc.cam.ac.uk or https://www.ccdc.cam.ac.uk/structures/).

References

1. Bruker. APEX-III. *Bruker AXS Inc.*, Madison, Wisconsin, USA, **2019**.
2. Krause, L.; Herbst-Irmer, R.; Sheldrick, G. M.; Stalke, D. Comparison of silver and molybdenum microfocus X-ray sources for single-crystal structure determination. *J. Appl. Cryst.* **2015**, 48, 3–10. http://doi.org/10.1107/S1600576714022985
3. Sheldrick, G. M. SHELXT - Integrated space-group and crystal-structure determination. *Acta Cryst.* **2015**, A71, 3-8. http://doi.org/10.1107/S2053273314026370
4. Sheldrick, G. M. Crystal structure refinement with SHELXL. *Acta Cryst.* **2015**, C71, 3-8. http://doi.org/10.1107/S2053229614024218
5. CrysAlisPro. Version 1.171.41. *Rigaku Oxford Diffraction*, **2021**.
6. Dolomanov O.V.; Bourhis L.J.; Gildea R.J.; Howard J.A.K.; Puschmann H. OLEX2: a complete structure solution, refinement and analysis program. *J. Appl. Cryst.* **2009**, 42, 229-341. http://doi.org/10.1107/S0021889808042726
7. Macrae, C. F.; Sovago, I.; Cottrell, S. J.; Galek, P. T. A.; McCabe, P.; Pidcock, E.; Platings, M.; Shields, G. P.; Stevens, J. S.; Towler, M.; Wood, P. A. Mercury 4.0: from visualization to analysis, design and prediction. *J. Appl. Cryst.* **2020**, 53, 226-235. https://doi.org/10.1107/S1600576719014092

Table S6. Crystal data, data collection and structure refinement details for **4h**, **4u** and **9f.**

Identification code	**4h**	**4u**	**9f**
Empirical formula	$C_{16}H_{16}N_4$	$C_{18}H_{28}N_4$	$C_{21}H_{18}N_4$
Formula weight	264.33	300.44	326.39
Temperature (K)	100(2)	100(2)	100.0(1)
Wavelength (Å)	0.71073	0.71073	1.54184
Crystal system	Monoclinic	Triclinic	Trigonal
Space group	$P2_1/c$	$P\bar{1}$	$P3_1$
Unit cell dimensions			
a (Å)	10.9515(3)	8.8745(2)	10.5968(2)
b (Å)	6.05280(10)	9.8920(2)	10.5968(2)
c (Å)	20.1410(5)	11.1653(3)	13.4314(3)
α (°)	90	91.1400(10)	90
β (°)	93.8980(10)	104.8090(10)	90
γ (°)	90	113.3590(10)	120
Volume ($Å^3$)	1332.00(5)	861.78(4)	1306.17(6)
Z	4	2	3
Calcd. density ($g \cdot cm^{-3}$)	1.318	1.158	1.245
Absorption coefficient, μ (mm^{-1})	0.082	0.070	0.595
F(000)	560	328	516
Crystal size	0.59×0.29×0.26	0.59×0.52×0.47	0.74×0.13×0.10
θ range for data collection (°)	1.864-33.148	1.904-33.496	4.819-77.907
Index ranges	-16<=h<=16, -9<=k<=9, -30<=l<=30	-13<=h<=13, -15<=k<=15, -17<=l<=17	-13<=h<=13, -13<=k<=13, -16<=l<=13
Reflections			
collected	46205	55140	18357
independent [R_{int}]	5081 [0.0360]	6773 [0.0236]	3060 [0.0449]
observed (I>2σ(I))	4375	5997	3023
Completeness to θ_{full} / θ_{max}	0.998 / 0.999	0.999 / 0.999	1.000 / 0.996
Transmission max. / min.	0.7471 / 0.7133	0.8023 / 0.7440	0.949 / 0.788
Data / restraints / parameters	5081 / 0 / 245	6773 / 0 / 311	3060 / 196 / 269
Goodness-of-fit on F^2	1.036	1.025	1.041
Final R1 / wR2 indices (I>2σ(I))	0.0425 / 0.1077	0.0398 / 0.1069	0.0585 / 0.1329
Final R1 / wR2 indices (all data)	0.0511 / 0.1152	0.0454 / 0.1114	0.0589 / 0.1332
Absolute structure parameter	-	-	0.1(3)
Extinction coefficient	-	-	0.0050(7)
$\Delta\rho(\bar{e})_{max}$ / $\Delta\rho(\bar{e})_{min}$ ($\bar{e} \cdot Å$)	0.443 / -0.335	0.501 / -0.266	0.228 / -0.267
CCDC number	2194495	2194496	2194497

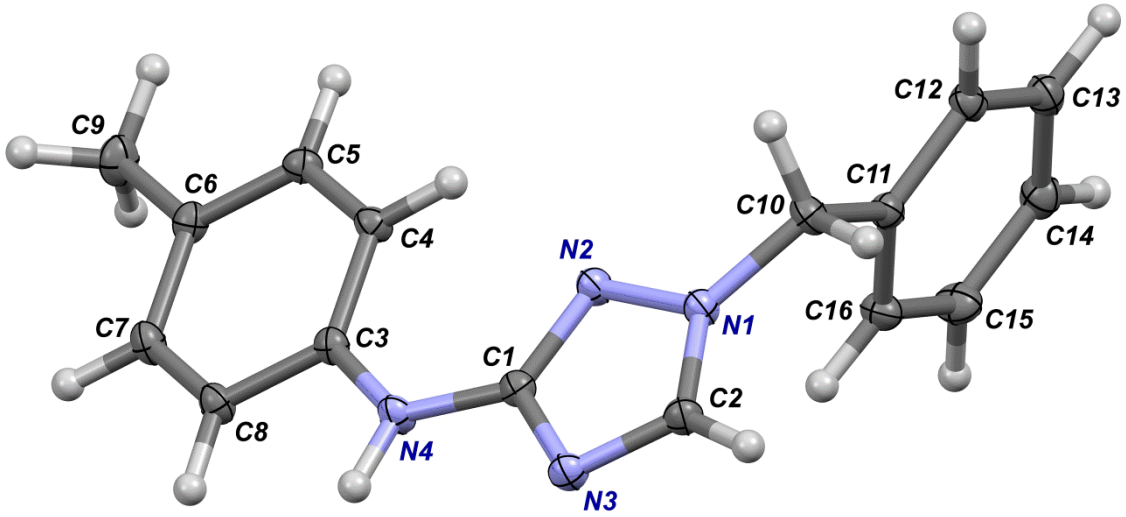

Figure S23. The molecular structure of compound **4h**. Thermal ellipsoids are shown at a 50% probability level. Hydrogen atoms are drawn as fixed-size spheres.

Table S7. Bond distances (Å) for **4h.**

N2-C1	1.3313(10)	C4-H4	0.973(12)	C10-H10B	0.998(13)
N2-N1	1.3763(10)	C5-C6	1.3926(11)	C11-C16	1.3946(12)
N3-C2	1.3275(11)	C5-H5	0.983(13)	C11-C12	1.3956(11)
N3-C1	1.3753(10)	C6-C7	1.4006(12)	C12-C13	1.3934(12)
N1-C2	1.3327(10)	C6-C9	1.5051(12)	C12-H12	0.993(13)
N1-C10	1.4469(11)	C7-C8	1.3866(11)	C13-C14	1.3896(13)
N4-C1	1.3652(10)	C7-H7	0.986(14)	C13-H13	0.976(14)
N4-C3	1.3982(10)	C8-H8	0.974(14)	C14-C15	1.3904(13)
N4-H4A	0.912(14)	C9-H9A	0.996(17)	C14-H14	0.990(14)
C2-H2	0.957(13)	C9-H9B	0.993(17)	C15-C16	1.3963(12)
C3-C4	1.4000(11)	C9-H9C	0.998(16)	C15-H15	0.988(15)
C3-C8	1.4040(11)	C10-C11	1.5137(12)	C16-H16	0.980(14)
C4-C5	1.3954(11)	C10-H10A	0.992(13)		

Table S8. Intermolecular hydrogen bond parameters (Å, °) for **4h**.

D-H...A	d(D-H)	d(H...A)	d(D...A)	<(DHA)
N(4)-H(4A)...N(3)#1	0.912(14)	2.099(14)	3.0050(10)	172.6(13)

Symmetry transformation to generate equivalent atoms: #1 -x+1, -y+2, -z+1

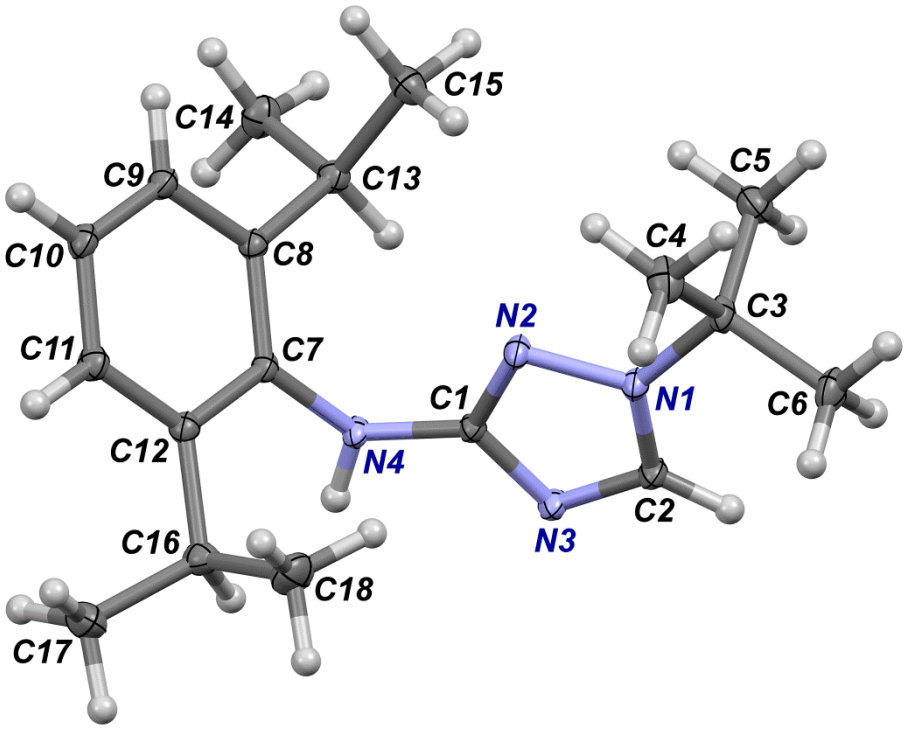

Figure S24. The molecular structure of compound **4u**. Thermal ellipsoids are shown at a 50% probability level. Hydrogen atoms are drawn as fixed-size spheres.

Table S9. Bond distances (Å) for **4u.**

N1-C2	1.3354(8)	C5-H5B	0.986(13)	C13-C14	1.5361(10)
N1-N2	1.3802(7)	C5-H5C	1.009(14)	C13-H13	0.995(11)
N1-C3	1.4807(8)	C6-H6A	0.977(13)	C14-H14A	0.992(13)
N2-C1	1.3322(8)	C6-H6B	0.984(14)	C14-H14B	0.990(14)
N3-C2	1.3288(8)	C6-H6C	1.014(14)	C14-H14C	0.974(14)
N3-C1	1.3712(8)	C7-C8	1.4063(9)	C15-H15A	1.027(14)
N4-C1	1.3667(8)	C7-C12	1.4141(9)	C15-H15B	1.030(13)
N4-C7	1.4295(8)	C8-C9	1.3997(9)	C15-H15C	0.982(13)
N4-H4	0.875(13)	C8-C13	1.5190(9)	C16-C17	1.5281(11)
C2-H2	0.968(13)	C9-C10	1.3858(10)	C16-C18	1.5336(12)
C3-C4	1.5263(10)	C9-H9	0.975(12)	C16-H16	0.981(13)
C3-C6	1.5273(10)	C10-C11	1.3928(10)	C17-H17A	1.022(14)
C3-C5	1.5323(10)	C10-H10	0.985(12)	C17-H17B	1.011(15)
C4-H4A	0.972(13)	C11-C12	1.3980(9)	C17-H17C	1.017(16)
C4-H4B	0.994(13)	C11-H11	1.002(12)	C18-H18A	1.013(16)
C4-H4C	0.989(13)	C12-C16	1.5212(10)	C18-H18B	1.030(15)
C5-H5A	0.992(13)	C13-C15	1.5319(10)	C18-H18C	0.966(14)

Table S10. Intermolecular hydrogen bond parameters (Å, °) for **4u**.

D-H...A	d(D-H)	d(H...A)	d(D...A)	<(DHA)
N(4)-H(4)...N(3)#1	0.875(13)	2.173(13)	3.0433(8)	172.6(11)

Symmetry transformation to generate equivalent atoms: #1 -x+1, -y+1, -z+1

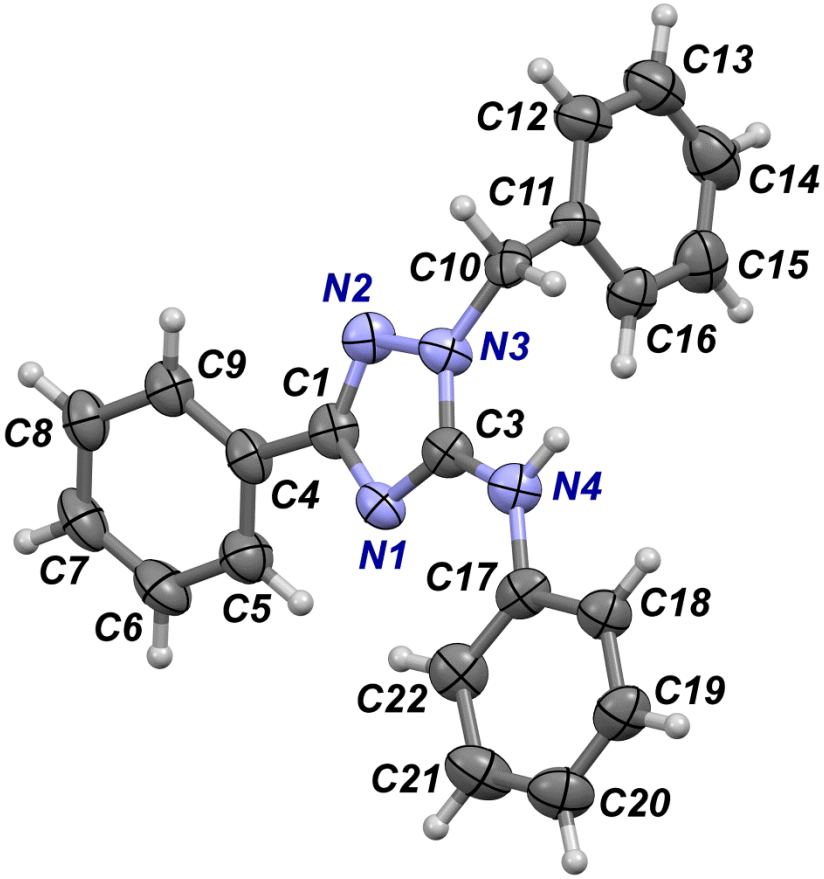

Figure S25. The molecular structure of compound **9f**. Thermal ellipsoids are shown at a 50% probability level. Hydrogen atoms are drawn as fixed-size spheres. Disorder is omitted for clarity on the figure.

Table S11. Selected bond distances (Å) for **9f.**

N1-C1	1.389(5)	C7-C8	1.386(3)	C15-C16	1.384(4)
N1-C3	1.309(5)	C8-C9	1.386(3)	C10A-C11A	1.507(8)
C1-N2	1.304(5)	C5A-C6A	1.386(4)	C11A-C12A	1.384(4)
C1-C4	1.476(5)	C6A-C7A	1.386(4)	C11A-C16A	1.386(4)
N2-N3	1.400(4)	C7A-C8A	1.386(4)	C12A-C13A	1.385(4)
N3-C3	1.348(5)	C8A-C9A	1.386(4)	C13A-C14A	1.384(4)
N3-C10	1.456(5)	N4-H4	0.90(2)	C14A-C15A	1.385(4)
N3-C10A	1.456(6)	N4-C17	1.427(5)	C15A-C16A	1.385(4)
C3-N4	1.362(5)	C10-C11	1.508(7)	C17-C18	1.398(6)
C4-C5	1.387(3)	C11-C12	1.386(4)	C17-C22	1.382(6)
C4-C9	1.386(3)	C11-C16	1.384(4)	C18-C19	1.369(6)
C4-C5A	1.386(3)	C12-C13	1.386(4)	C19-C20	1.377(7)
C4-C9A	1.386(3)	C13-C14	1.386(4)	C20-C21	1.380(7)
C5-C6	1.385(3)	C14-C15	1.384(4)	C21-C22	1.399(6)
C6-C7	1.384(3)				

Table S12. Intermolecular hydrogen bond parameters (Å, °) for **9f**.

D-H...A	d(D-H)	d(H...A)	d(D...A)	<(DHA)
N(4)-H(4)...N(2)#1	0.90(2)	2.22(3)	3.070(5)	158(4)

Symmetry transformation to generate equivalent atoms: #1 -y+1, x-y+1, z+1/3

NMR spectra

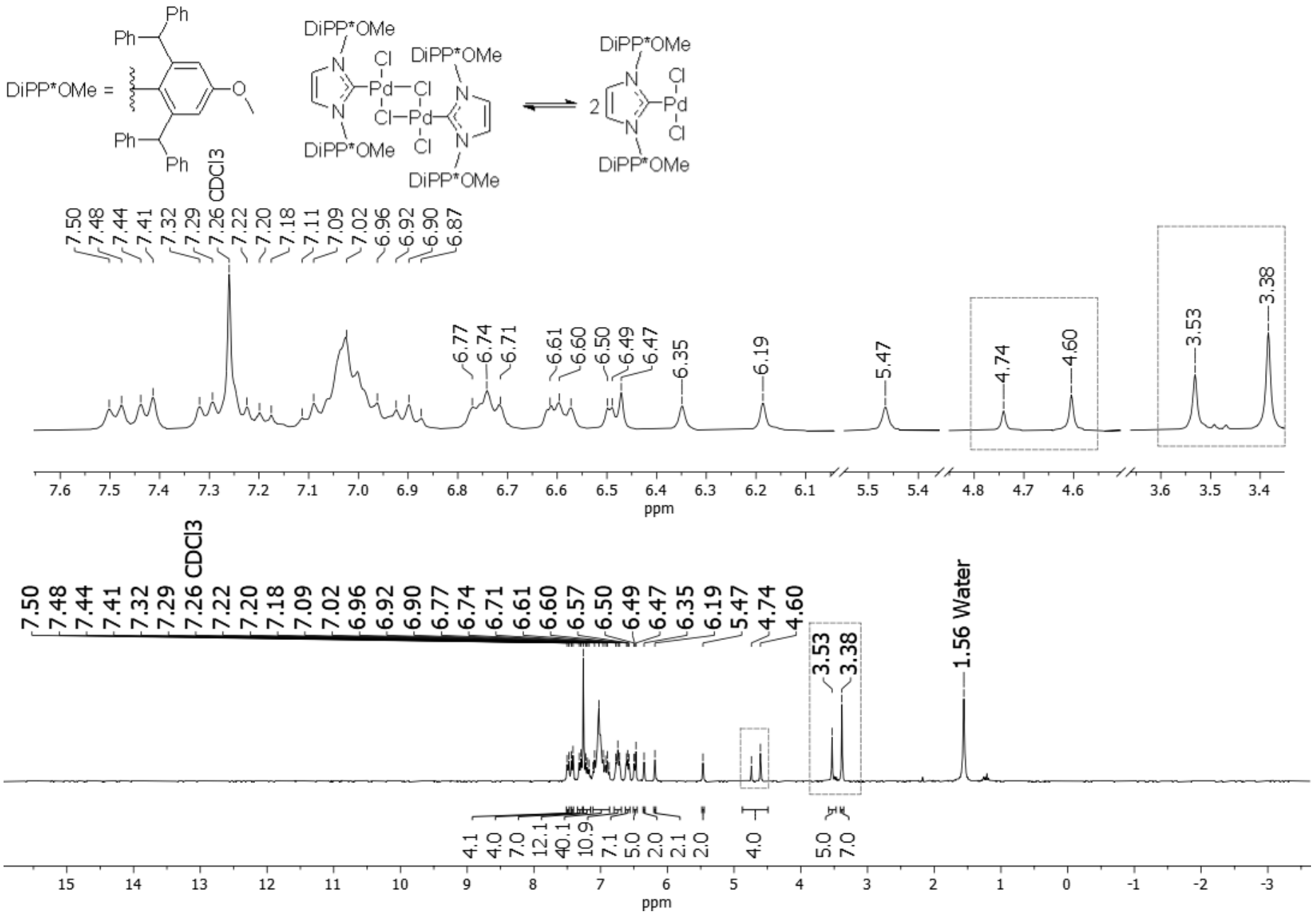

Figure S26. ^{1}H NMR spectrum of compound **1h** ($CDCl_3$, 300 MHz)

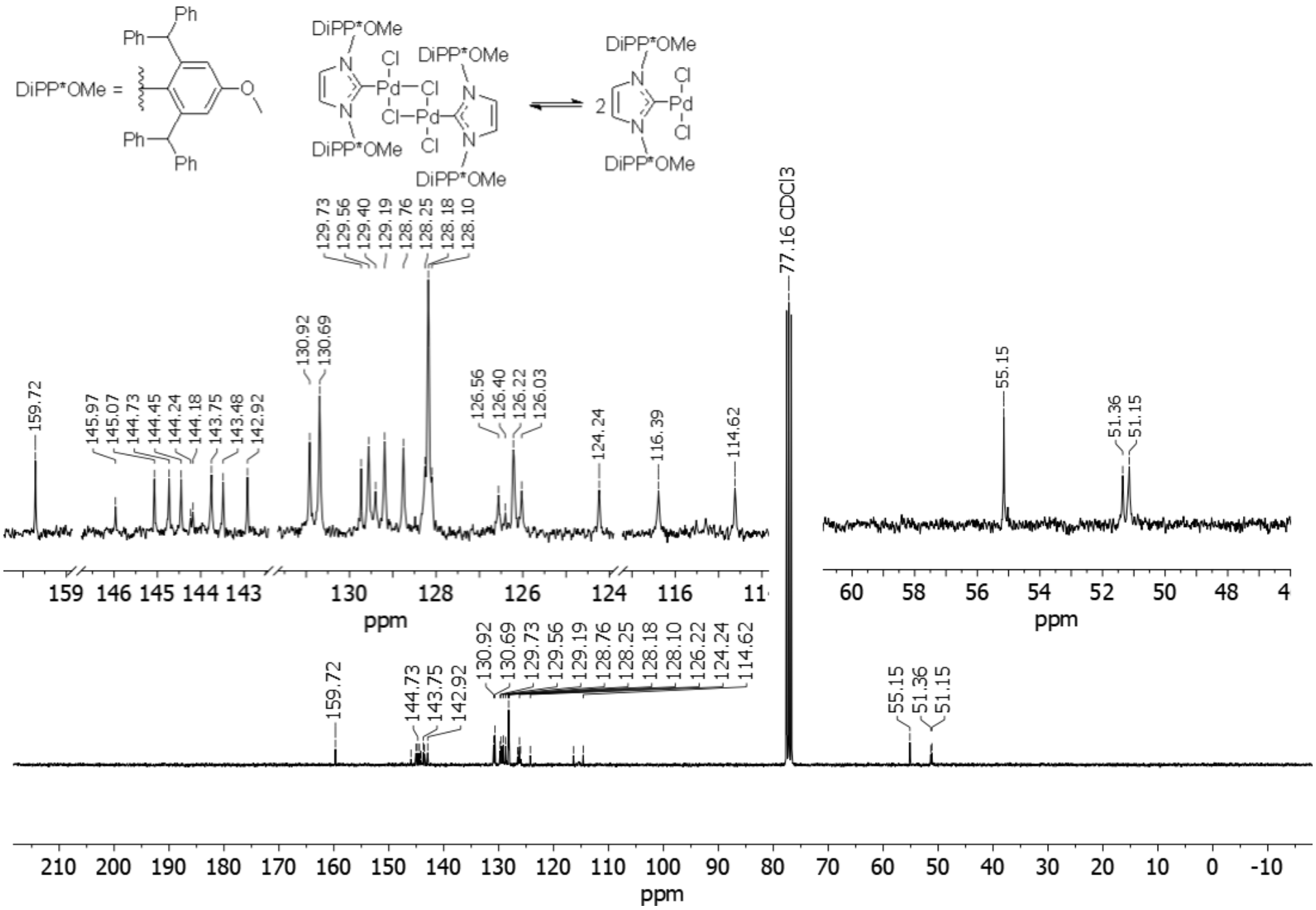

Figure S27. ^{13}C NMR spectrum of compound **1h** ($CDCl_3$, 75 MHz)

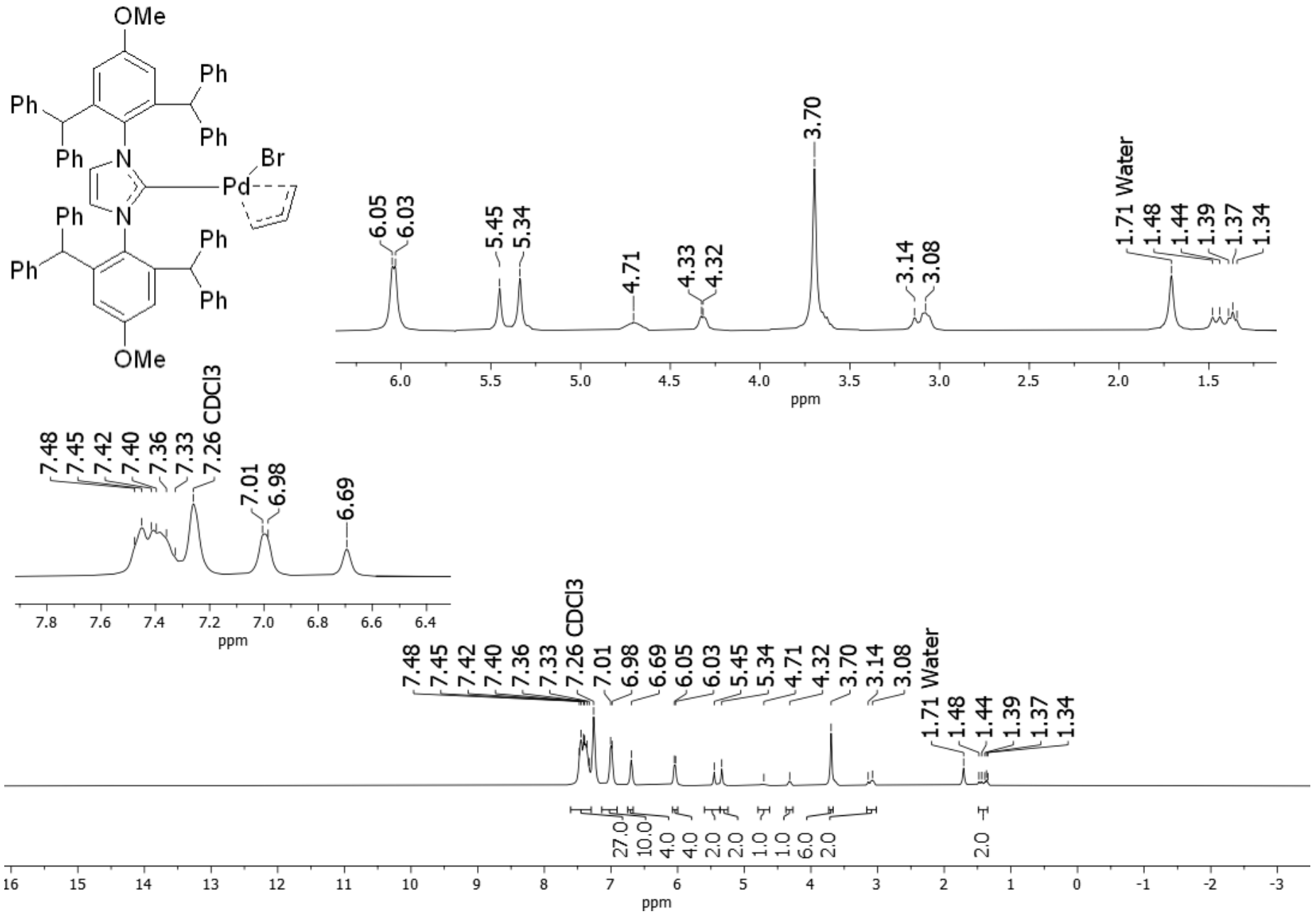

Figure S28. ^{1}H NMR spectrum of compound **1i** ($CDCl_3$, 300 MHz)

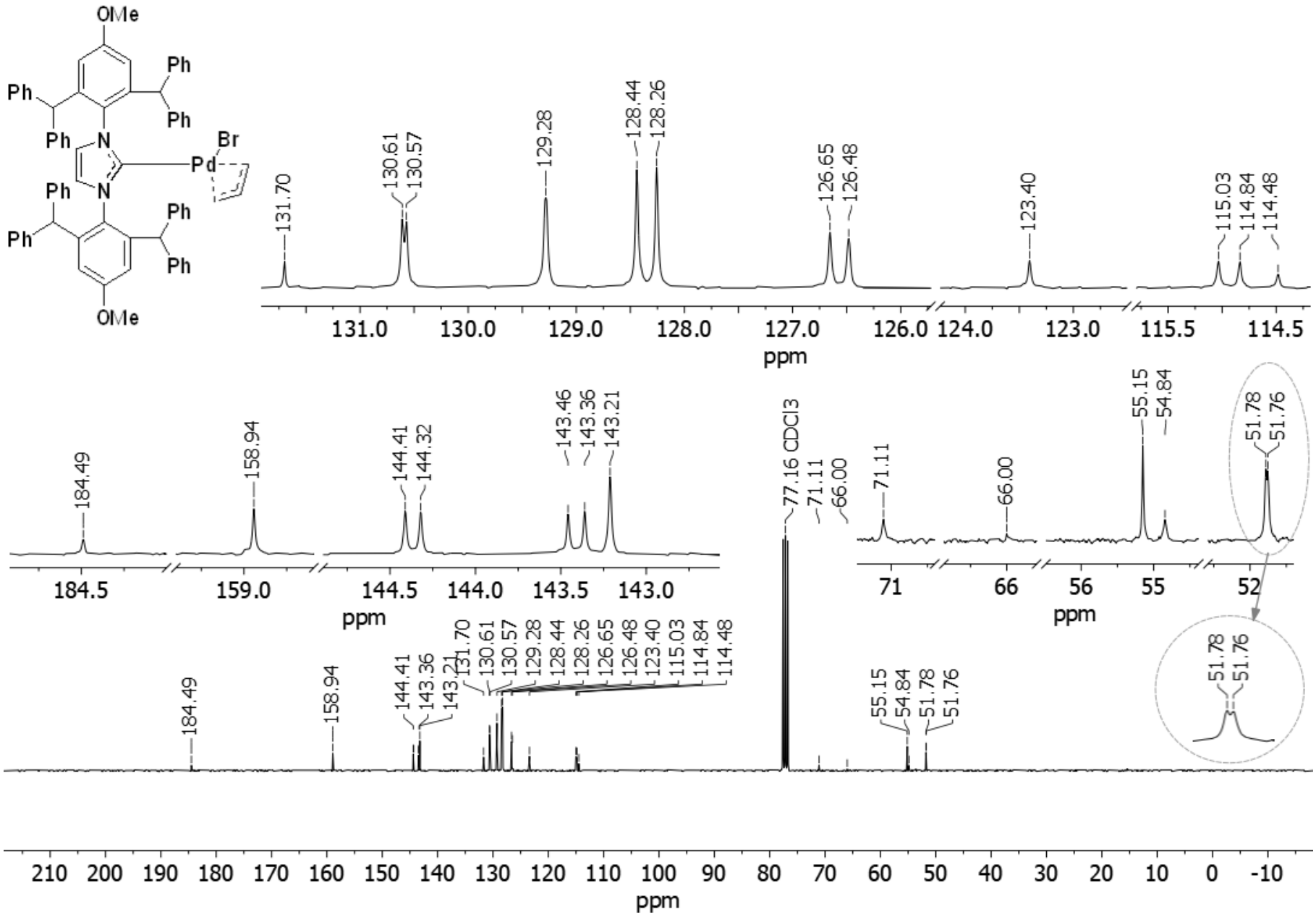

Figure S29. ^{13}C NMR spectrum of compound **1i** ($CDCl_3$, 75 MHz)

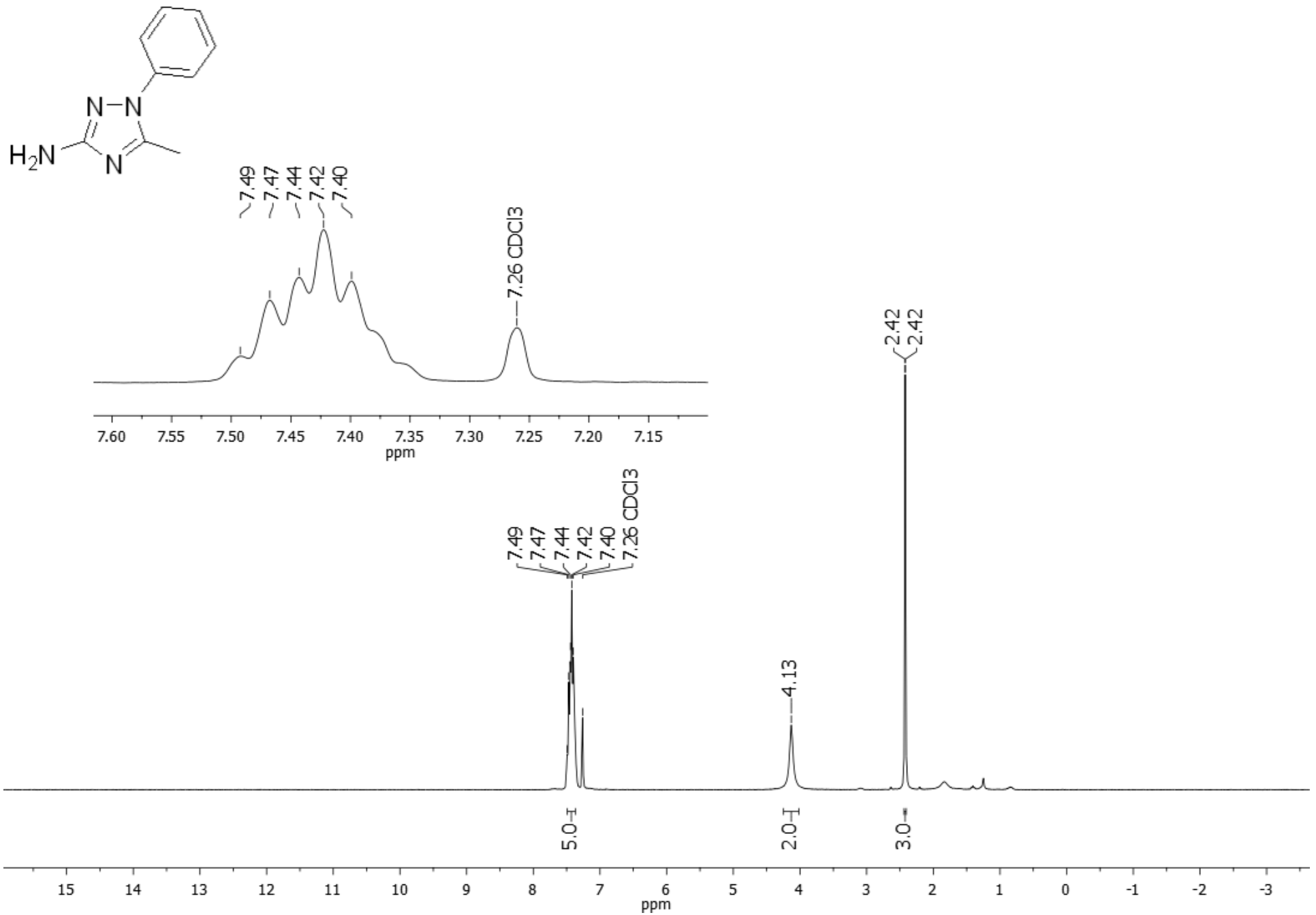

Figure S30. ^{1}H NMR spectrum of compound **2d** ($CDCl_3$, 300 MHz)

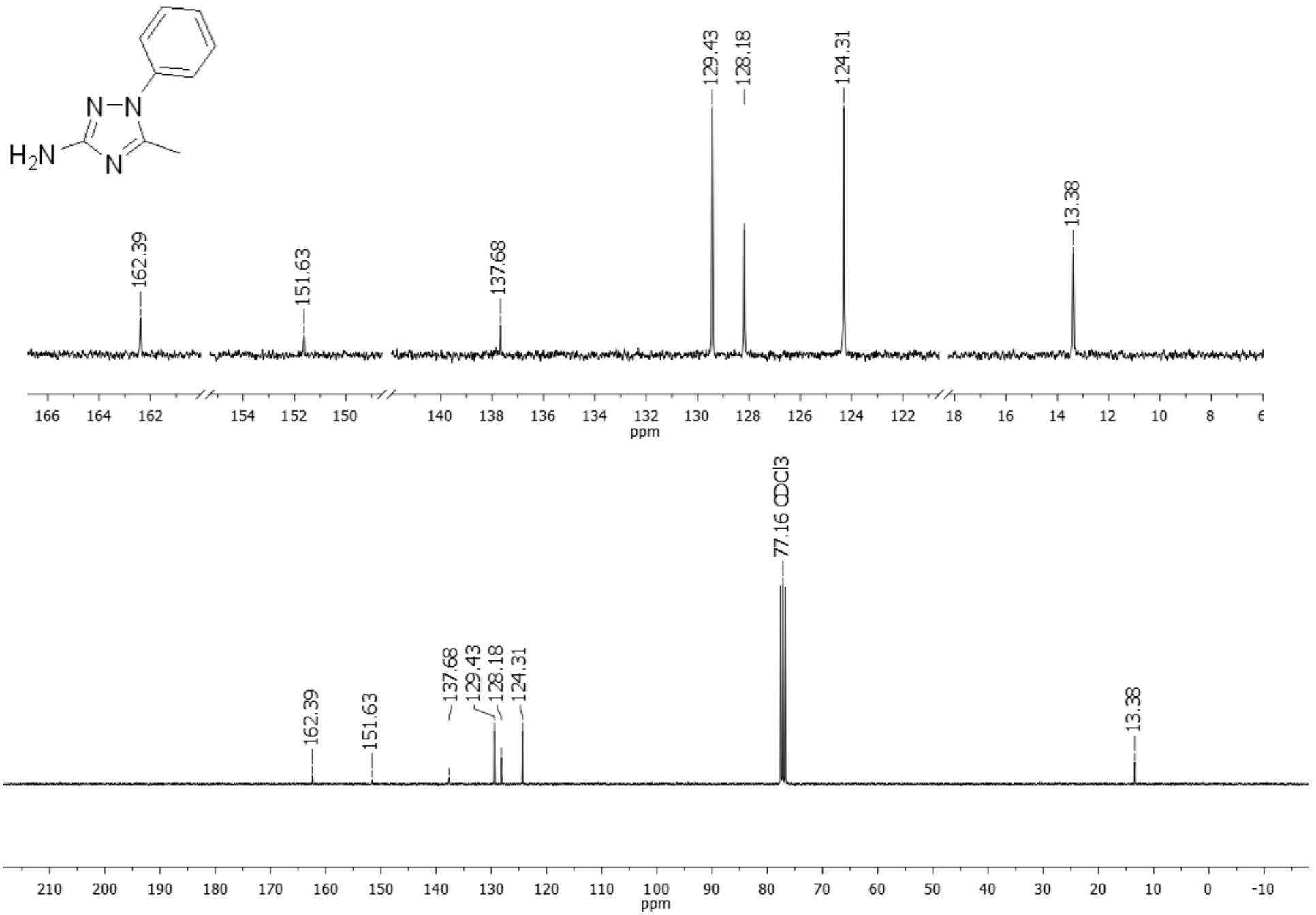

Figure S31. ^{13}C NMR spectrum of compound **2d** ($CDCl_3$, 75 MHz)

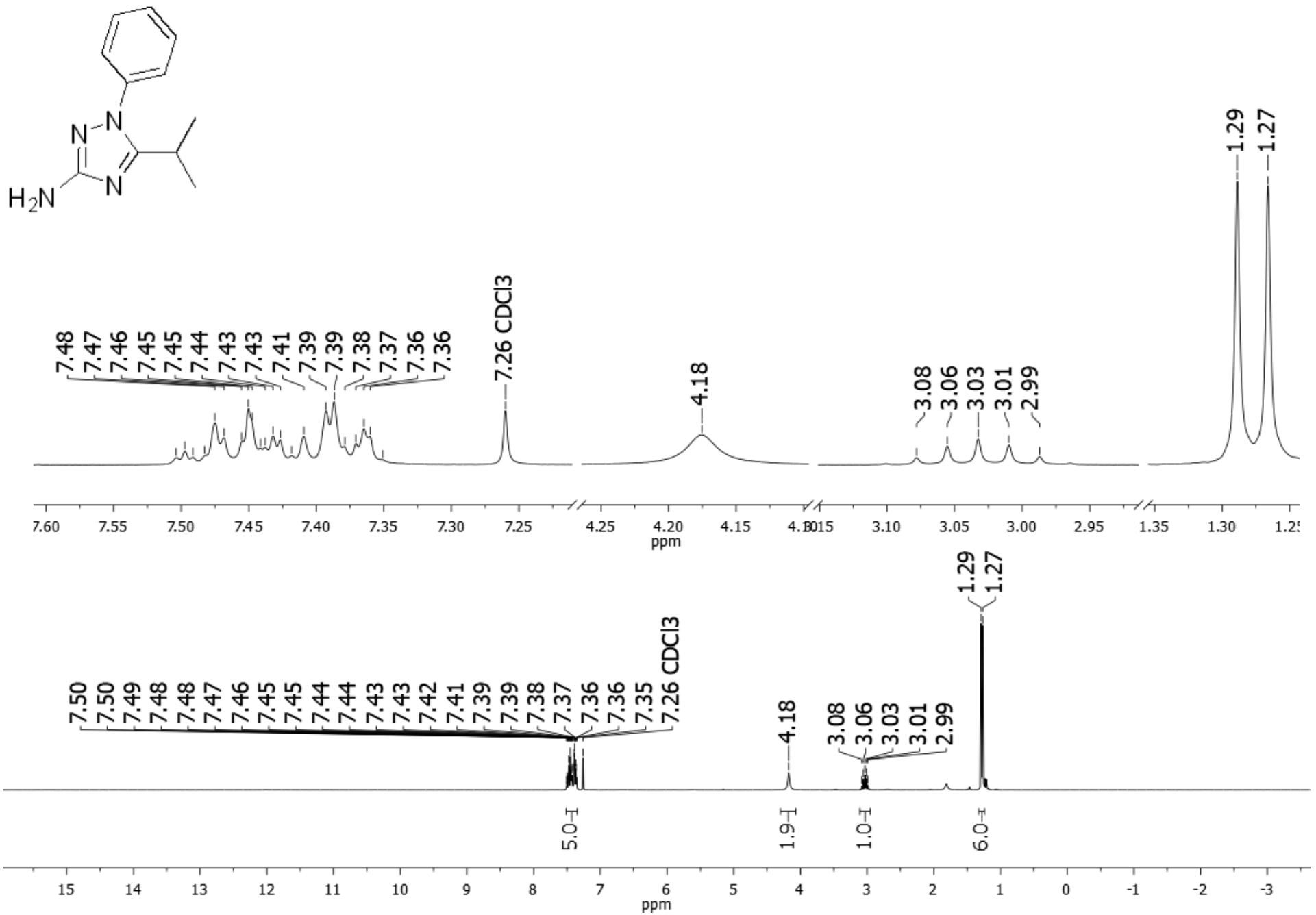

Figure S32. ^{1}H NMR spectrum of compound **2e** ($CDCl_3$, 300 MHz)

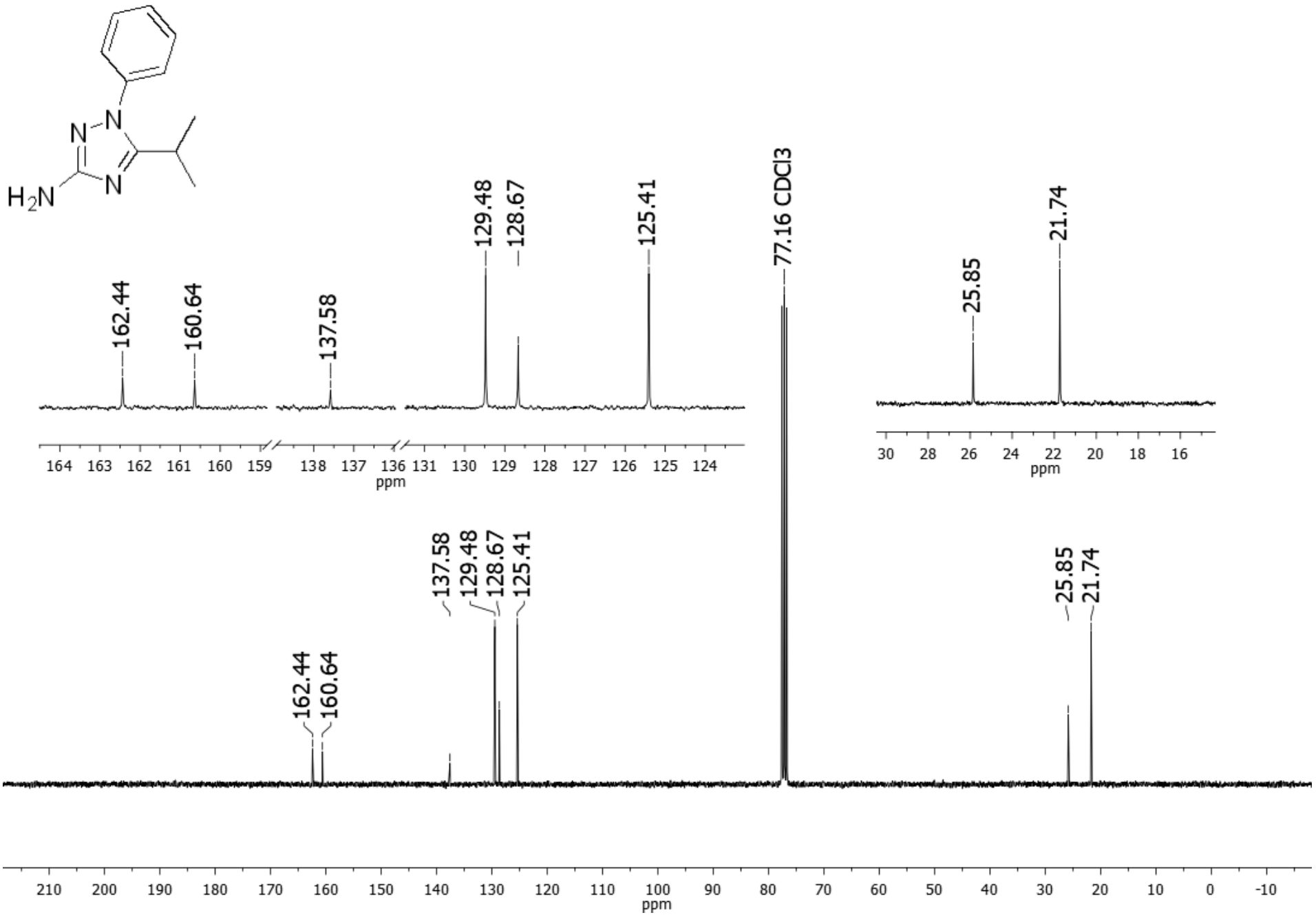

Figure S33. ^{13}C NMR spectrum of compound **2e** ($CDCl_3$, 75 MHz)

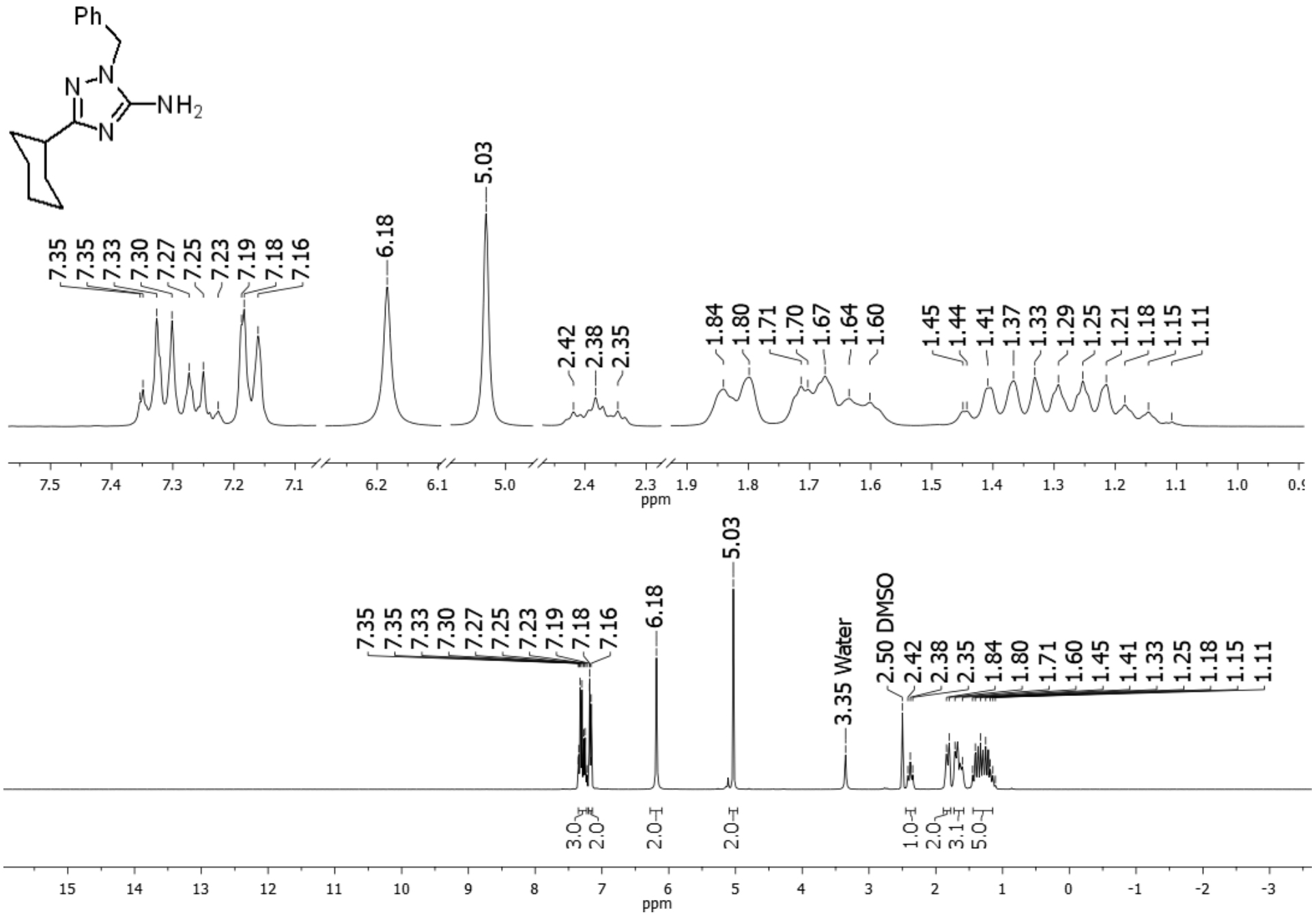

Figure S34. ^{1}H NMR spectrum of compound **6a** (DMSO-d_6, 300 MHz)

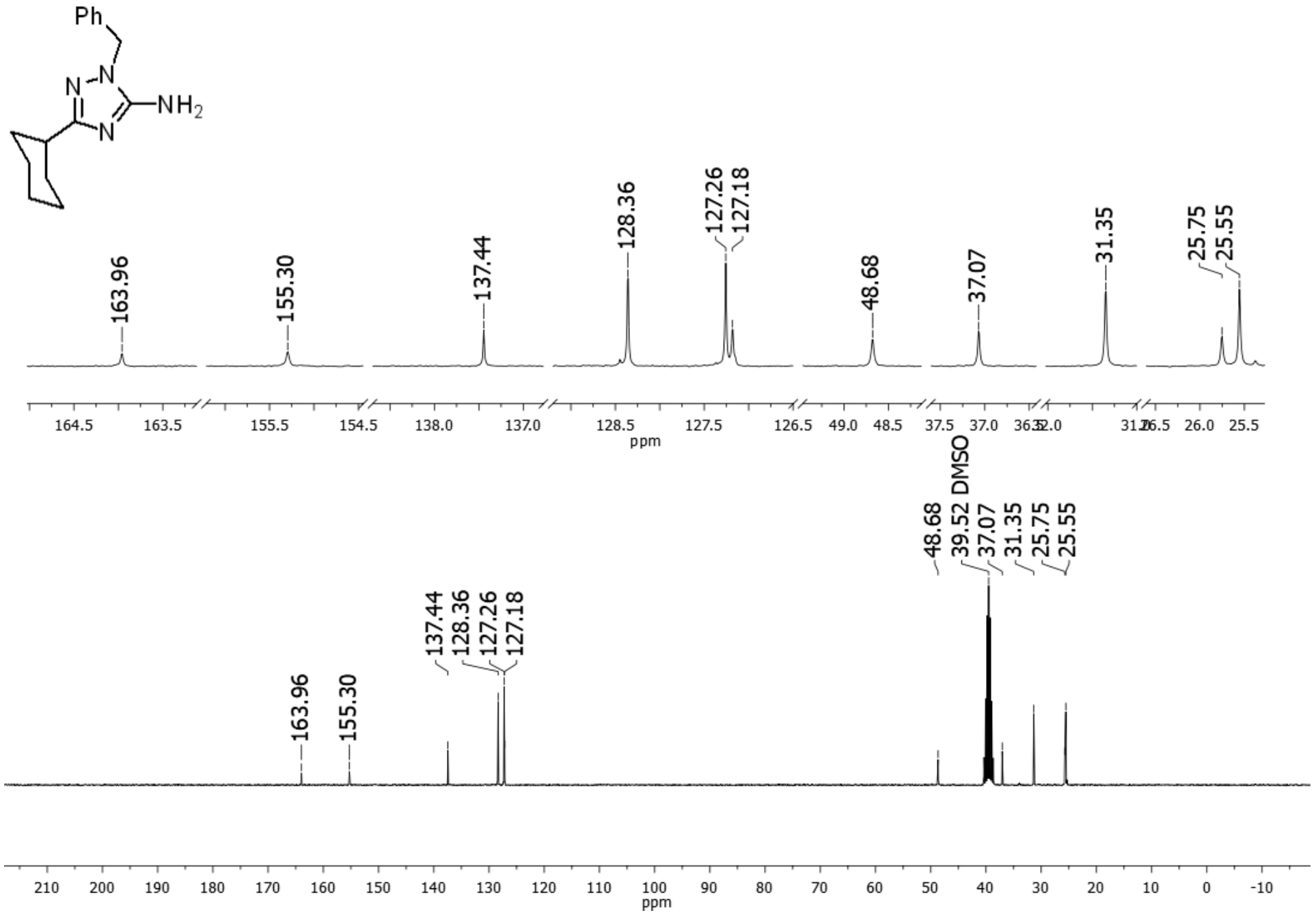

Figure S35. ^{13}C NMR spectrum of compound **6a** (DMSO-d_6, 75 MHz)

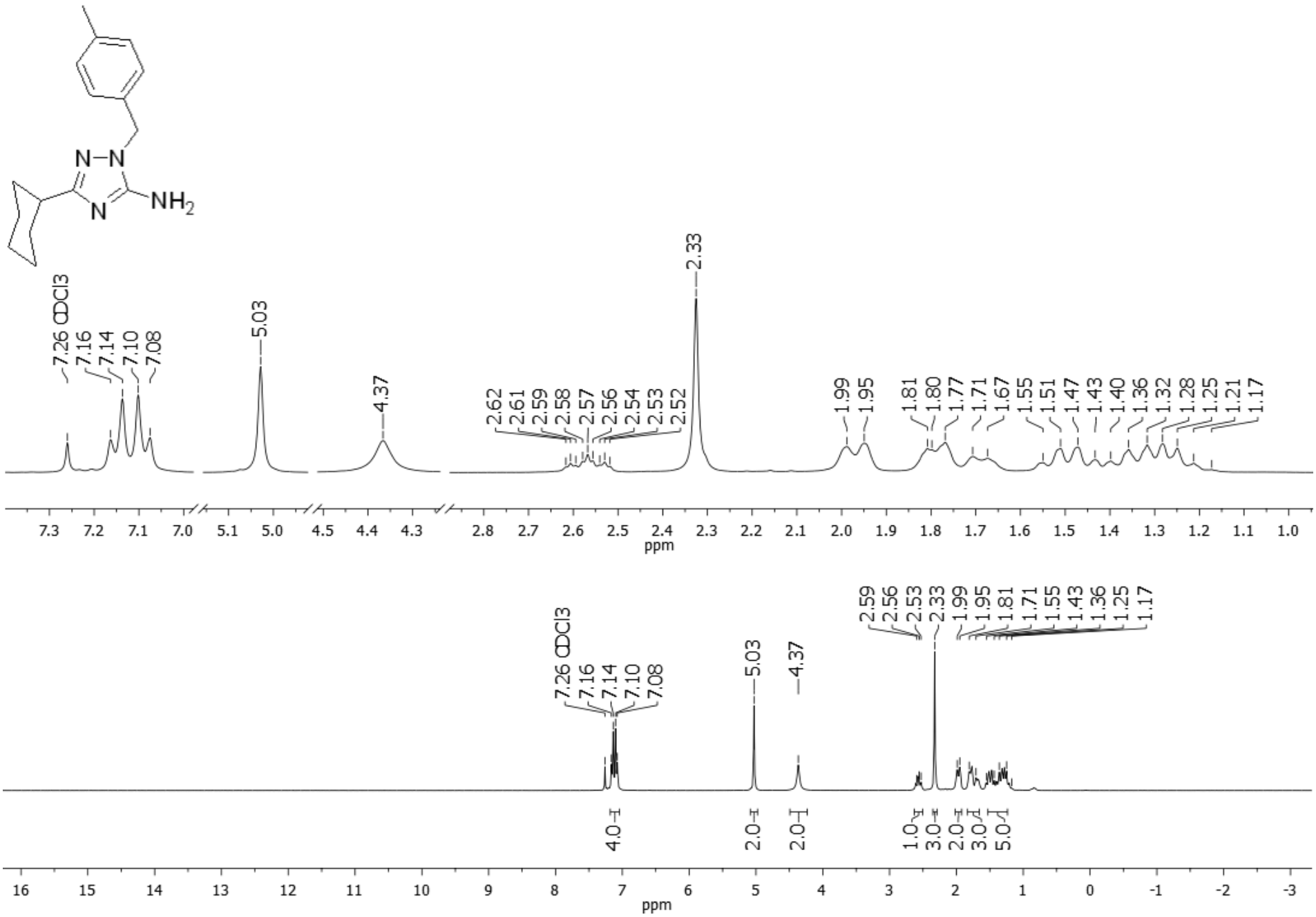

Figure S36. ^{1}H NMR spectrum of compound **6b** ($CDCl_3$, 300 MHz)

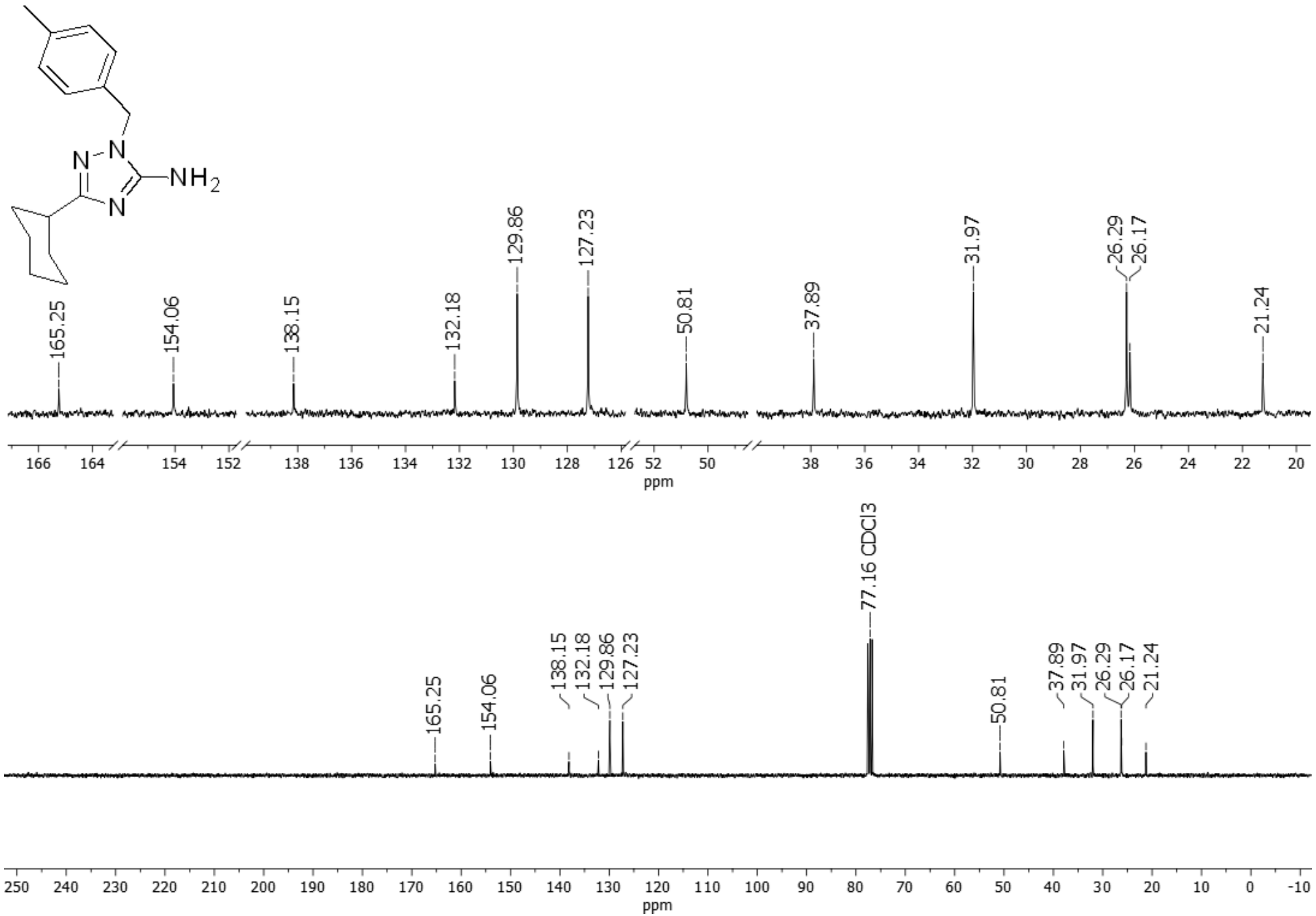

Figure S37. ^{13}C NMR spectrum of compound **6b** ($CDCl_3$, 75 MHz)

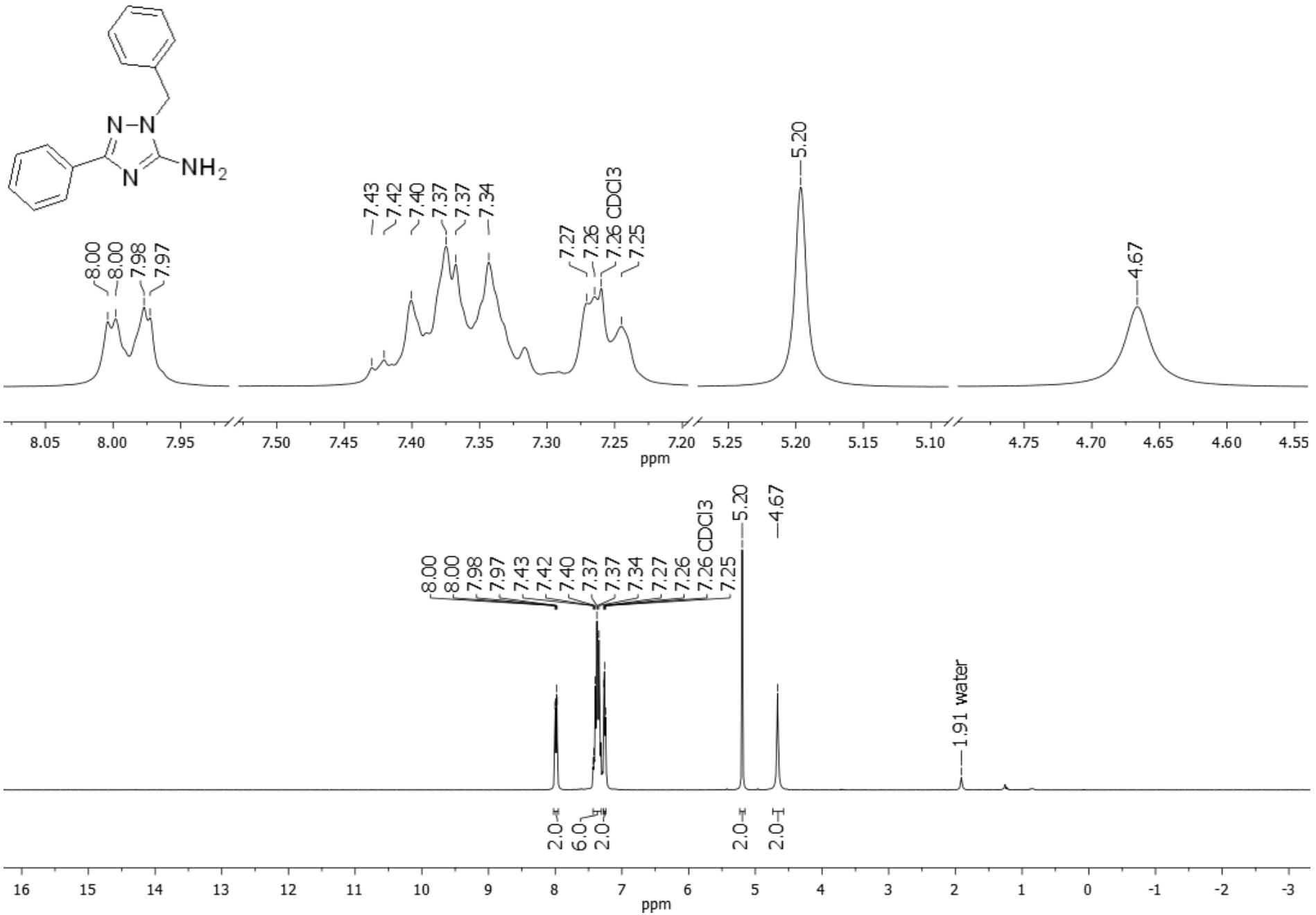

Figure S38. ^{1}H NMR spectrum of compound **6c** ($CDCl_3$, 300 MHz)

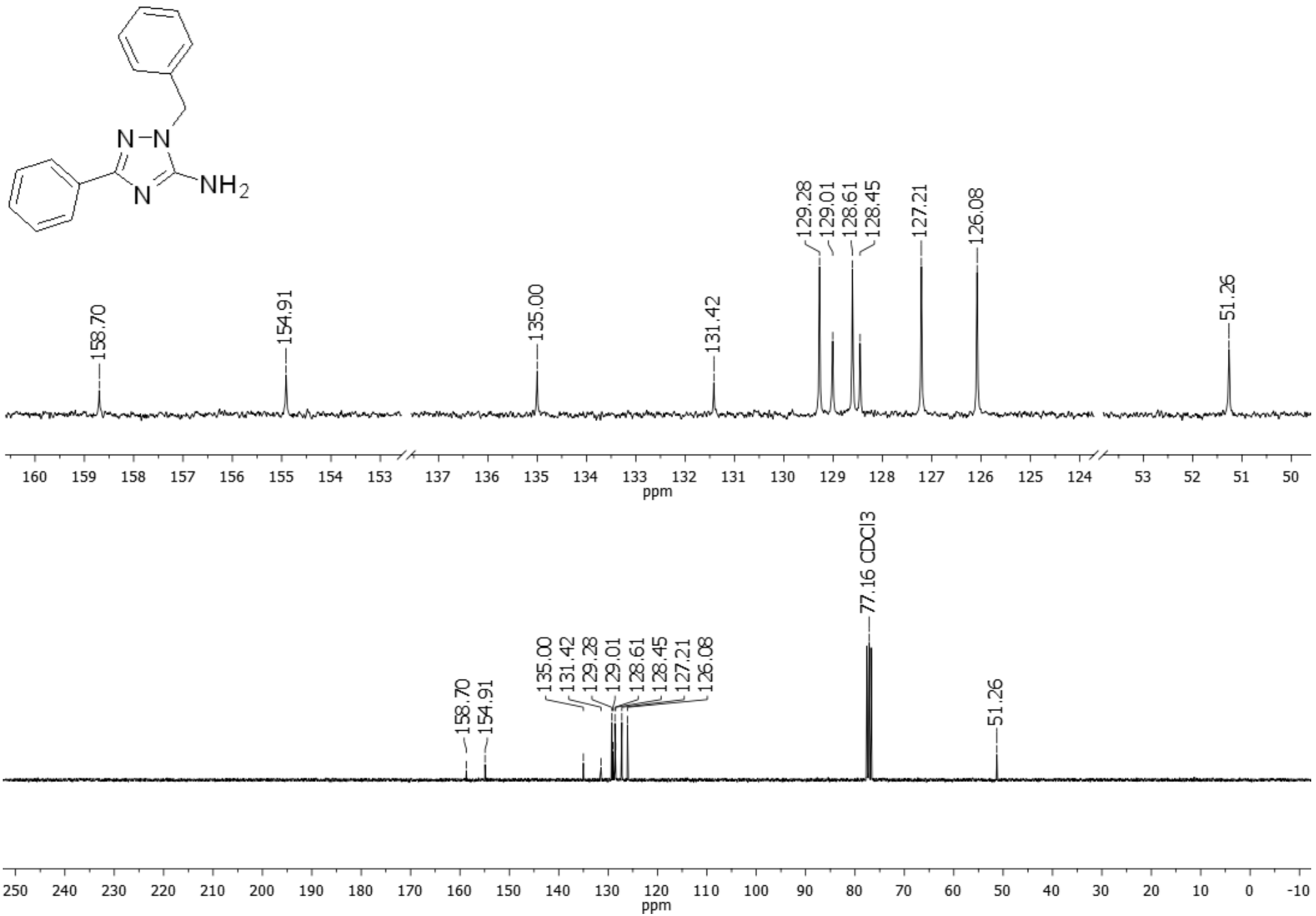

Figure S39. ^{13}C NMR spectrum of compound **6c** ($CDCl_3$, 75 MHz)

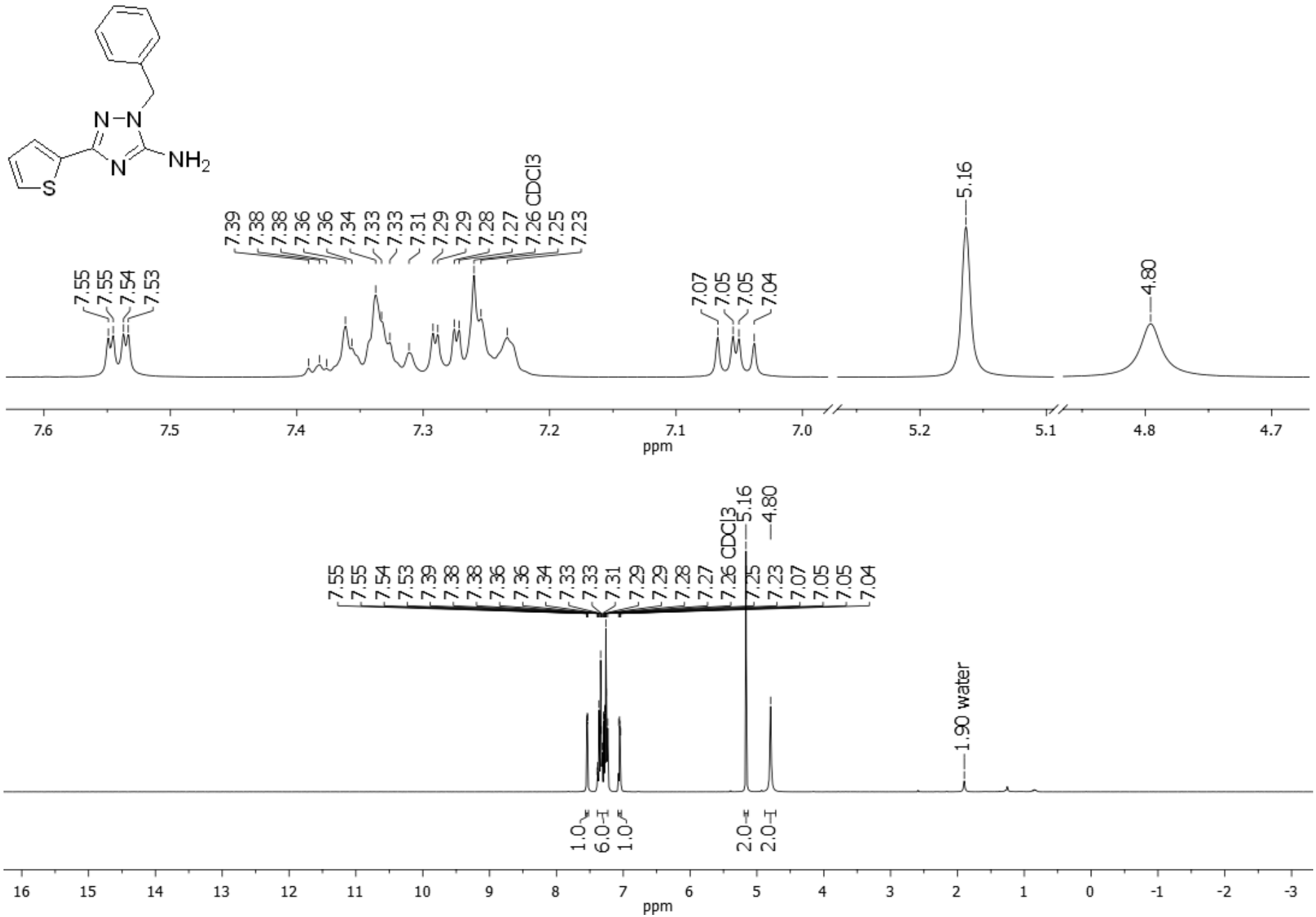

Figure S40. ^{1}H NMR spectrum of compound **6d** ($CDCl_3$, 300 MHz)

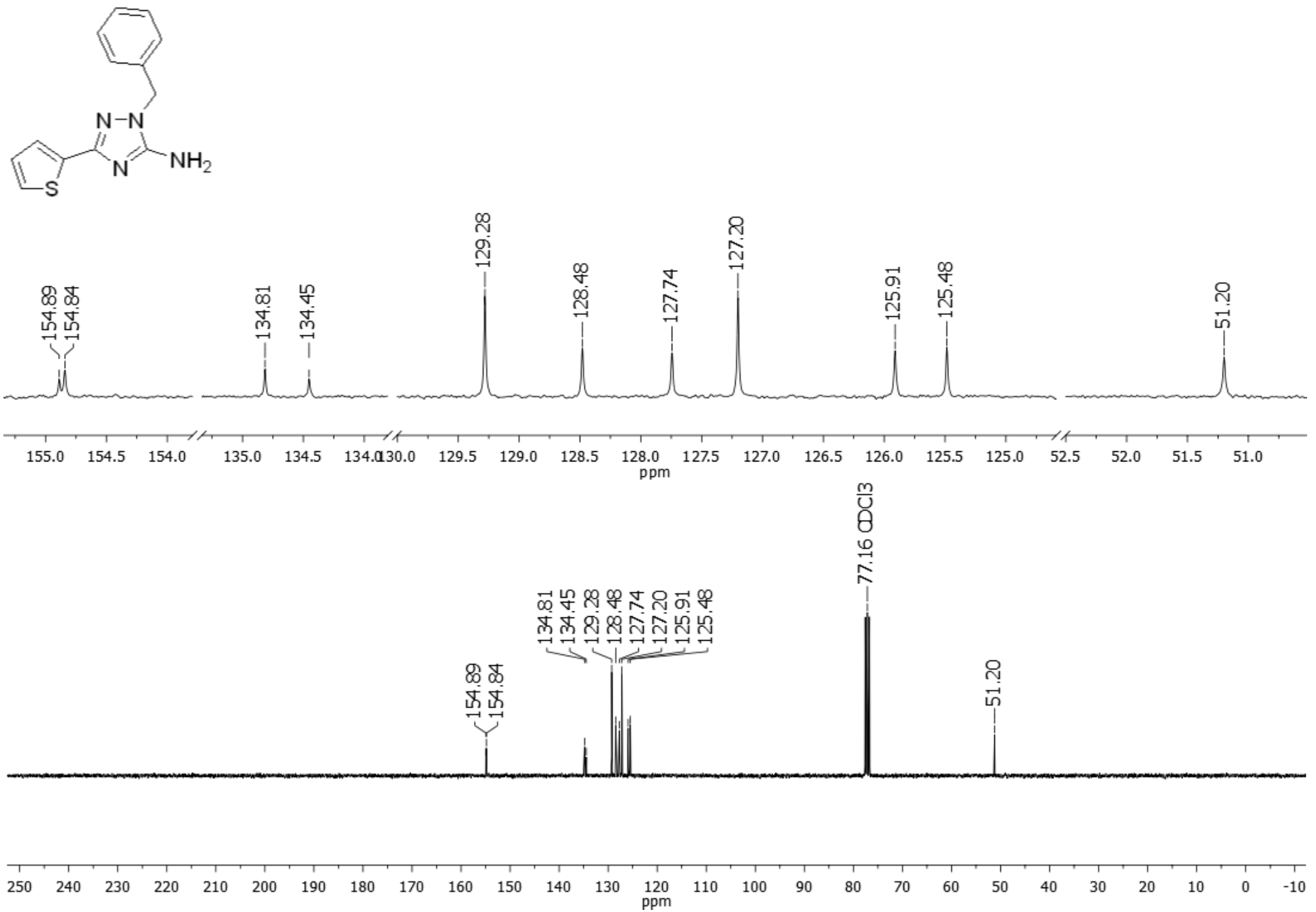

Figure S41. ^{13}C NMR spectrum of compound **6d** ($CDCl_3$, 75 MHz)

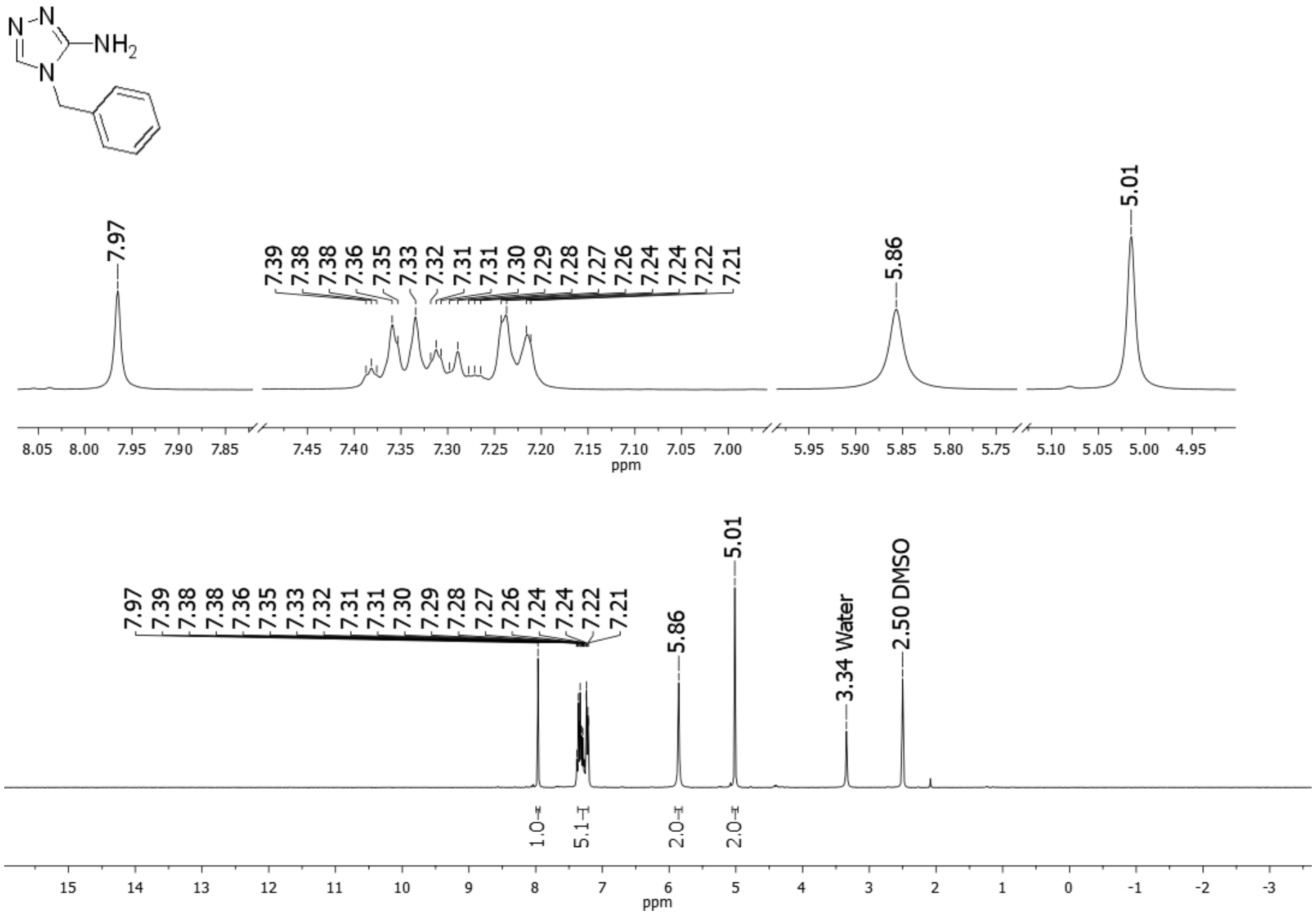

Figure S42. ^{1}H NMR spectrum of compound **7a** (DMSO-d_6, 300 MHz)

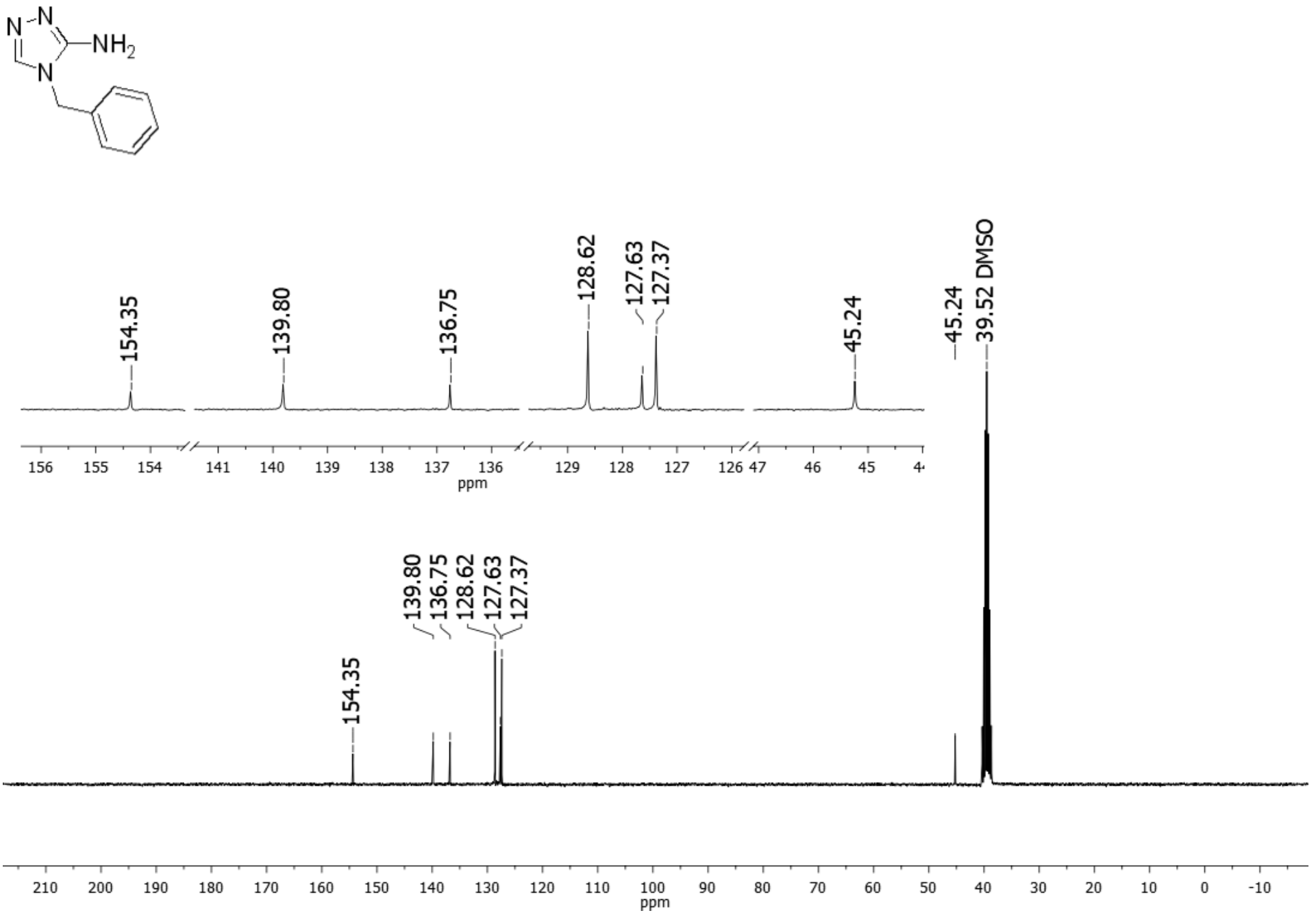

Figure S43. ^{13}C NMR spectrum of compound **7a** (DMSO-d_6, 75 MHz)

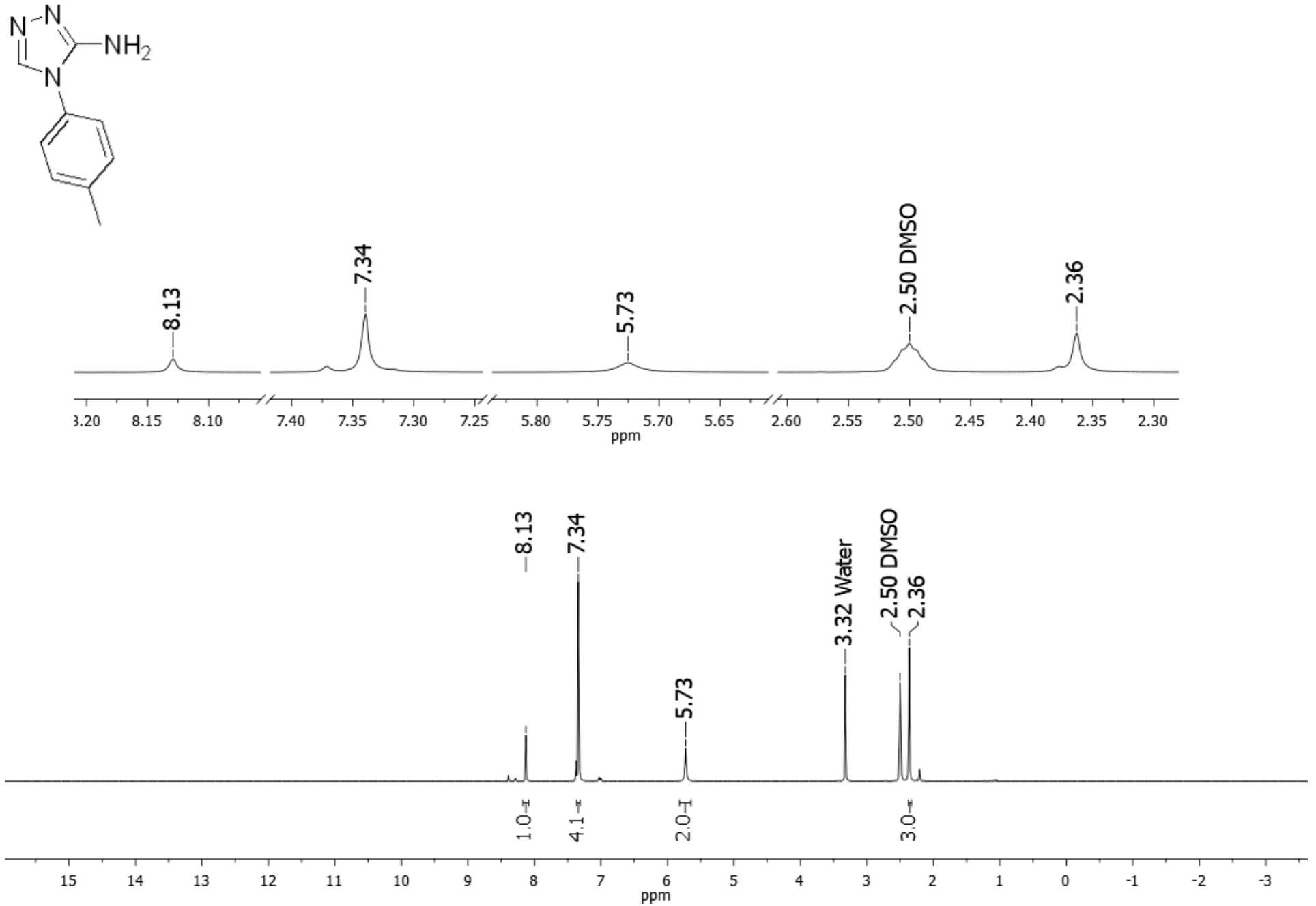

Figure S44. ^{1}H NMR spectrum of compound **7c** (DMSO-d_6, 300 MHz)

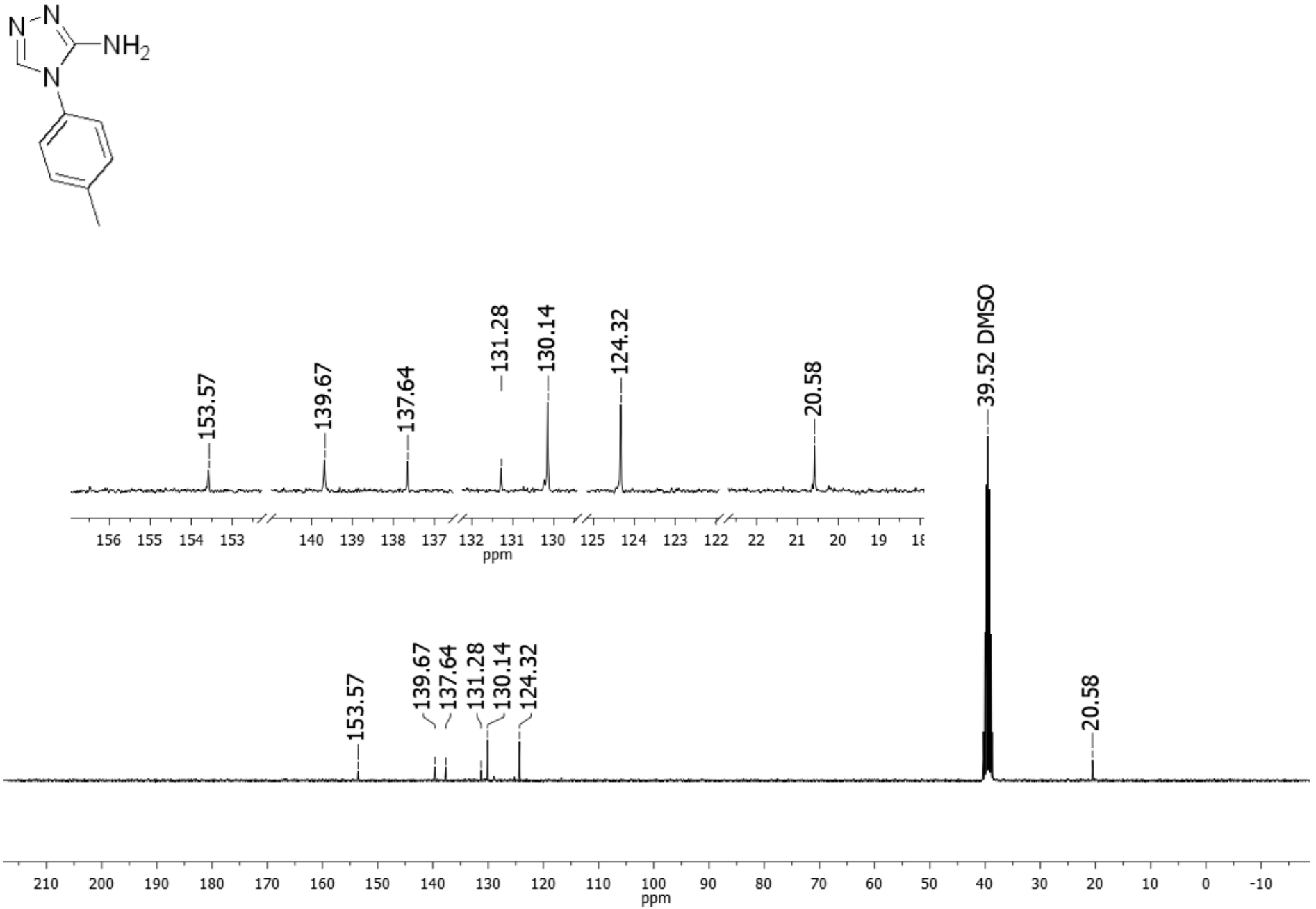

Figure S45. ^{13}C NMR spectrum of compound **7c** (DMSO-d_6, 75 MHz)

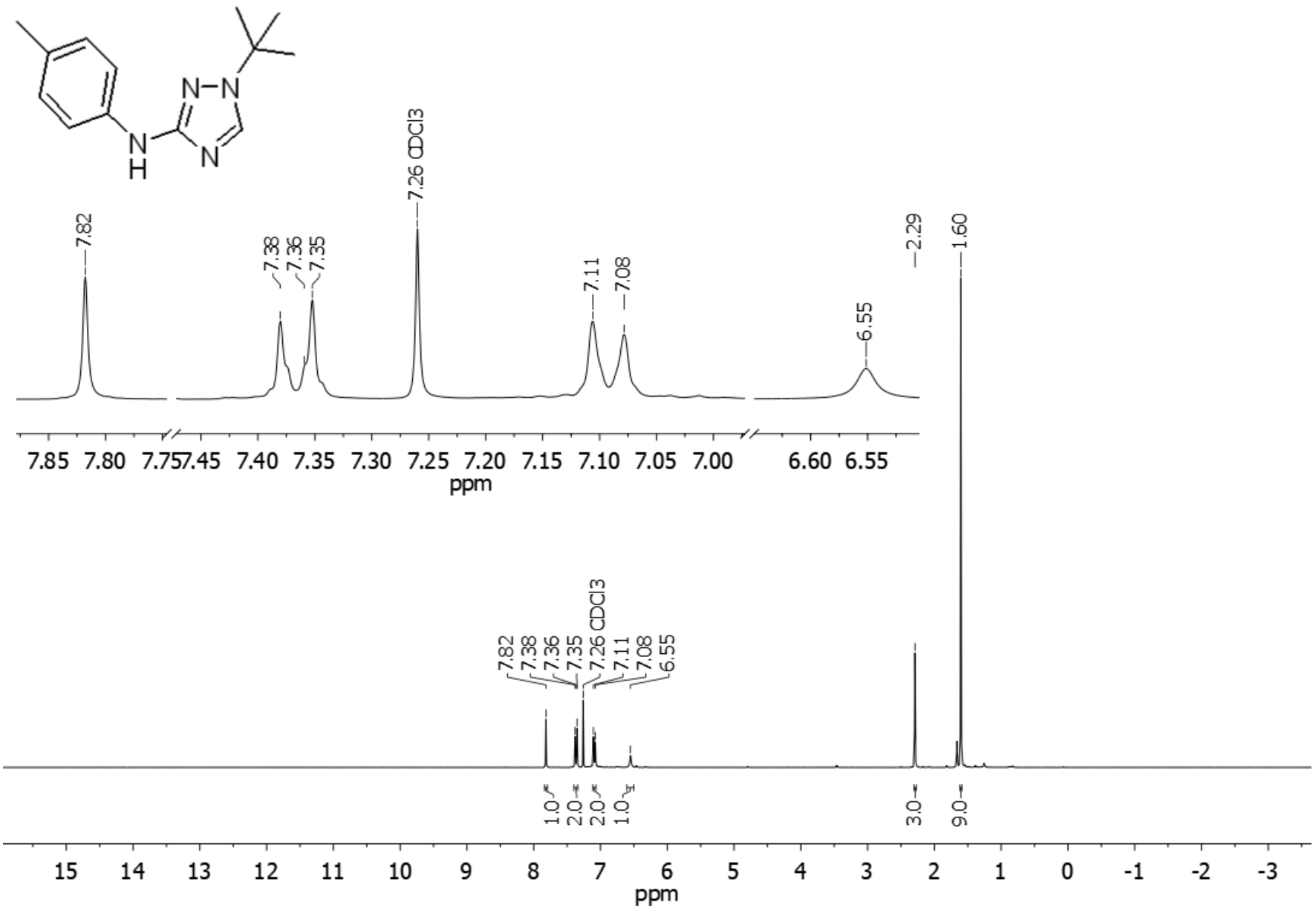

Figure S46. ^{1}H NMR spectrum of compound **4a** ($CDCl_3$, 300 MHz)

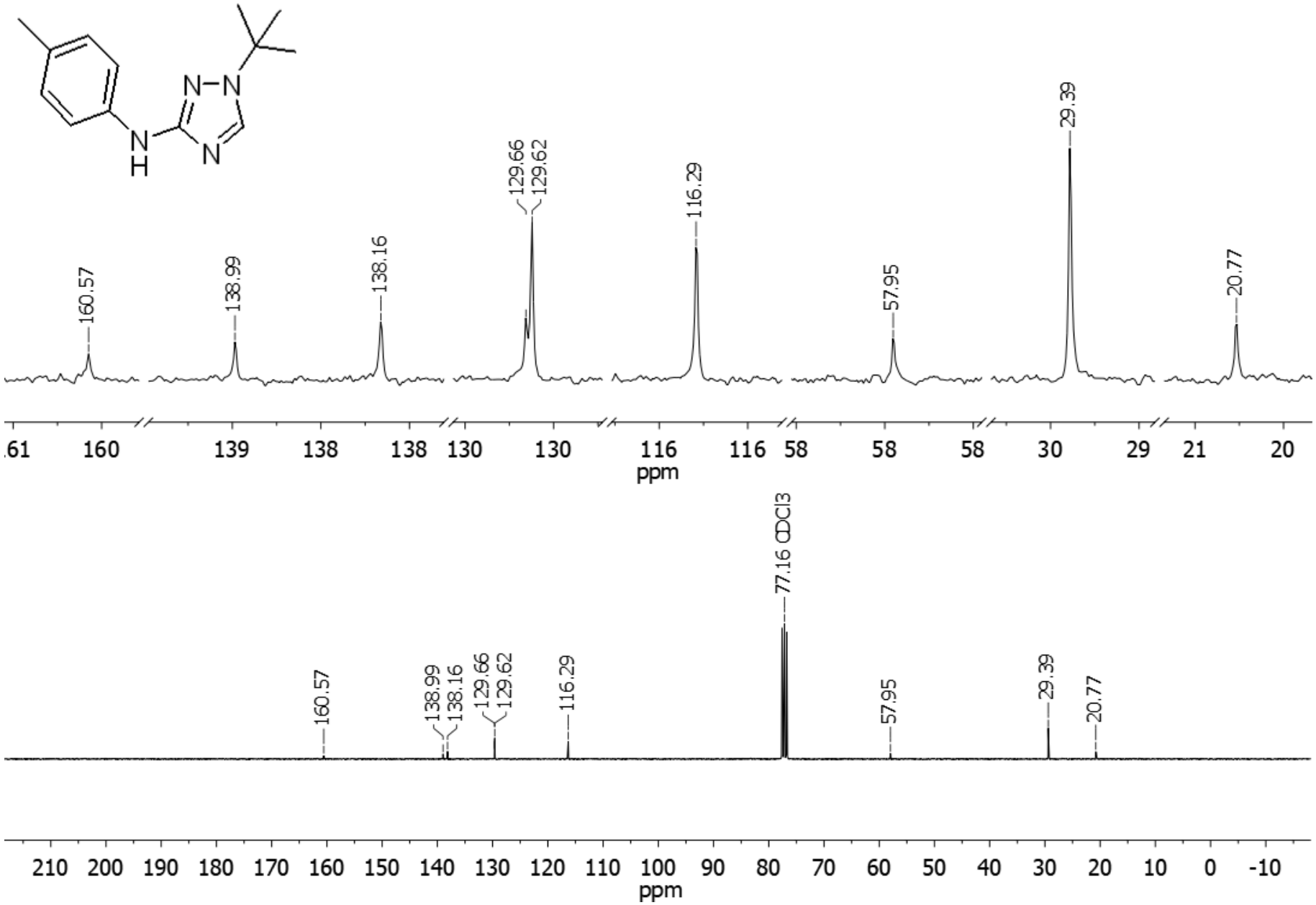

Figure S47. ^{13}C NMR spectrum of compound **4a** ($CDCl_3$, 75 MHz)

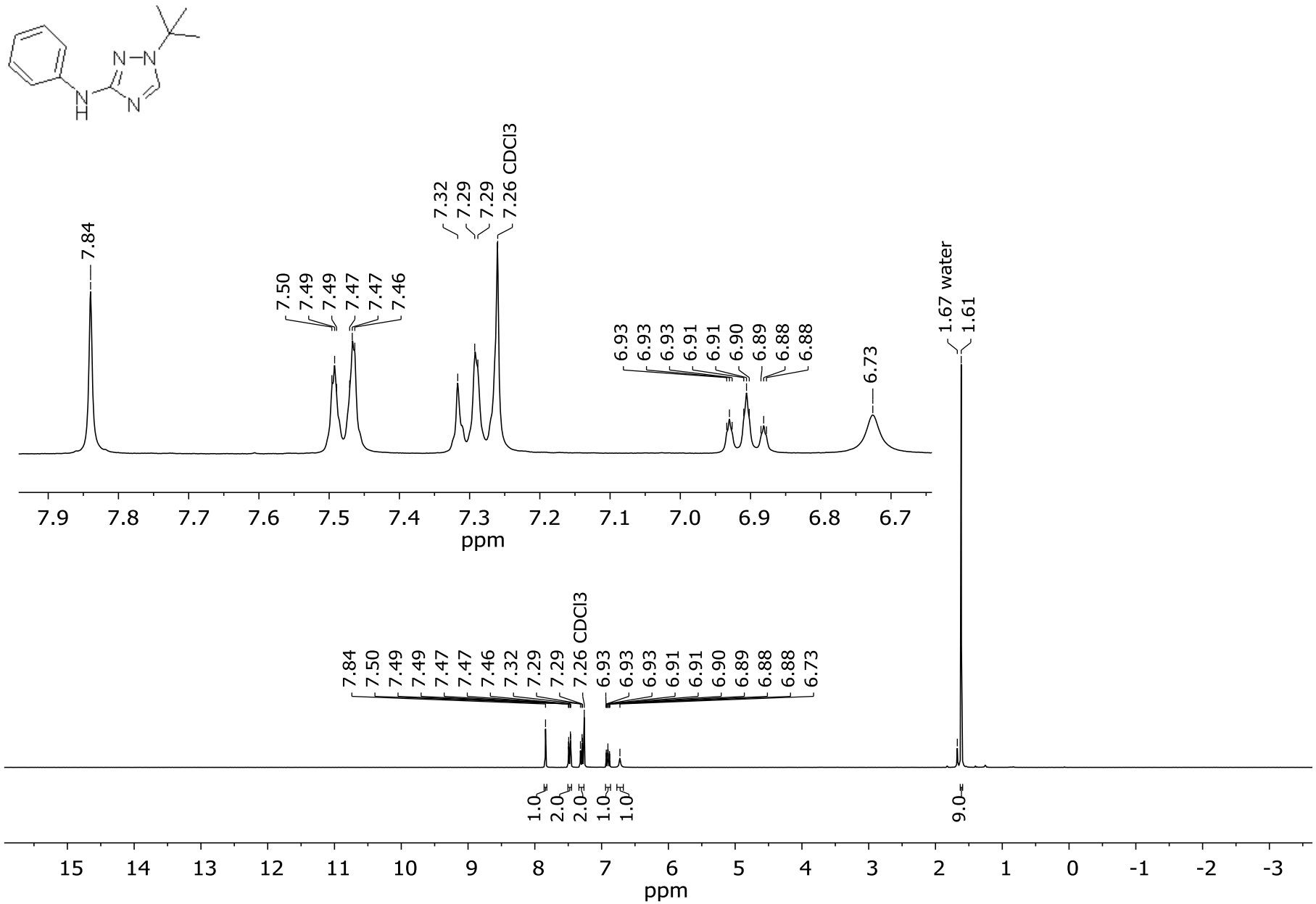

Figure S48. ^{1}H NMR spectrum of compound **4b** ($CDCl_3$, 300 MHz)

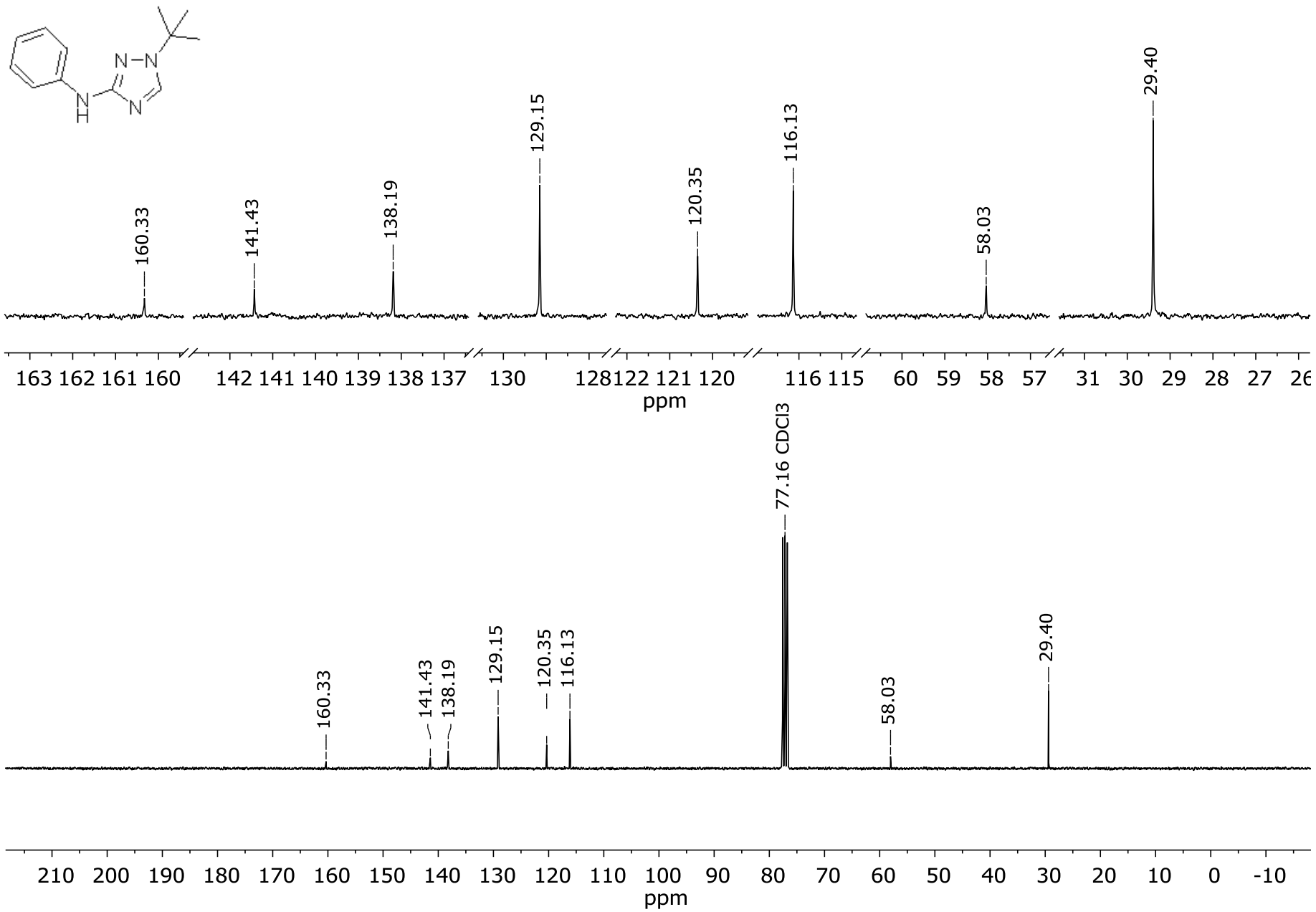

Figure S49. ^{13}C NMR spectrum of compound **4b** ($CDCl_3$, 75 MHz)

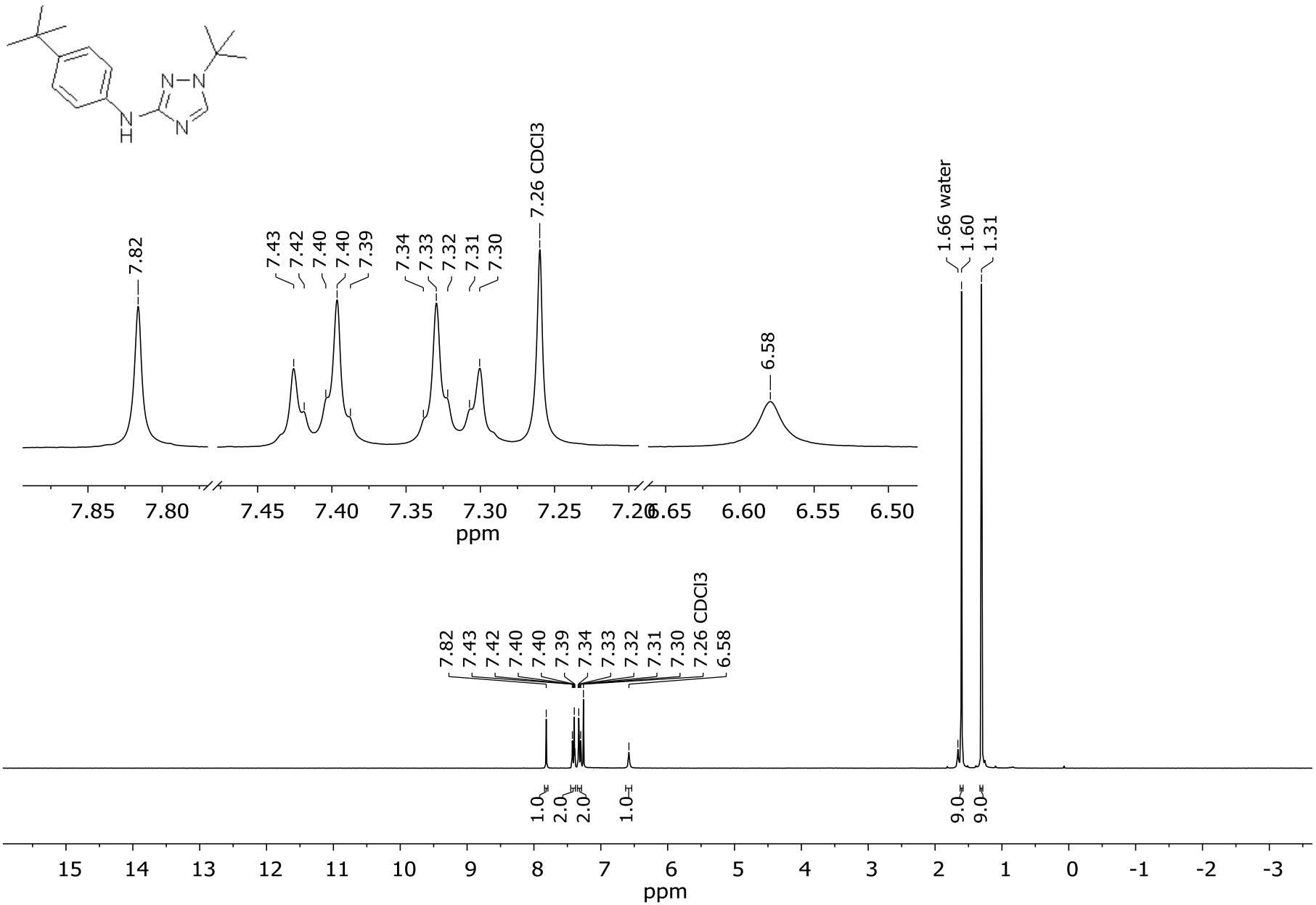

Figure S50. ^{1}H NMR spectrum of compound **4c** ($CDCl_3$, 300 MHz)

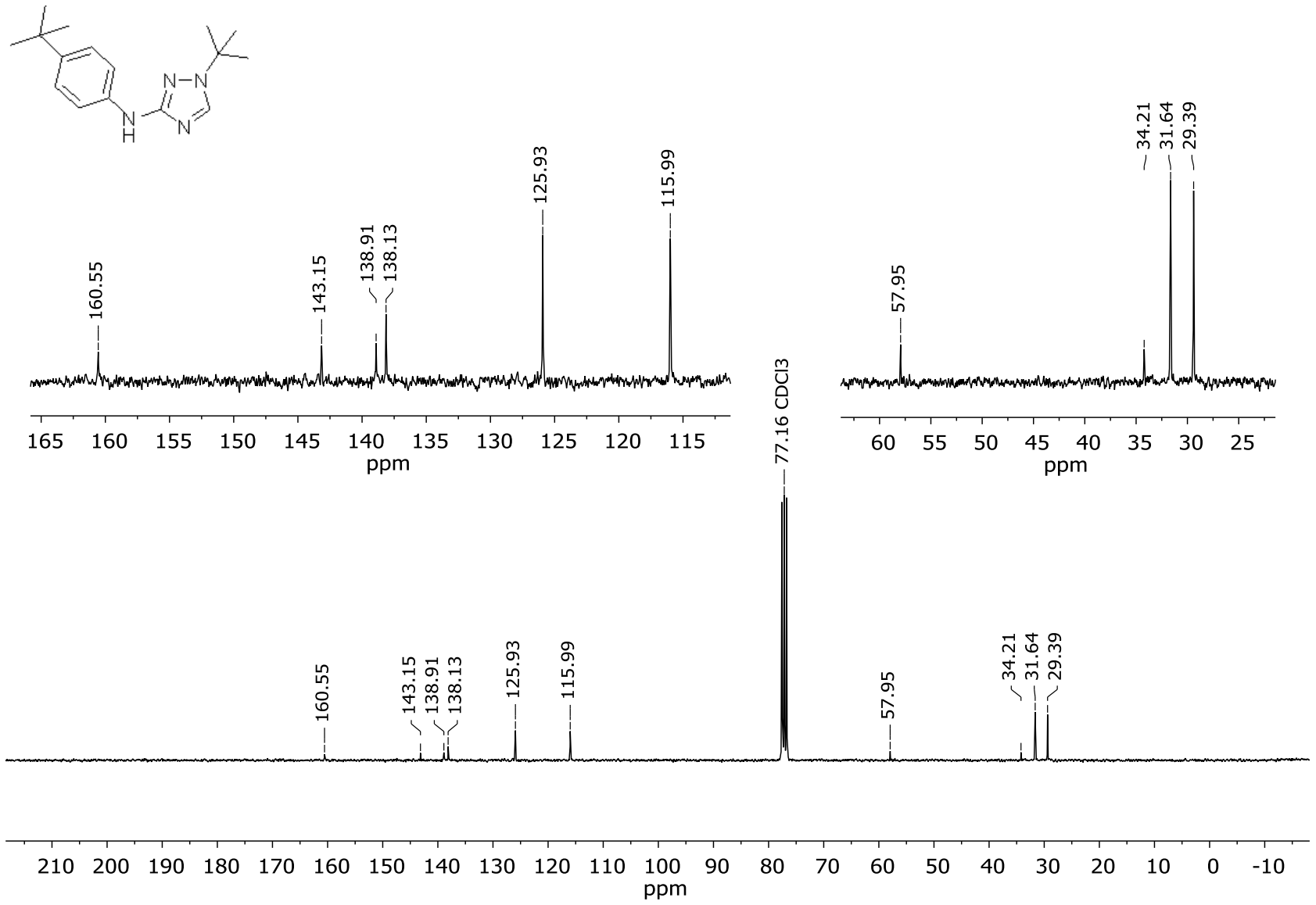

Figure S51. ^{13}C NMR spectrum of compound **4c** ($CDCl_3$, 75 MHz)

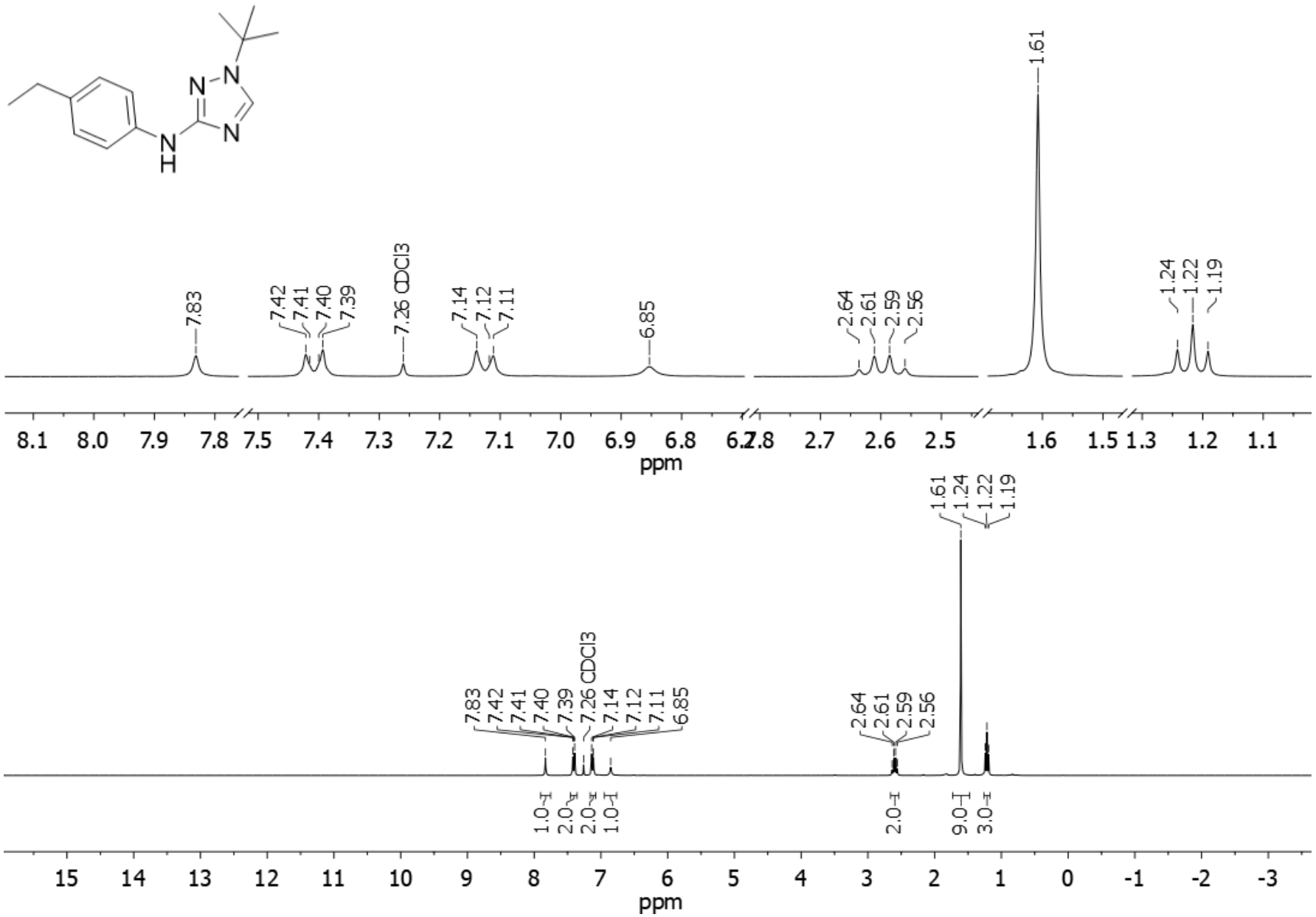

Figure S52. ^{1}H NMR spectrum of compound **4d** ($CDCl_3$, 300 MHz)

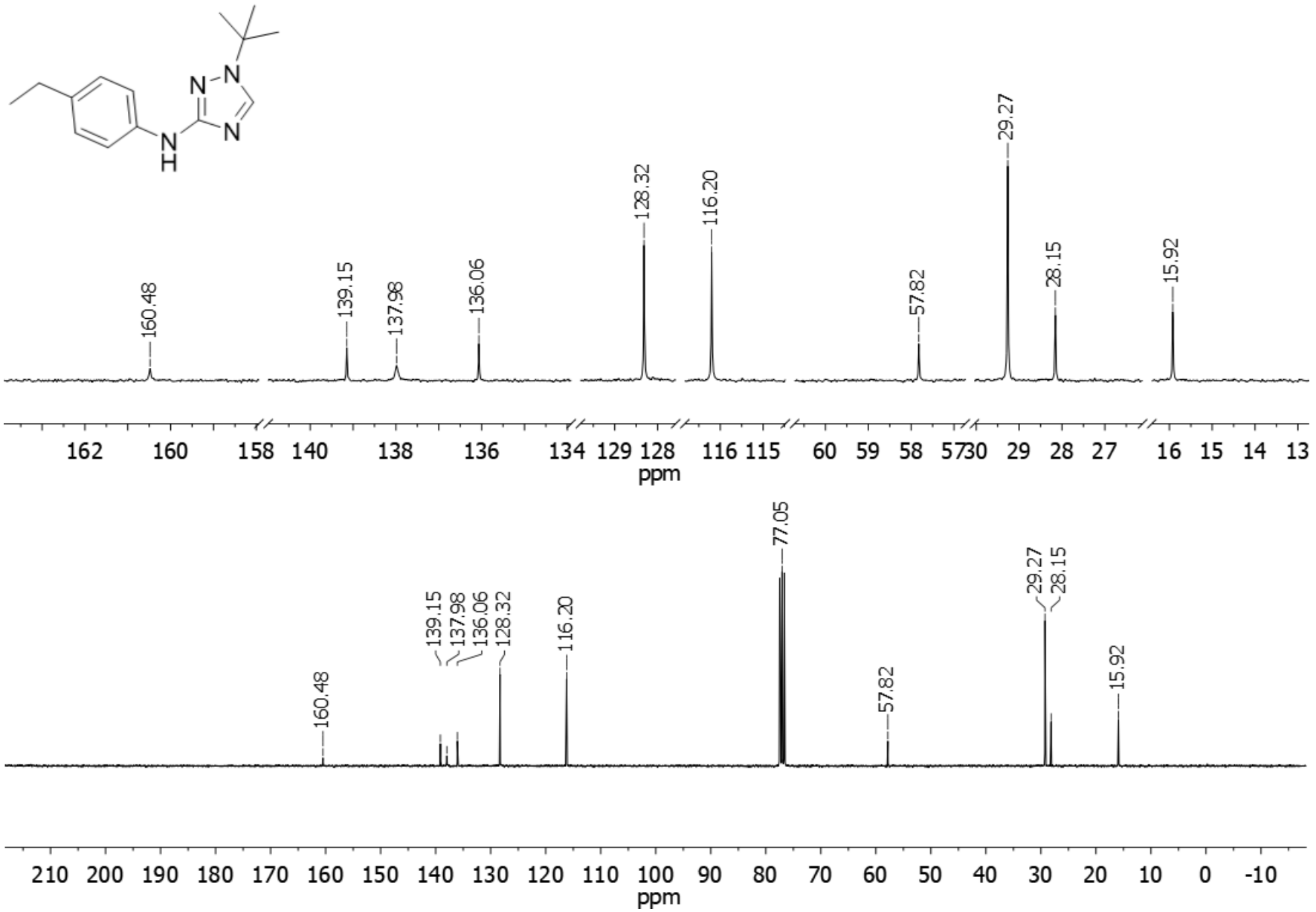

Figure S53. ^{13}C NMR spectrum of compound **4d** ($CDCl_3$, 75 MHz)

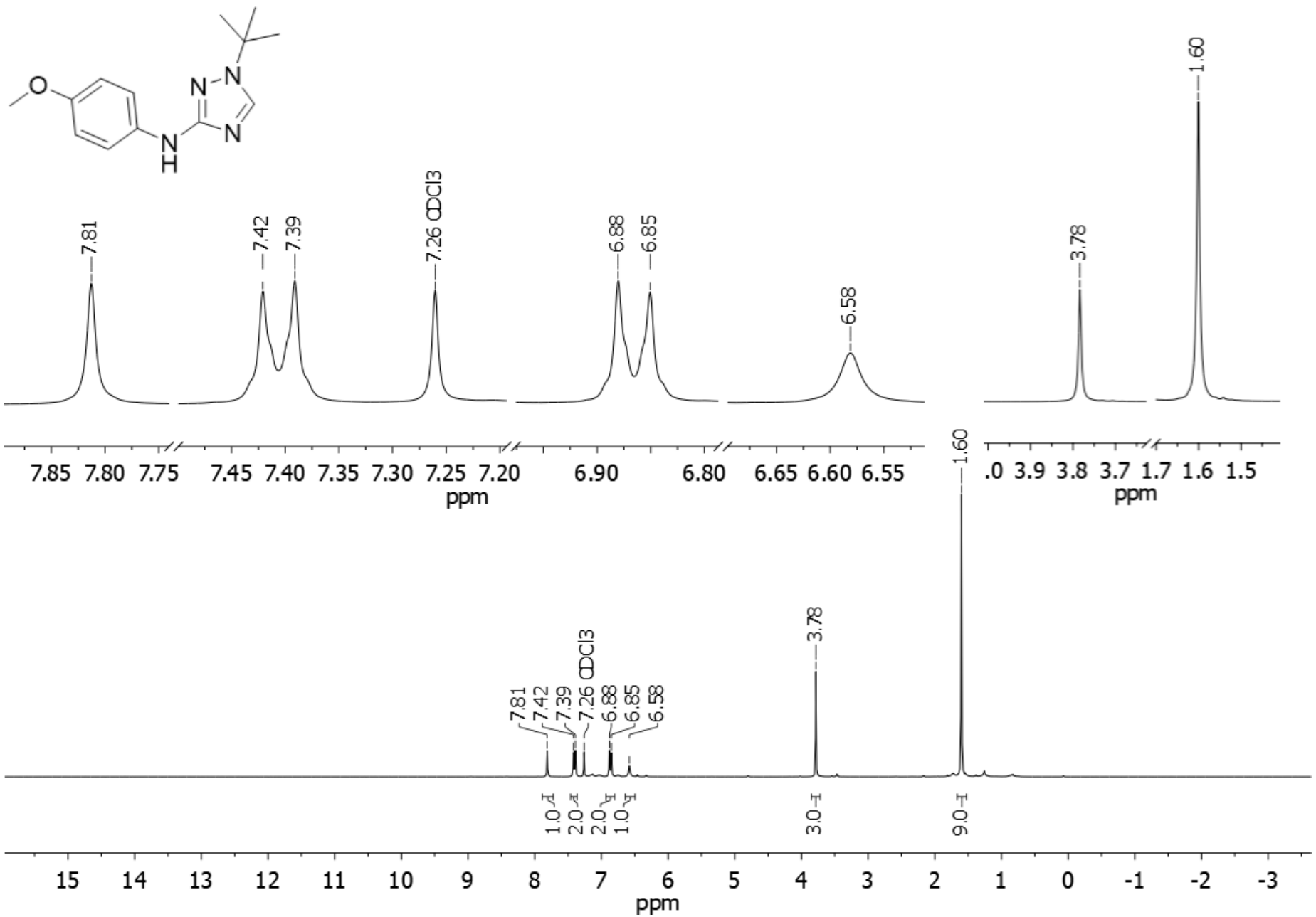

Figure S54. ^{1}H NMR spectrum of compound **4e** ($CDCl_3$, 300 MHz)

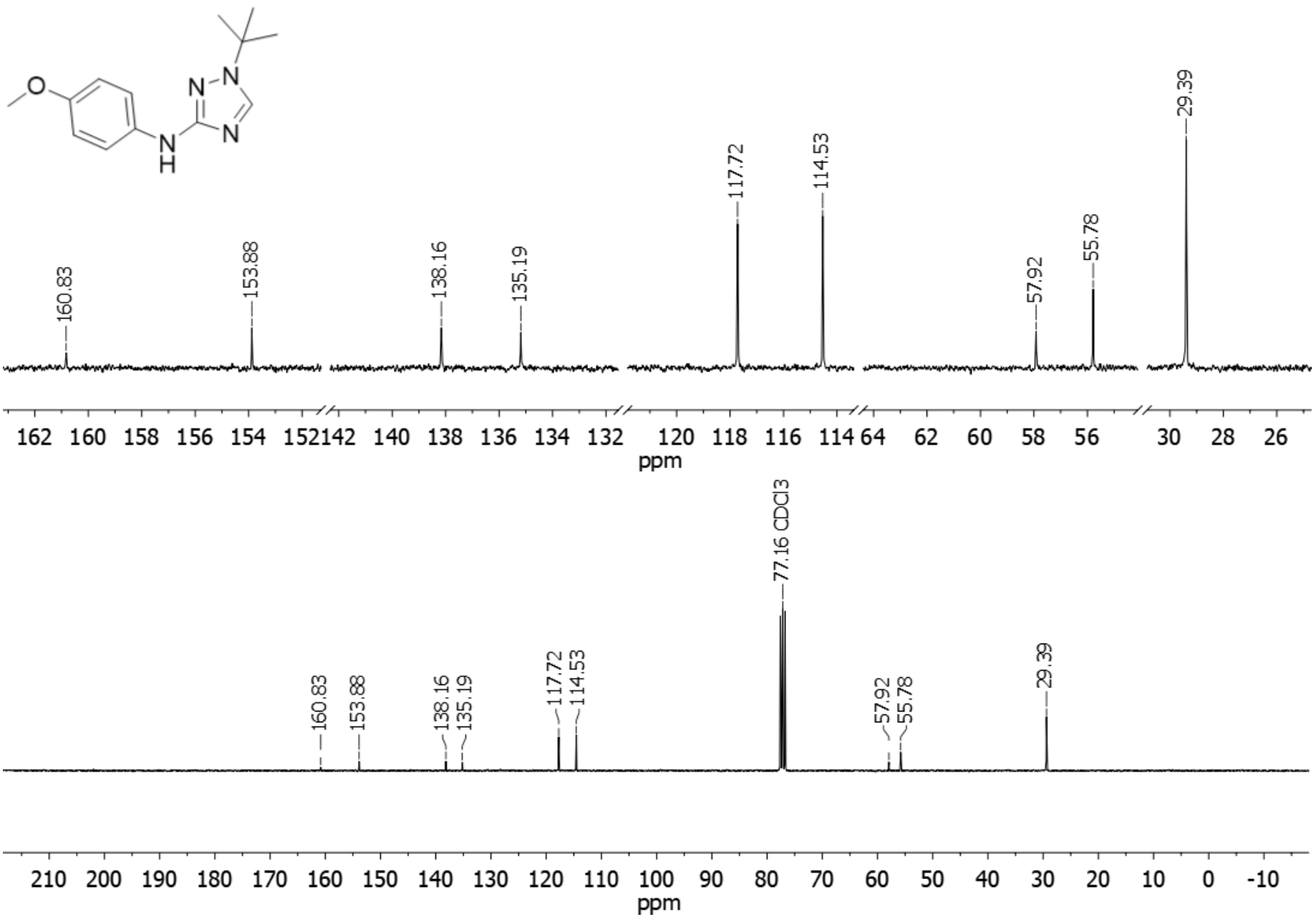

Figure S55. ^{13}C NMR spectrum of compound **4e** ($CDCl_3$, 75 MHz)

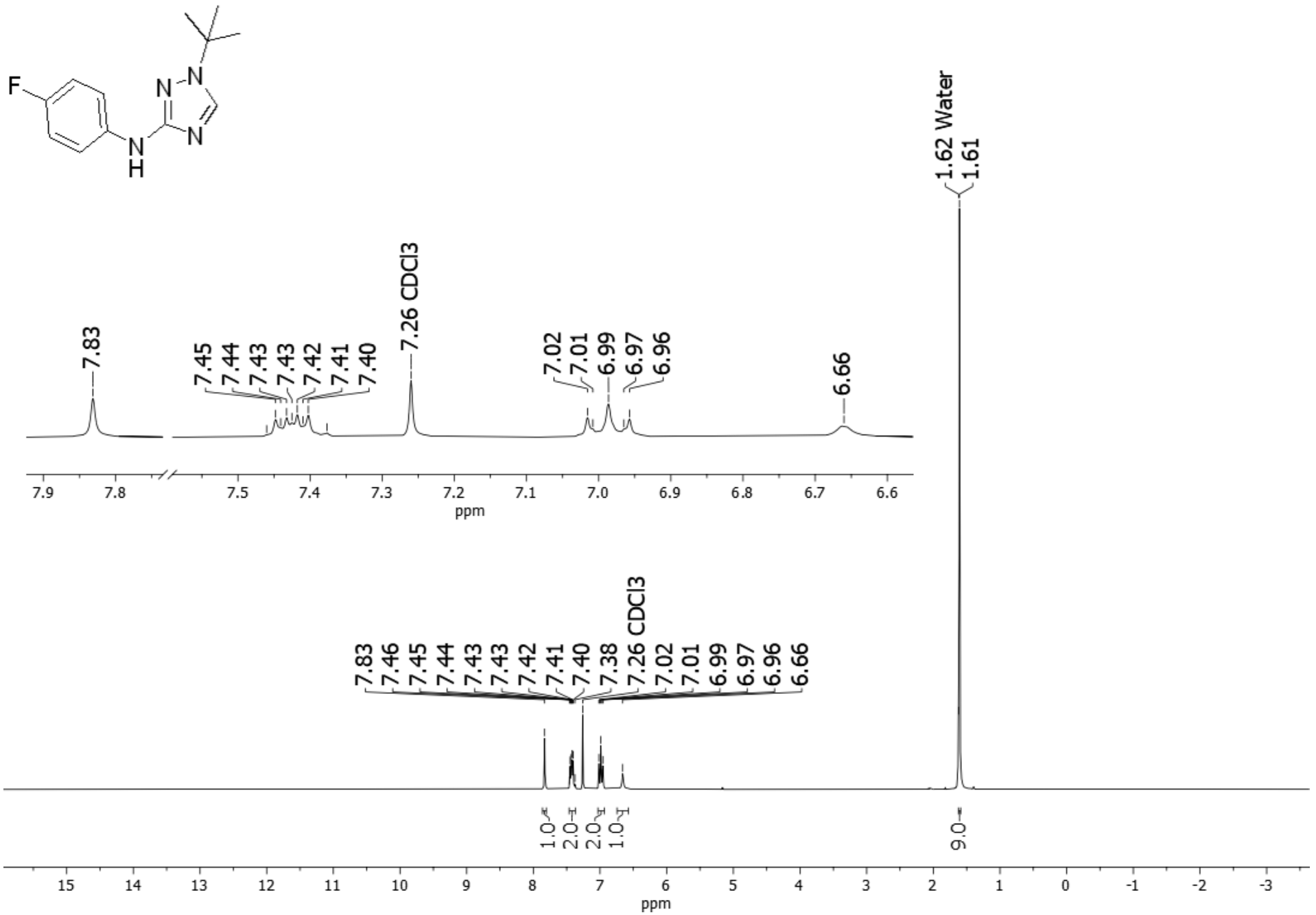

Figure S56. ^{1}H NMR spectrum of compound **4f** ($CDCl_3$, 300 MHz)

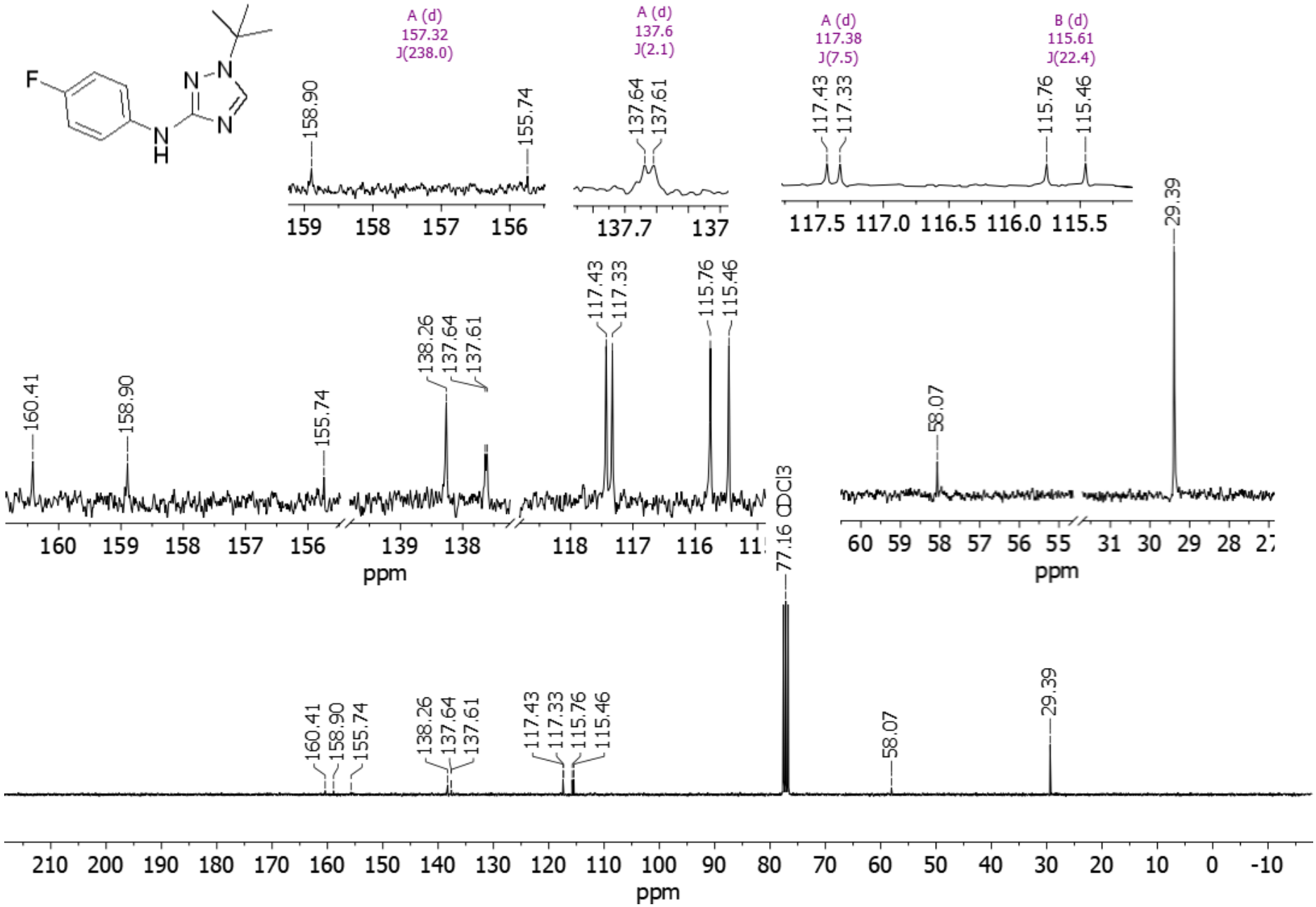

Figure S57. ^{13}C NMR spectrum of compound **4f** ($CDCl_3$, 75 MHz)

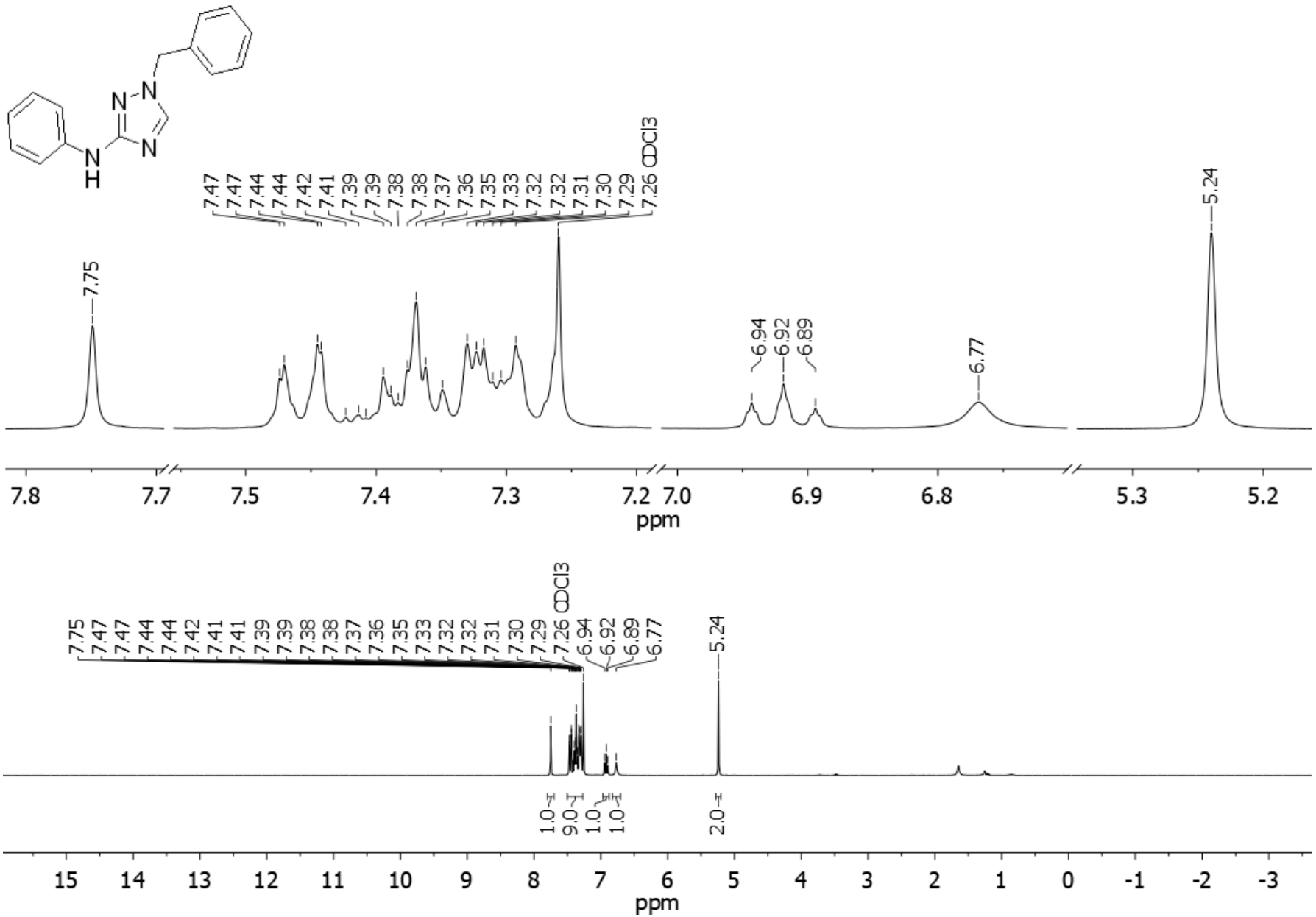

Figure S58. ^{1}H NMR spectrum of compound **4g** ($CDCl_3$, 300 MHz)

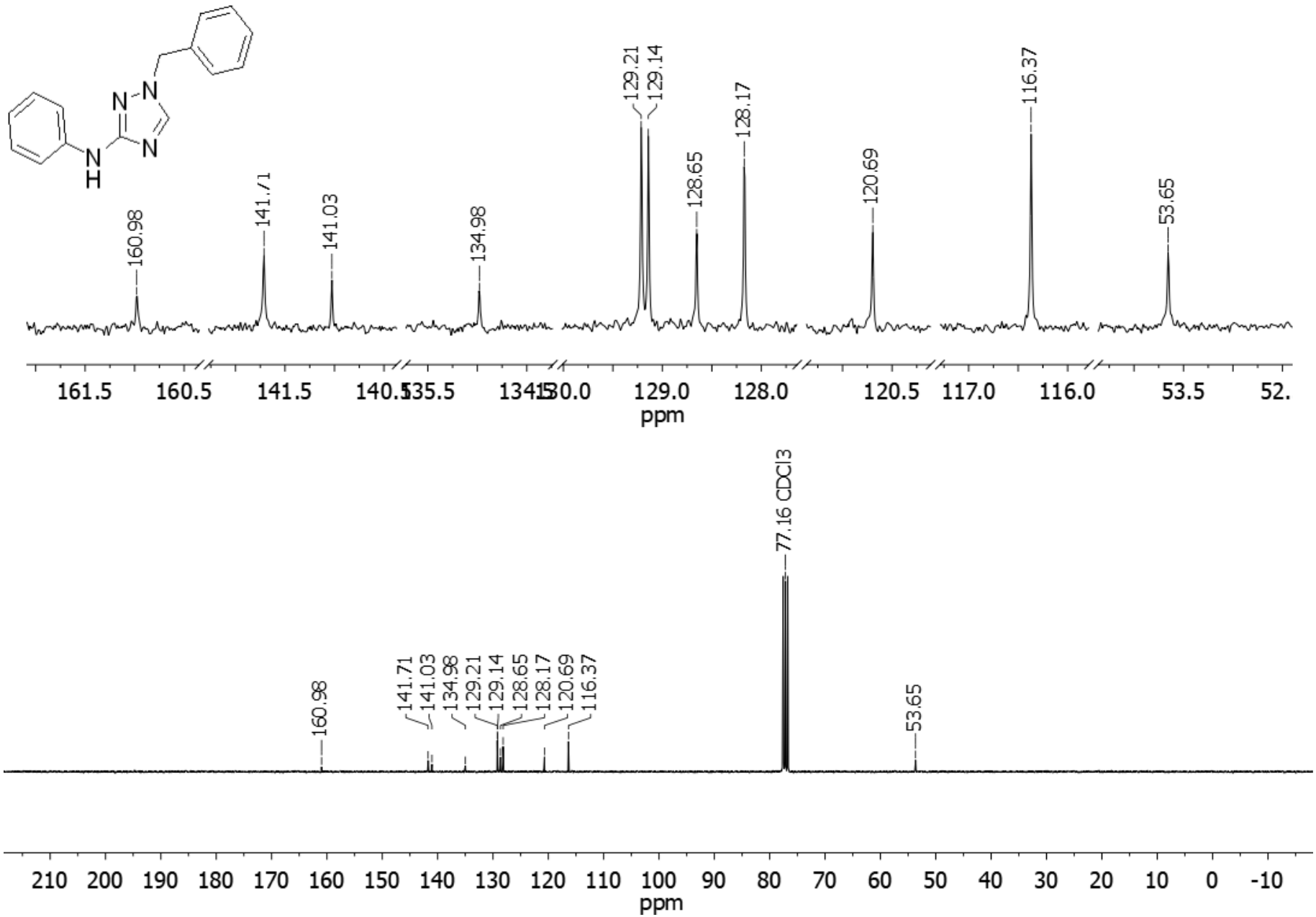

Figure S59. ^{13}C NMR spectrum of compound **4g** ($CDCl_3$, 75 MHz)

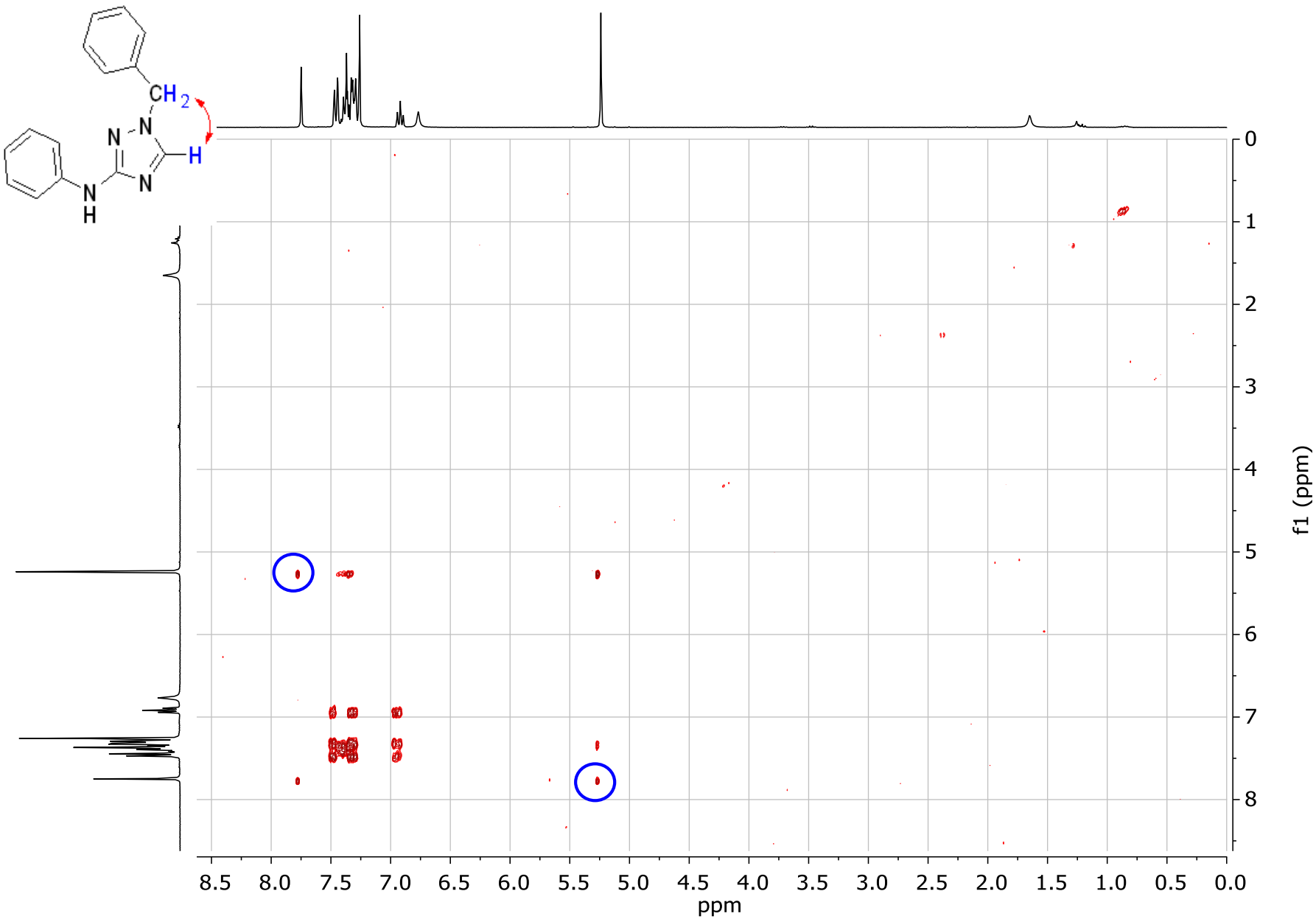

Figure S60. ^{1}H-^{1}H NOESY spectrum of compound **4g** ($CDCl_3$)

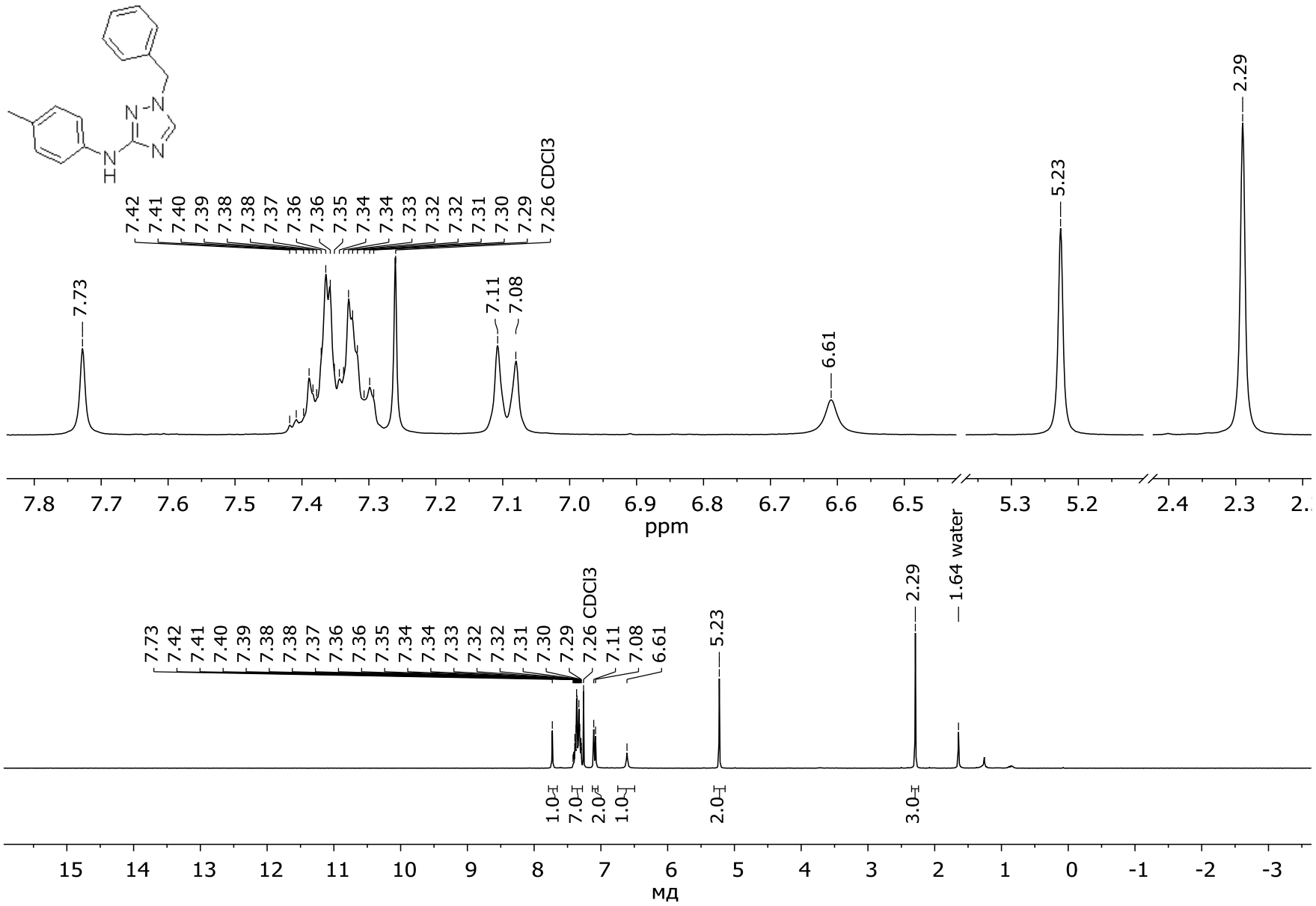

Figure S61. ^{1}H NMR spectrum of compound **4h** ($CDCl_3$, 300 MHz)

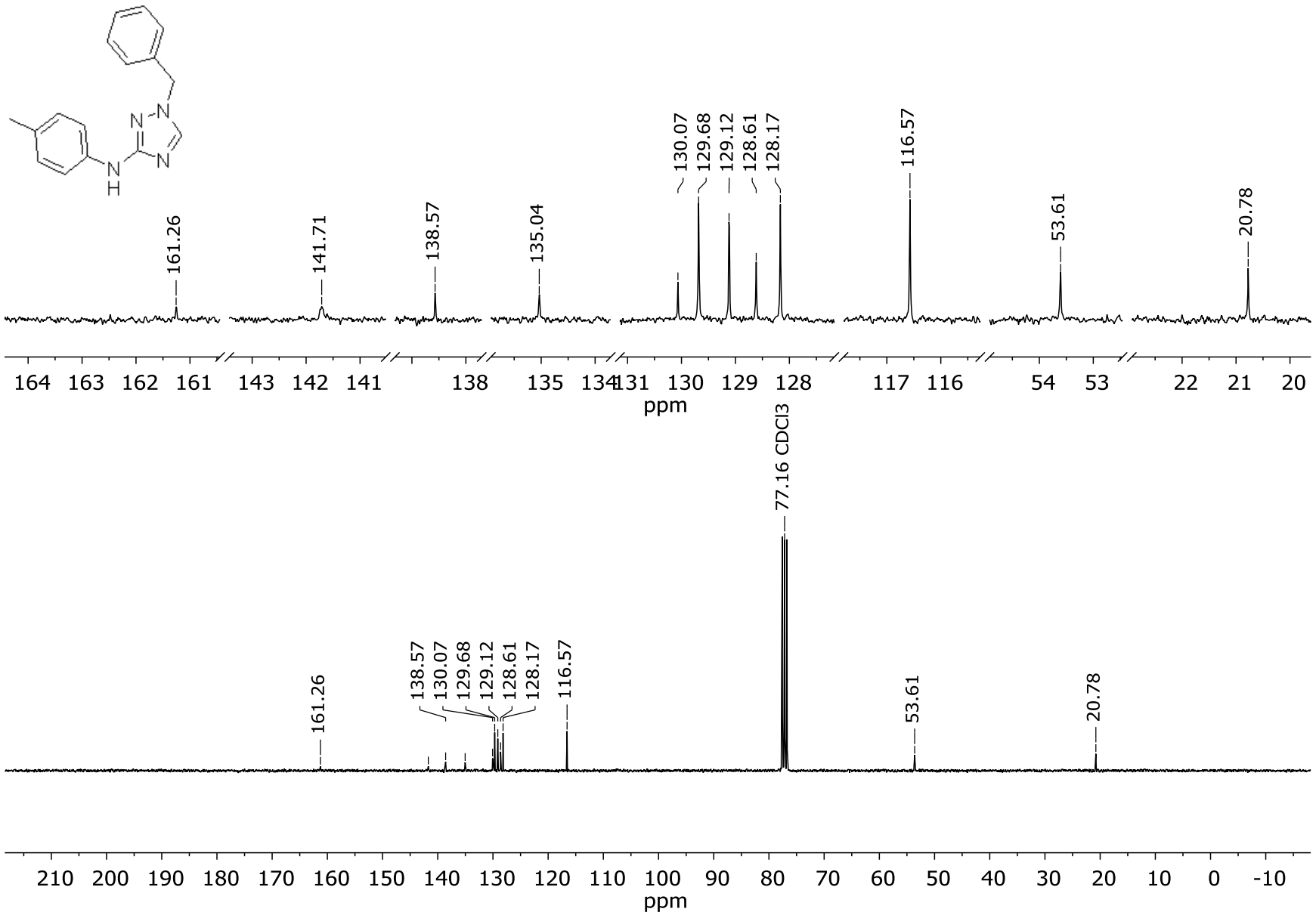

Figure S62. ^{13}C NMR spectrum of compound **4h** ($CDCl_3$, 75 MHz)

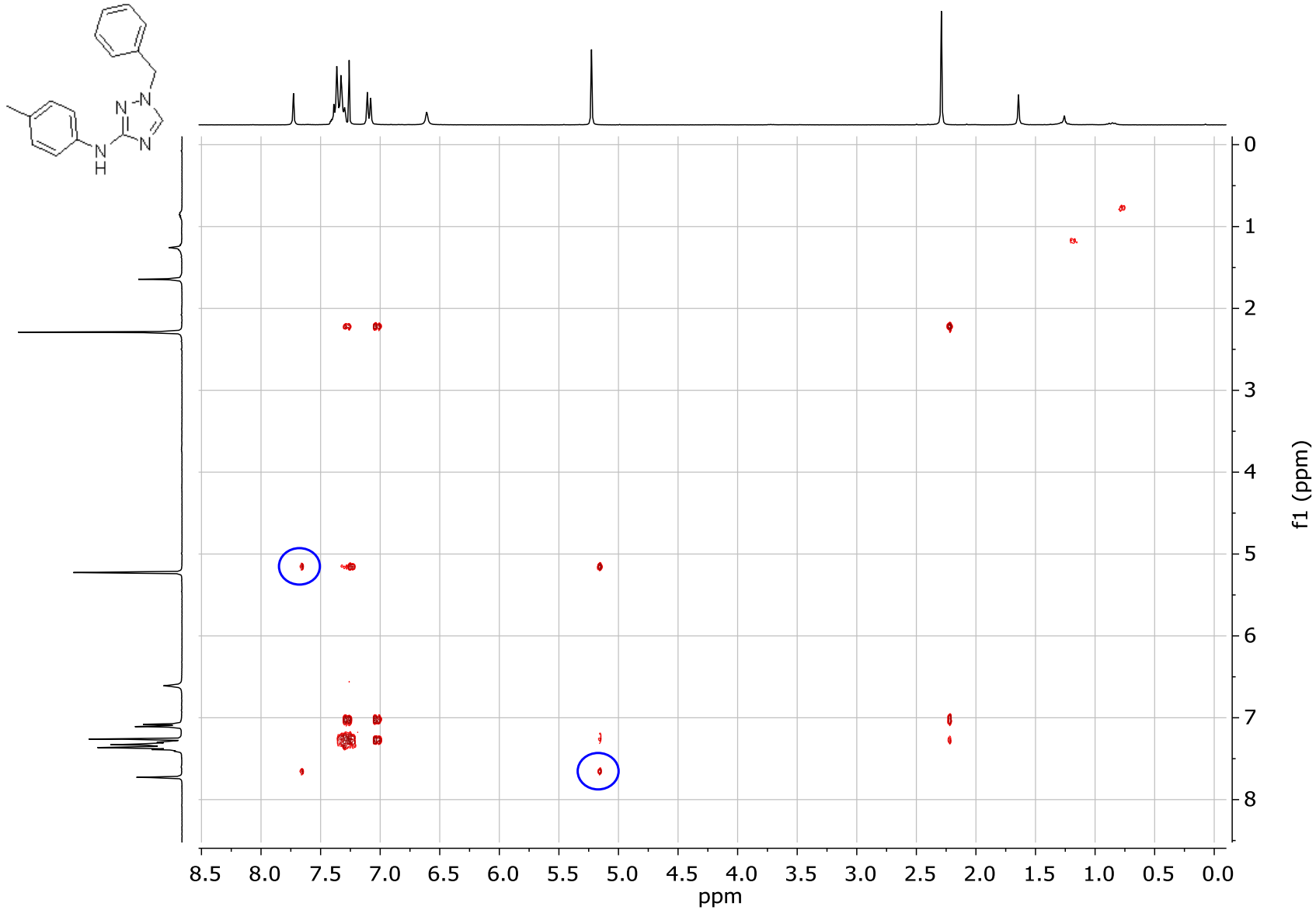

Figure S63. ^{1}H-^{1}H NOESY spectrum of compound **4h** ($CDCl_3$)

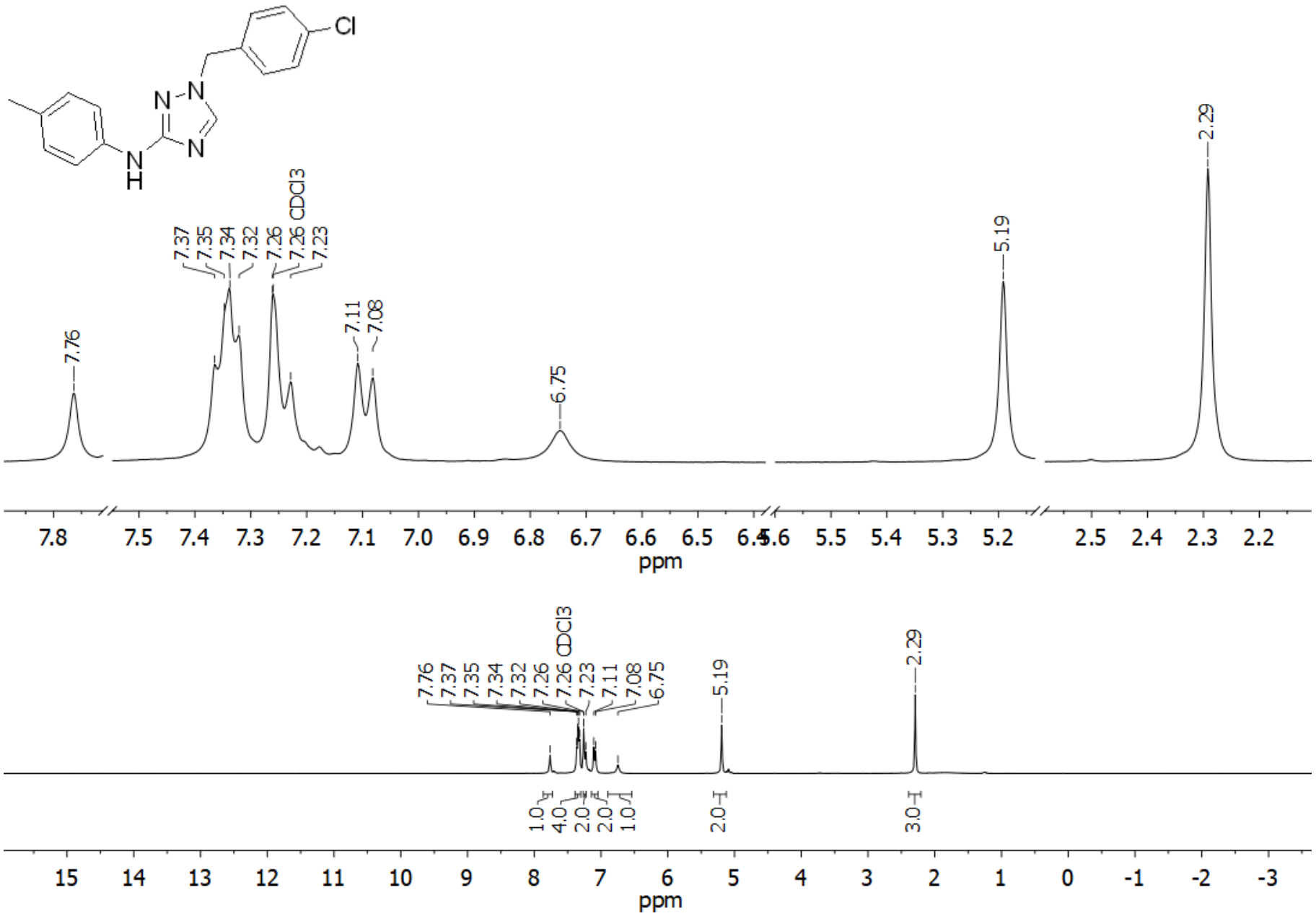

Figure S64. ^{1}H NMR spectrum of compound **4i** ($CDCl_3$, 300 MHz)

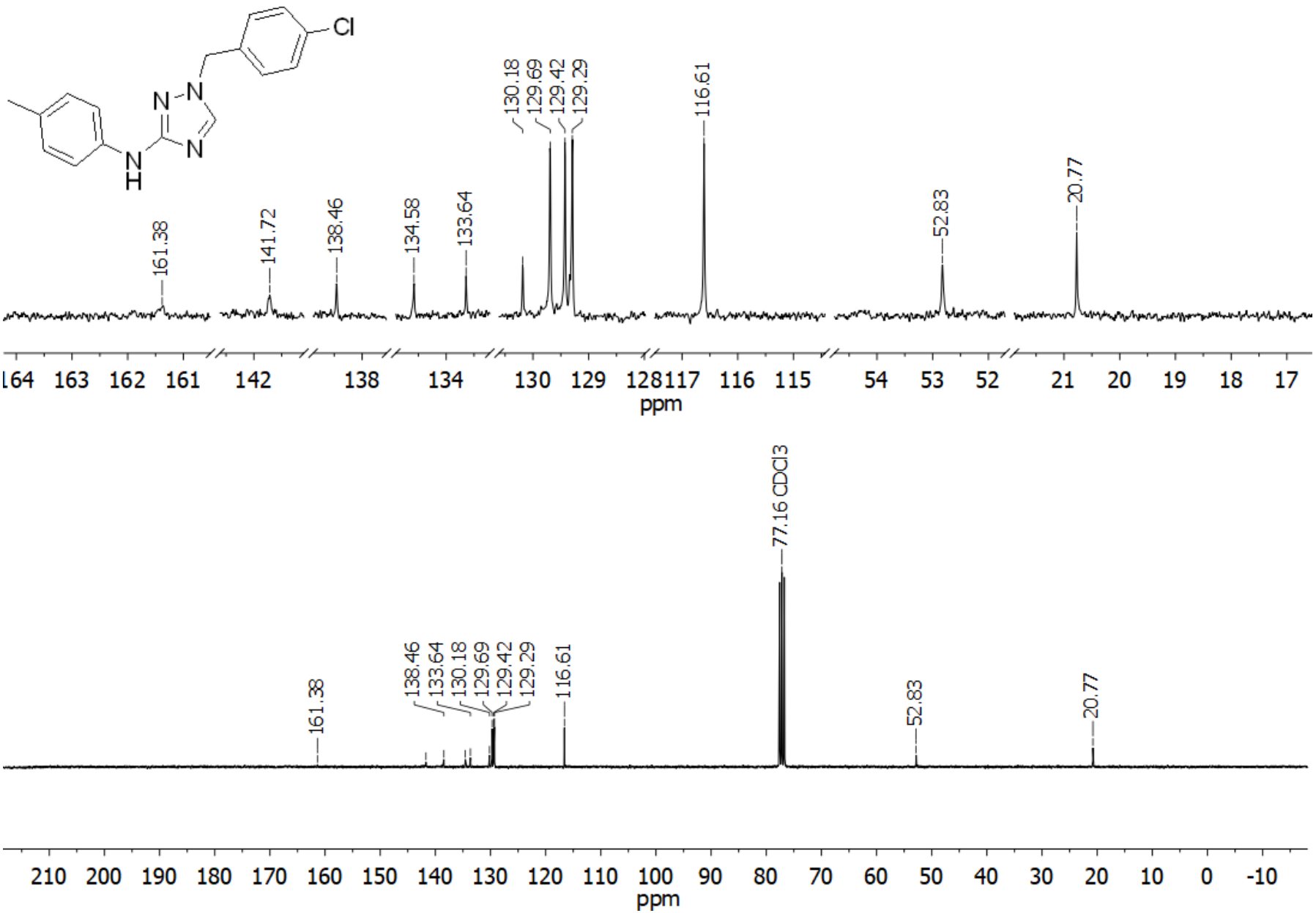

Figure S65. ^{13}C NMR spectrum of compound **4i** ($CDCl_3$, 75 MHz)

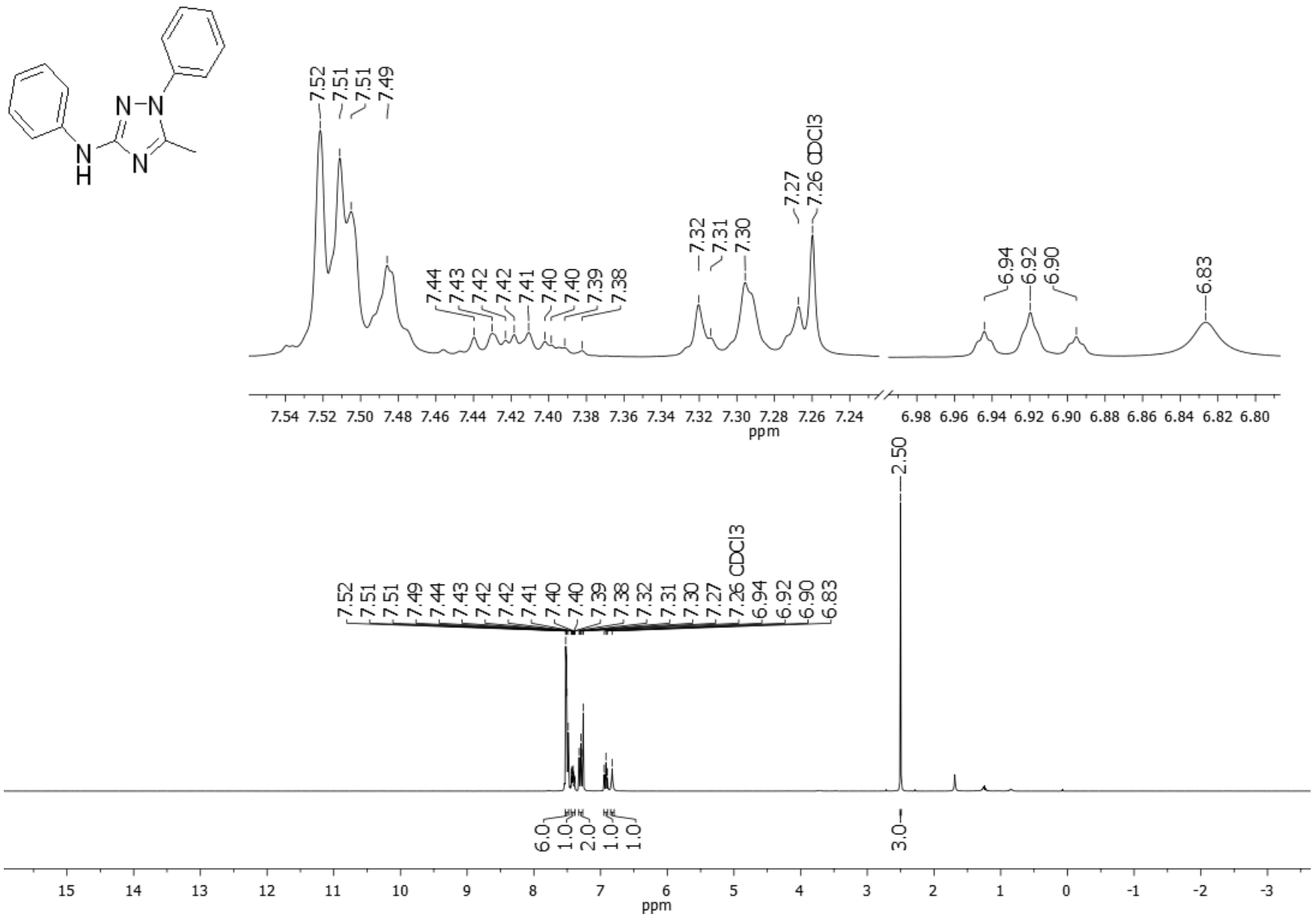

Figure S66. ^{1}H NMR spectrum of compound **4j** ($CDCl_3$, 300 MHz)

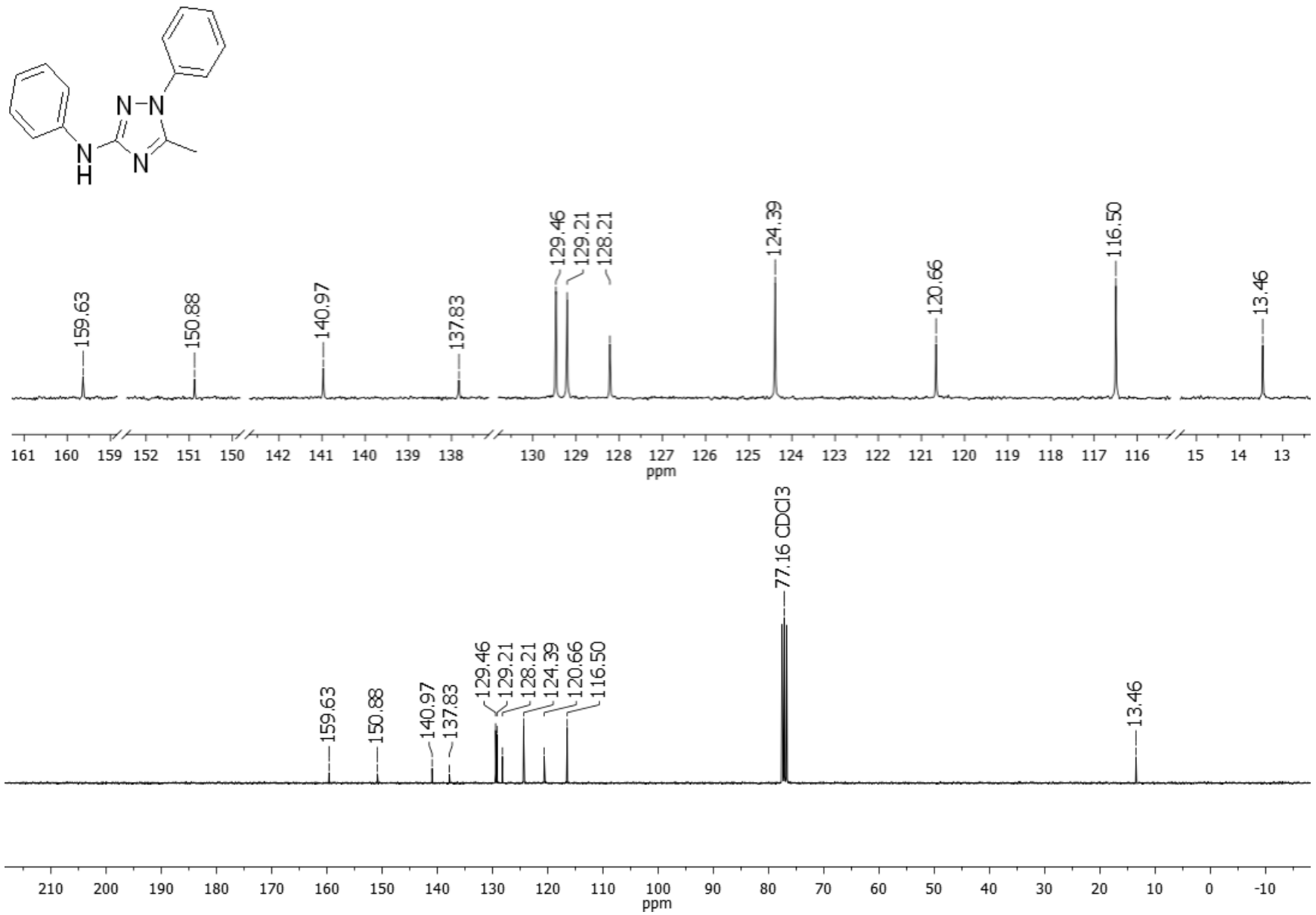

Figure S67. ^{13}C NMR spectrum of compound **4j** ($CDCl_3$, 75 MHz)

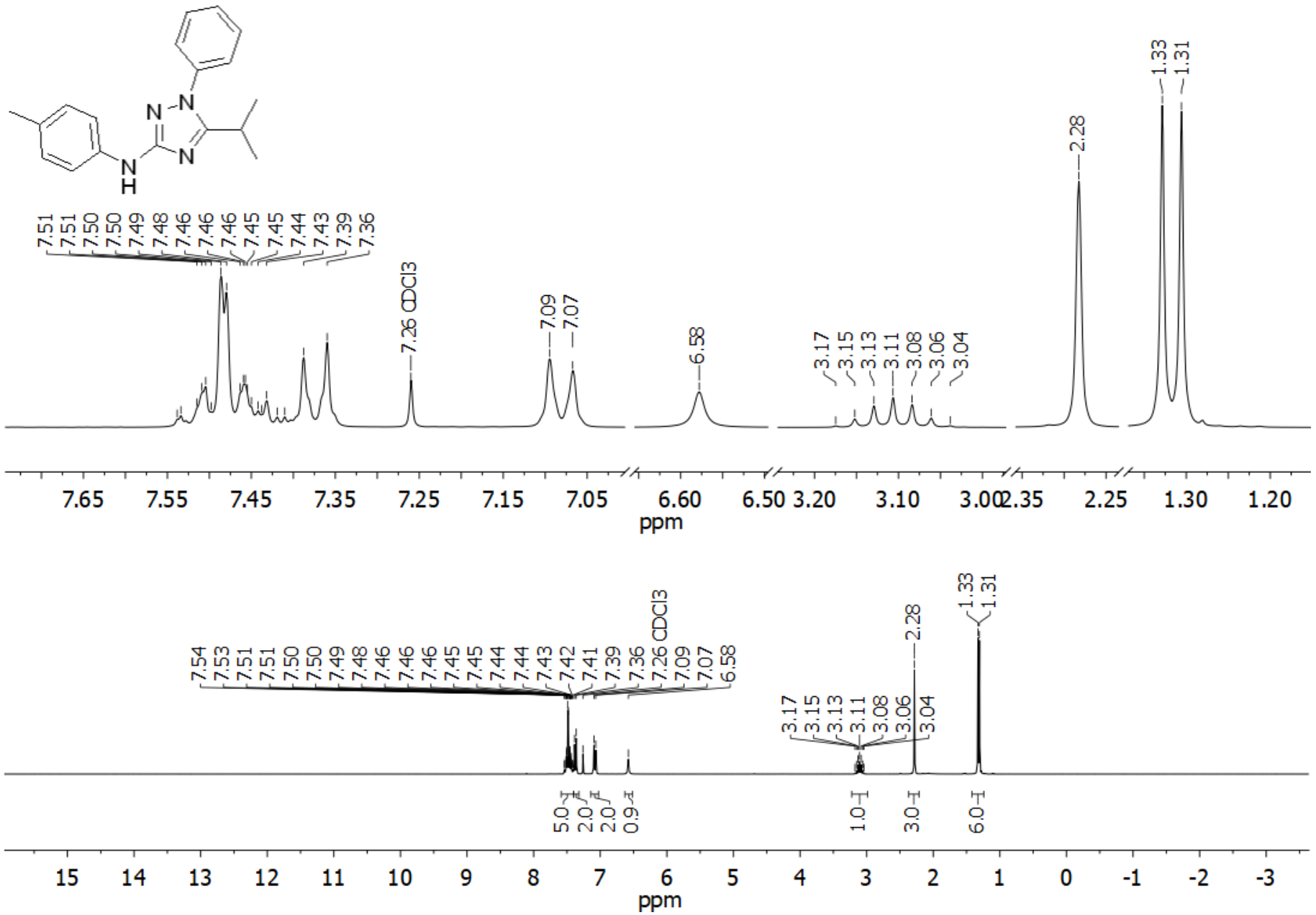

Figure S68. ^{1}H NMR spectrum of compound **4k** ($CDCl_3$, 300 MHz)

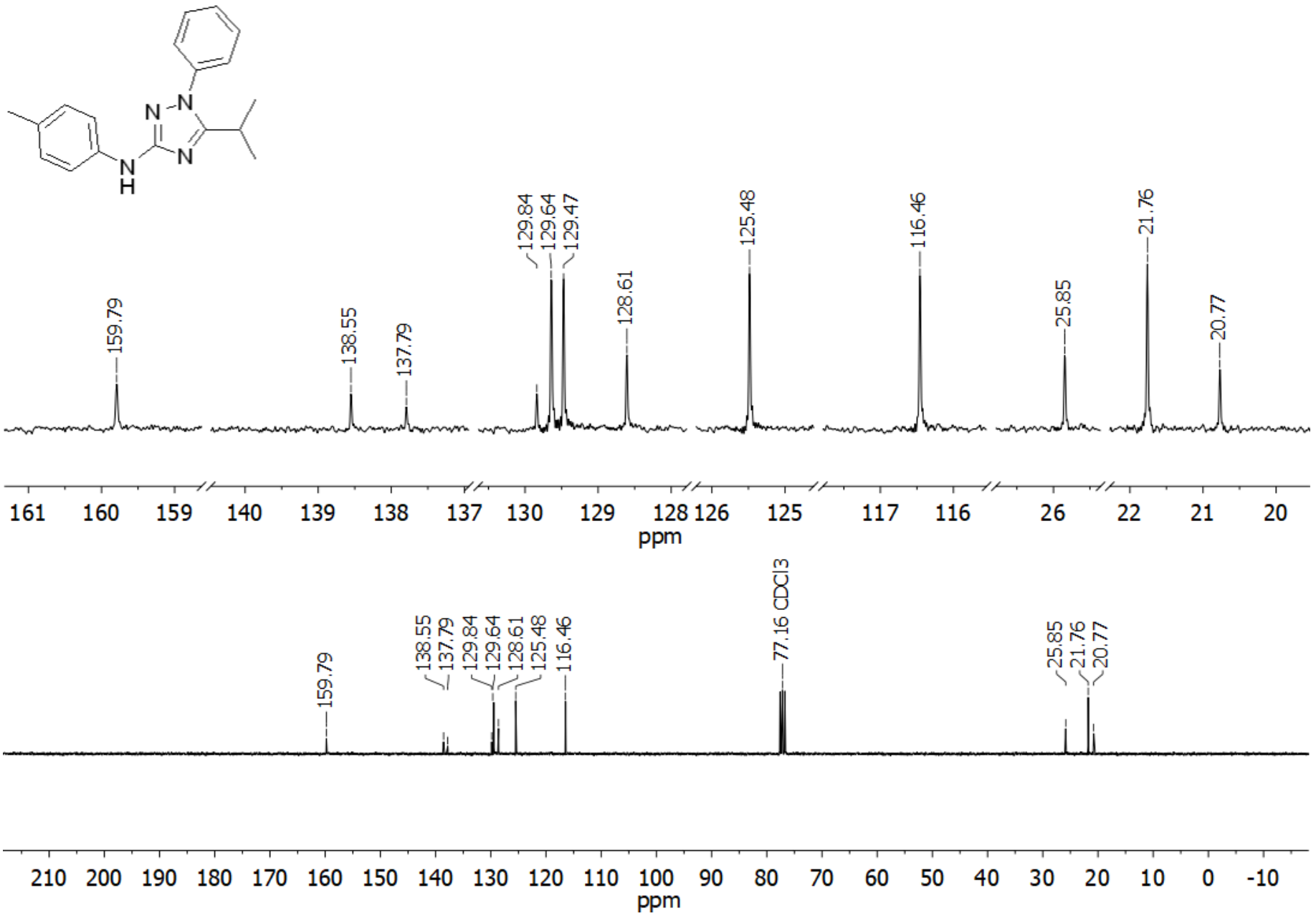

Figure S69. ^{13}C NMR spectrum of compound **4k** ($CDCl_3$, 75 MHz)

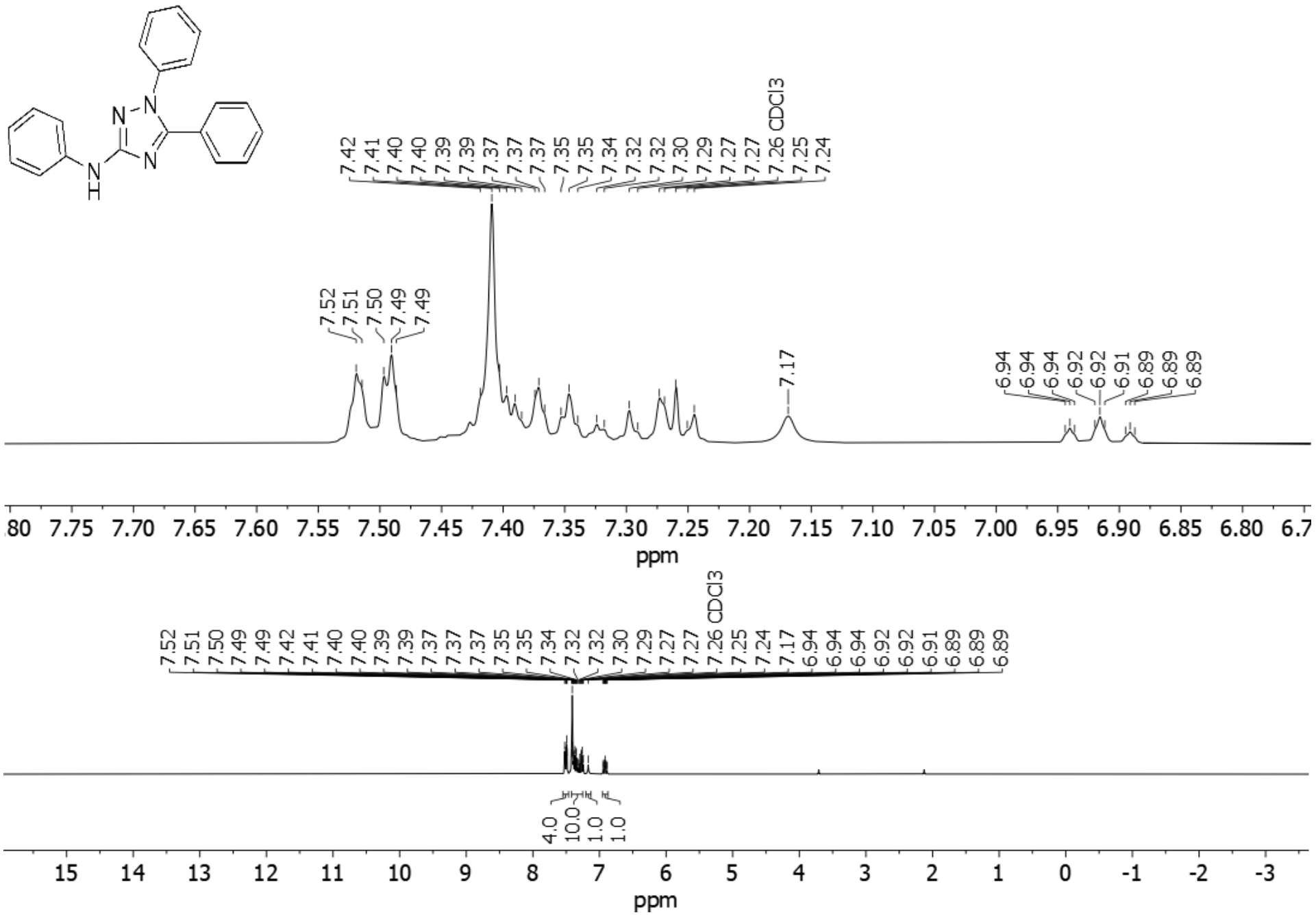

Figure S70. ^{1}H NMR spectrum of compound **4l** ($CDCl_3$, 300 MHz)

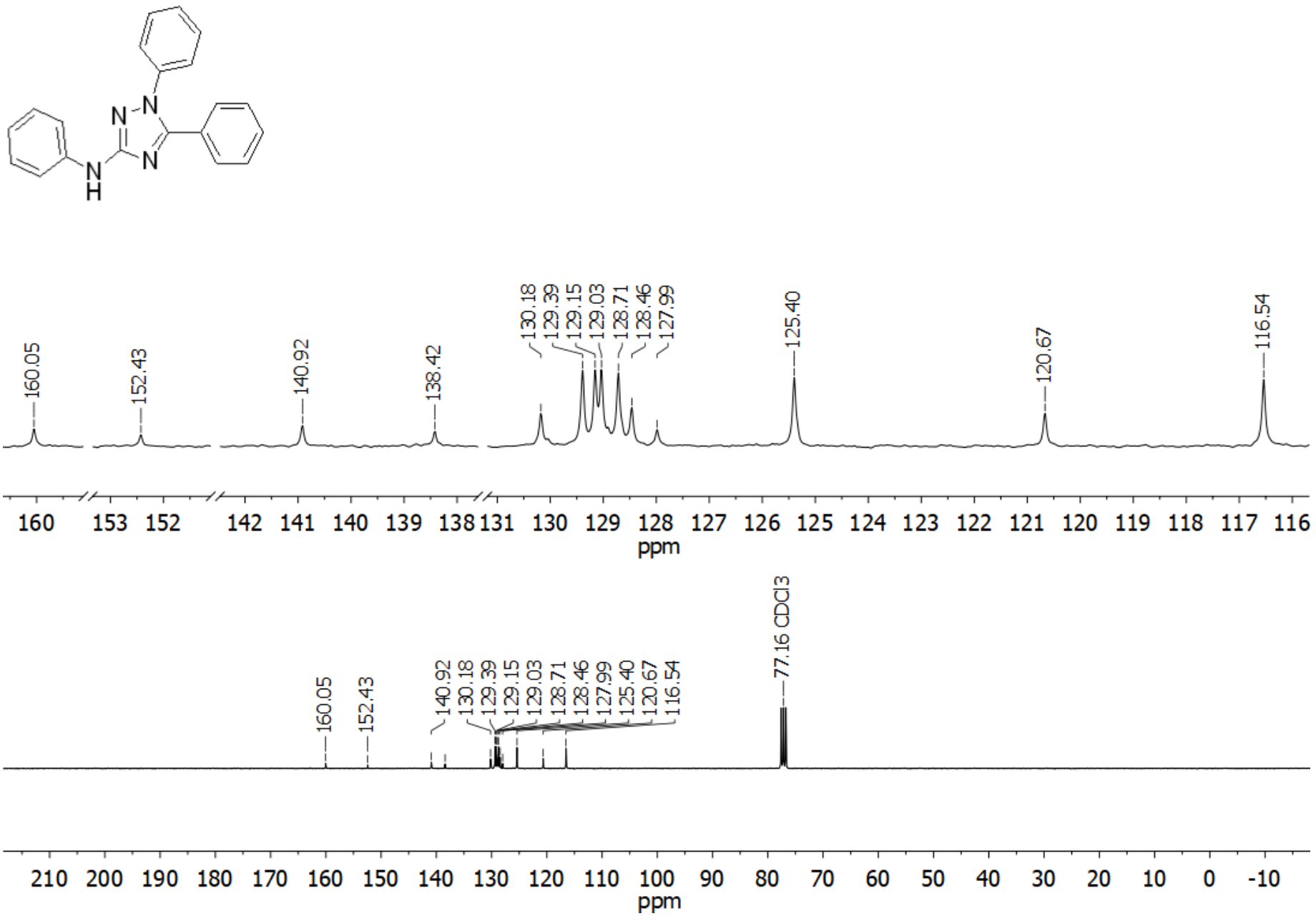

Figure S71. ^{13}C NMR spectrum of compound **4l** ($CDCl_3$, 75 MHz)

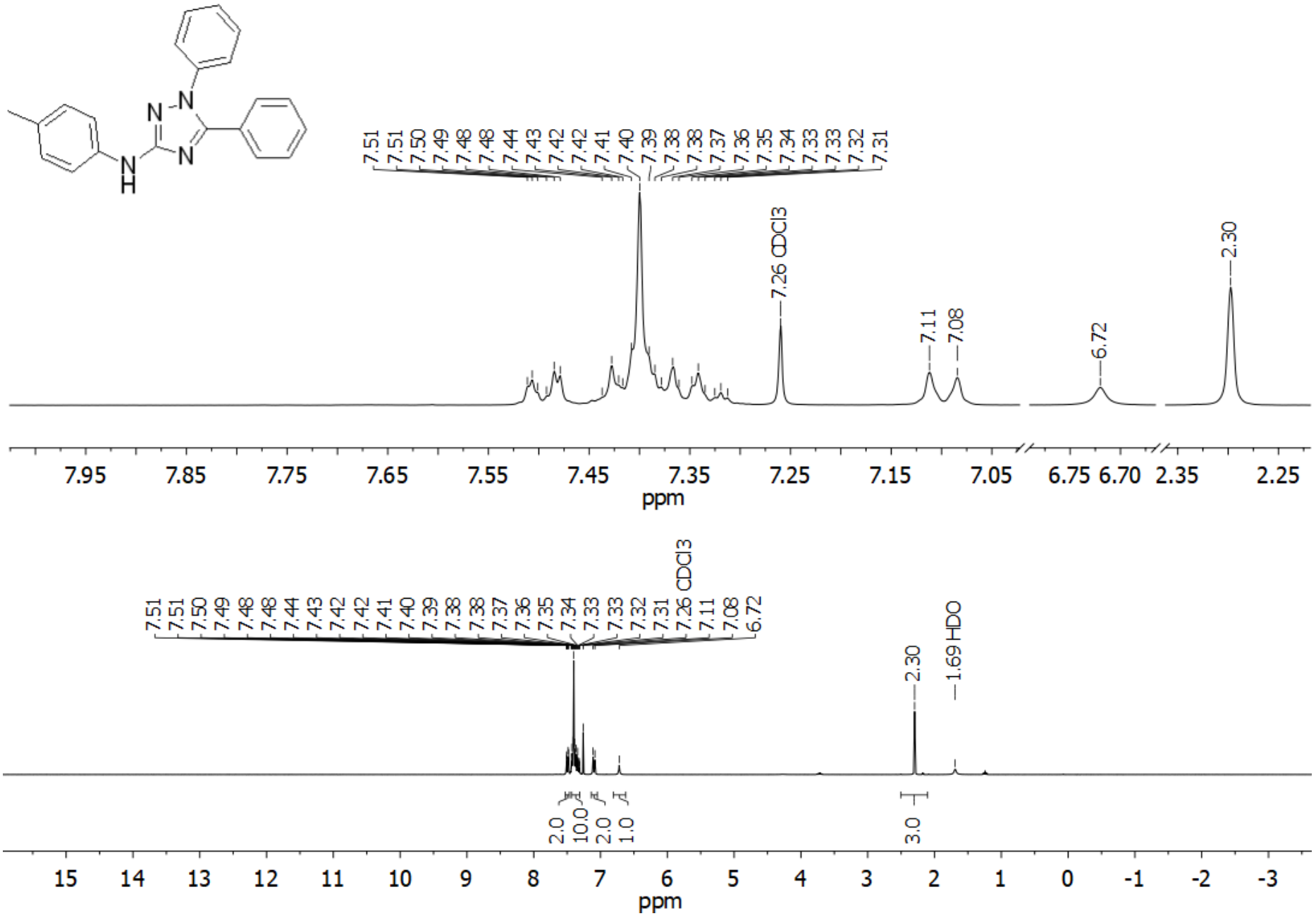

Figure S72. ^{1}H NMR spectrum of compound **4m** ($CDCl_3$, 300 MHz)

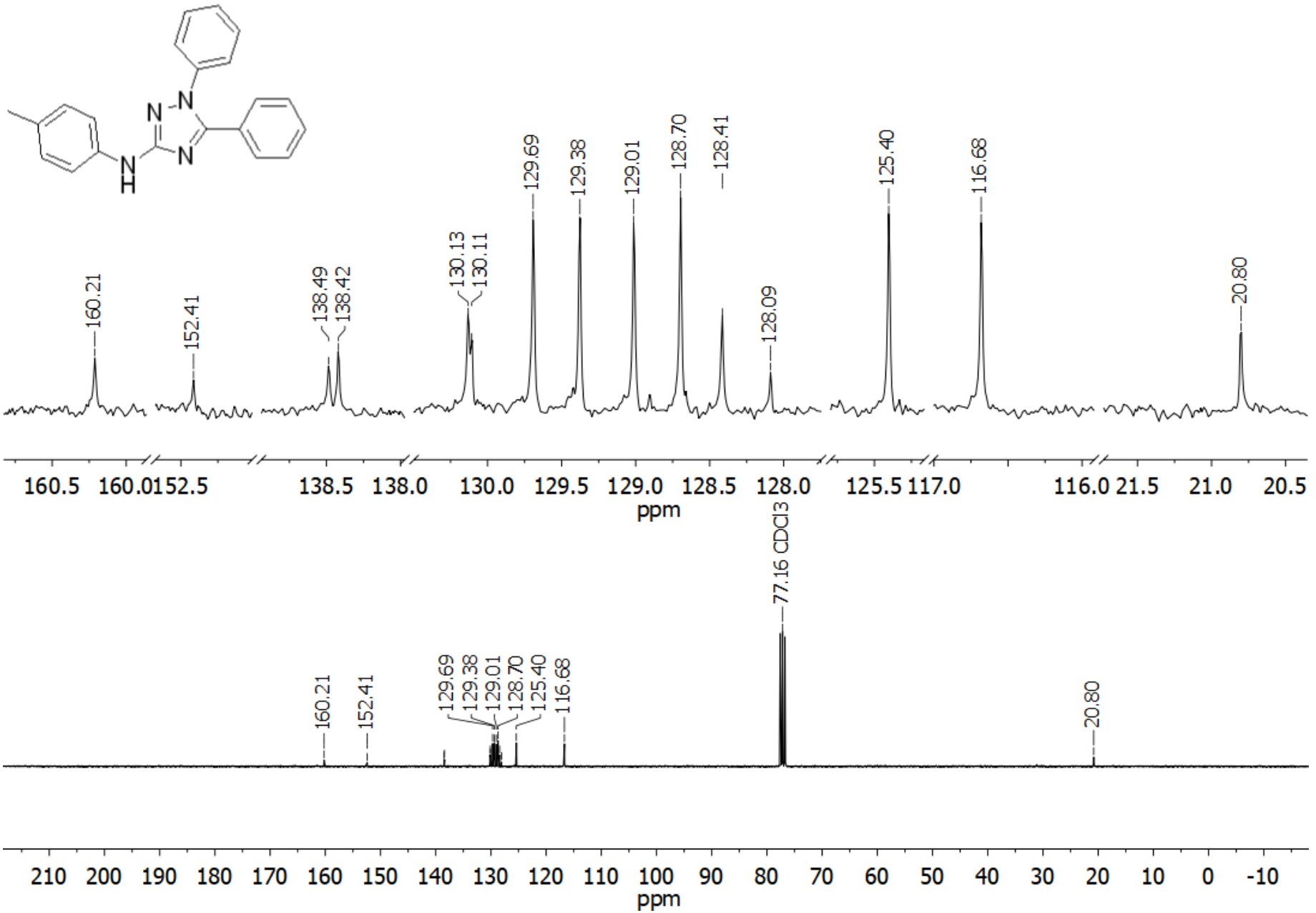

Figure S73. ^{13}C NMR spectrum of compound **4m** ($CDCl_3$, 75 MHz)

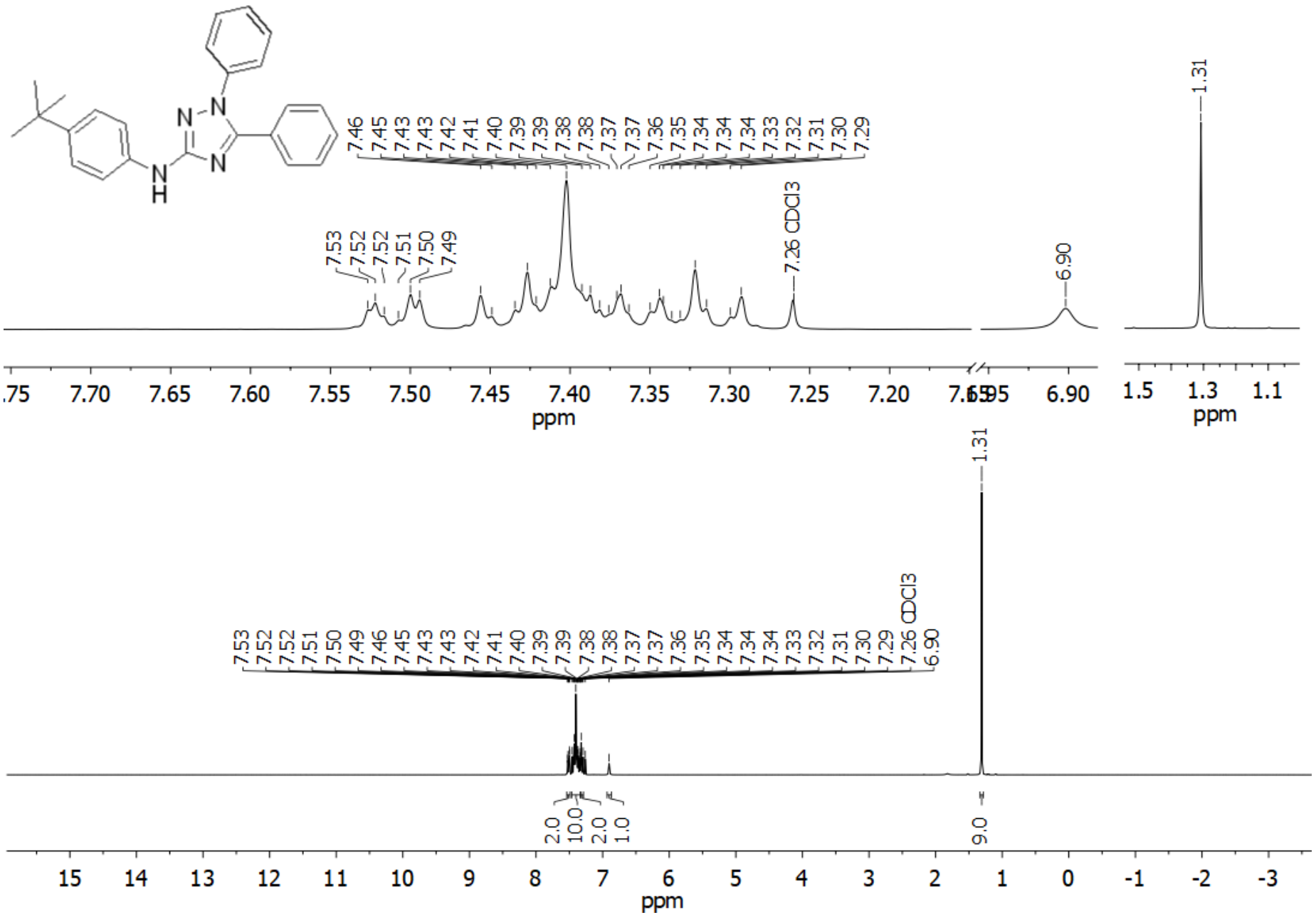

Figure S74. ^{1}H NMR spectrum of compound **4n** ($CDCl_3$, 300 MHz)

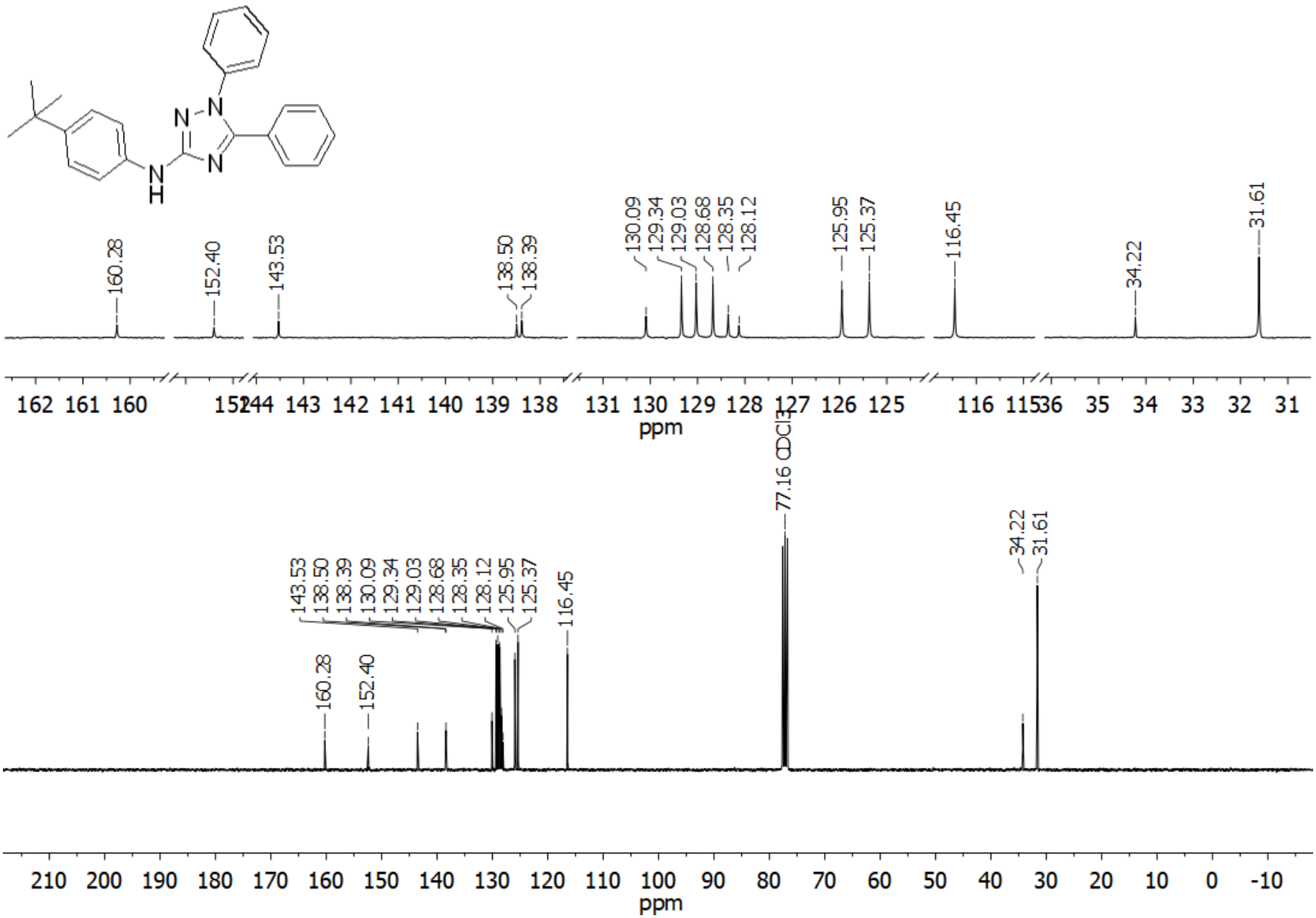

Figure S75. ^{13}C NMR spectrum of compound **4n** ($CDCl_3$, 75 MHz)

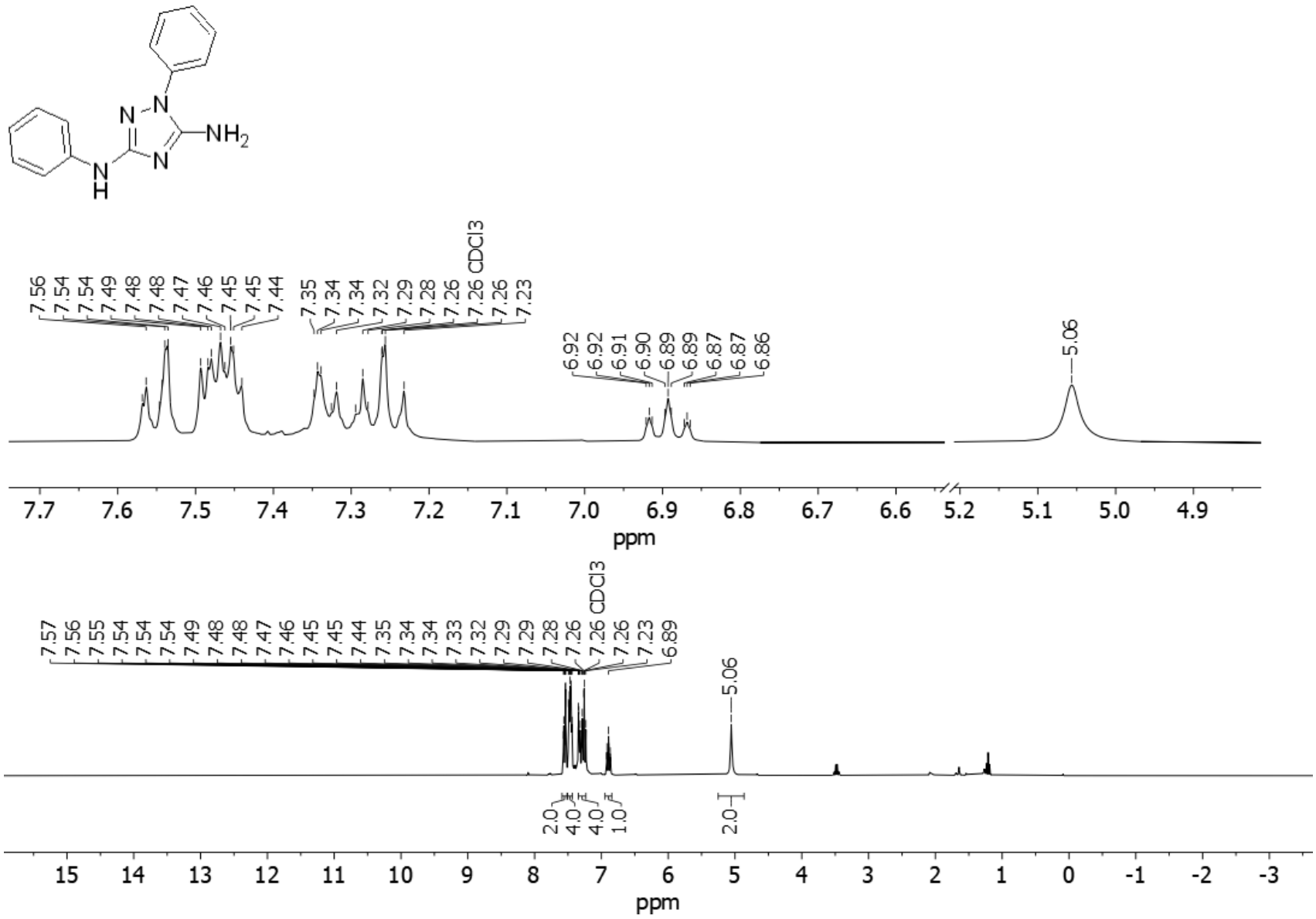

Figure S76. ^{1}H NMR spectrum of compound **4o** ($CDCl_3$, 300 MHz)

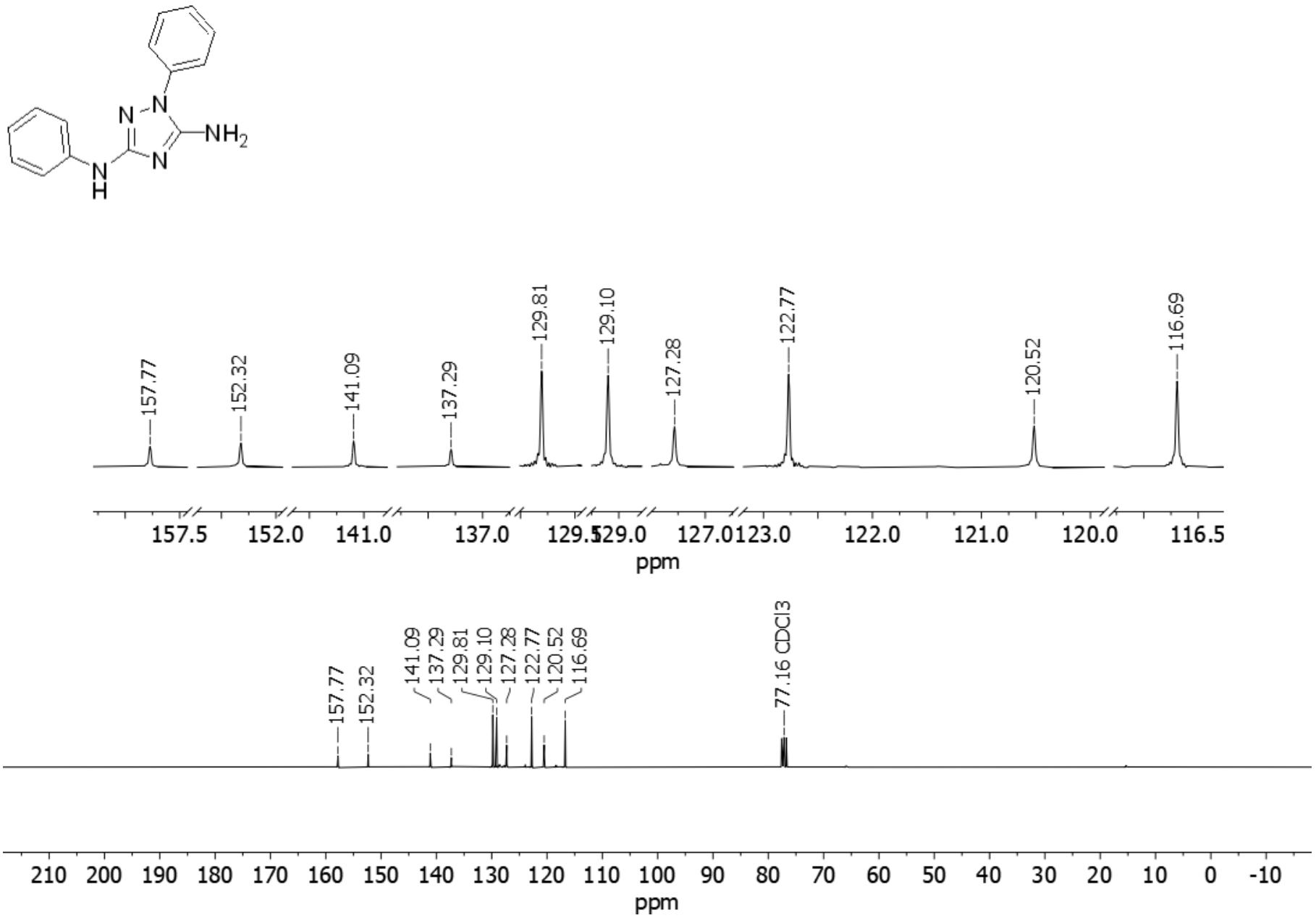

Figure S77. ^{13}C NMR spectrum of compound **4o** ($CDCl_3$, 75 MHz)

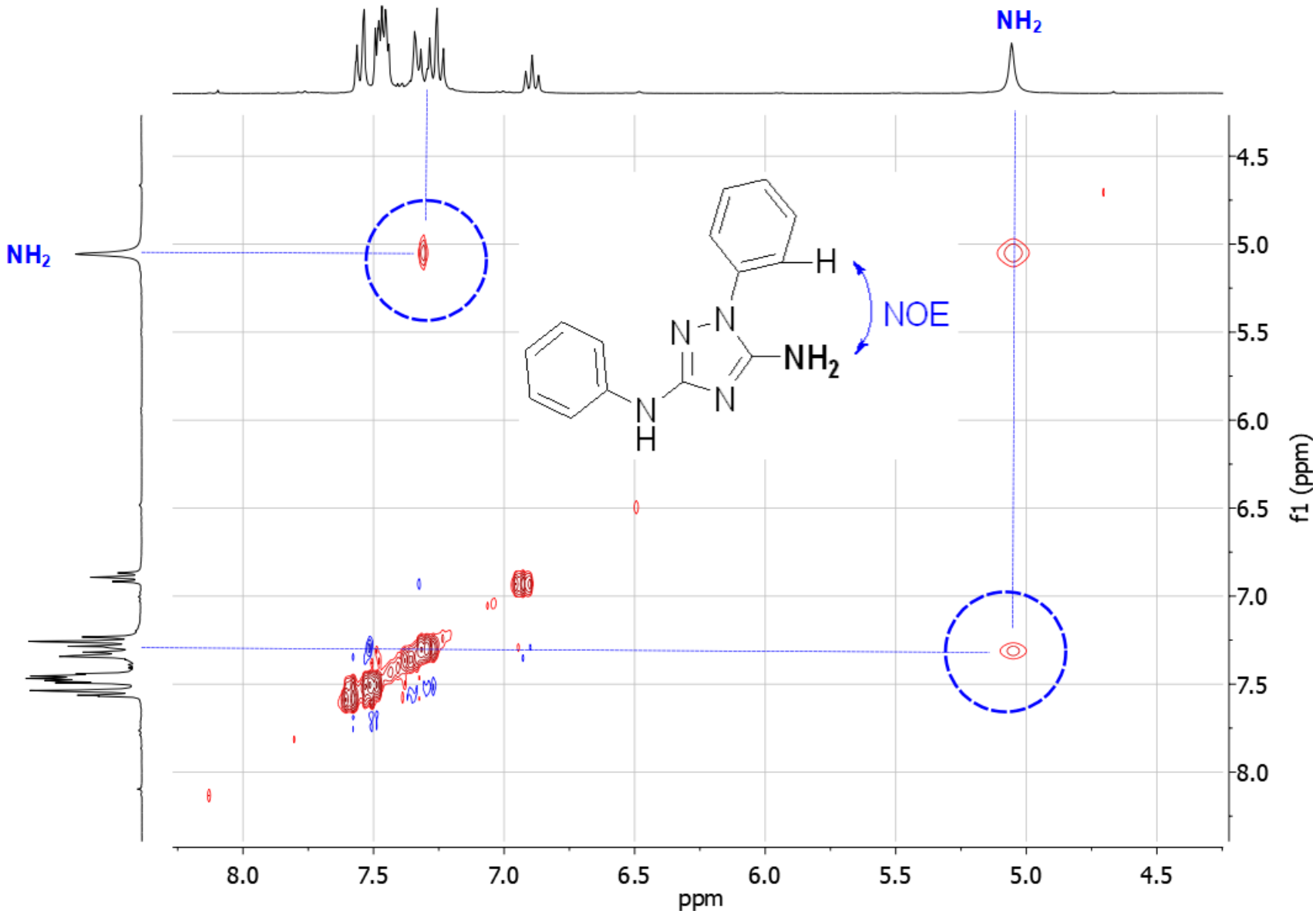

Figure S78. ^{1}H-^{1}H NOESY spectrum of compound **4o** ($CDCl_3$)

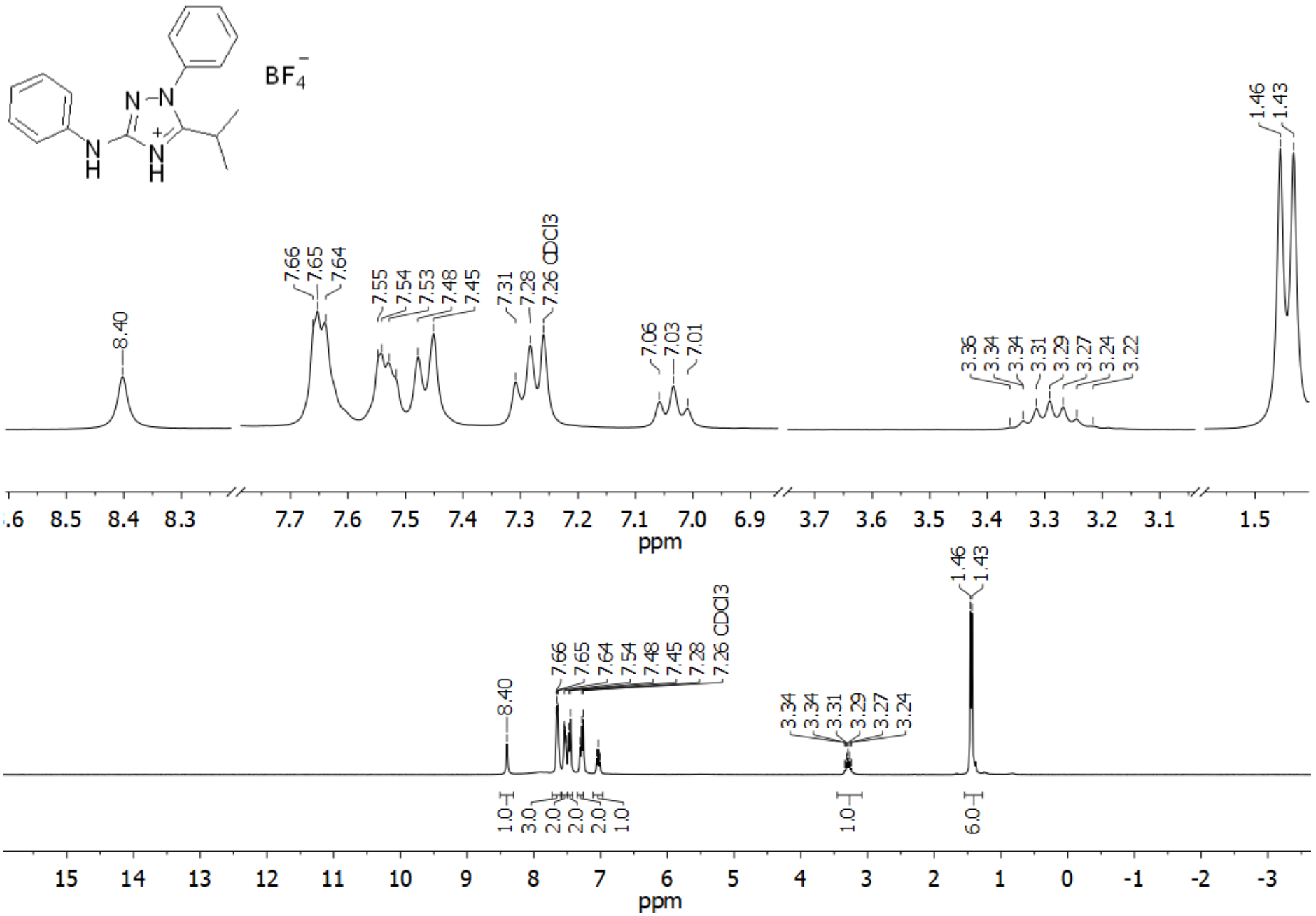

Figure S79. ^{1}H NMR spectrum of compound **4p** ($CDCl_3$, 300 MHz)

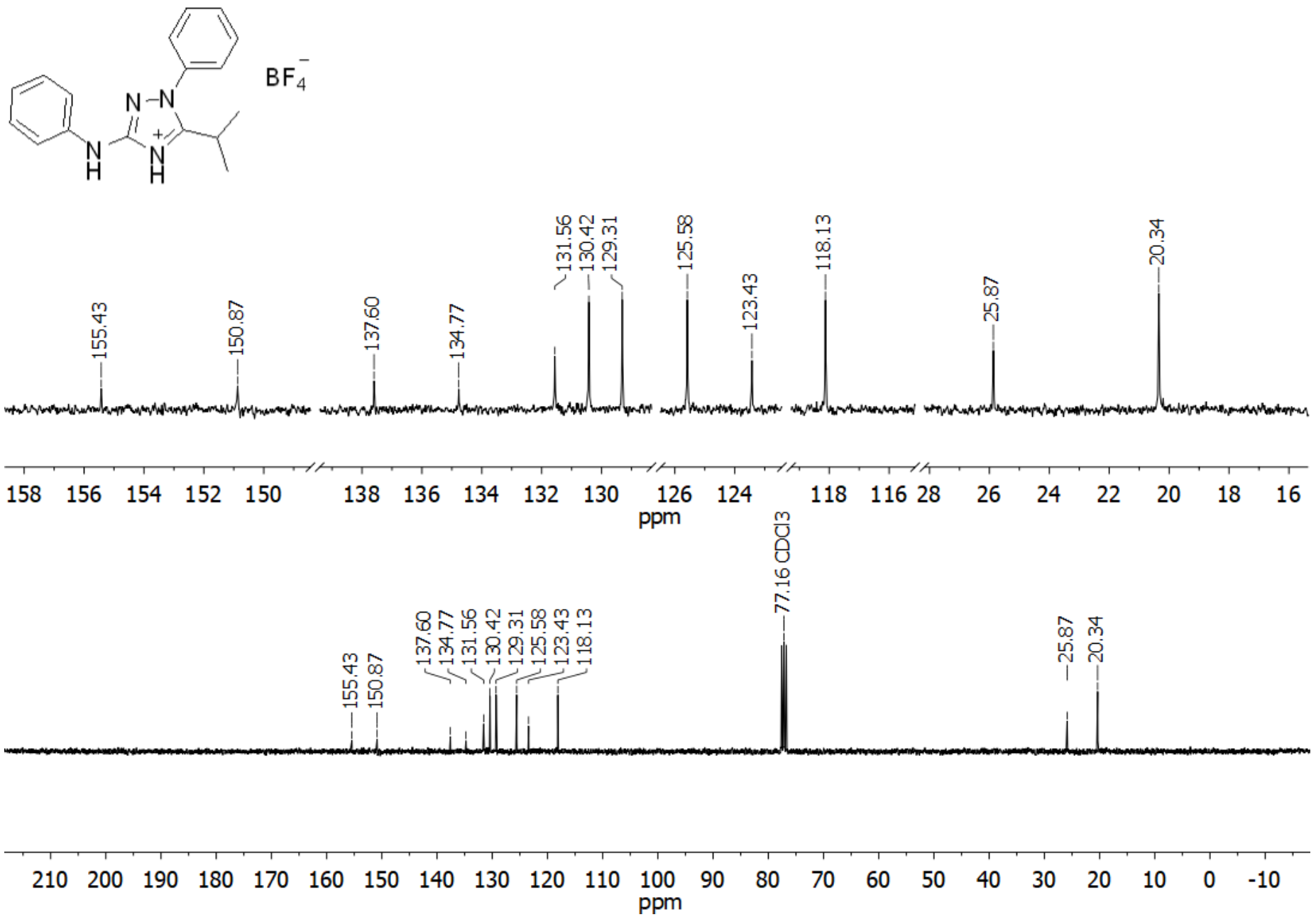

Figure S80. ^{13}C NMR spectrum of compound **4p** ($CDCl_3$, 75 MHz)

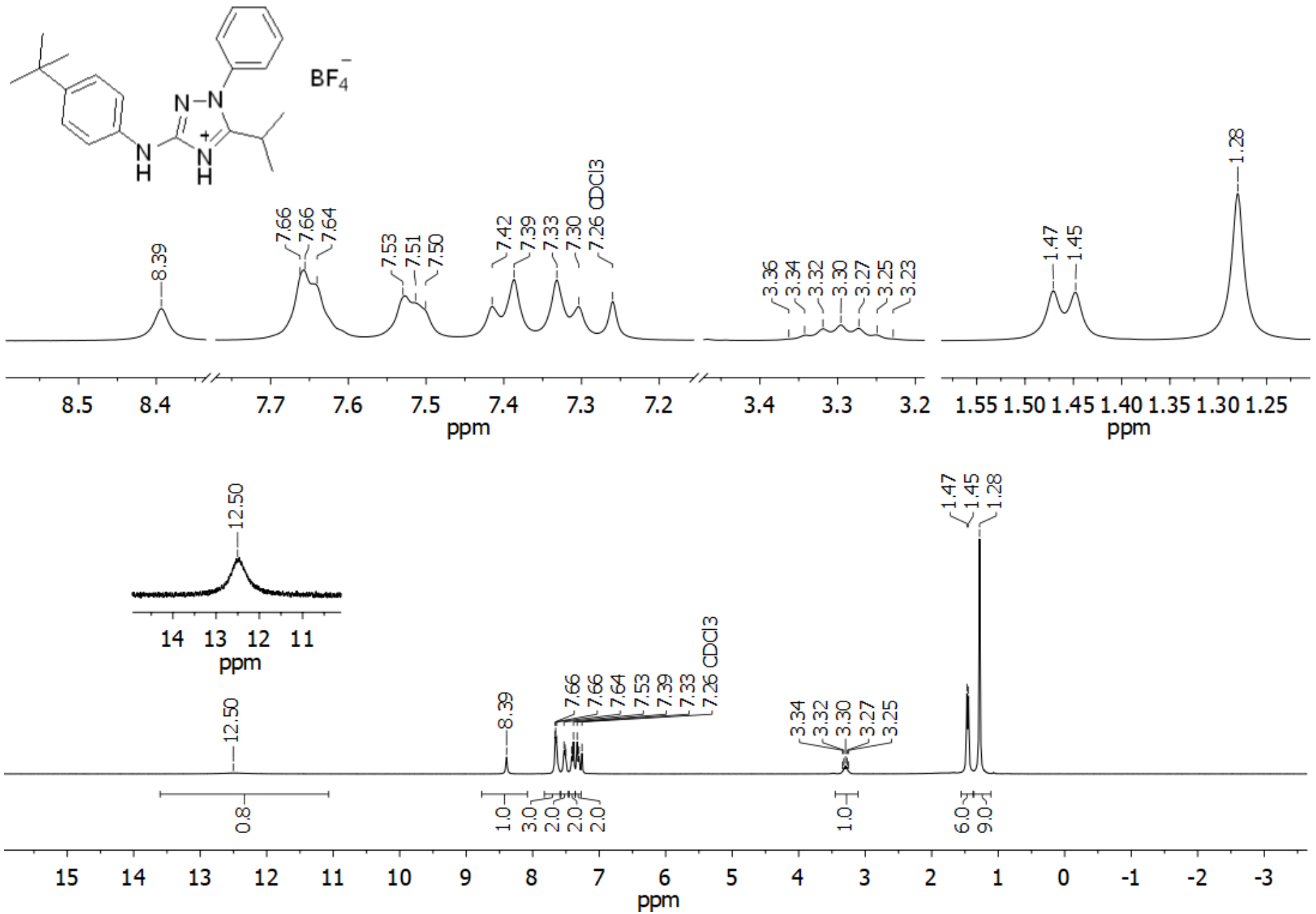

Figure S81. ^{1}H NMR spectrum of compound **4q** ($CDCl_3$, 300 MHz)

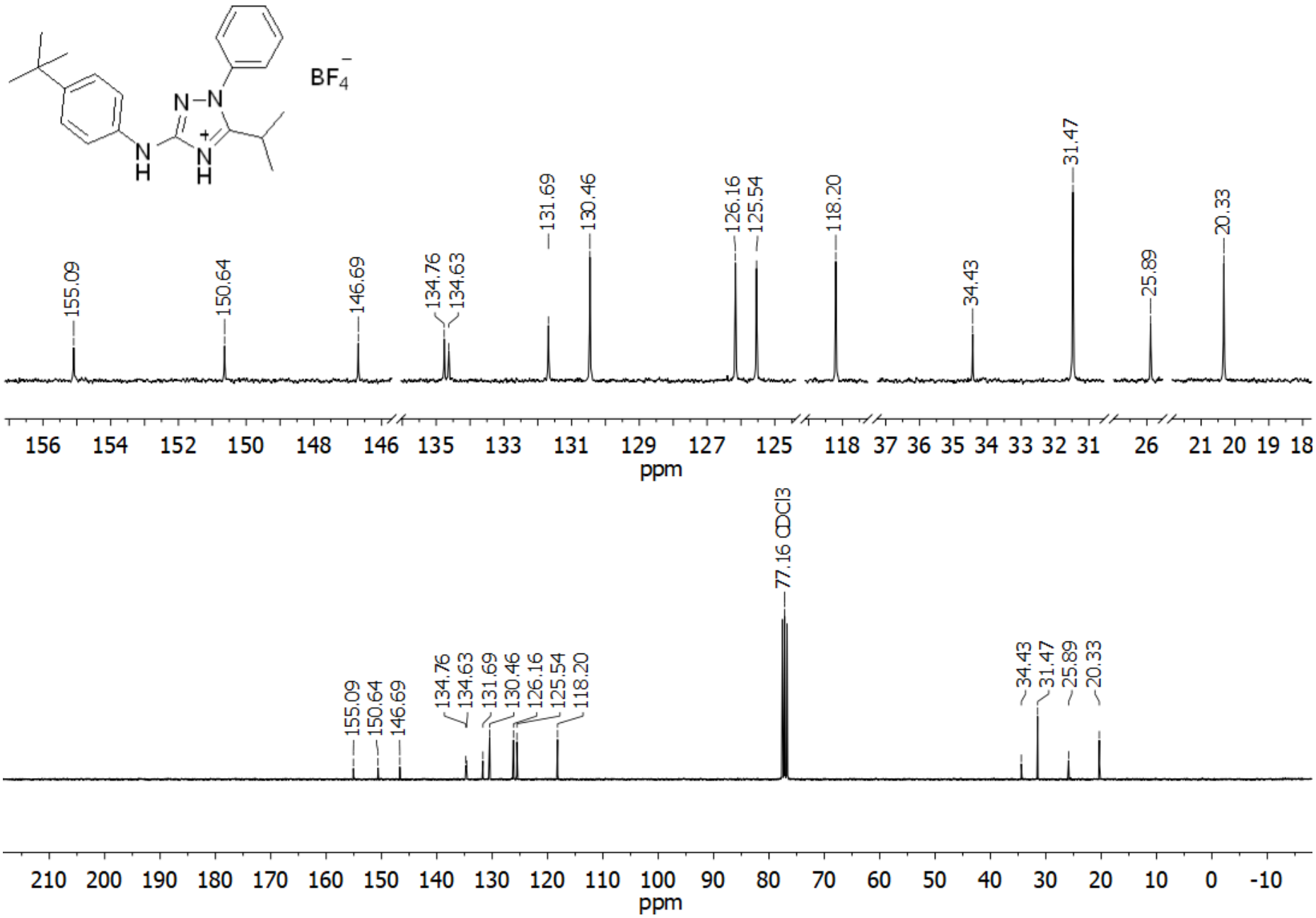

Figure S82. ^{13}C NMR spectrum of compound **4q** ($CDCl_3$, 75 MHz)

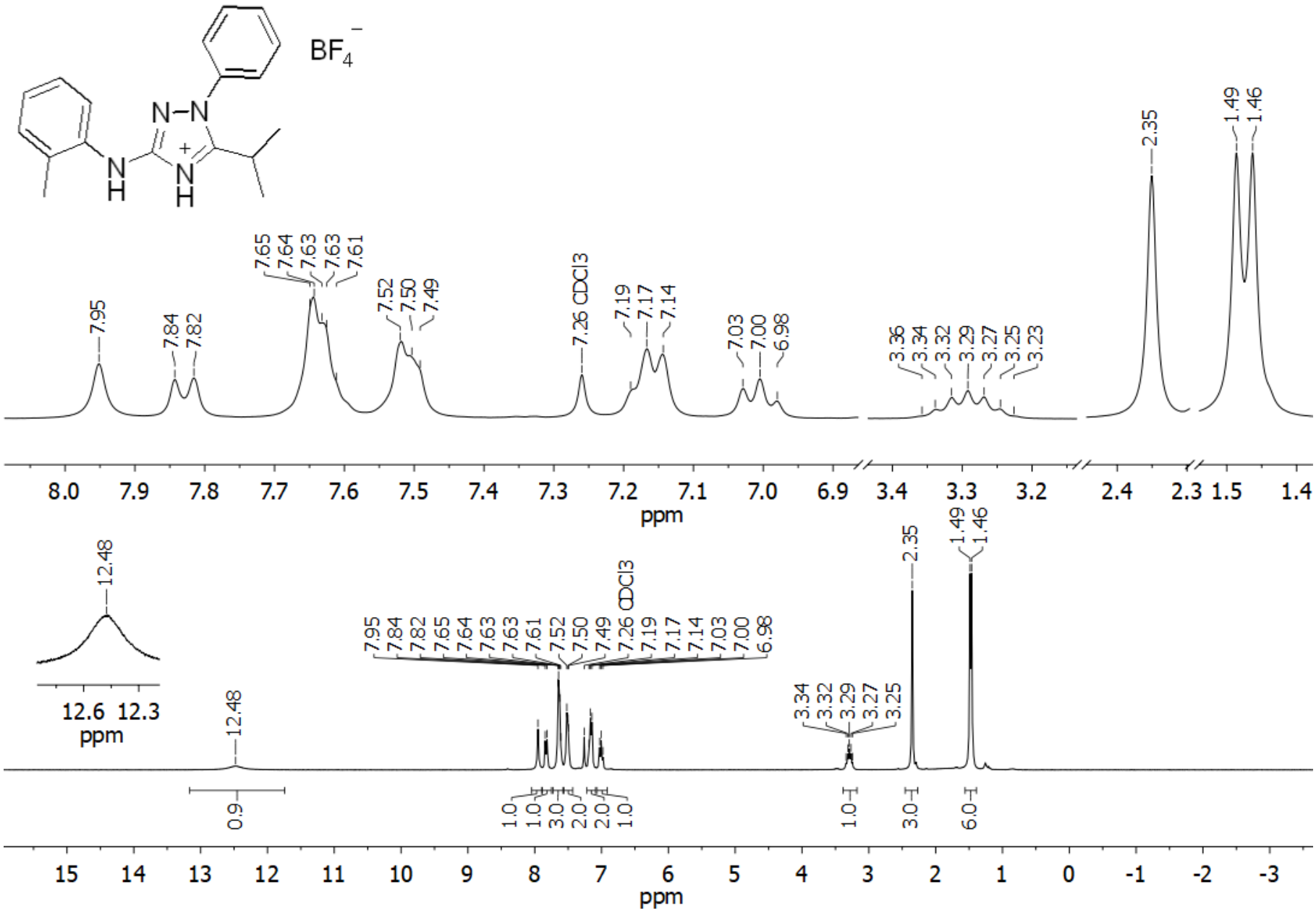

Figure S83. ^{1}H NMR spectrum of compound **4r** ($CDCl_3$, 300 MHz)

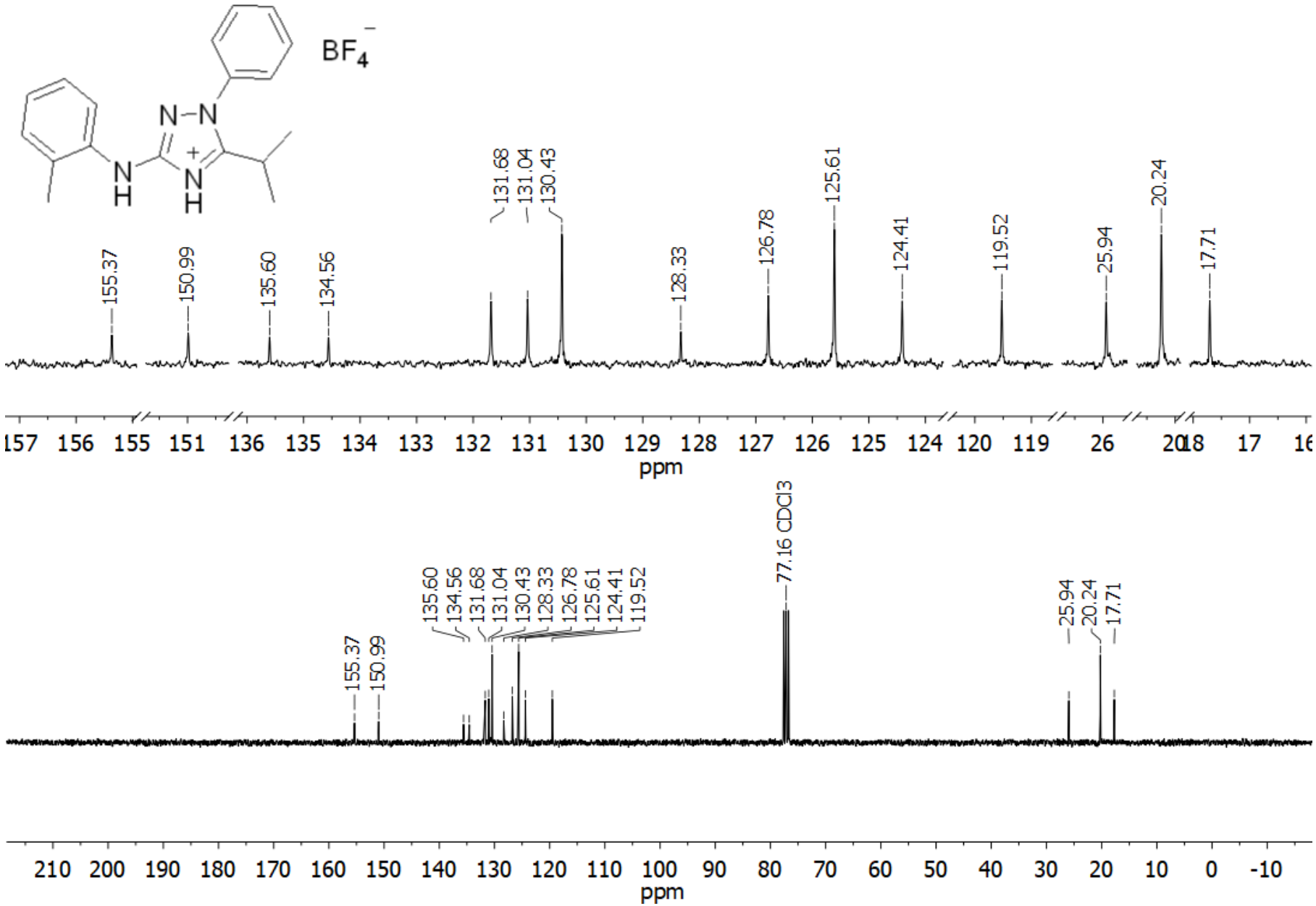

Figure S84. ^{13}C NMR spectrum of compound **4r** ($CDCl_3$, 75 MHz)

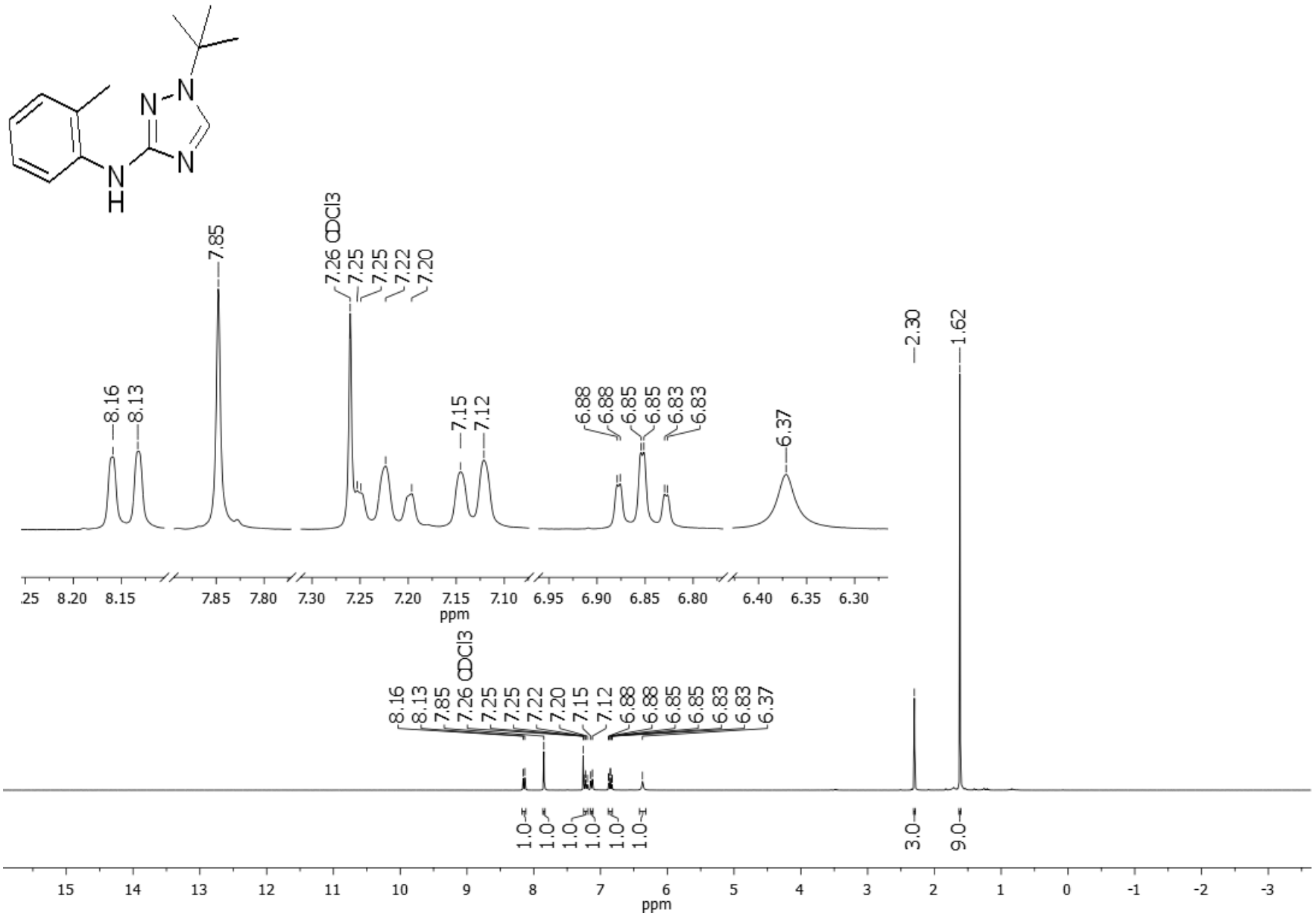

Figure S85. ^{1}H NMR spectrum of compound **4s** ($CDCl_3$, 300 MHz)

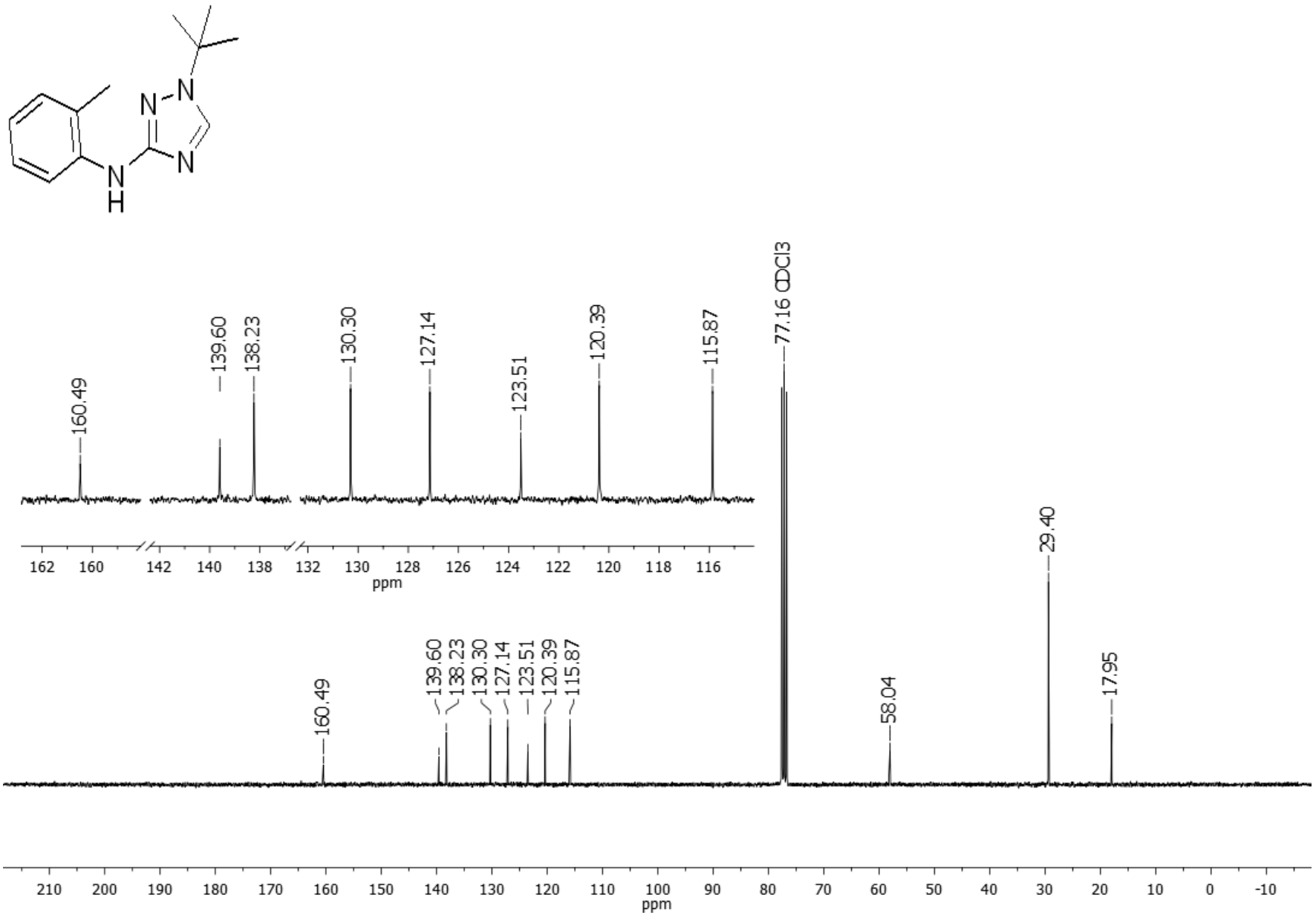

Figure S86. ^{13}C NMR spectrum of compound **4s** ($CDCl_3$, 75 MHz)

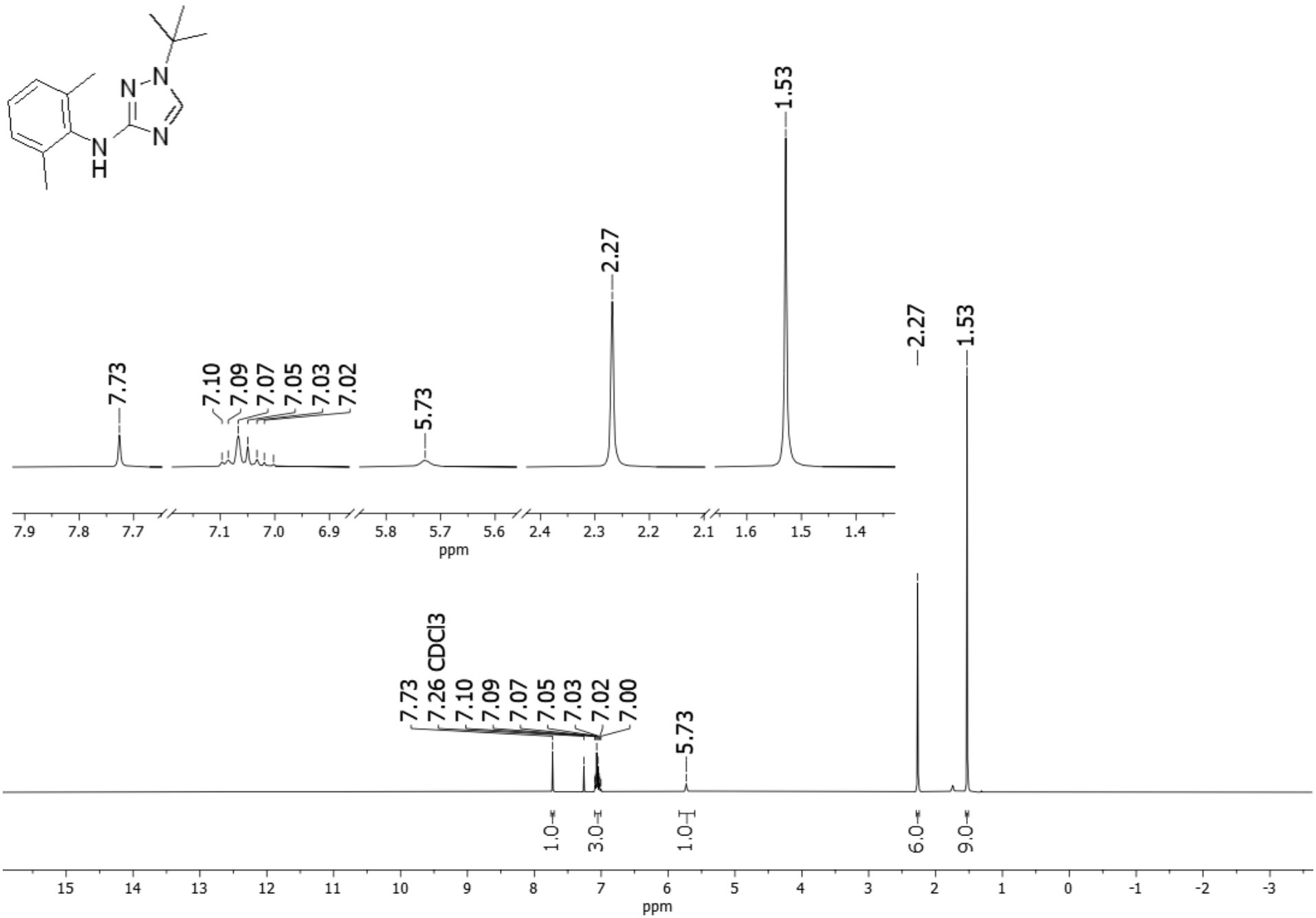

Figure S87. ^{1}H NMR spectrum of compound **4t** ($CDCl_3$, 300 MHz)

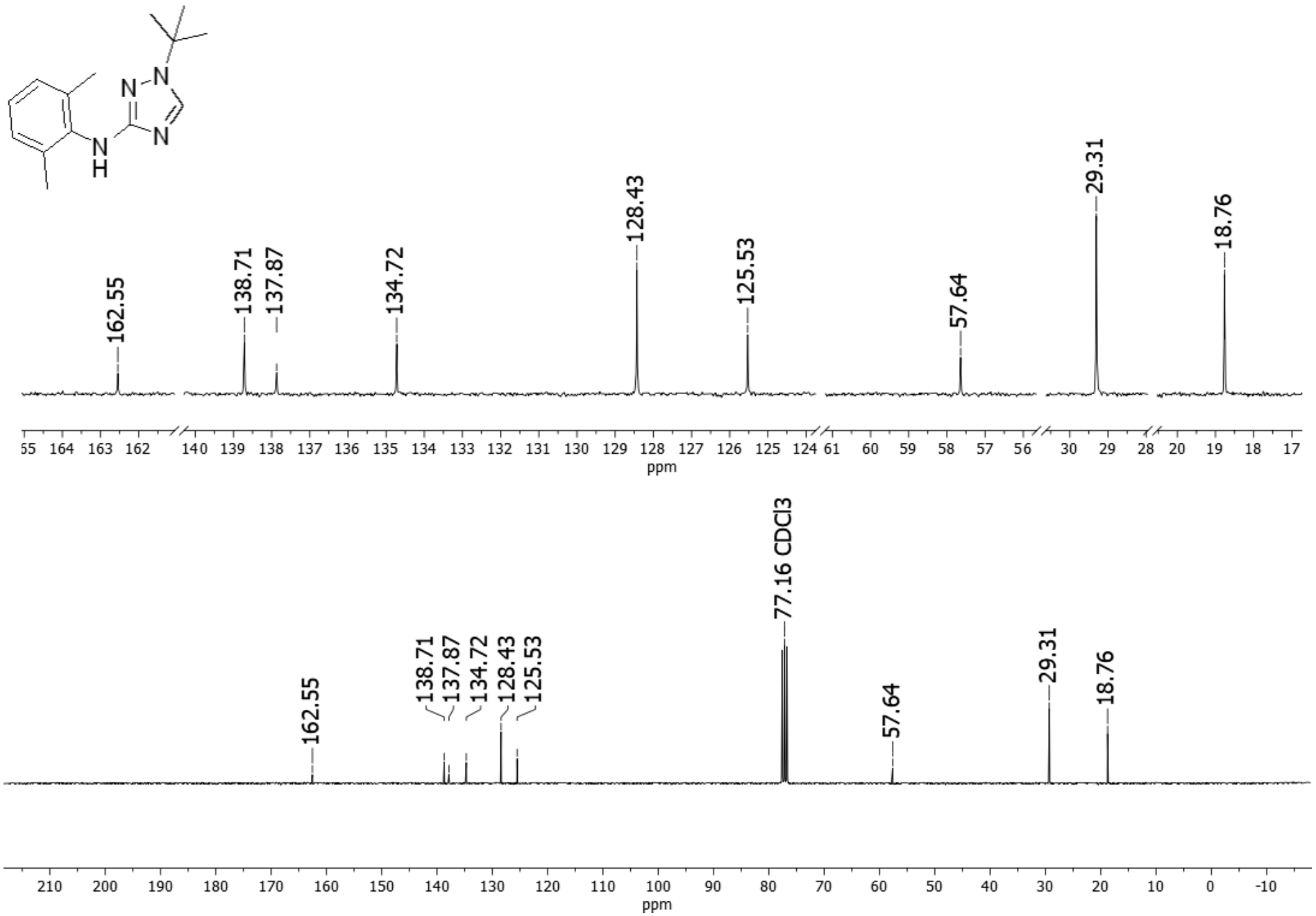

Figure S88. ^{13}C NMR spectrum of compound **4t** ($CDCl_3$, 75 MHz)

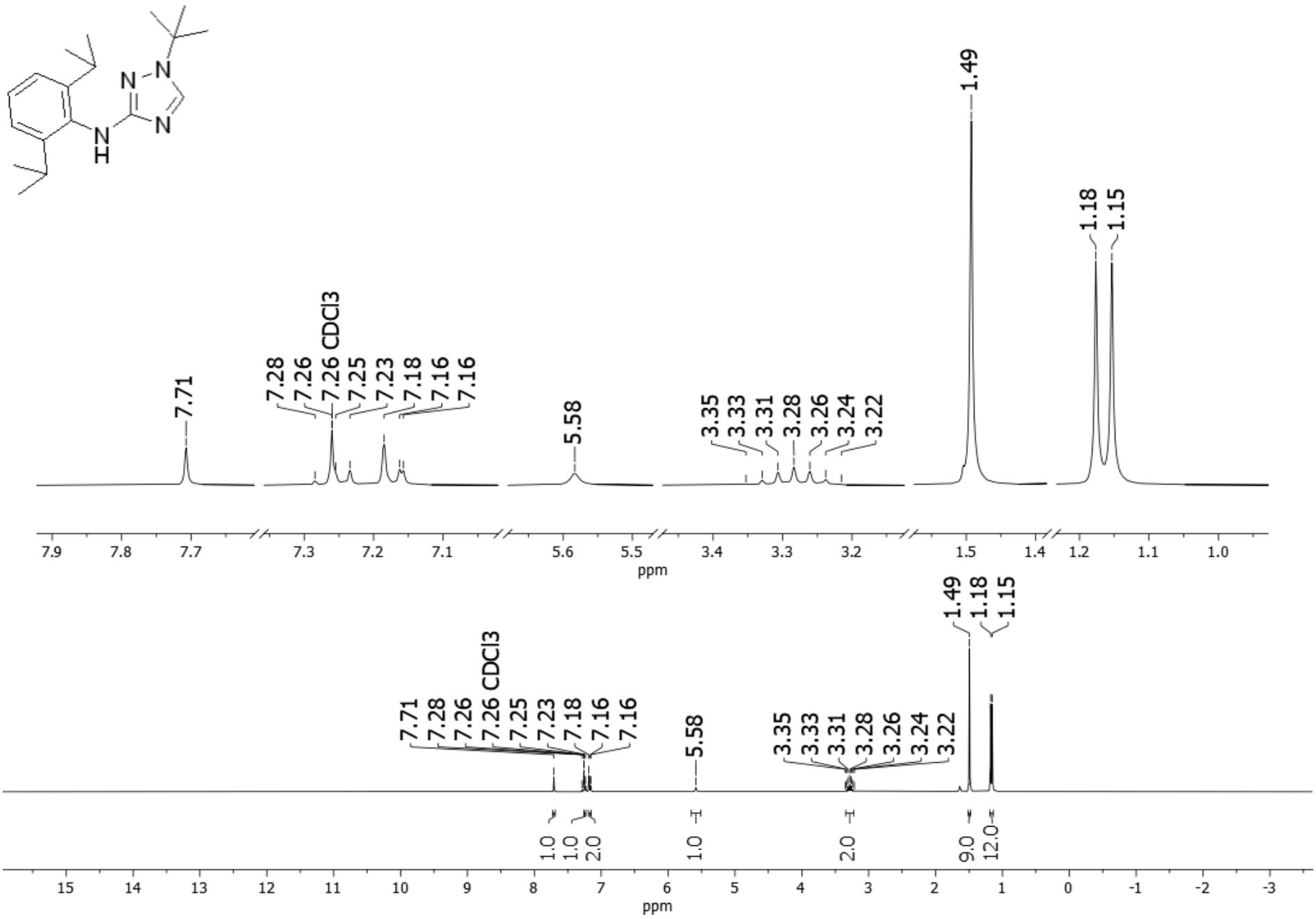

Figure S89. ^{1}H NMR spectrum of compound **4u** ($CDCl_3$, 300 MHz)

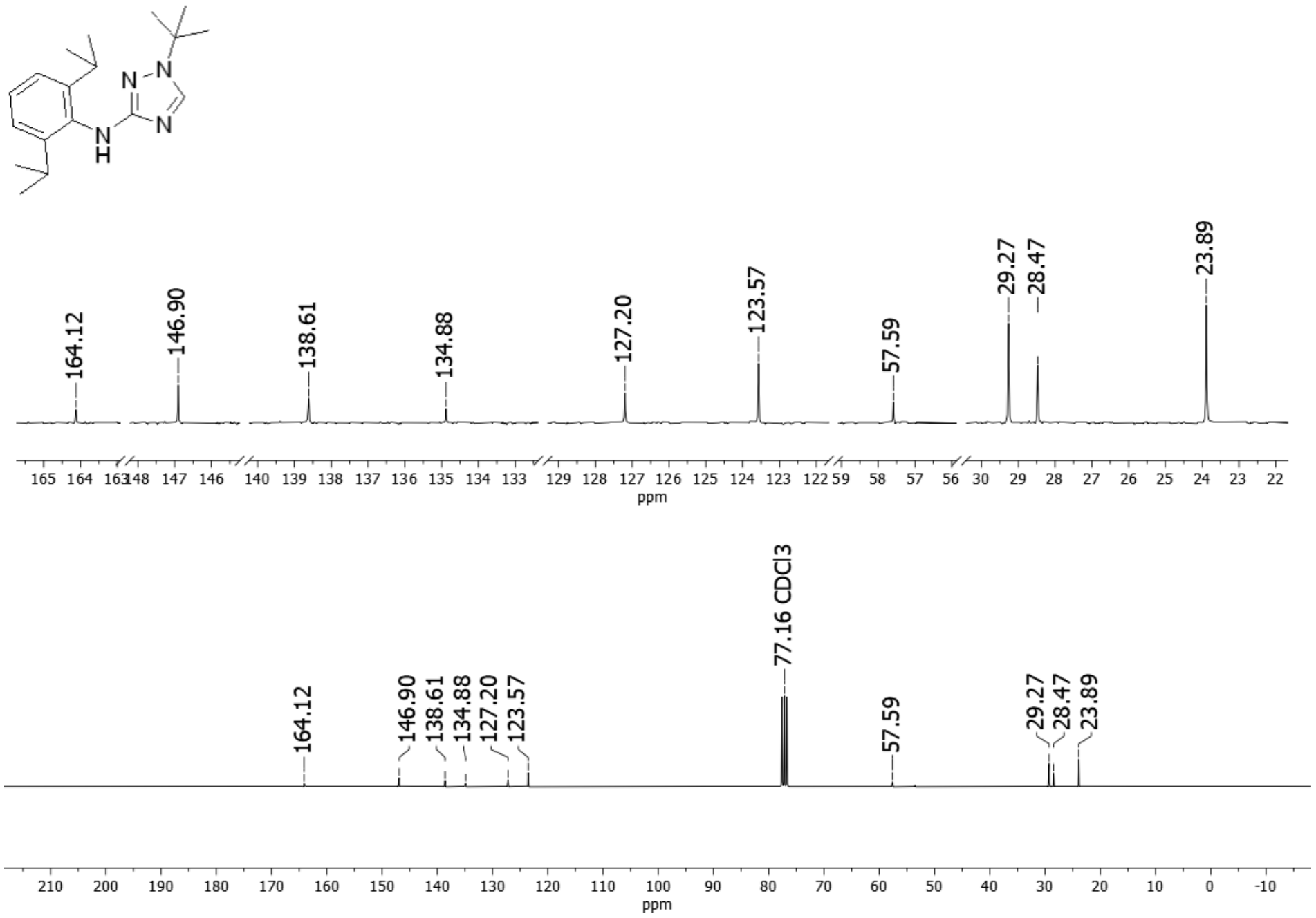

Figure S90. ^{13}C NMR spectrum of compound **4u** ($CDCl_3$, 75 MHz)

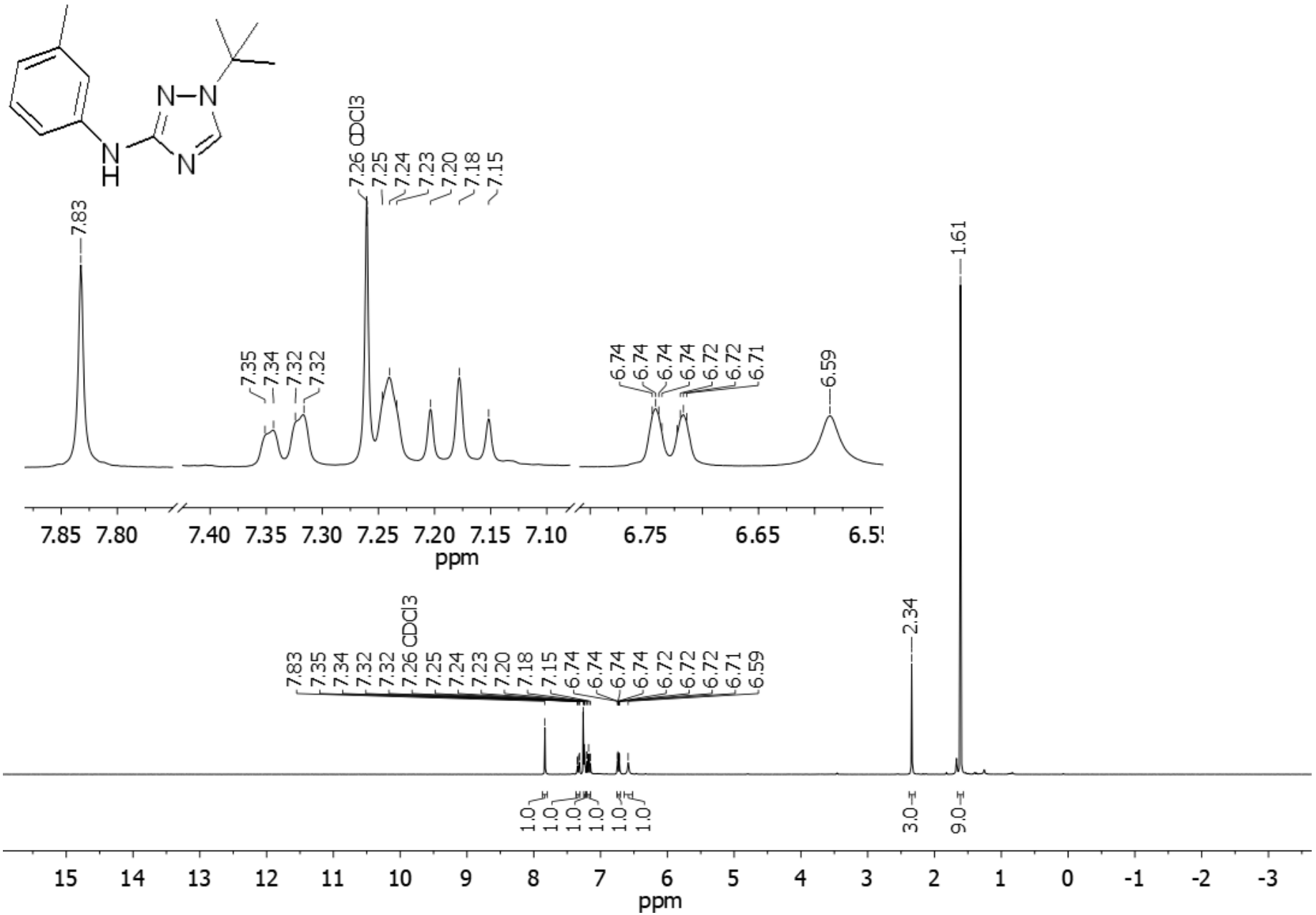

Figure S91. ^{1}H NMR spectrum of compound **4v** ($CDCl_3$, 300 MHz)

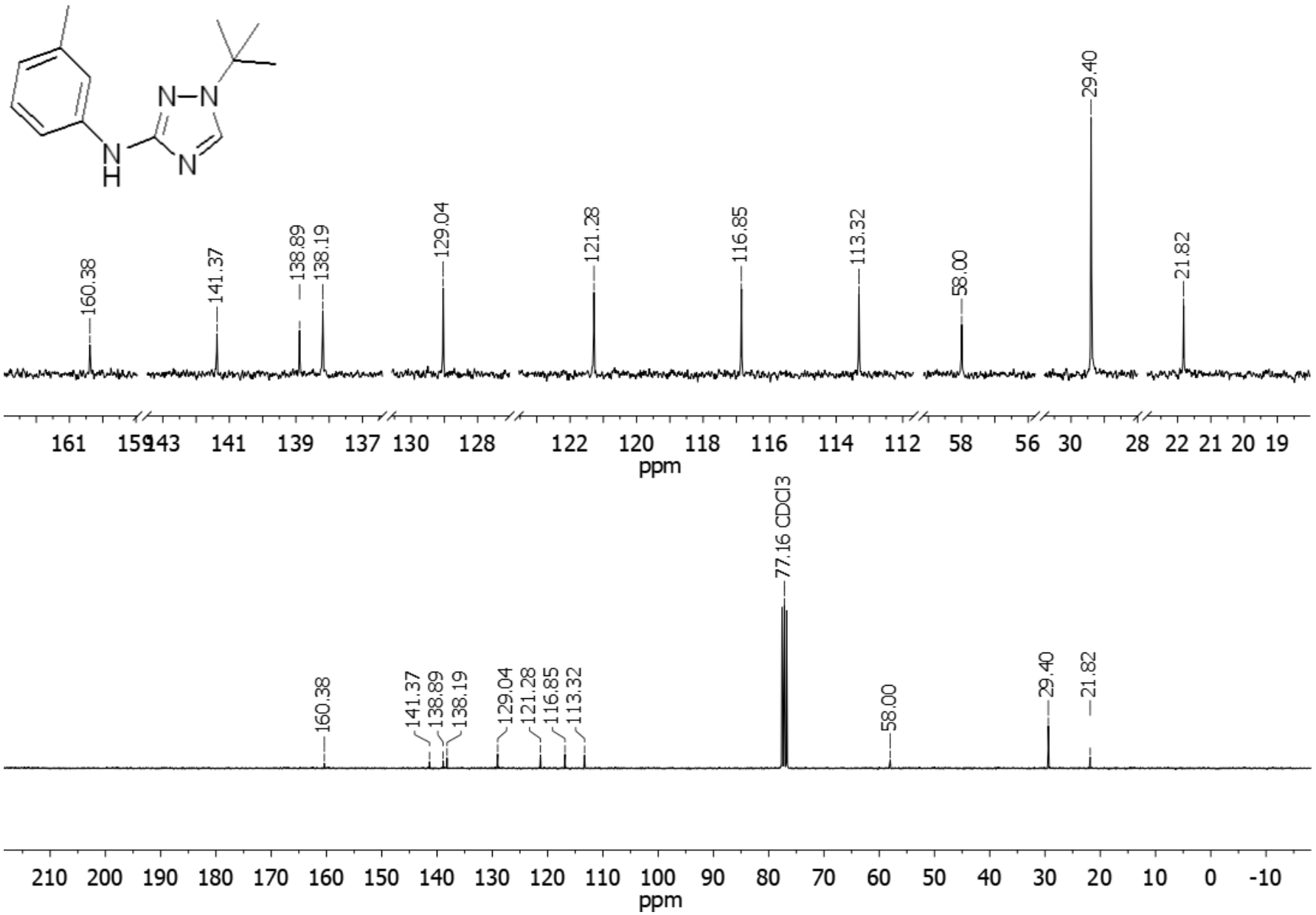

Figure S92. ^{13}C NMR spectrum of compound **4v** ($CDCl_3$, 75 MHz)

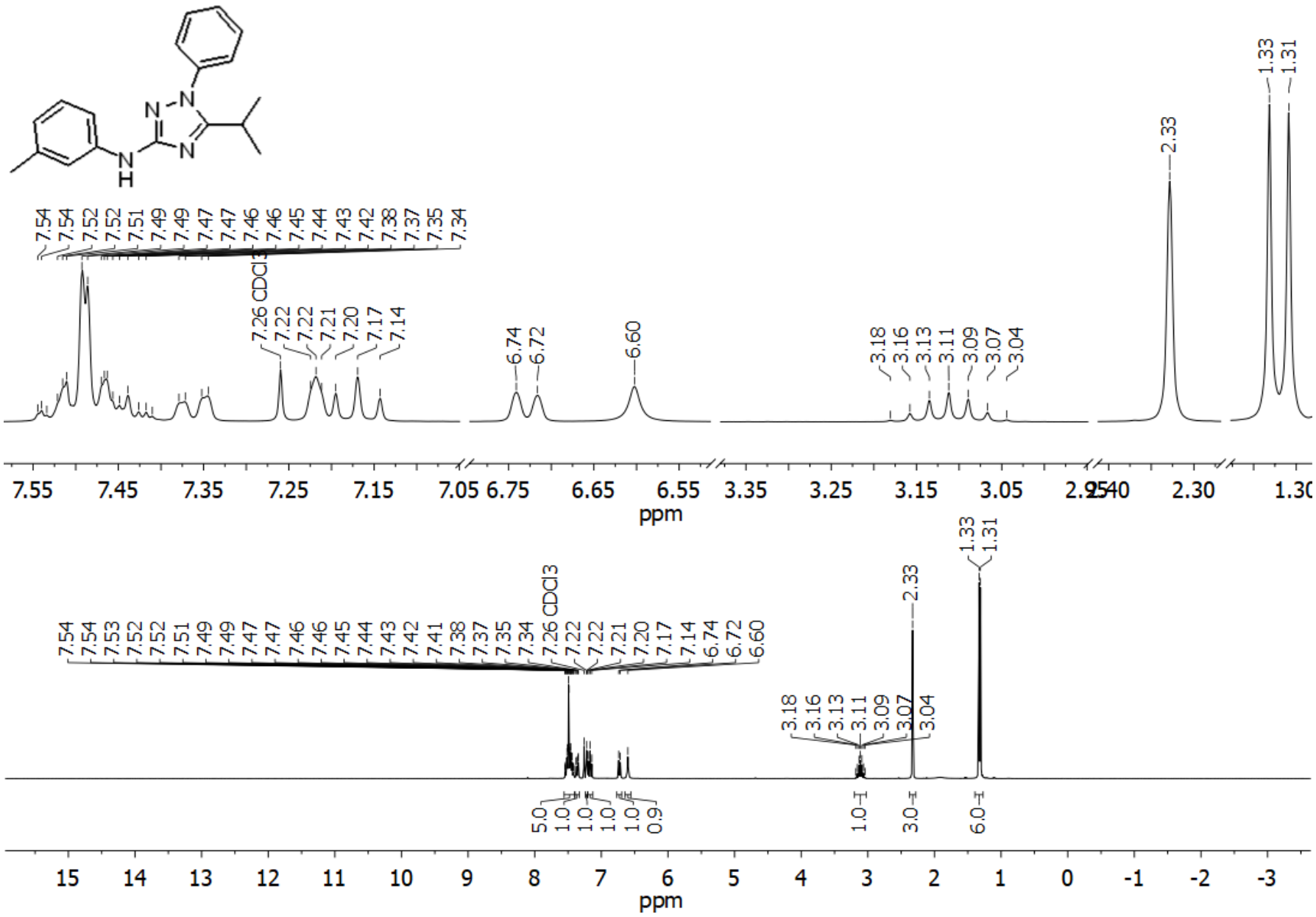

Figure S93. ^{1}H NMR spectrum of compound **4w** ($CDCl_3$, 300 MHz)

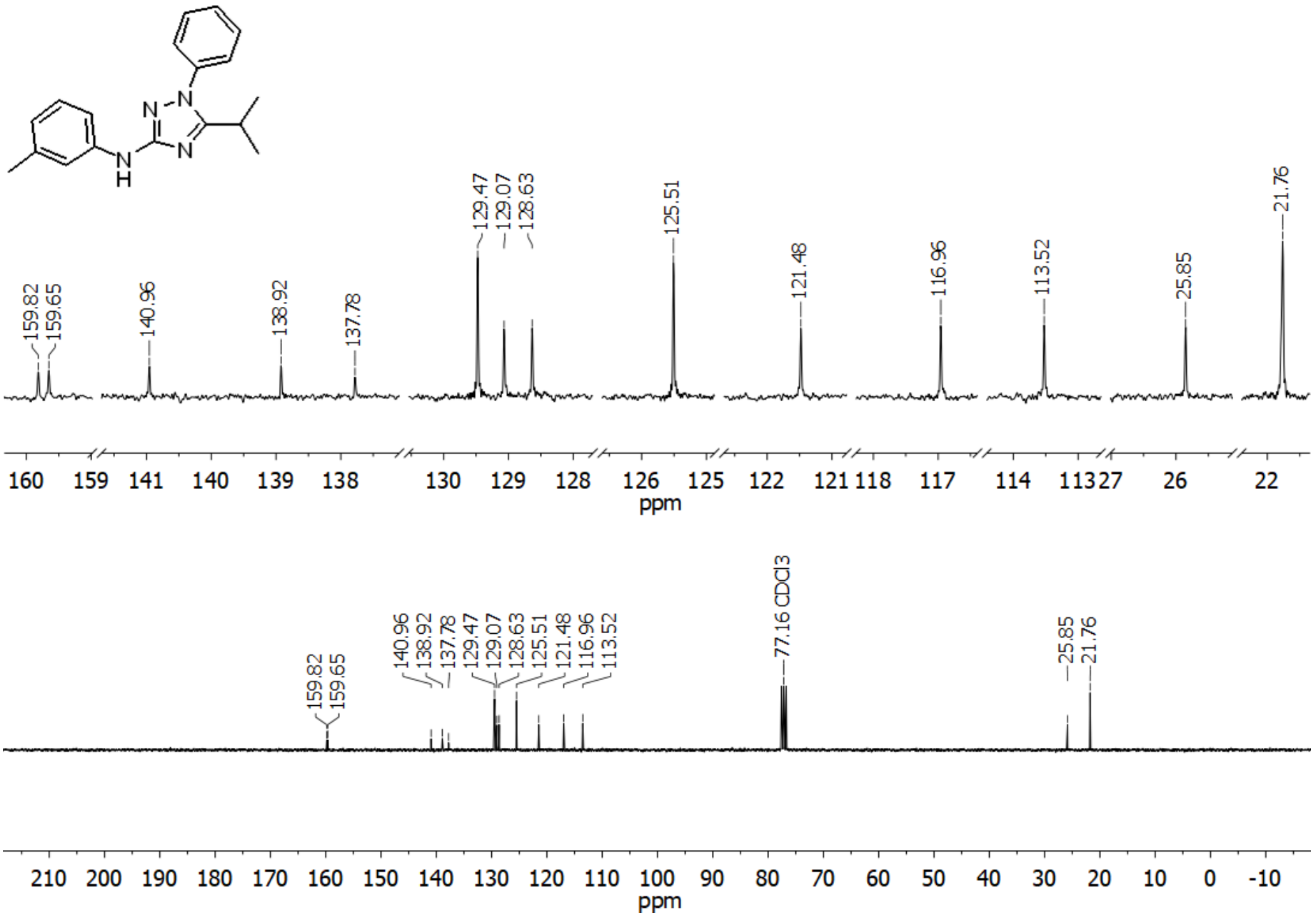

Figure S94. ^{13}C NMR spectrum of compound **4w** ($CDCl_3$, 75 MHz)

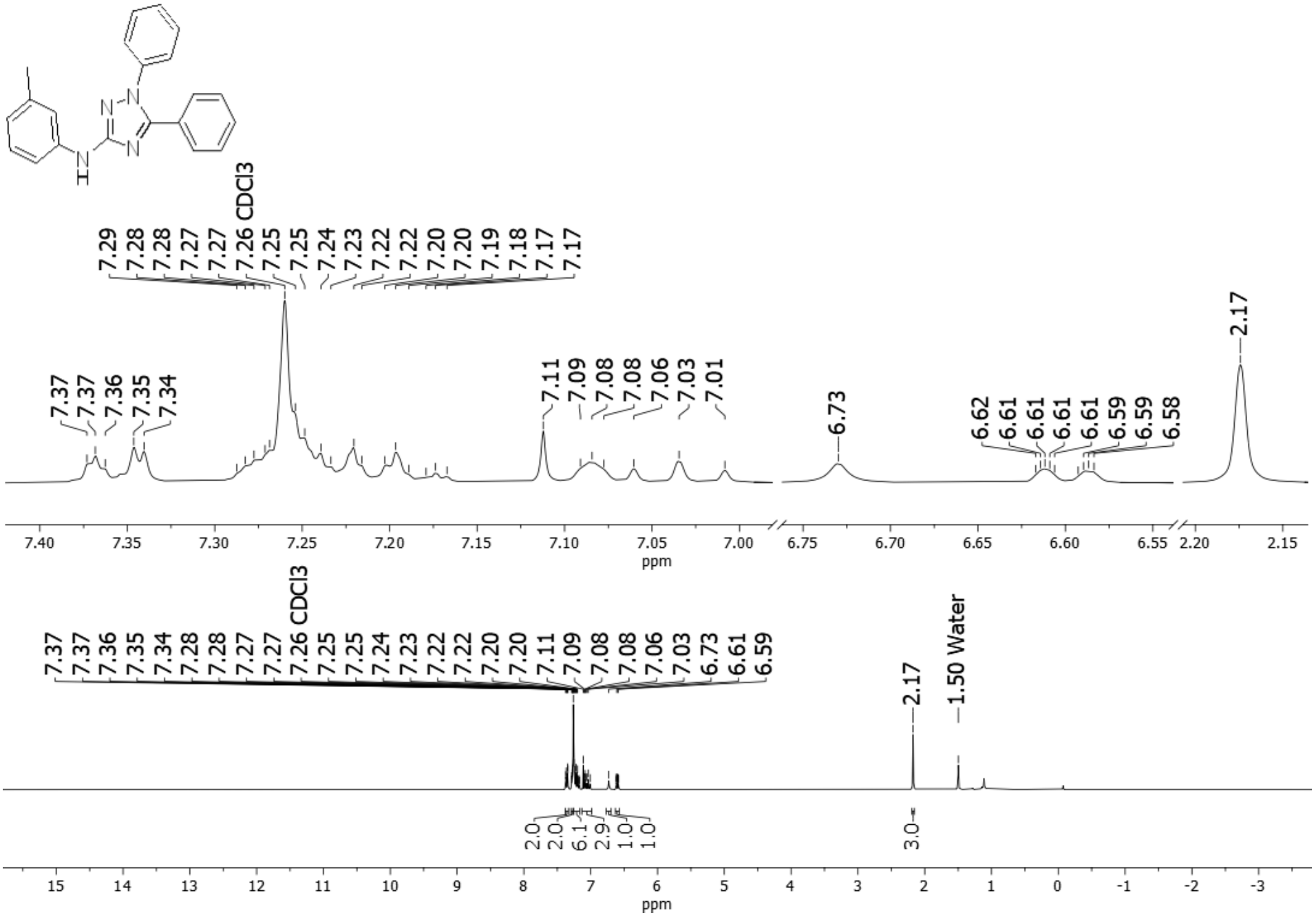

Figure S95. ^{1}H NMR spectrum of compound **4x** ($CDCl_3$, 300 MHz)

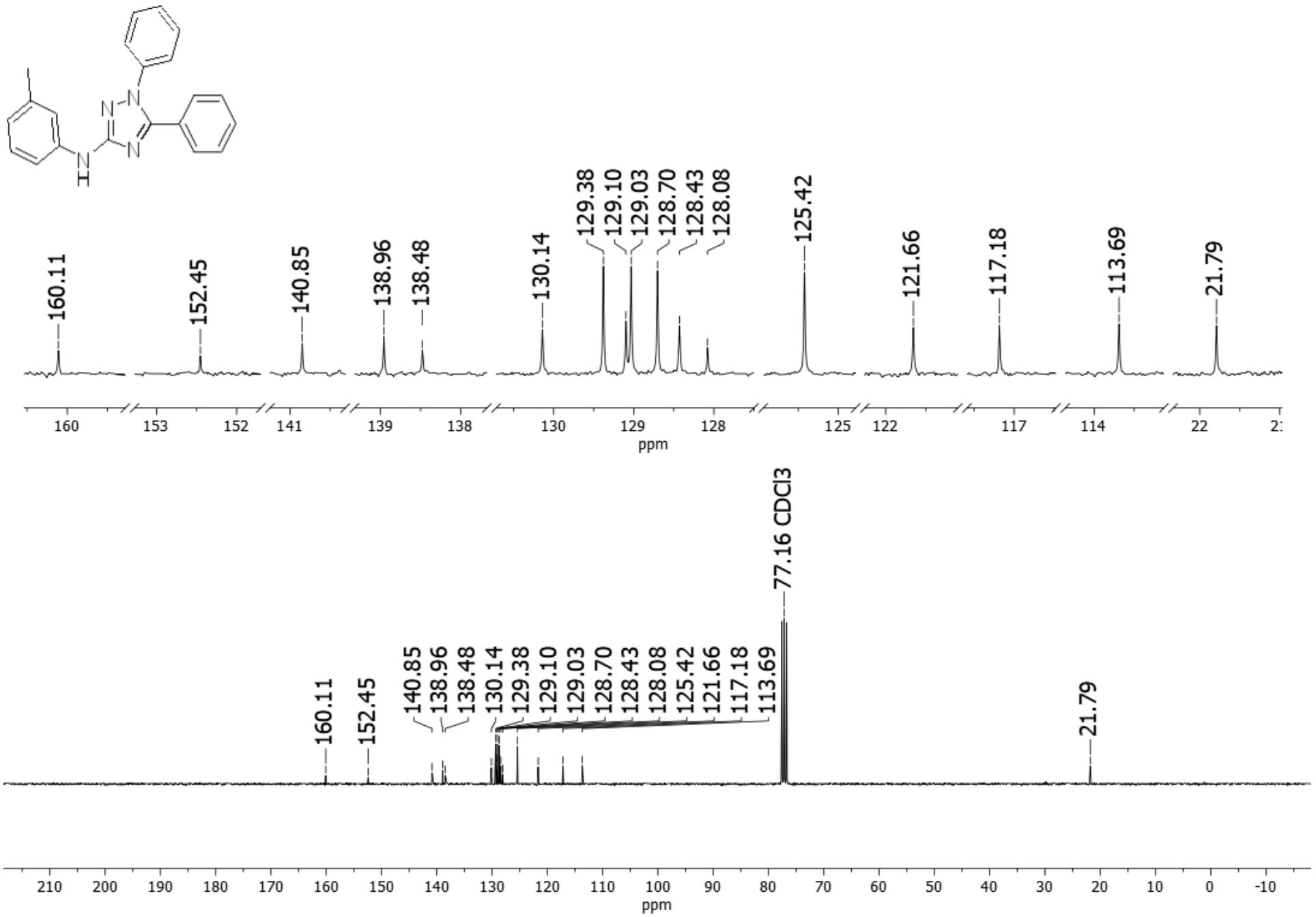

Figure S96. ^{13}C NMR spectrum of compound **4x** ($CDCl_3$, 75 MHz)

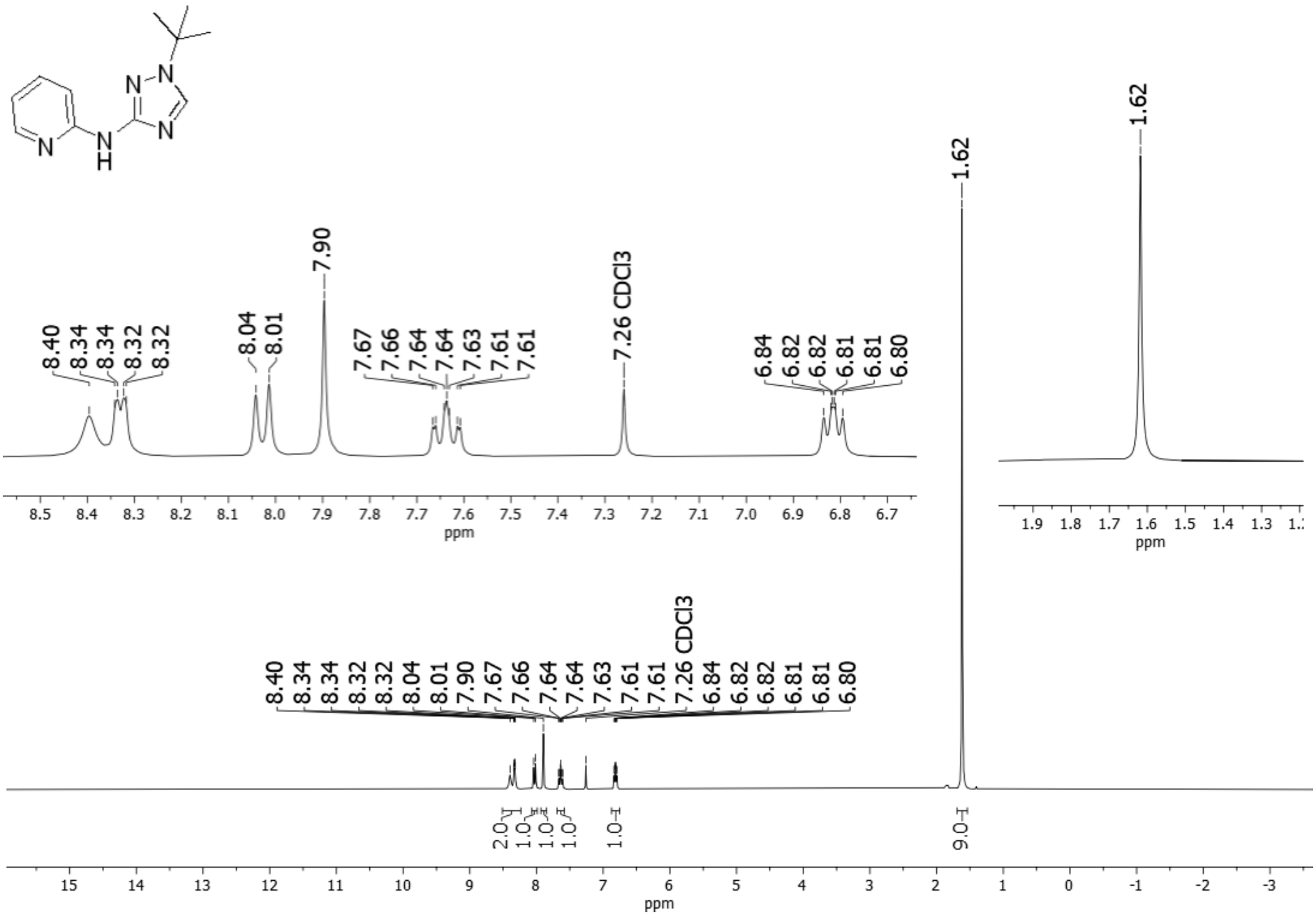

Figure S97. ^{1}H NMR spectrum of compound **4y** ($CDCl_3$, 300 MHz)

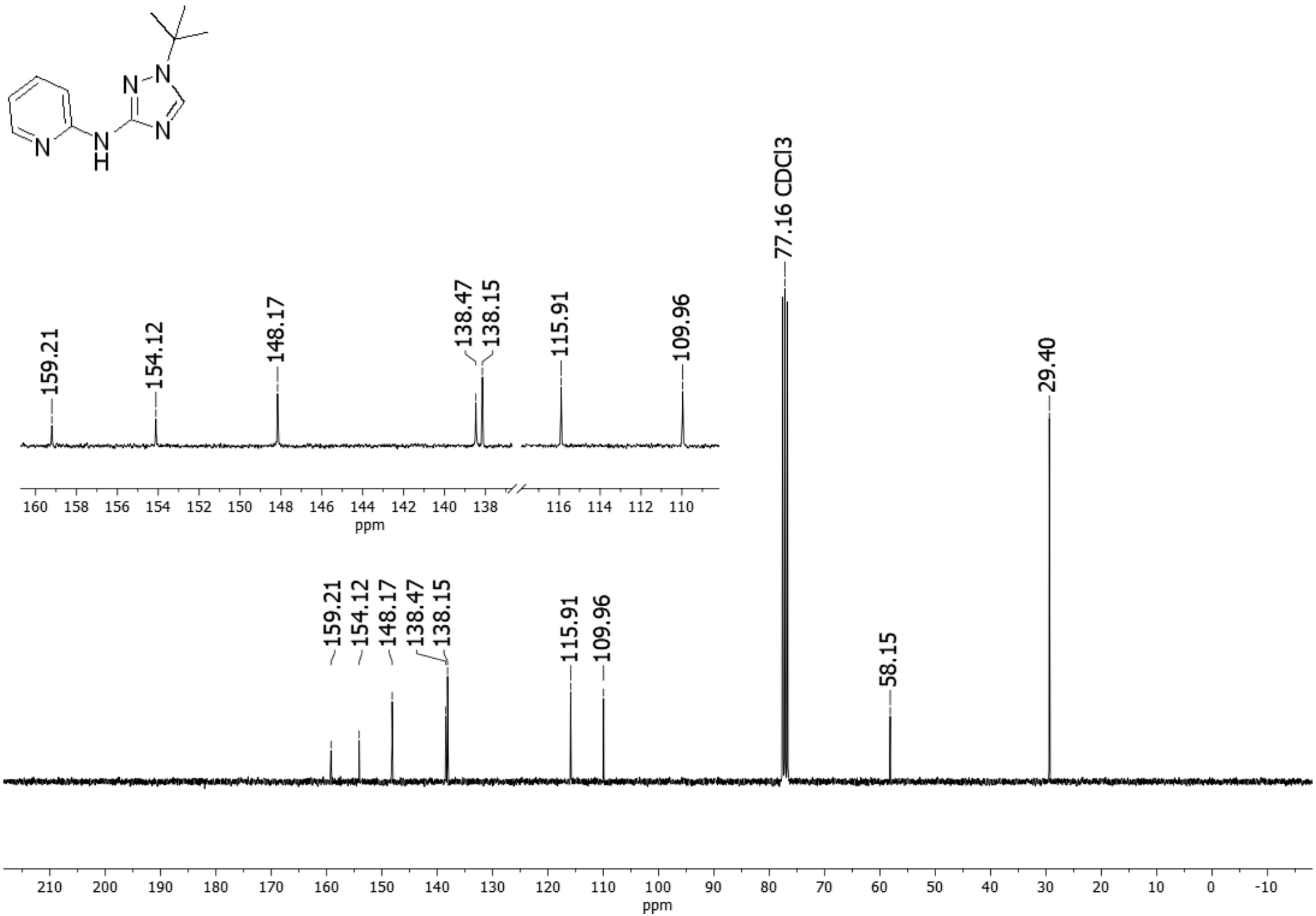

Figure S98. ^{13}C NMR spectrum of compound **4y** ($CDCl_3$, 75 MHz)

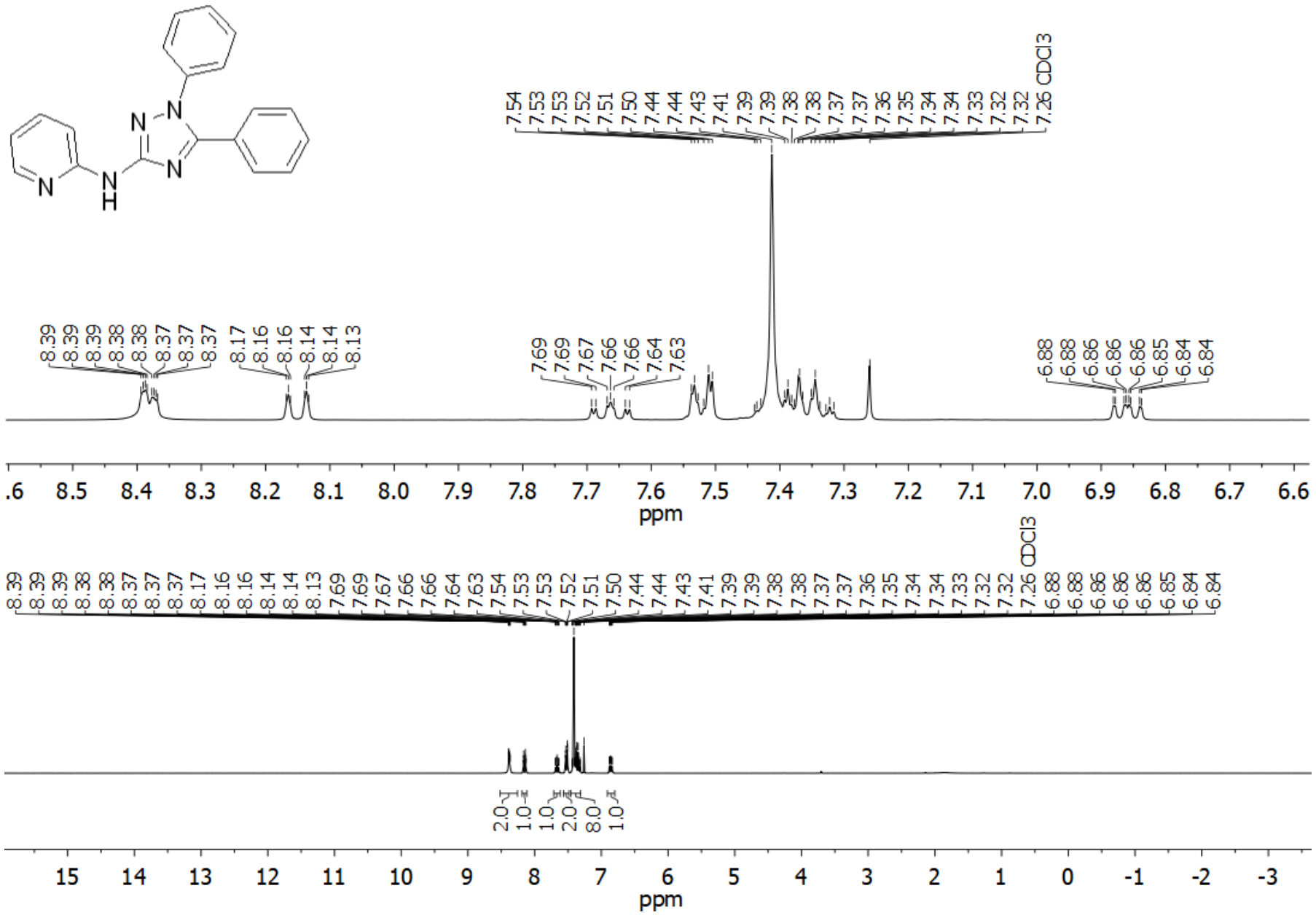

Figure S99. ^{1}H NMR spectrum of compound **4z** ($CDCl_3$, 300 MHz)

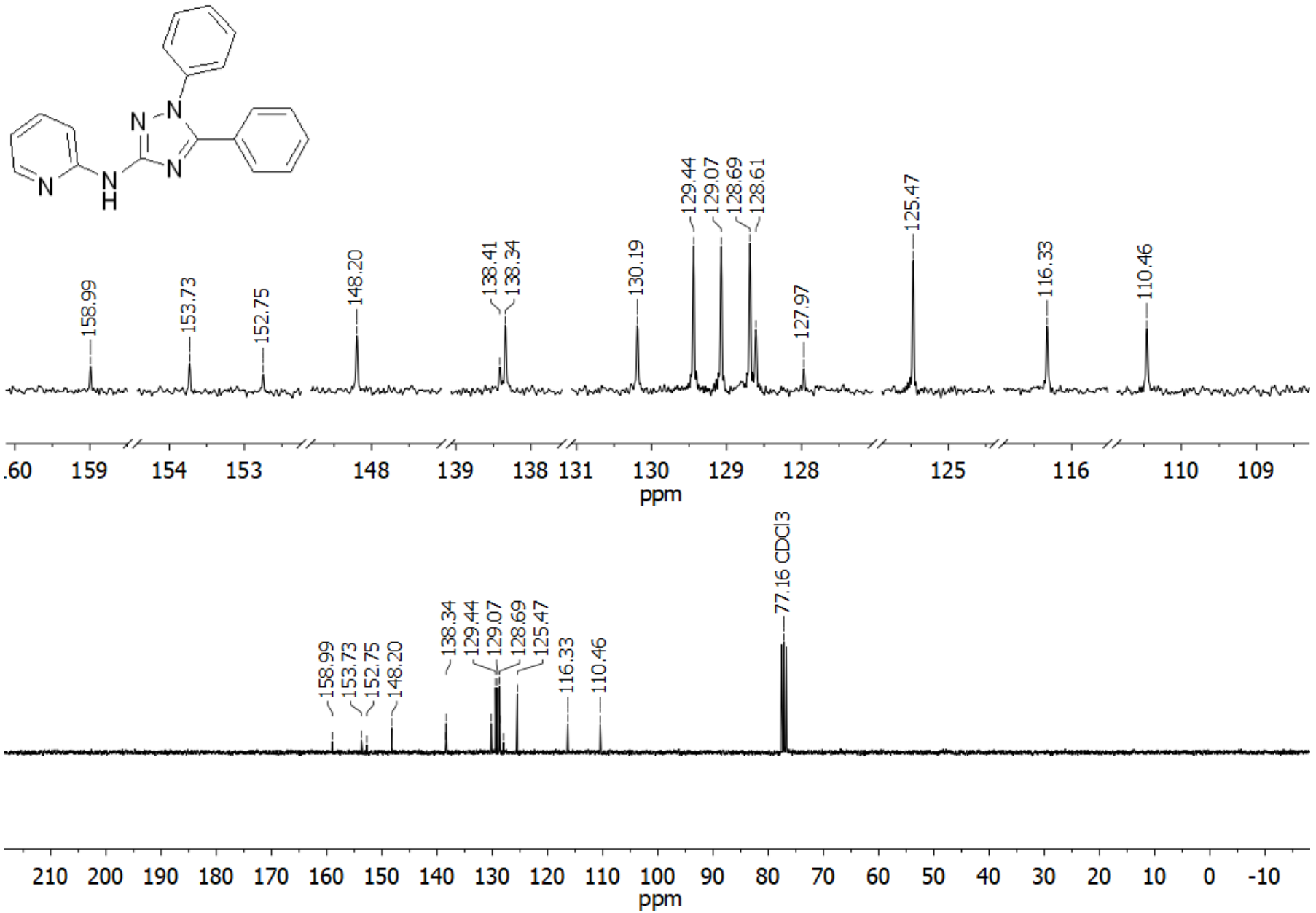

Figure S100. ^{13}C NMR spectrum of compound **4z** ($CDCl_3$, 75 MHz)

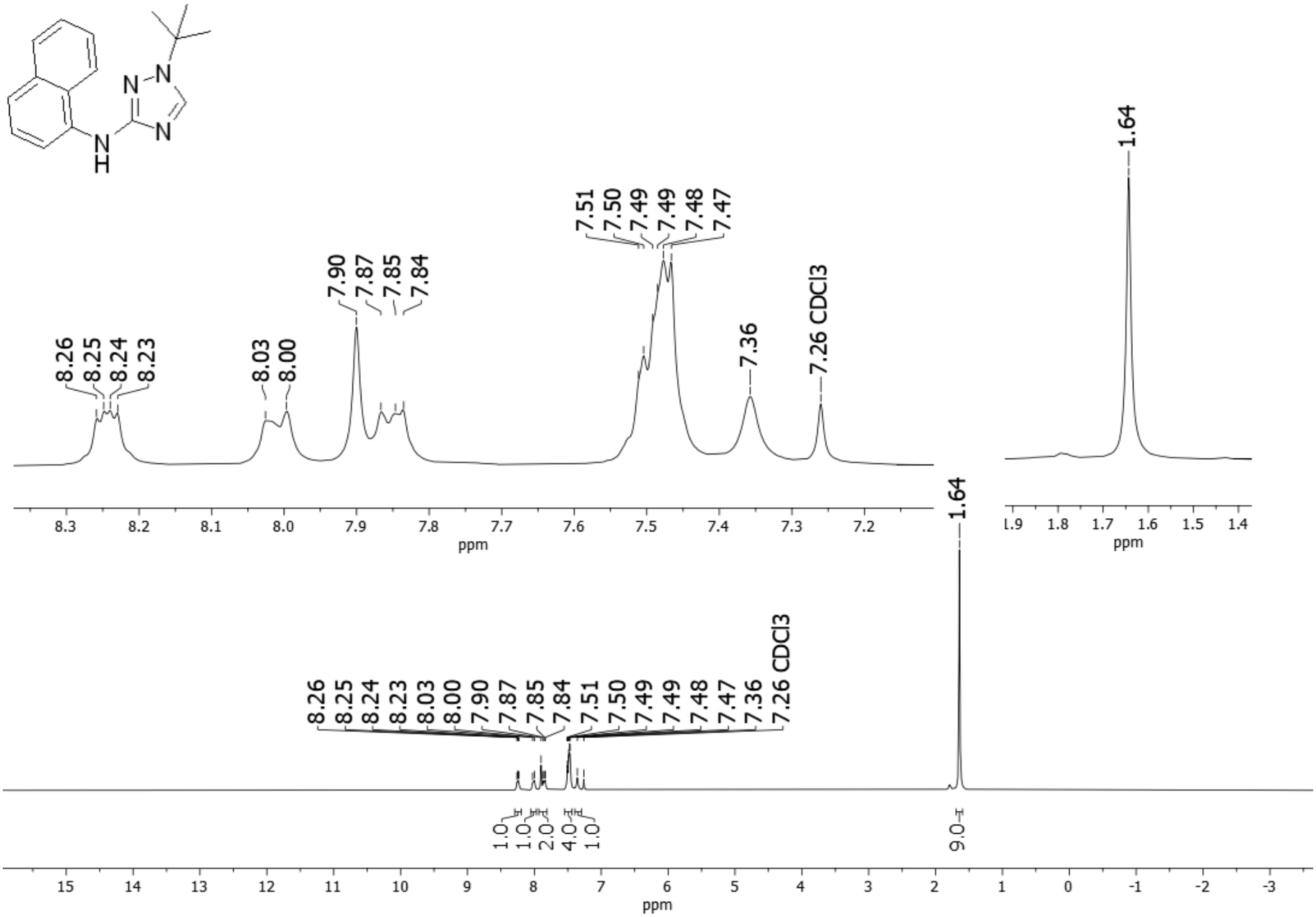

Figure S101. ^{1}H NMR spectrum of compound **4aa** ($CDCl_3$, 300 MHz)

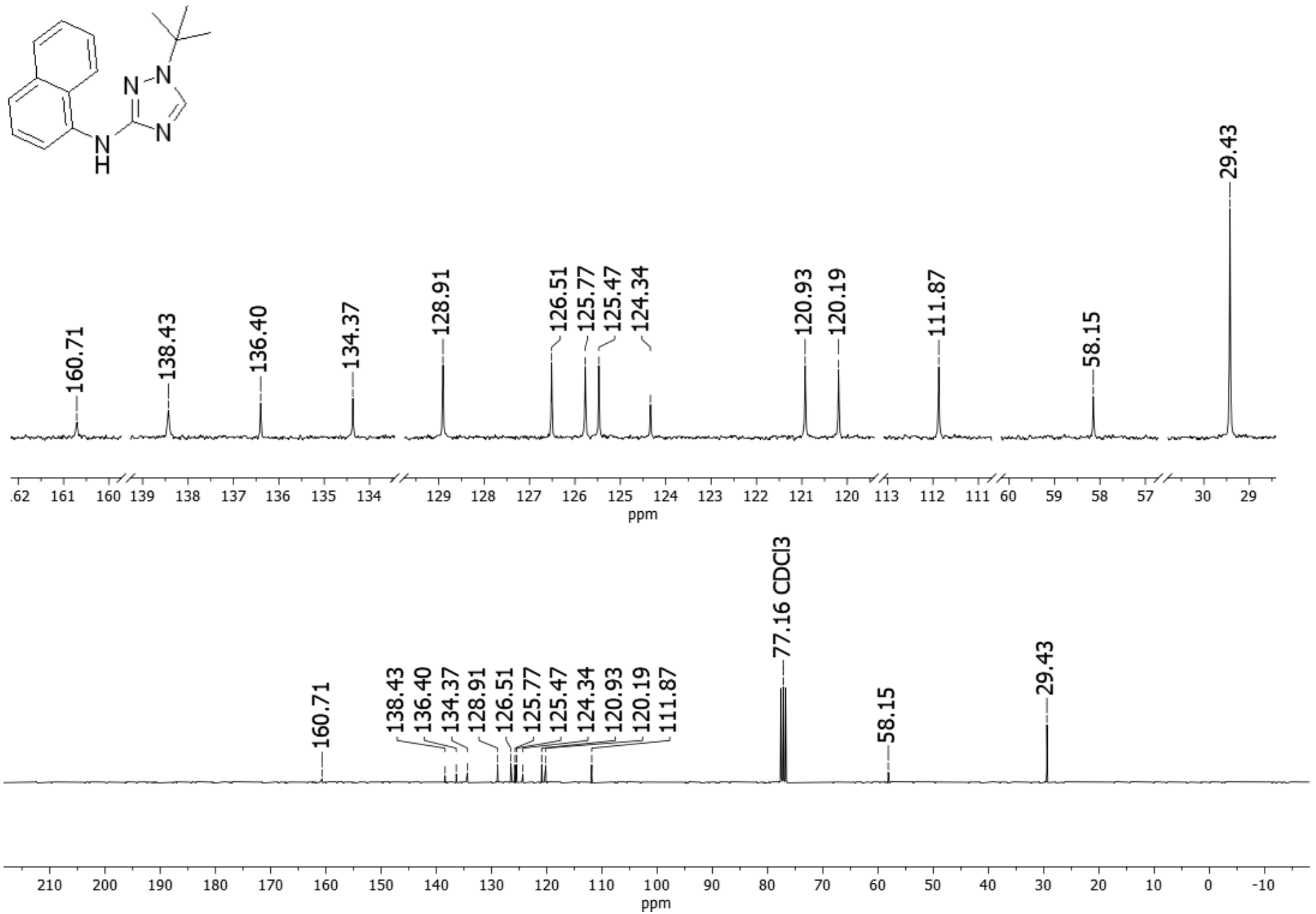

Figure S102. ^{13}C NMR spectrum of compound **4aa** ($CDCl_3$, 75 MHz)

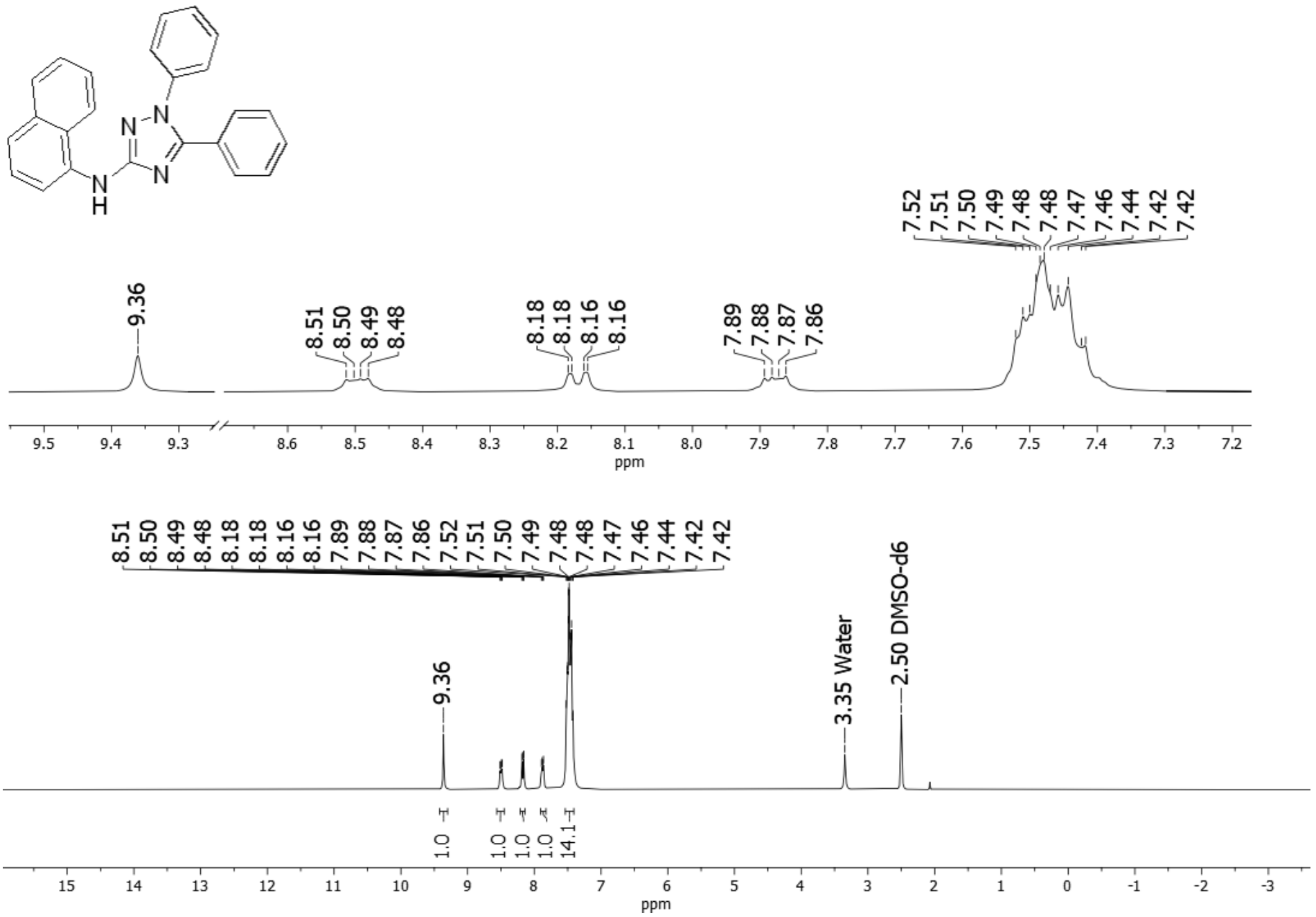

Figure S103. ^{1}H NMR spectrum of compound **4ab** (DMSO-d_6, 300 MHz)

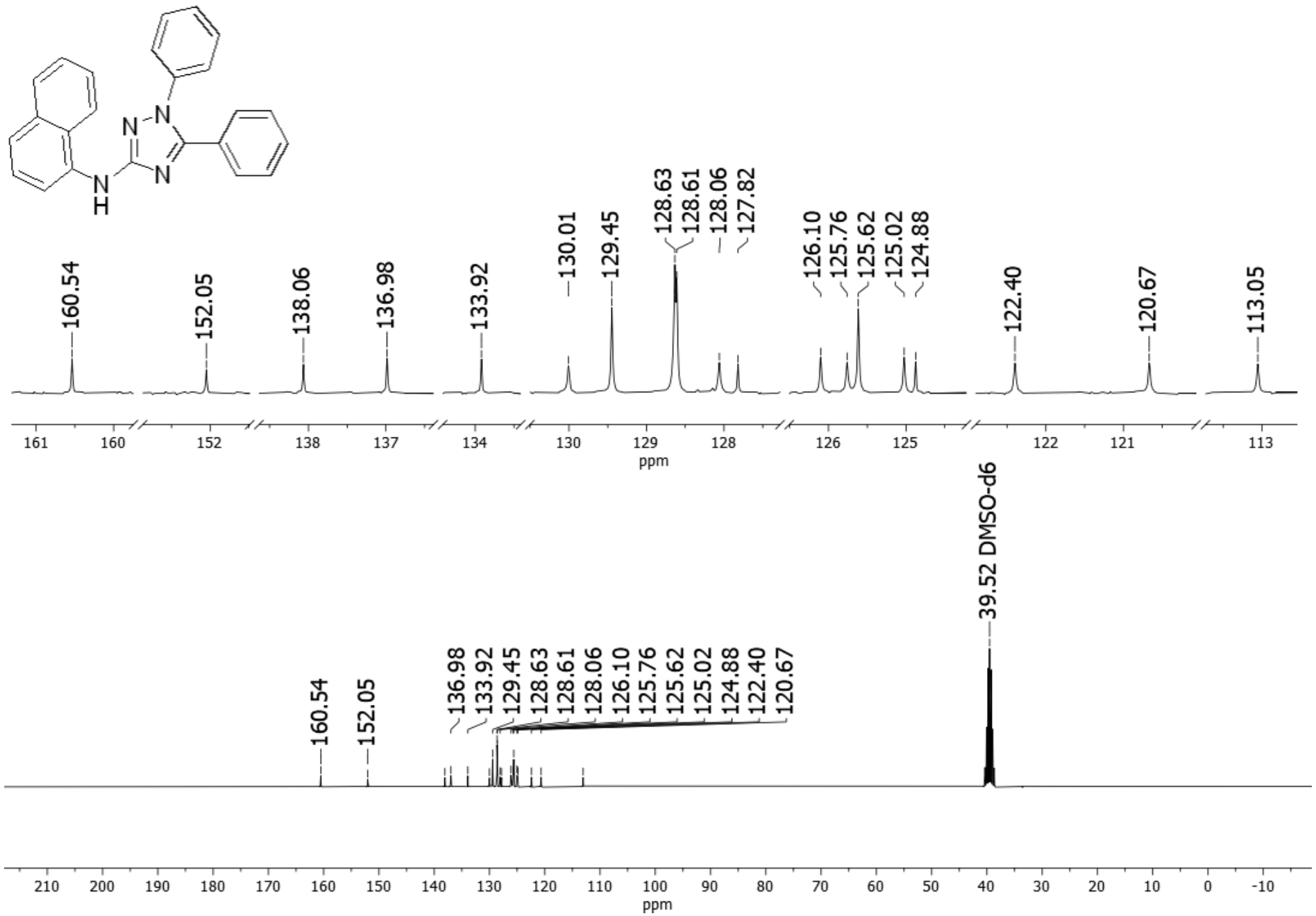

Figure S104. ^{13}C NMR spectrum of compound **4ab** (DMSO-d_6, 75 MHz)

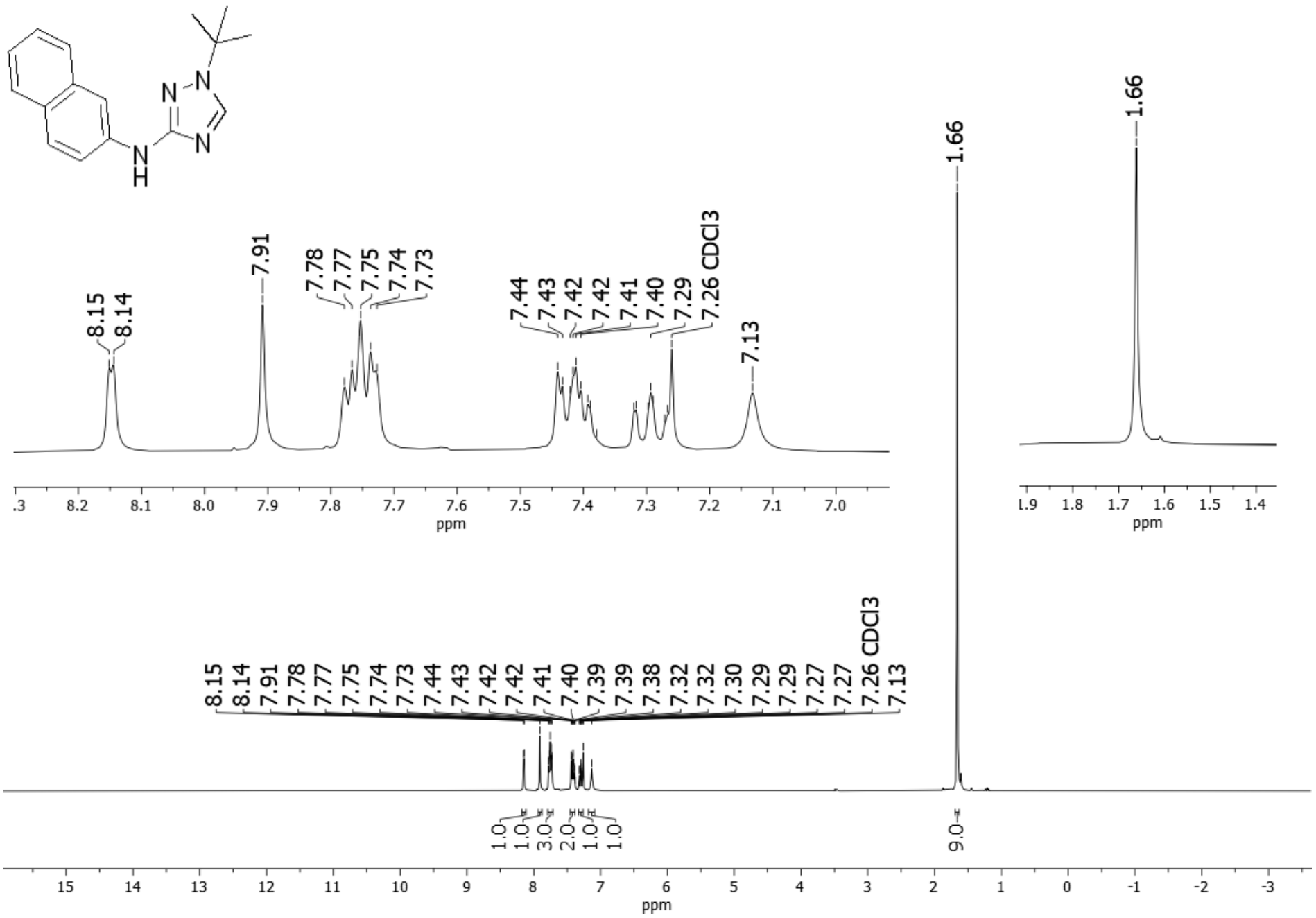

Figure S105. ^{1}H NMR spectrum of compound **4ac** ($CDCl_3$, 300 MHz)

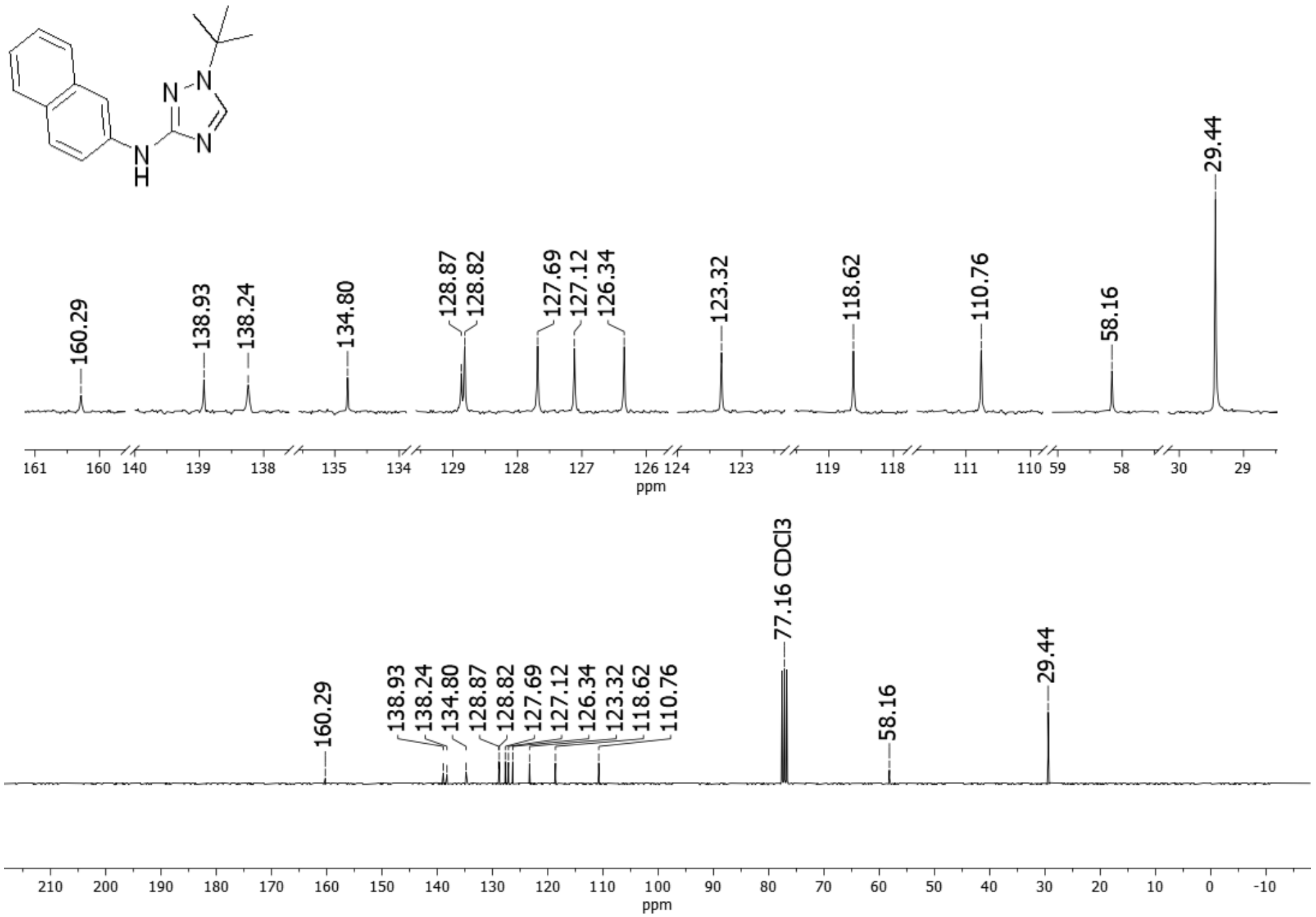

Figure S106. ^{13}C NMR spectrum of compound **4ac** ($CDCl_3$, 75 MHz)

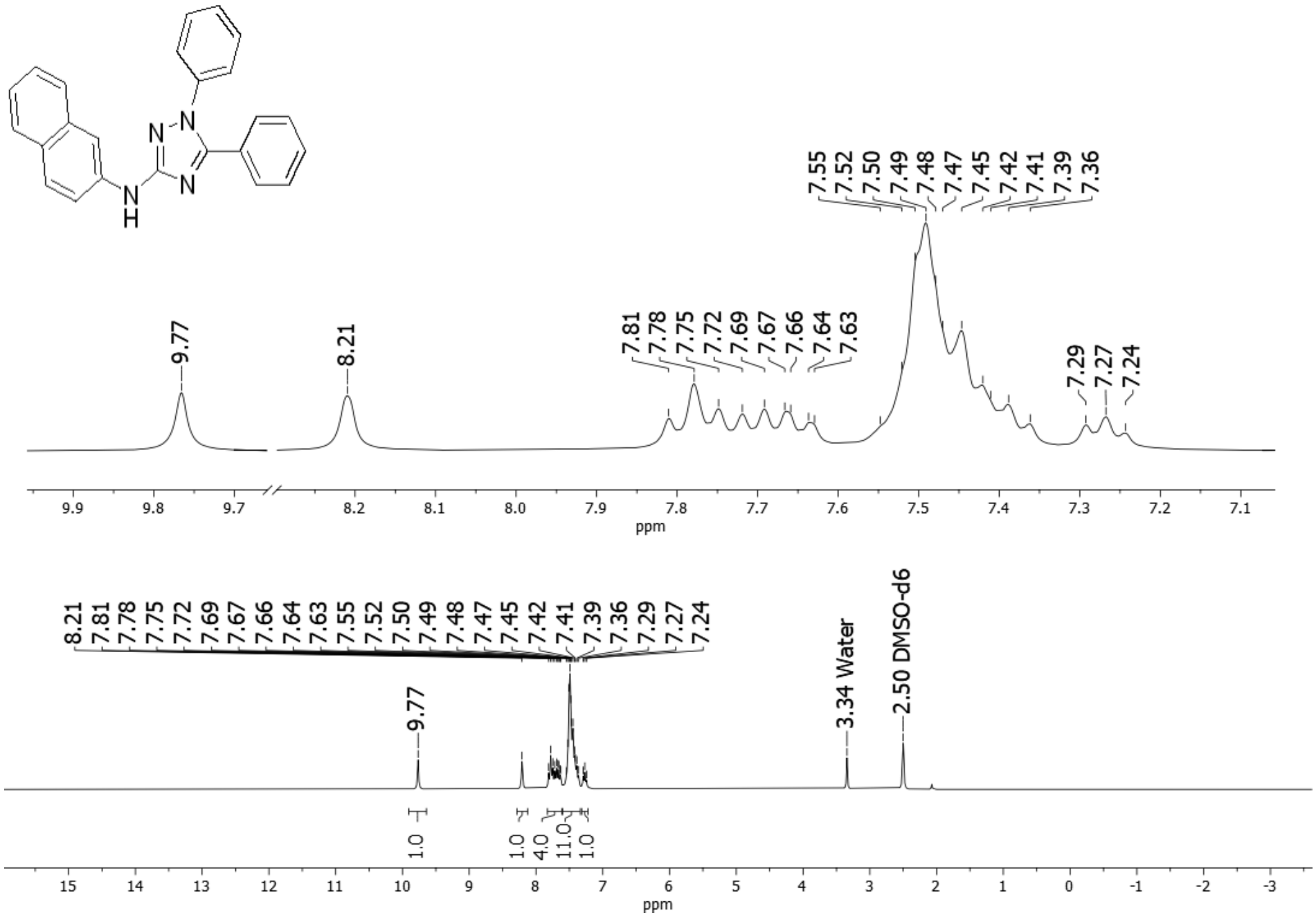

Figure S107. ^{1}H NMR spectrum of compound **4ad** (DMSO-d_6, 300 MHz)

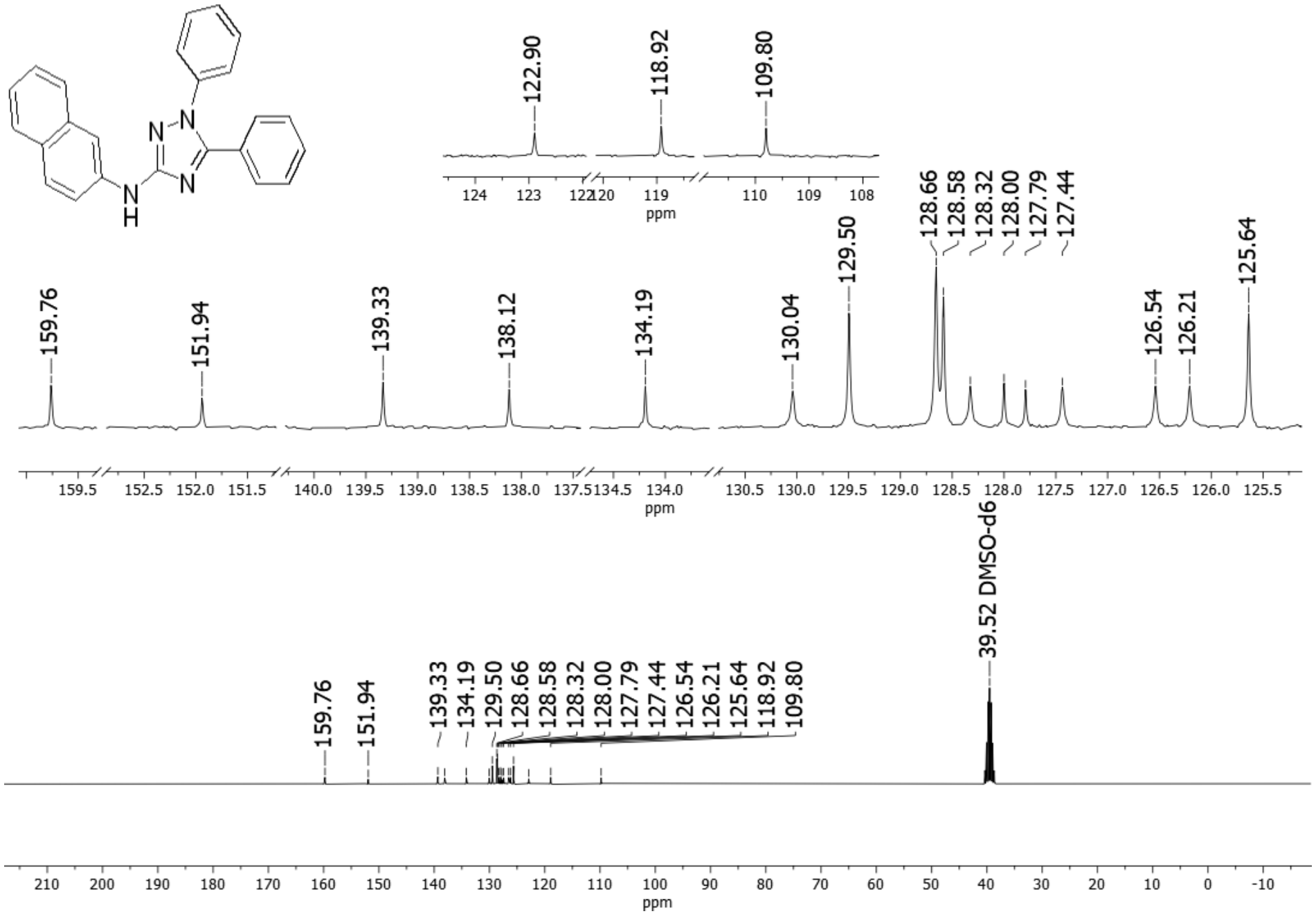

Figure S108. ^{13}C NMR spectrum of compound **4ad** (DMSO-*d*$_6$, 75 MHz)

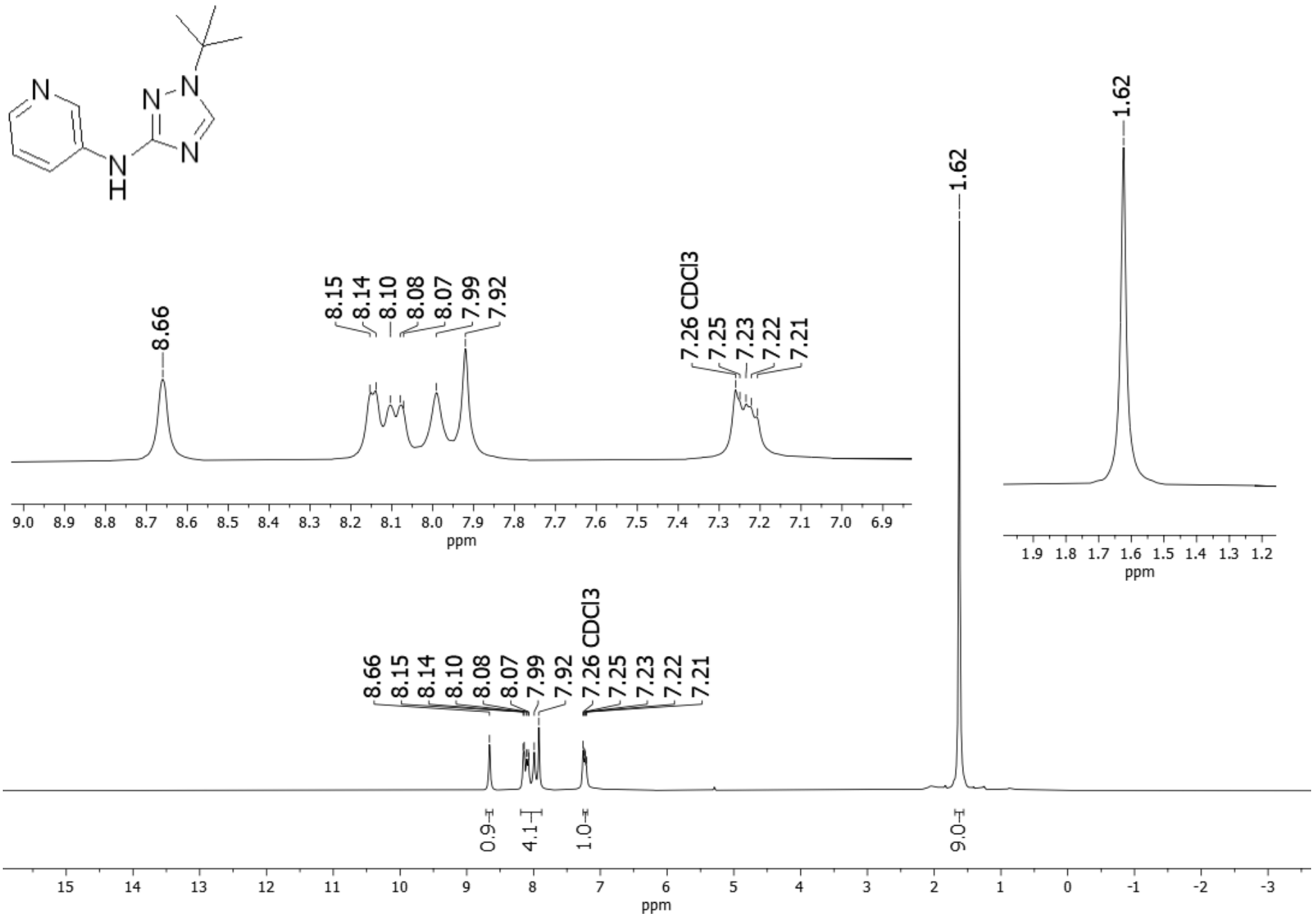

Figure S109. ^{1}H NMR spectrum of compound **4ae** ($CDCl_3$, 300 MHz)

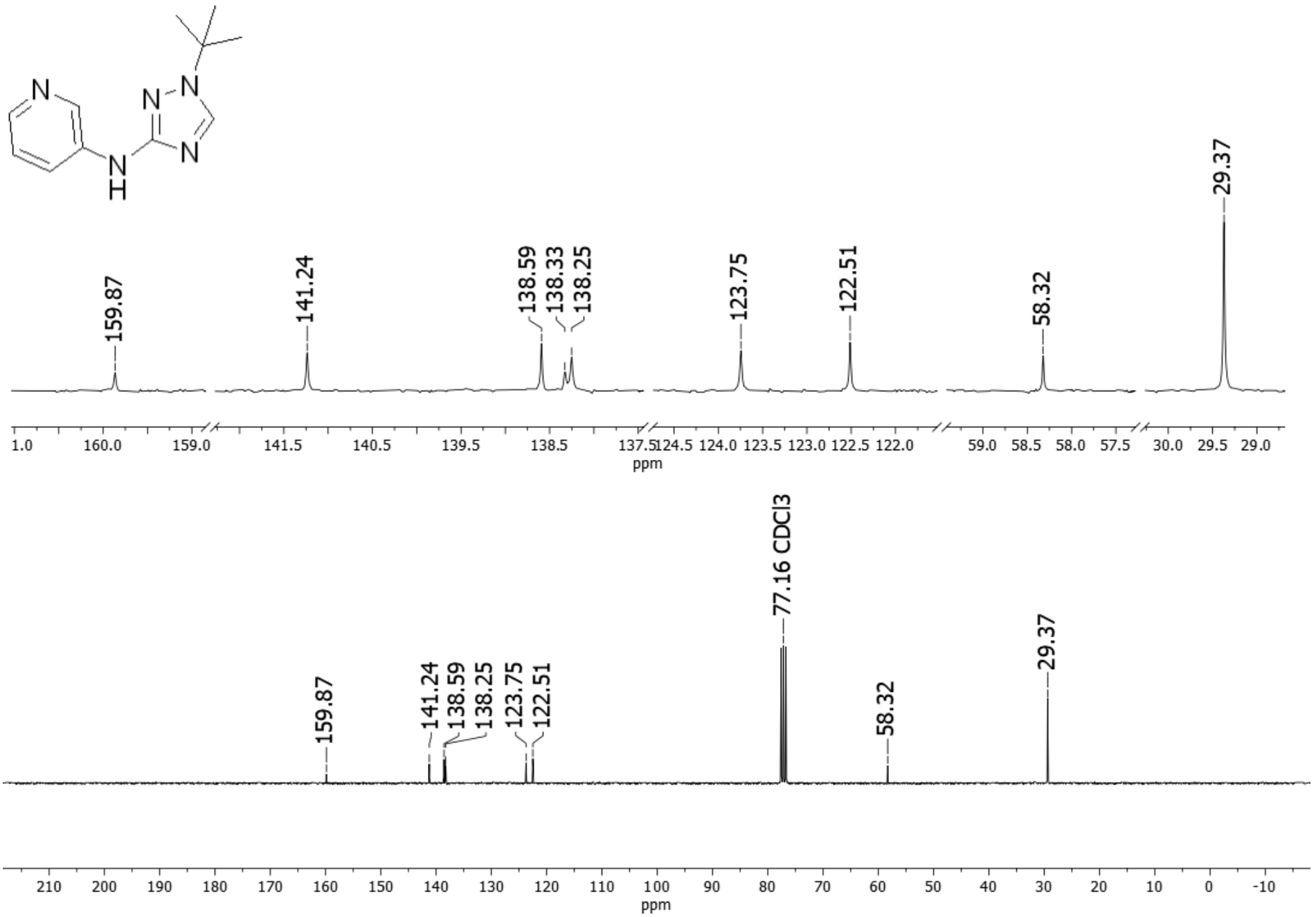

Figure S110. ^{13}C NMR spectrum of compound **4ae** ($CDCl_3$, 75 MHz)

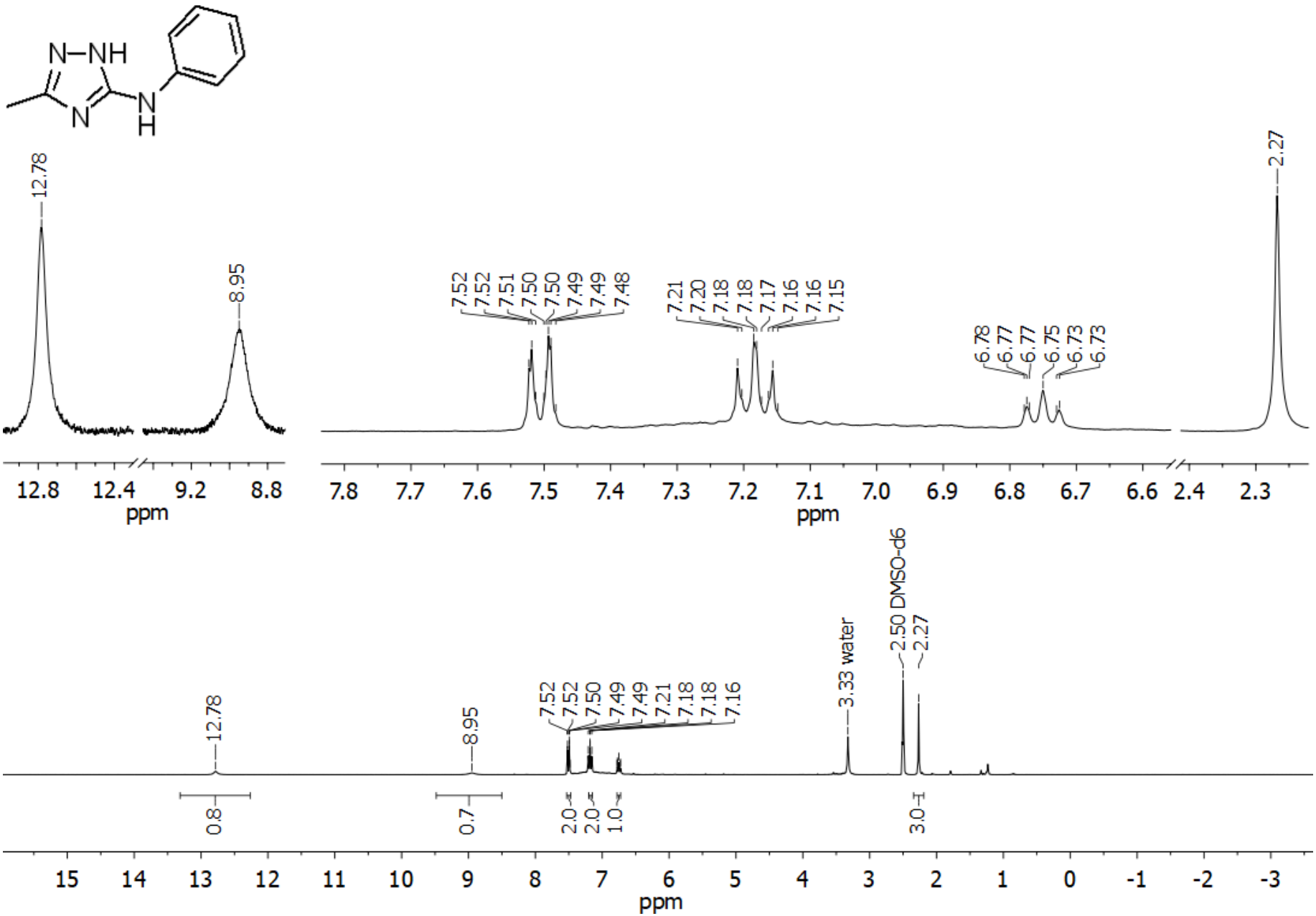

Figure S111. ^{1}H NMR spectrum of compound **8a** (DMSO-d_6, 300 MHz)

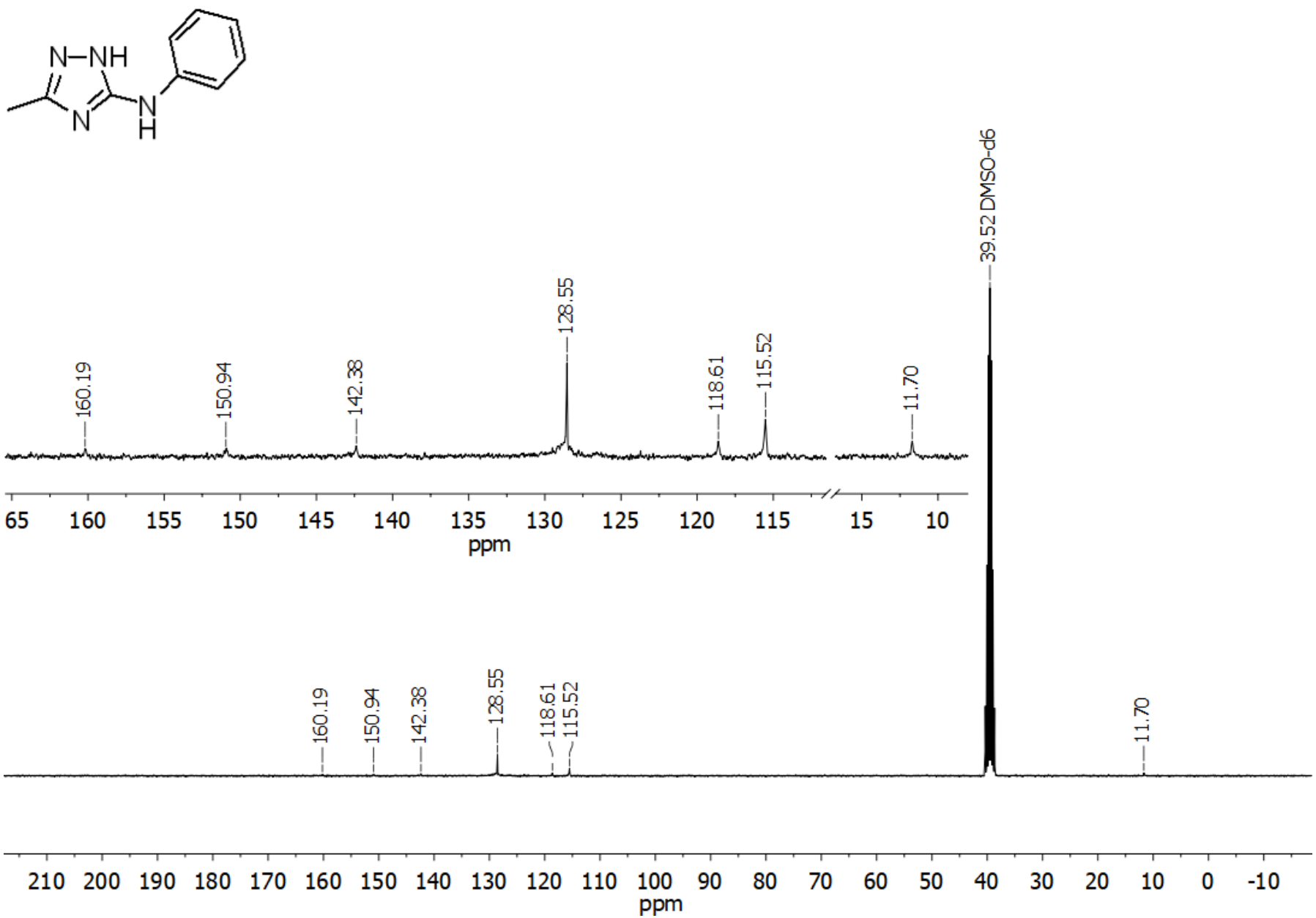

Figure S112. ^{13}C NMR spectrum of compound **8a** (DMSO-d_6, 75 MHz)

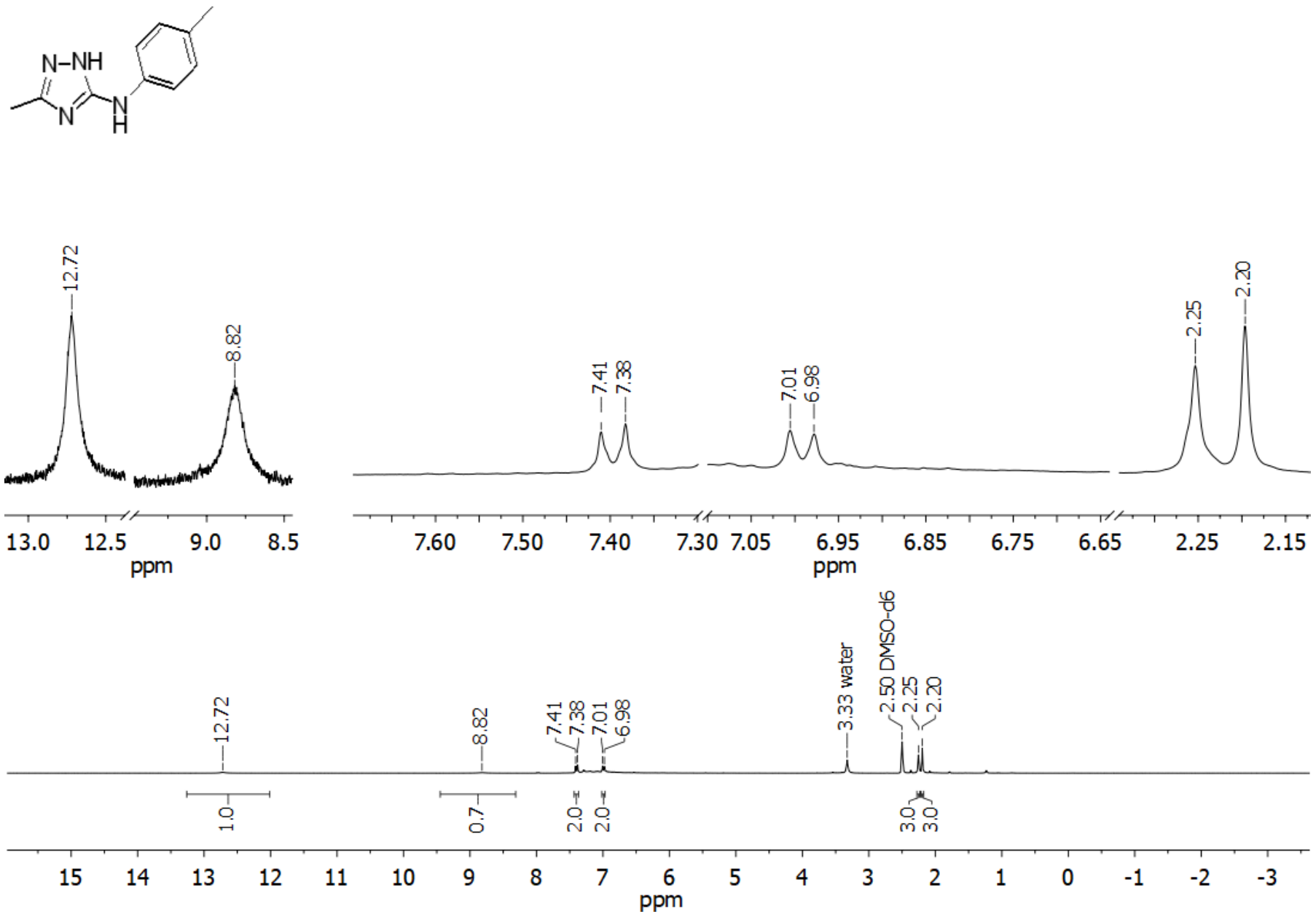

Figure S113. ^{1}H NMR spectrum of compound **8b** (DMSO-d_6, 300 MHz)

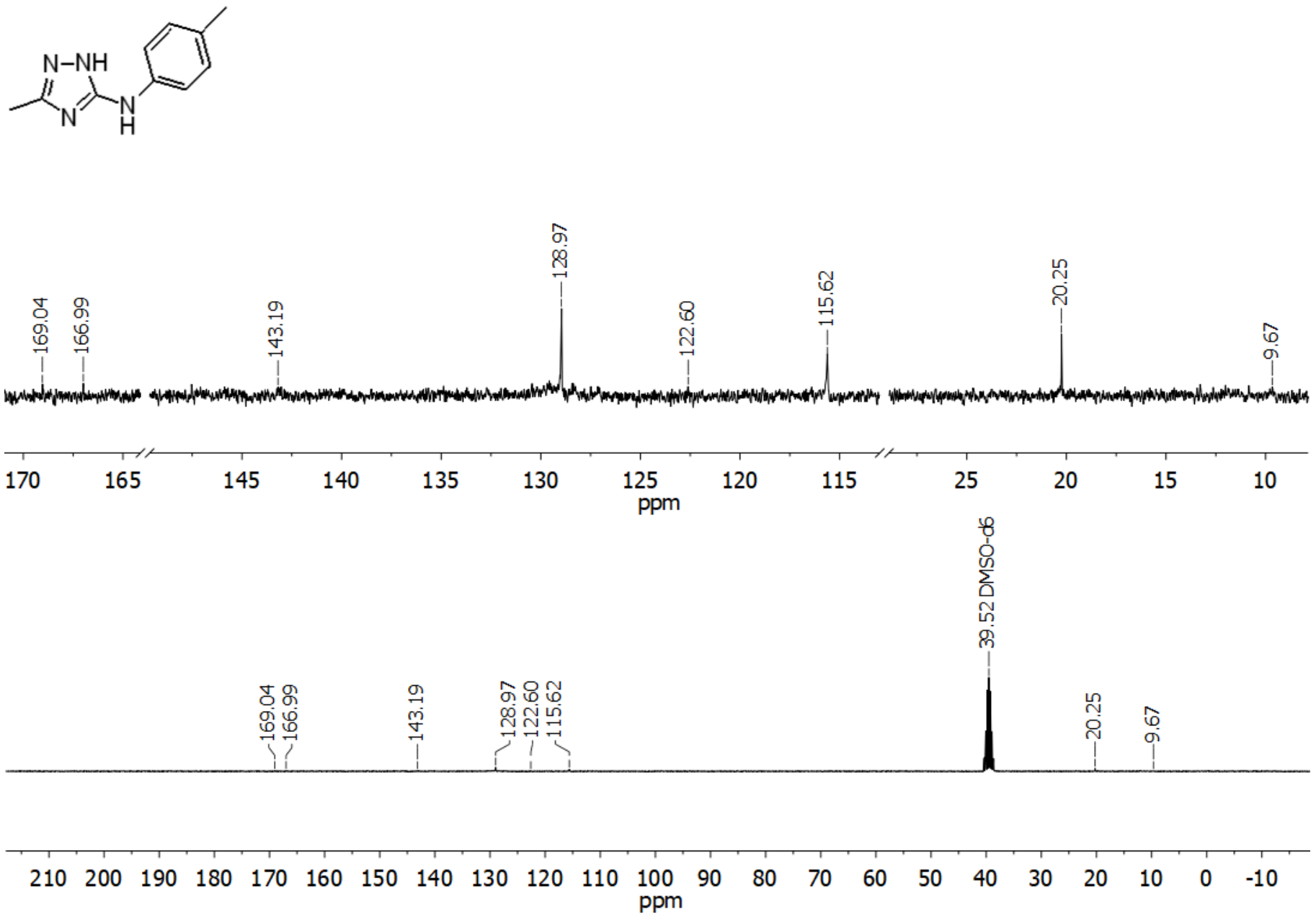

Figure S114. ^{13}C NMR spectrum of compound **8b** (DMSO-d_6, 75 MHz)

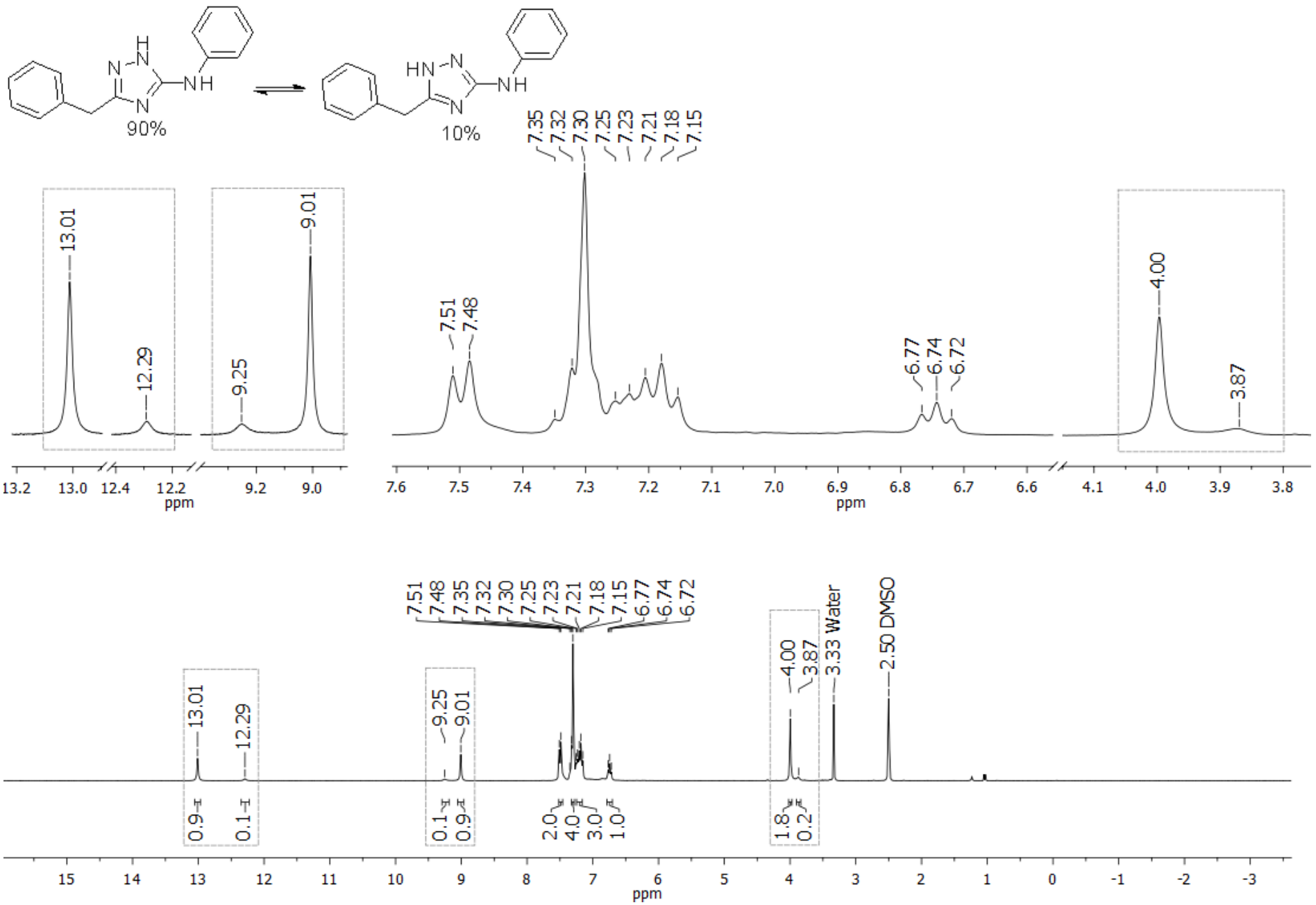

Figure S115. ^{1}H NMR spectrum of compound **8c** (DMSO-d_6, 300 MHz)

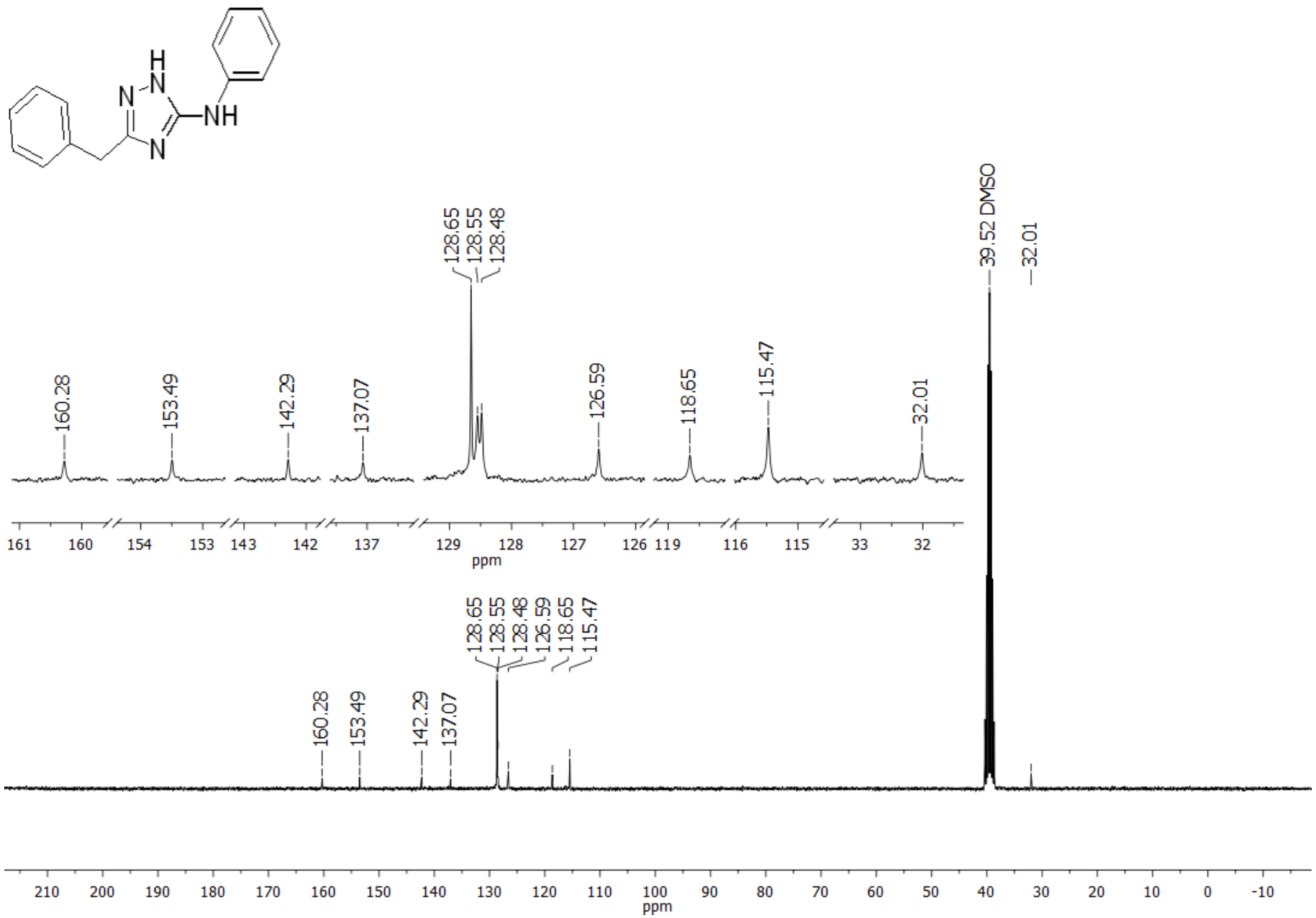

Figure S116. ^{13}C NMR spectrum of compound **8c** (DMSO-d_6, 75 MHz)

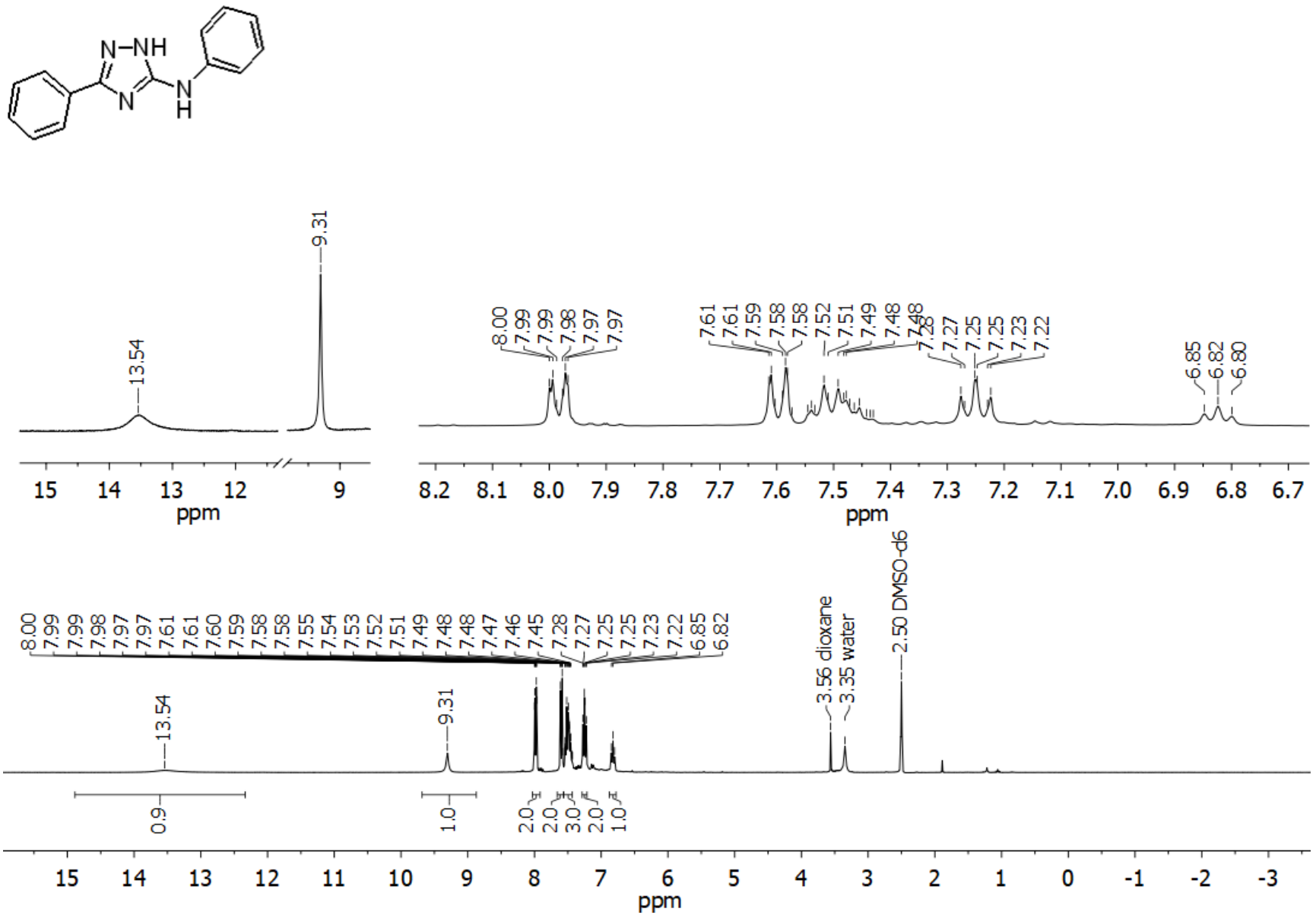

Figure S117. ^{1}H NMR spectrum of compound **8d** (DMSO-d_6, 300 MHz)

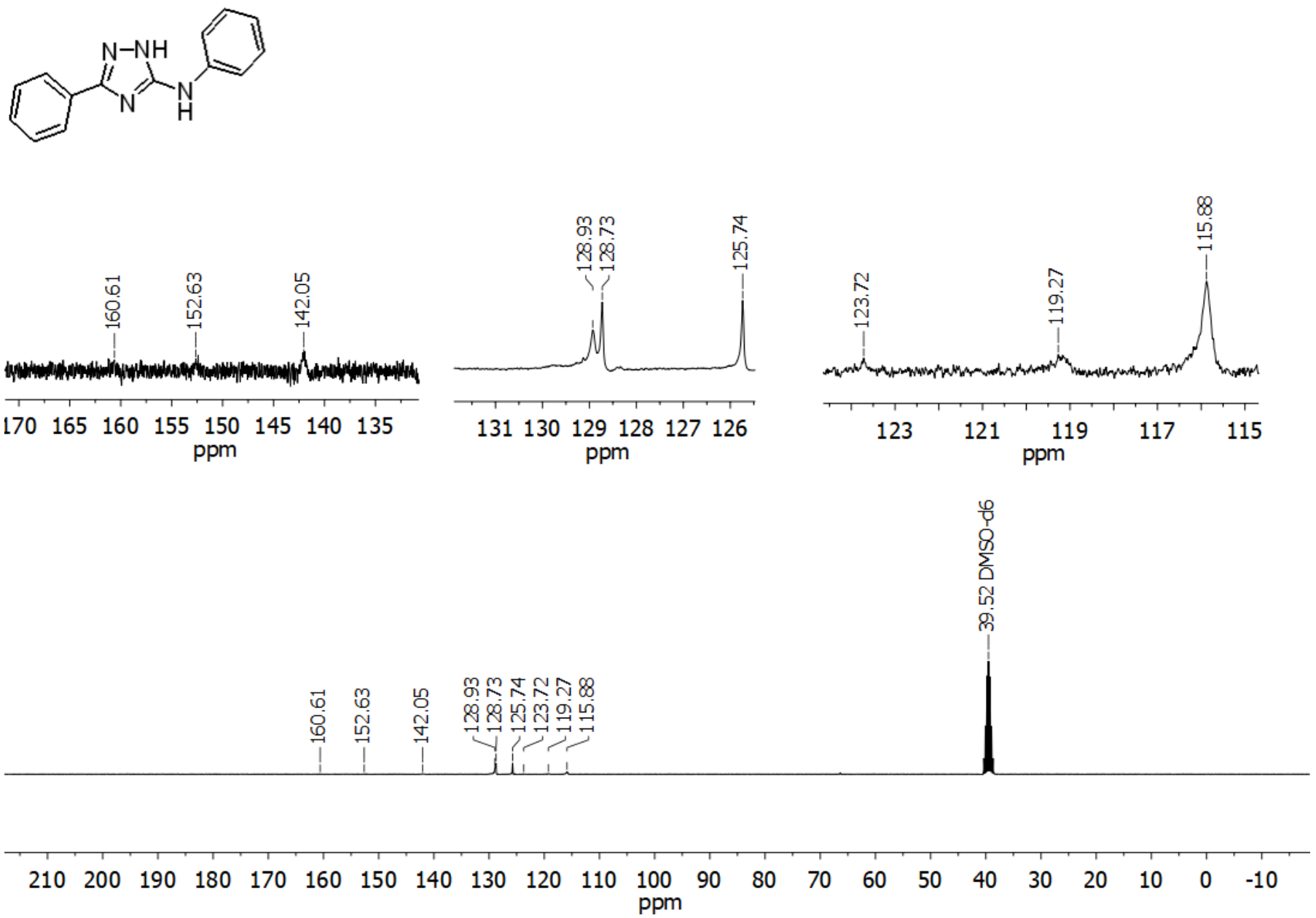

Figure S118. ^{13}C NMR spectrum of compound **8d** (DMSO-d_6, 75 MHz)

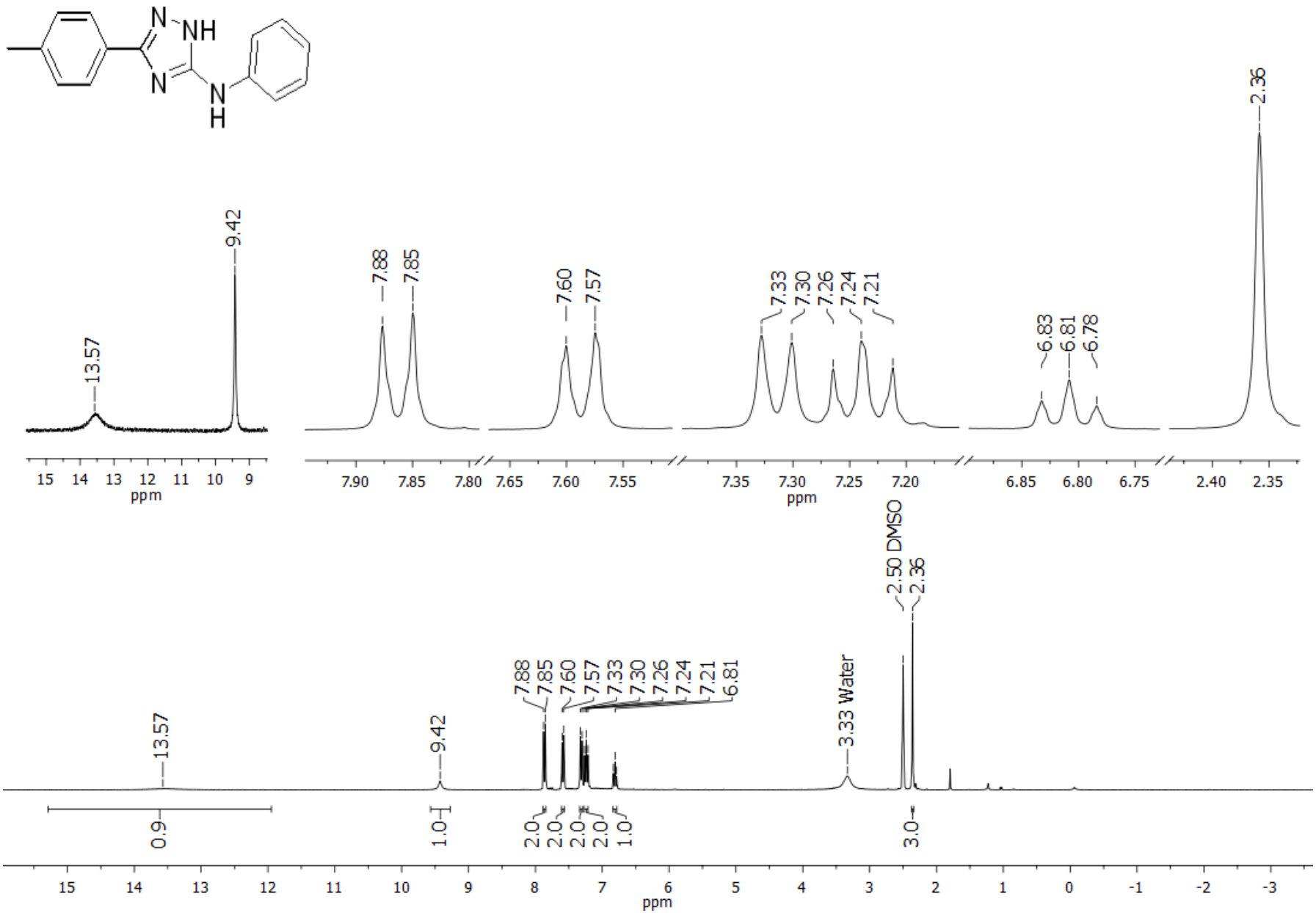

Figure S119. ^{1}H NMR spectrum of compound **8e** (DMSO-d_6, 300 MHz)

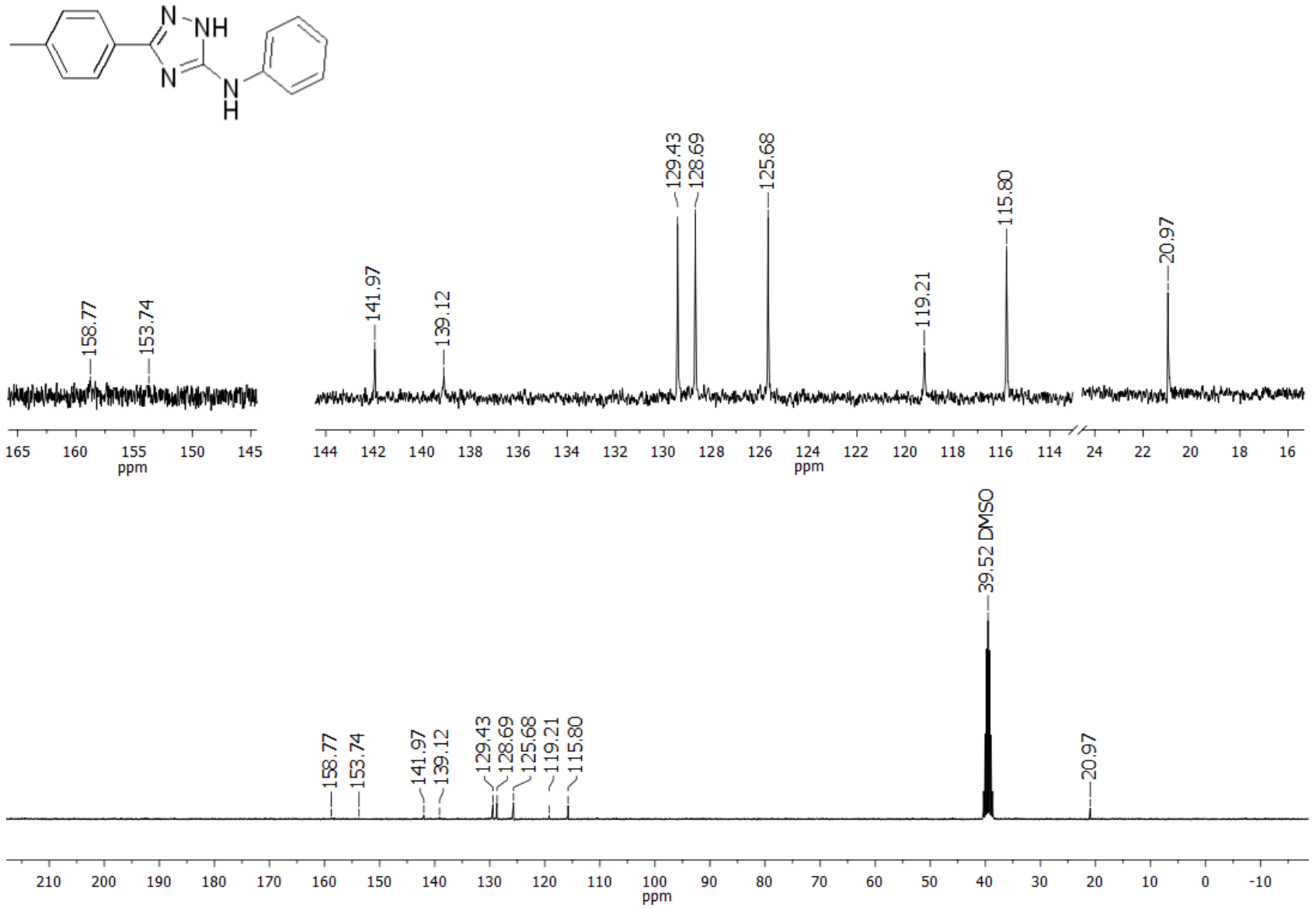

Figure S120. ^{13}C NMR spectrum of compound **8e** (DMSO-d_6, 75 MHz)

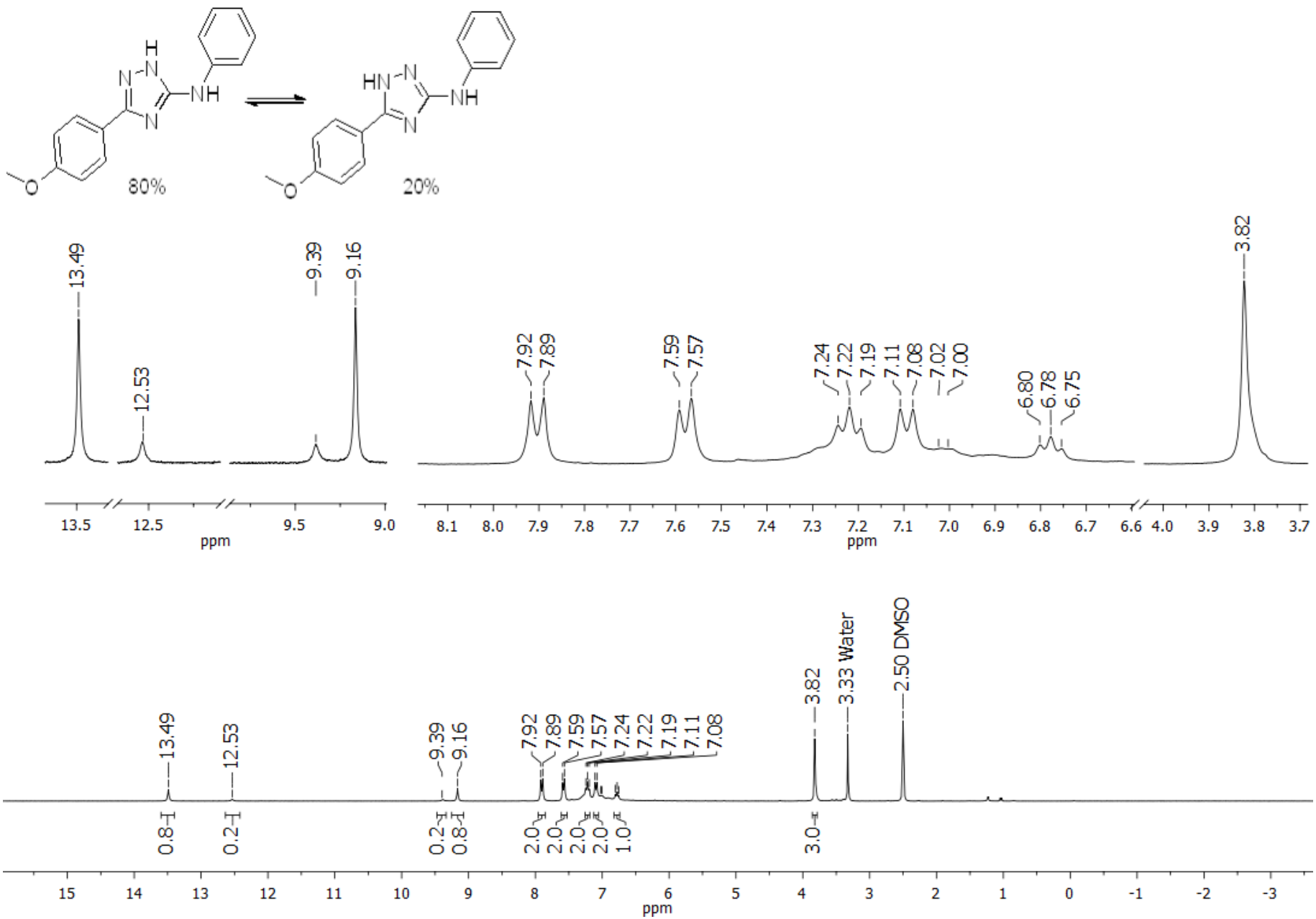

Figure S121. ^{1}H NMR spectrum of compound **8f** (DMSO-d_6, 300 MHz)

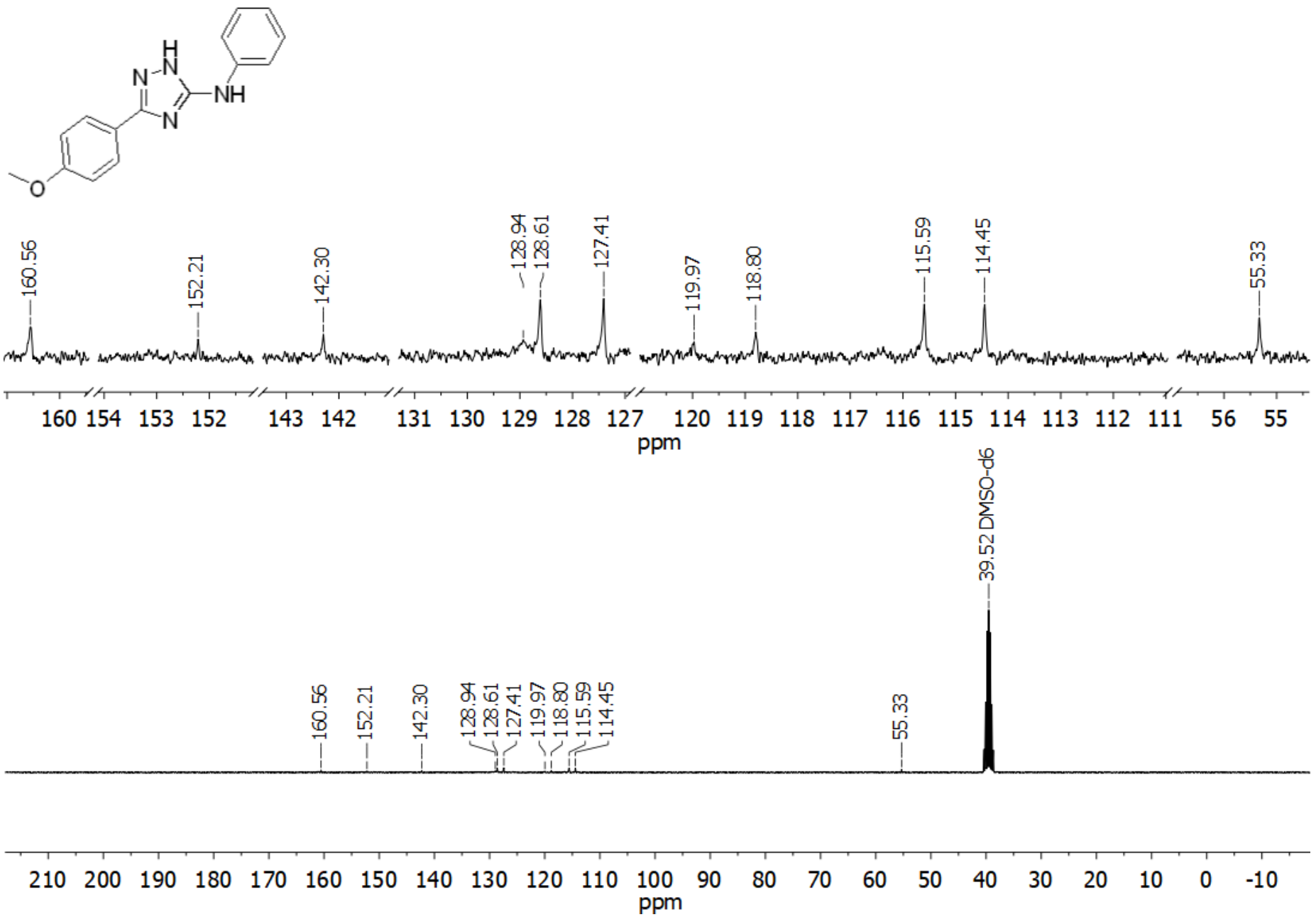

Figure S122. ^{13}C NMR spectrum of compound **8f** (DMSO-d_6, 75 MHz)

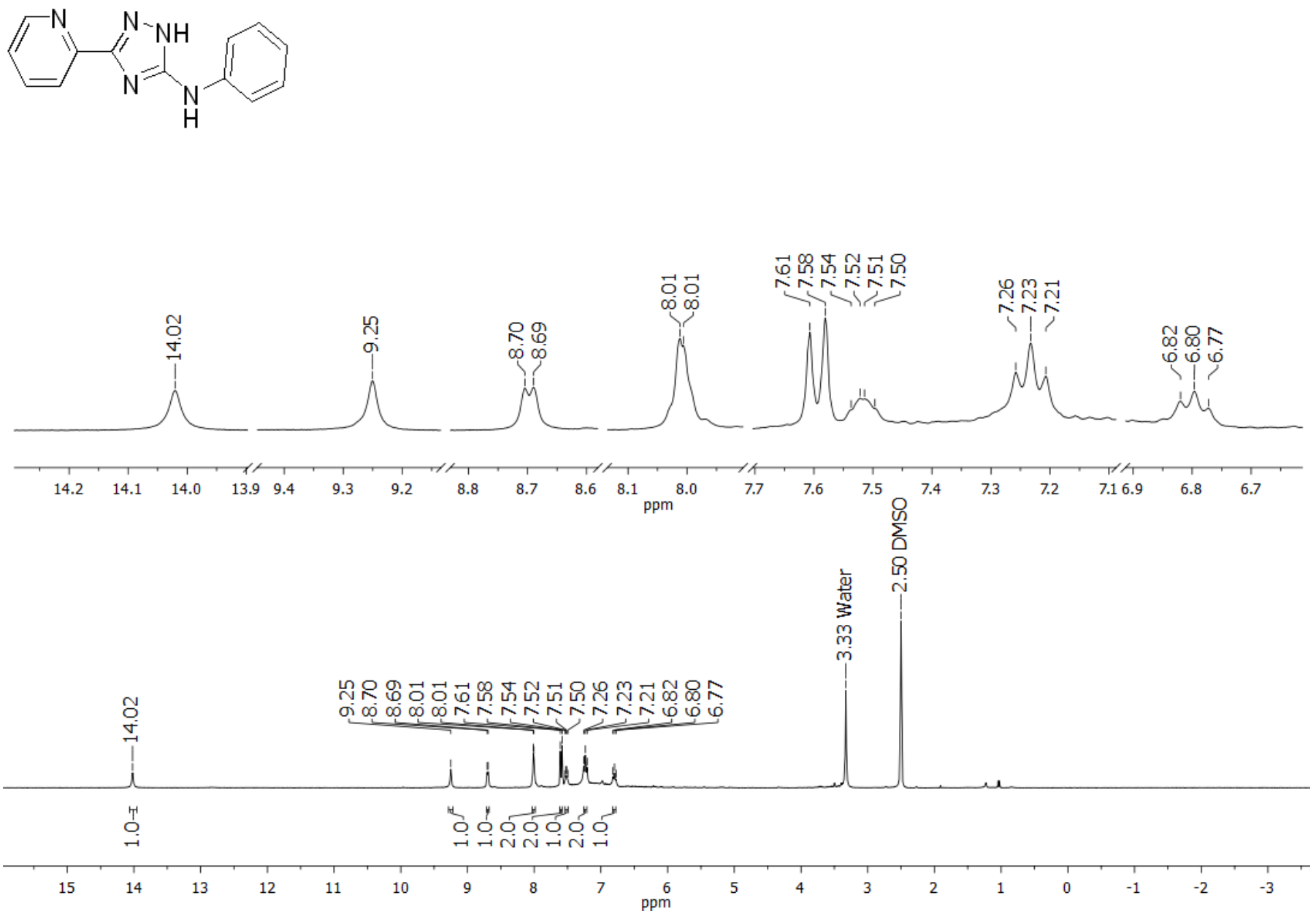

Figure S123. ^{1}H NMR spectrum of compound **8g** (DMSO-d_6, 300 MHz)

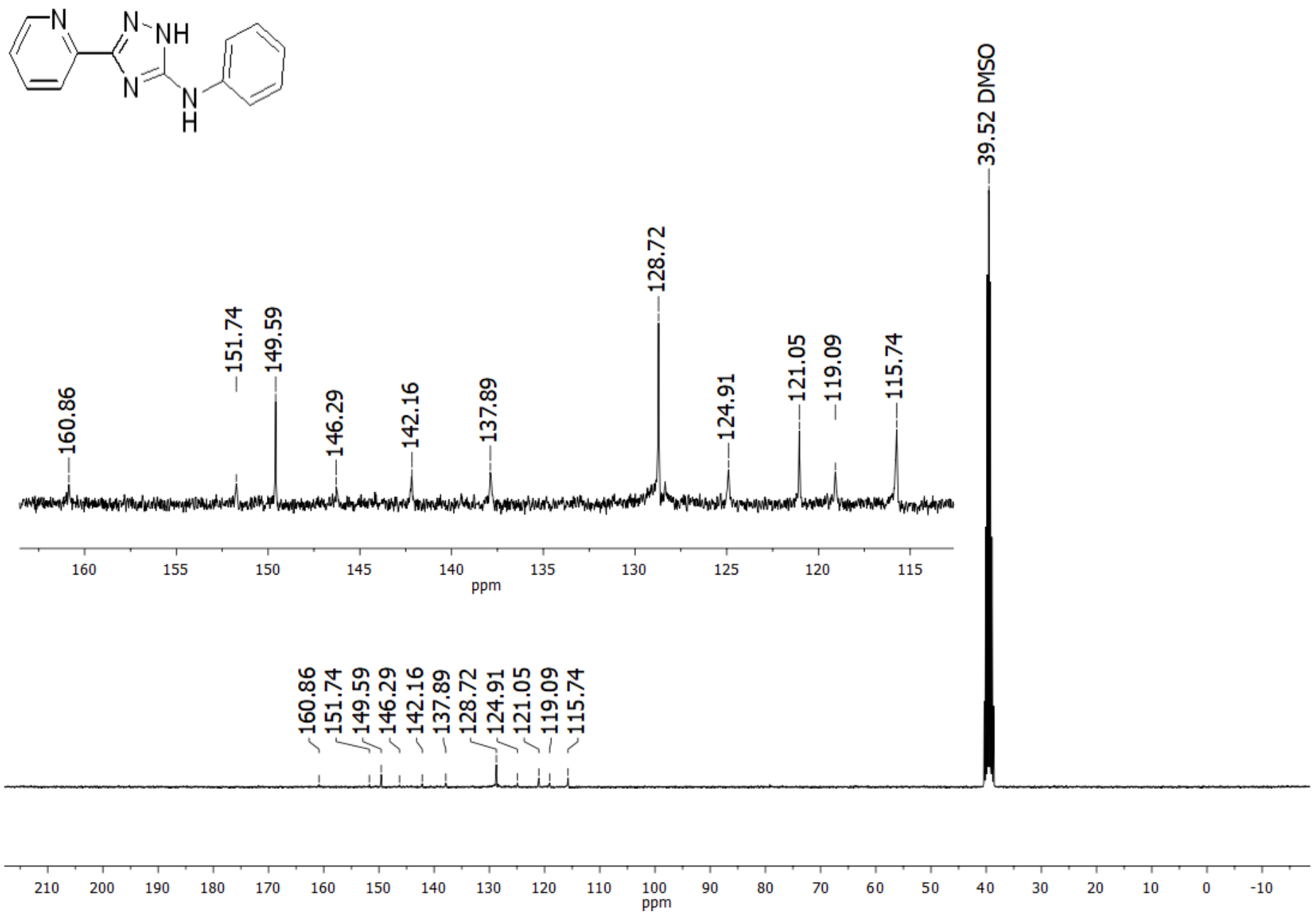

Figure S124. ^{13}C NMR spectrum of compound **8g** (DMSO-d_6, 75 MHz)

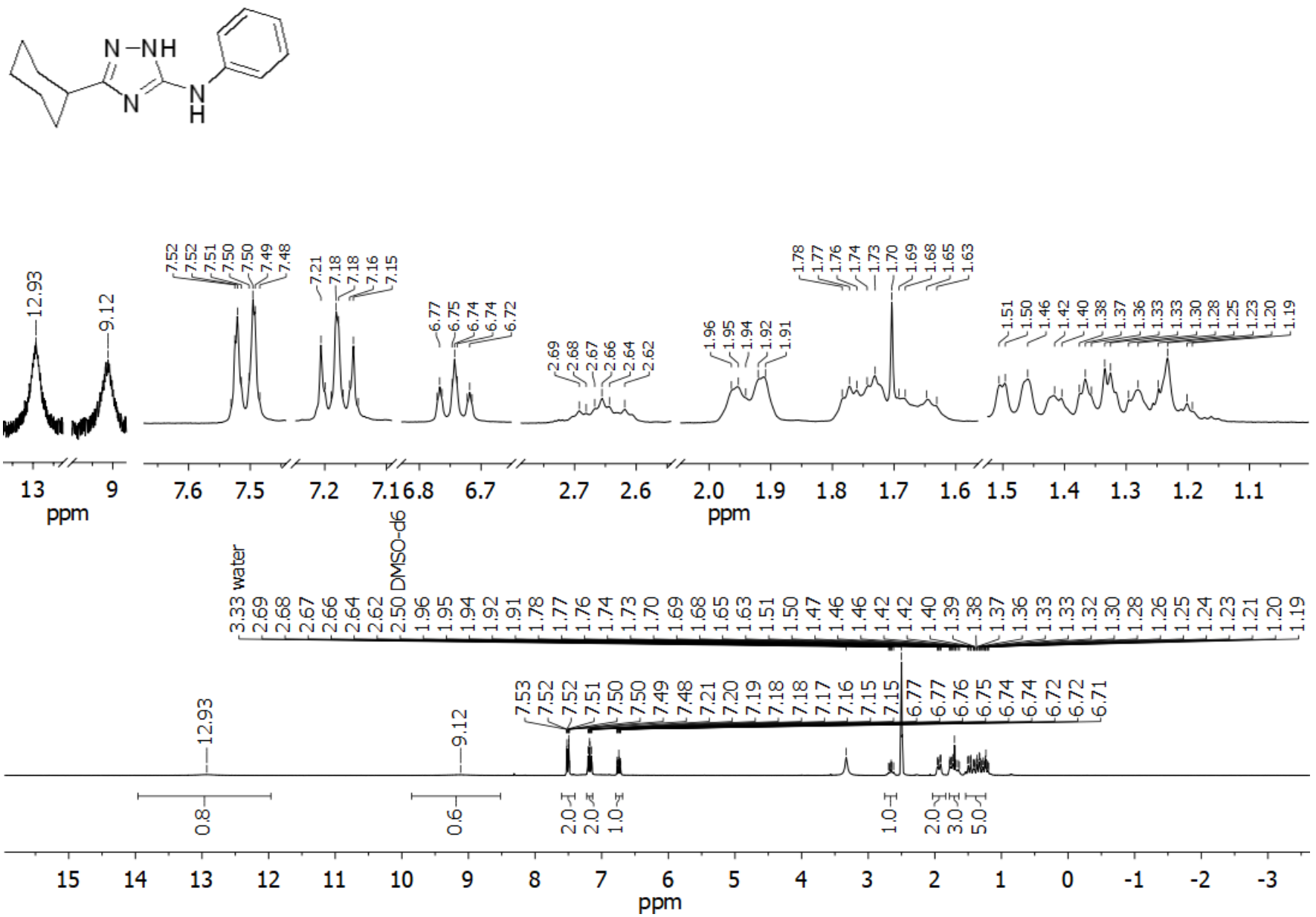

Figure S125. ^{1}H NMR spectrum of compound **8h** (DMSO-d_6, 300 MHz)

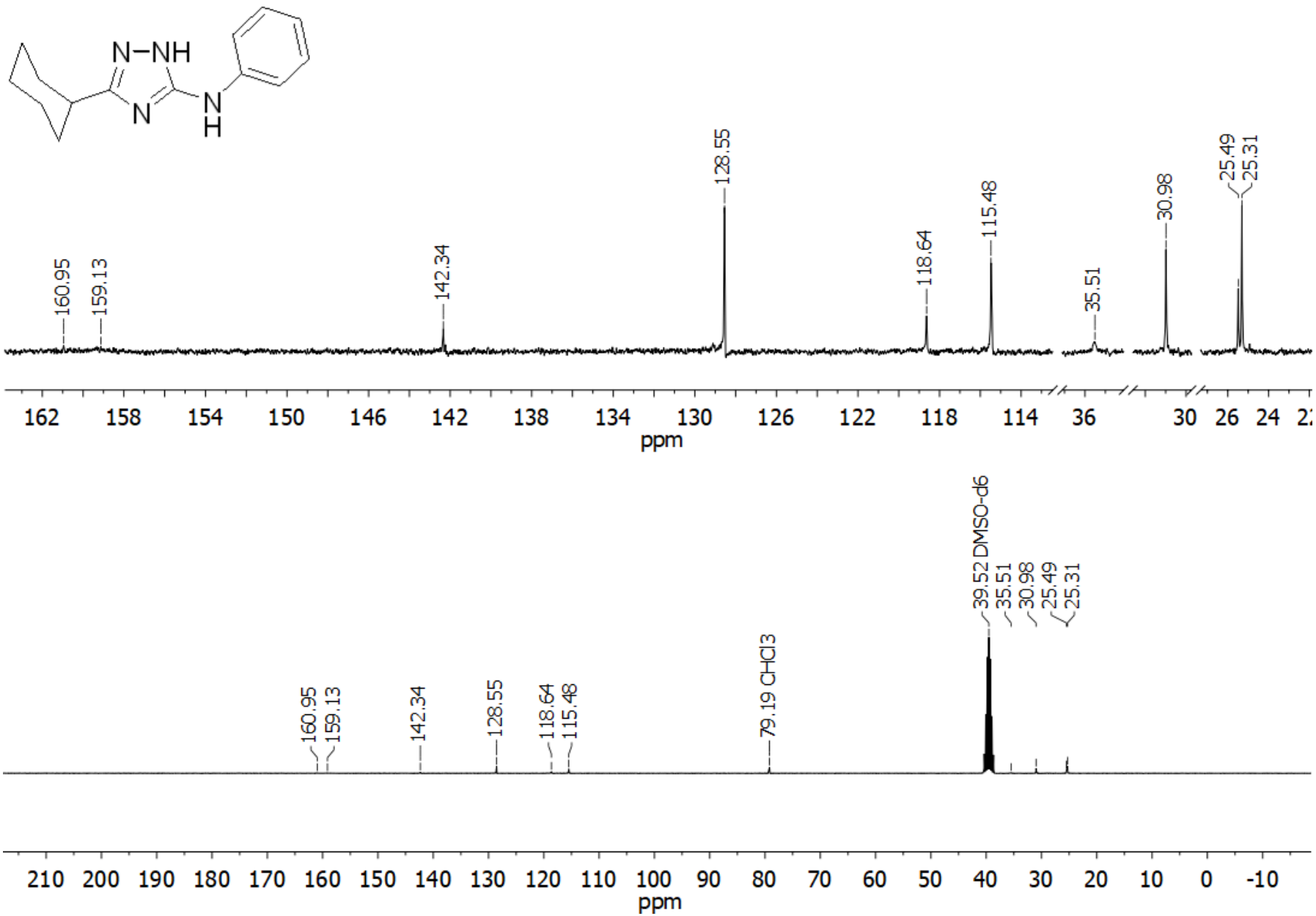

Figure S126. ^{13}C NMR spectrum of compound **8h** (DMSO-d_6, 75 MHz)

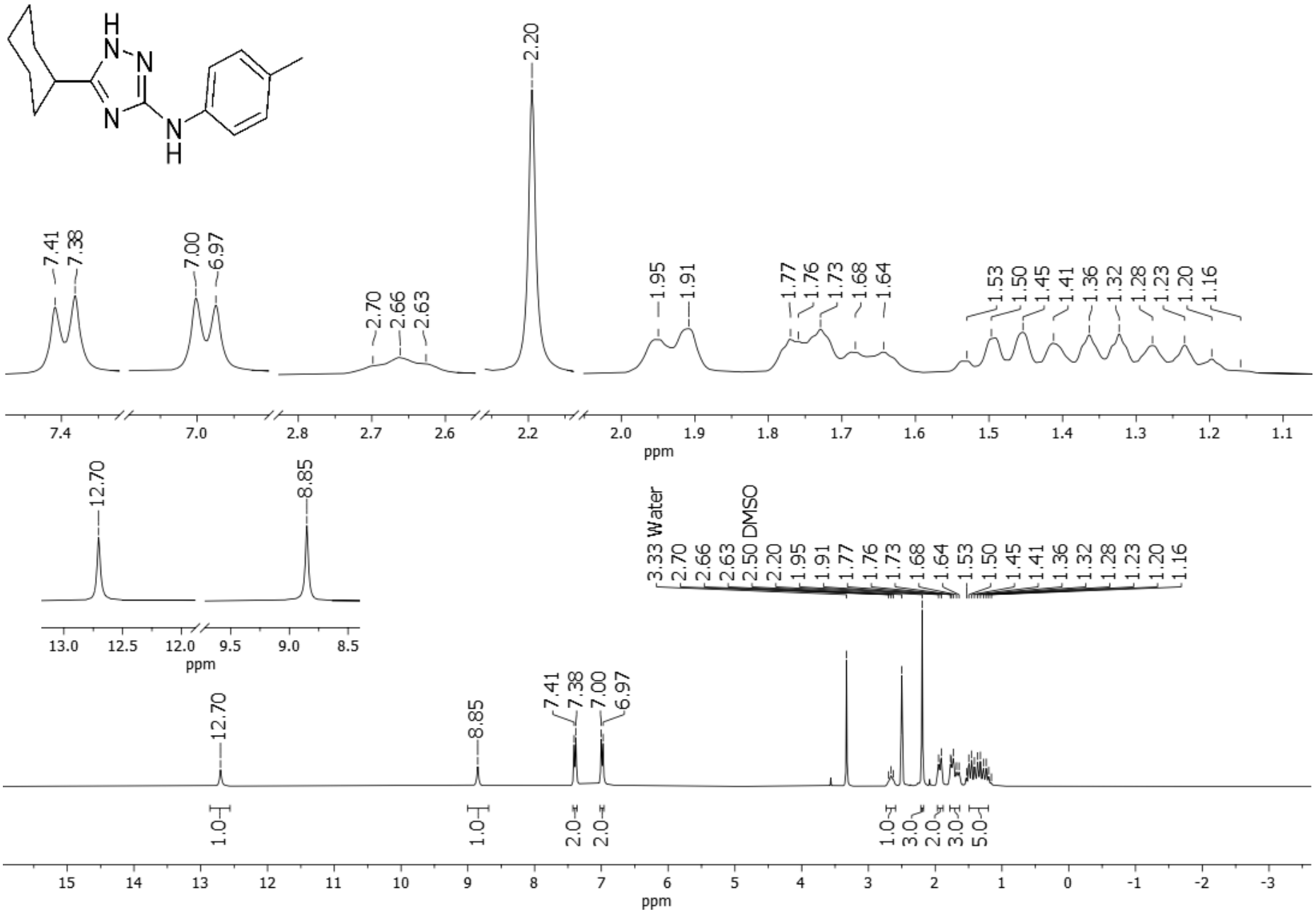

Figure S127. ^{1}H NMR spectrum of compound **8i** (DMSO-d_6, 300 MHz)

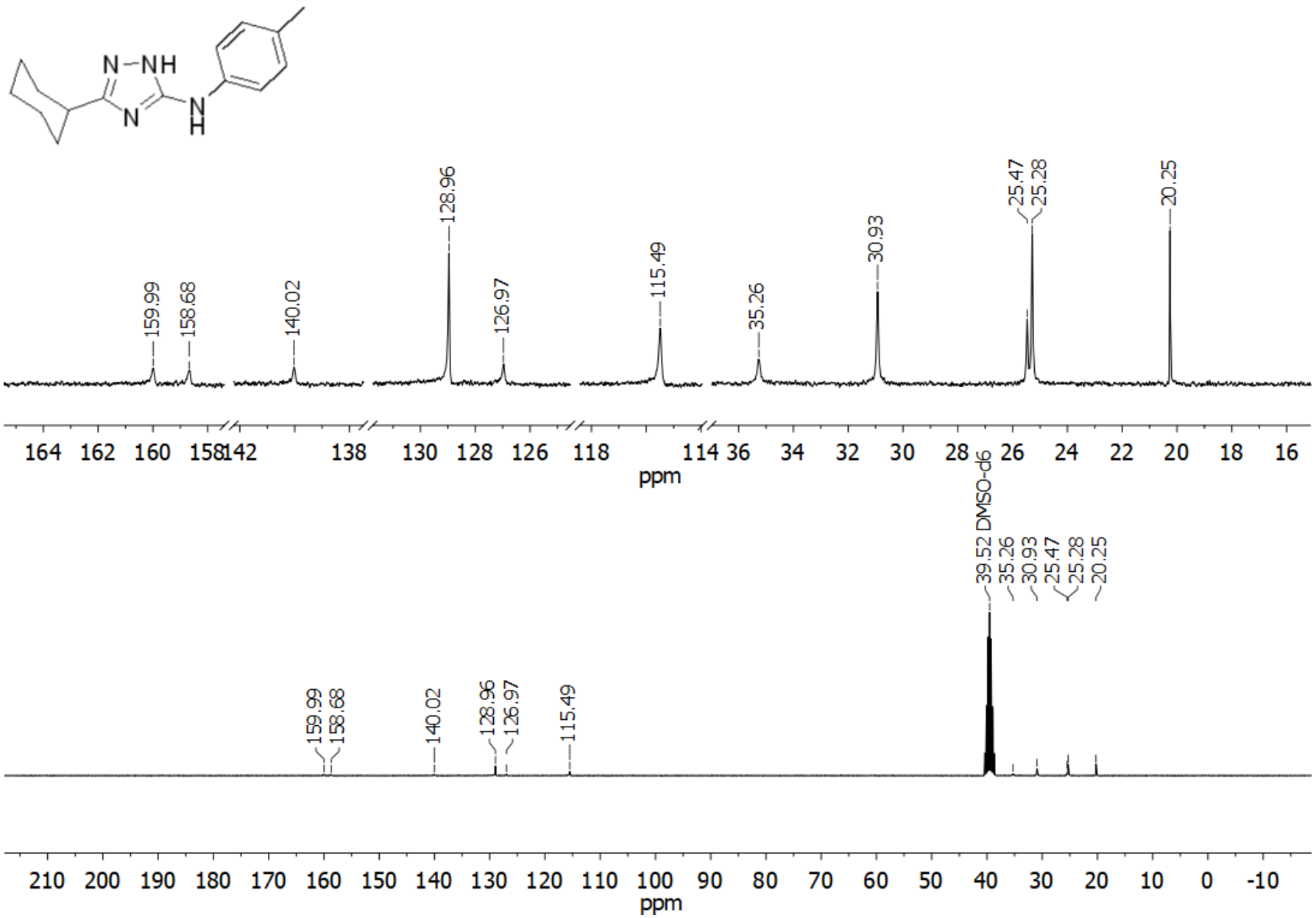

Figure S128. ^{13}C NMR spectrum of compound **8i** (DMSO-d_6, 75 MHz)

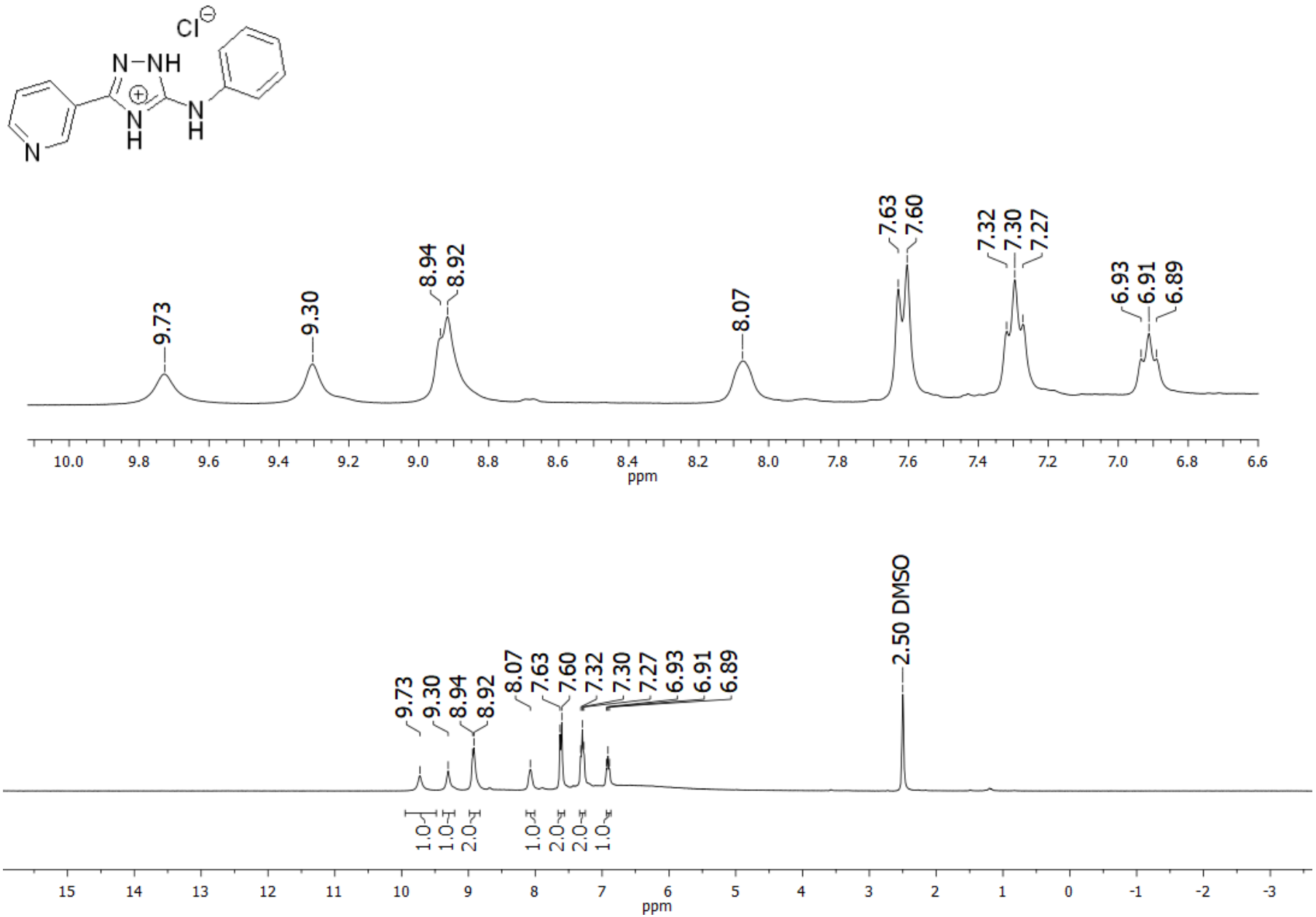

Figure S129. ^{1}H NMR spectrum of compound **8j** (DMSO-d_6, 300 MHz)

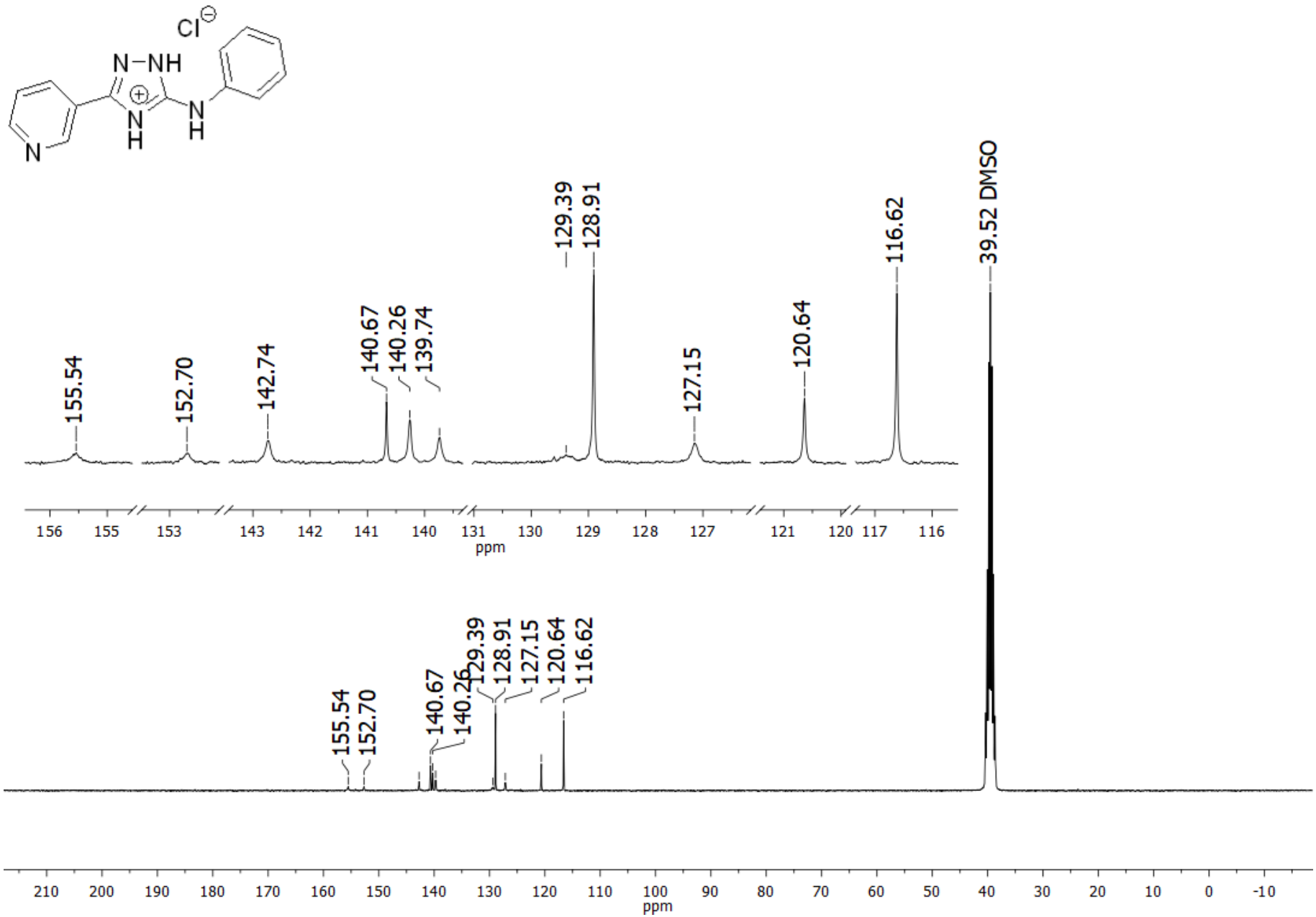

Figure S130. ^{13}C NMR spectrum of compound **8j** (DMSO-*d*$_6$, 75 MHz)

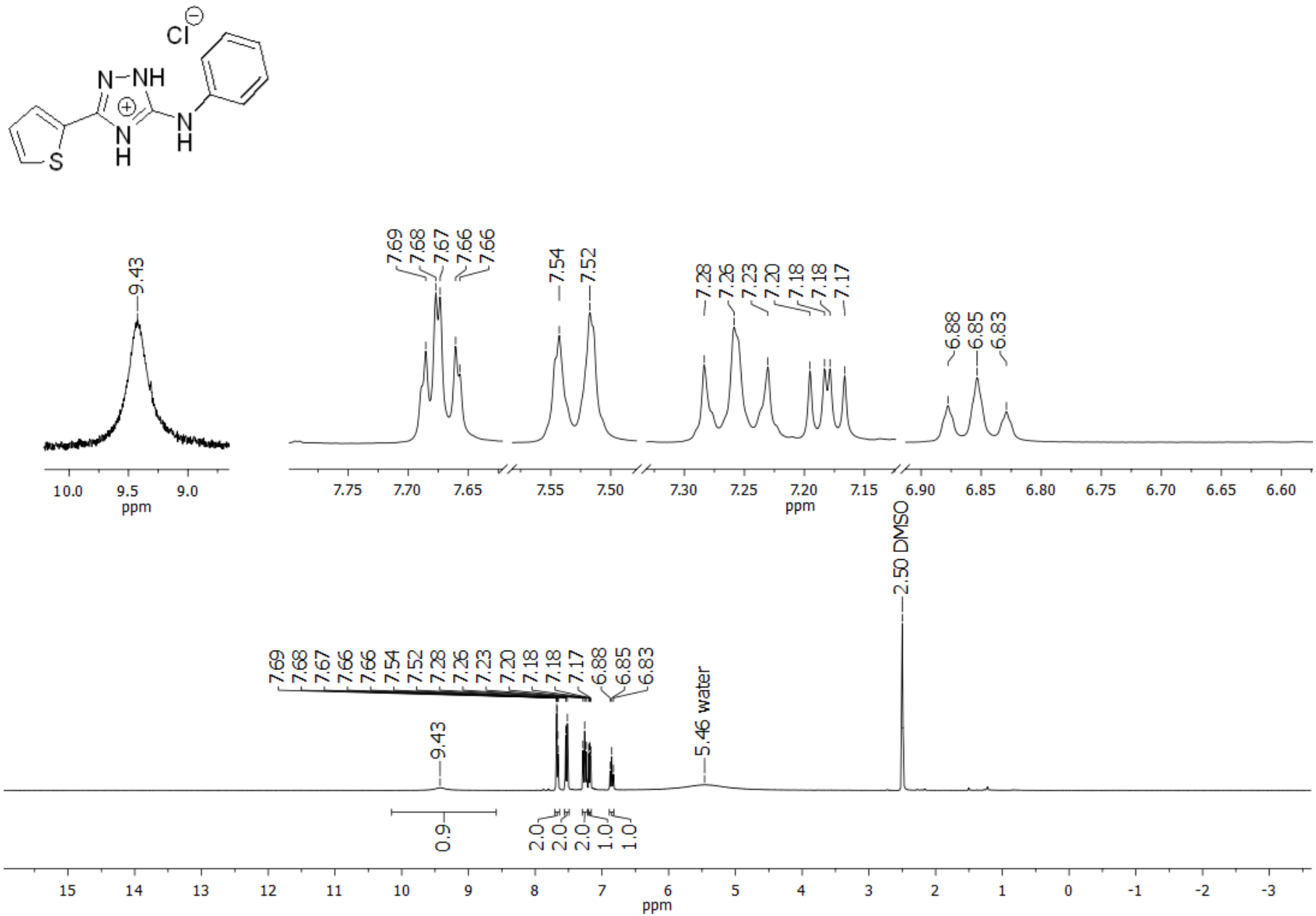

Figure S131. ^{1}H NMR spectrum of compound **8k** (DMSO-d_6, 300 MHz)

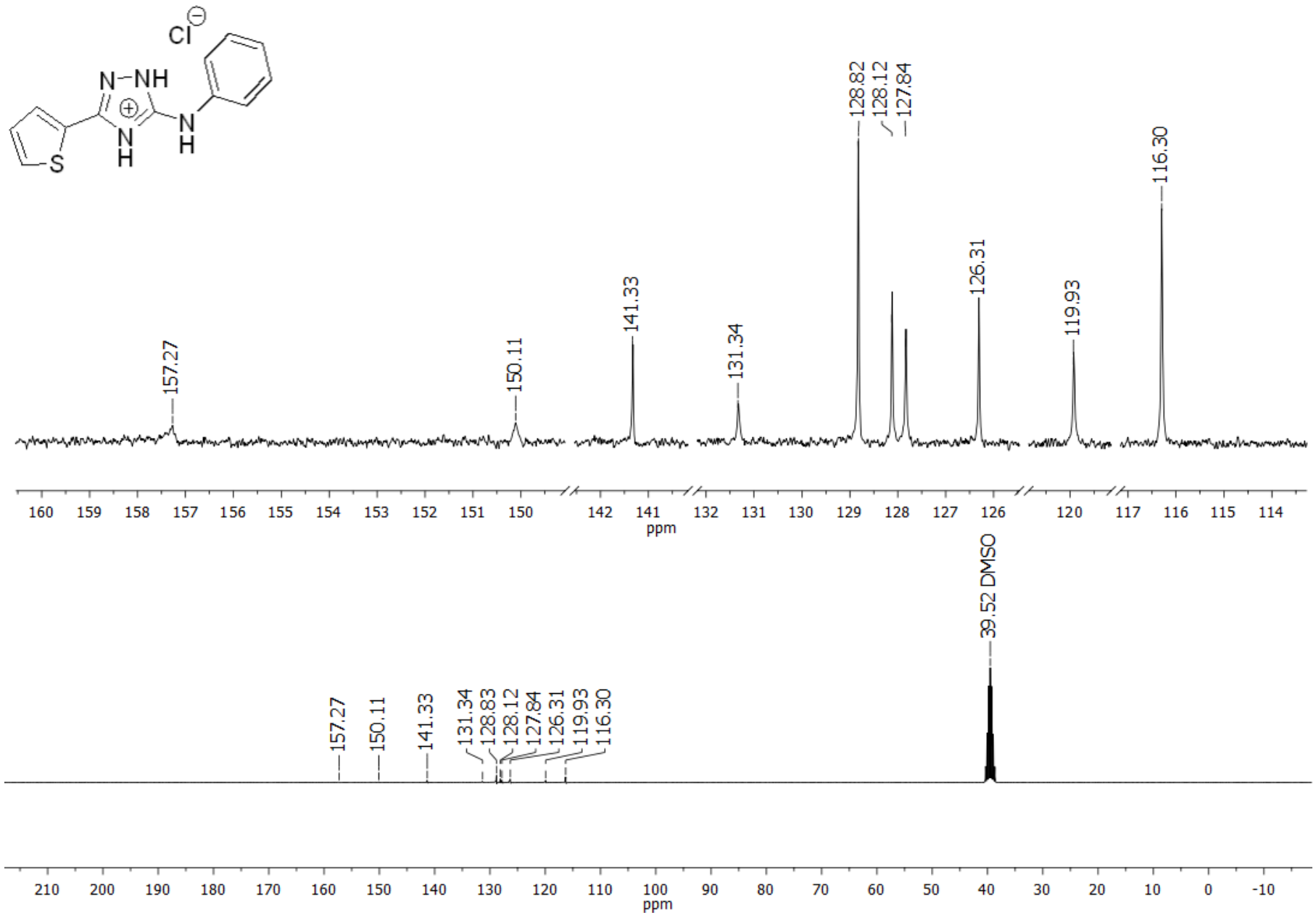

Figure S132. ^{13}C NMR spectrum of compound **8k** (DMSO-d_6, 75 MHz)

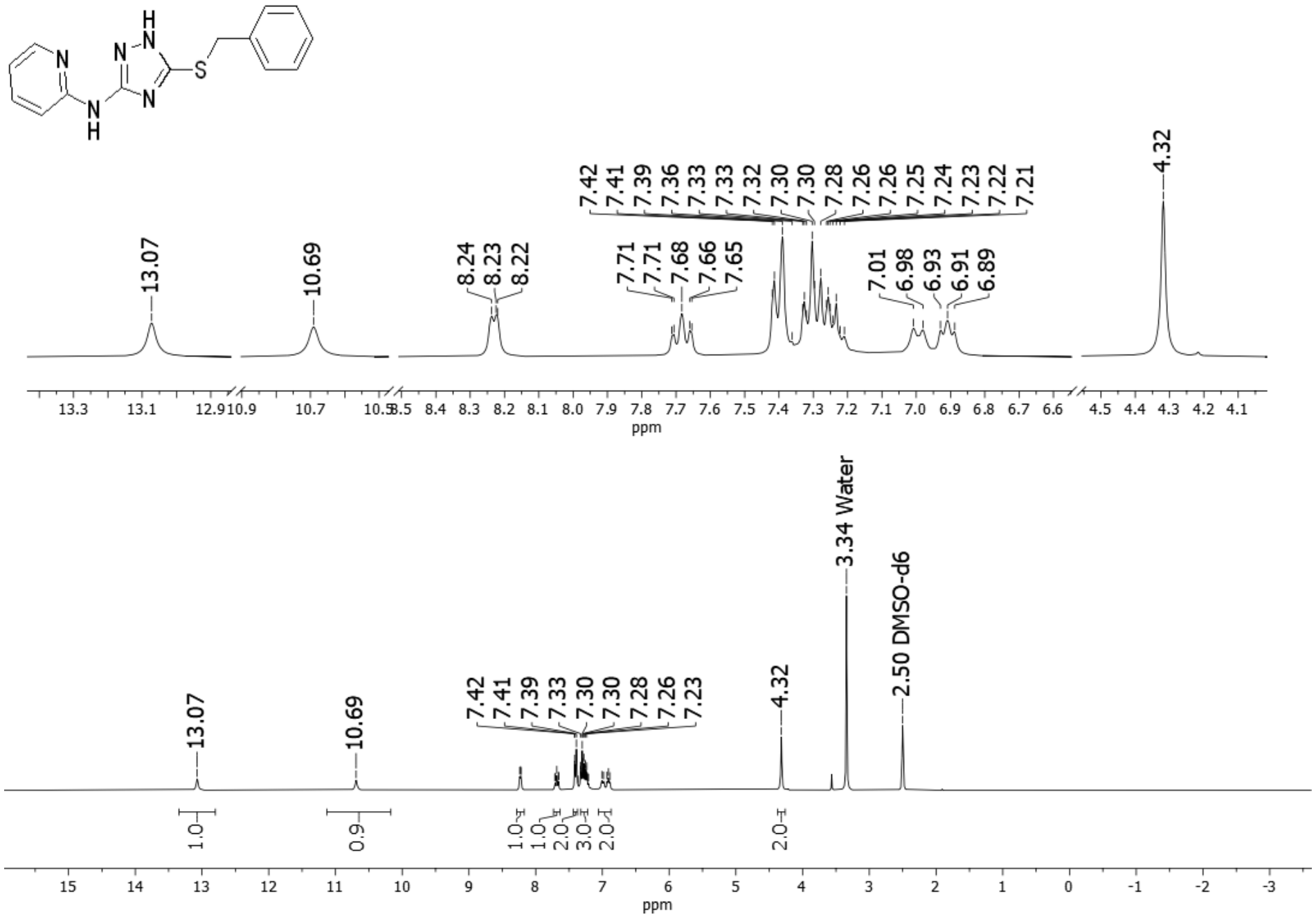

Figure S133. ^{1}H NMR spectrum of compound **8l** (DMSO-d_6, 300 MHz)

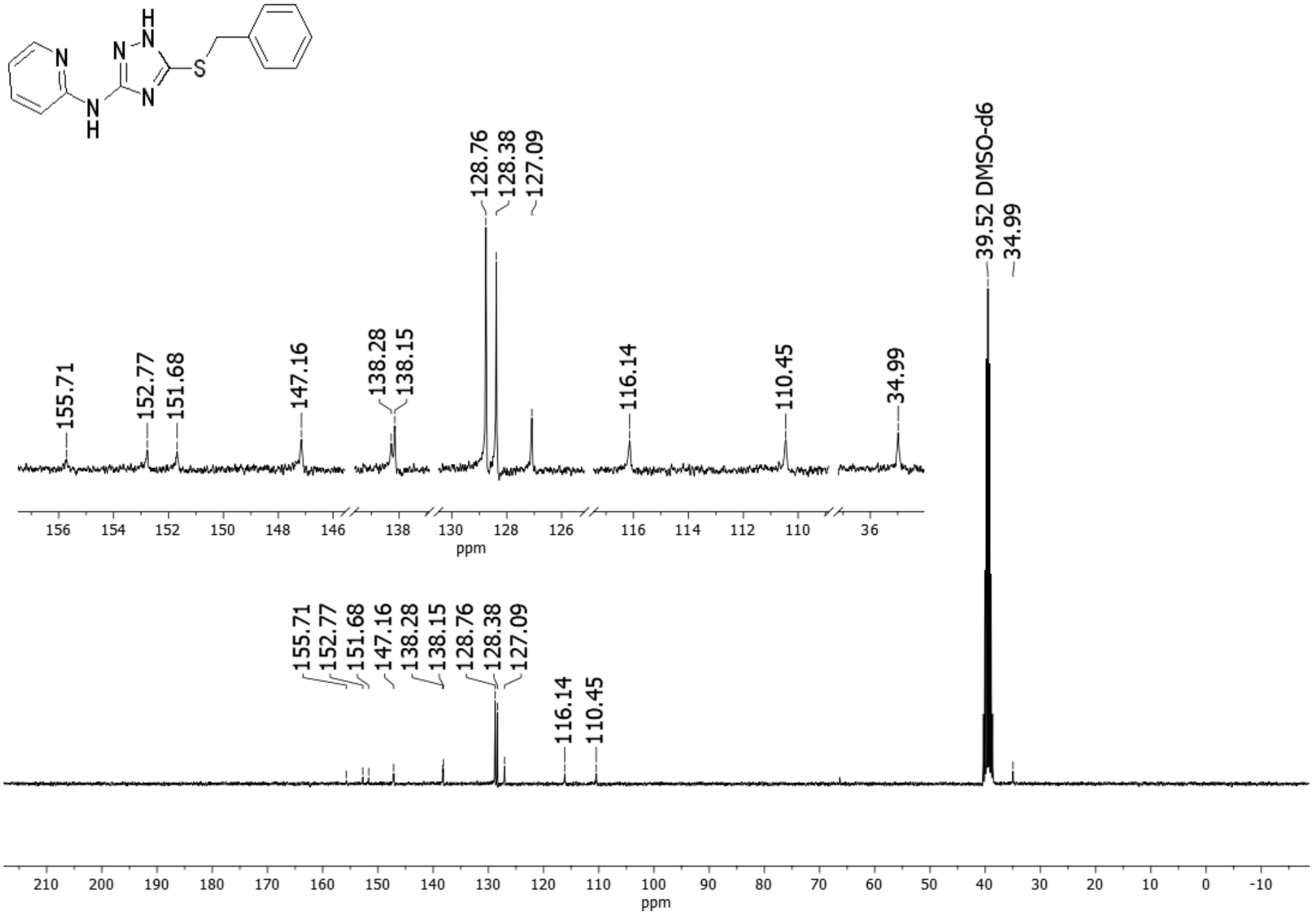

Figure S134. ^{13}C NMR spectrum of compound **8l** (DMSO-d_6, 75 MHz)

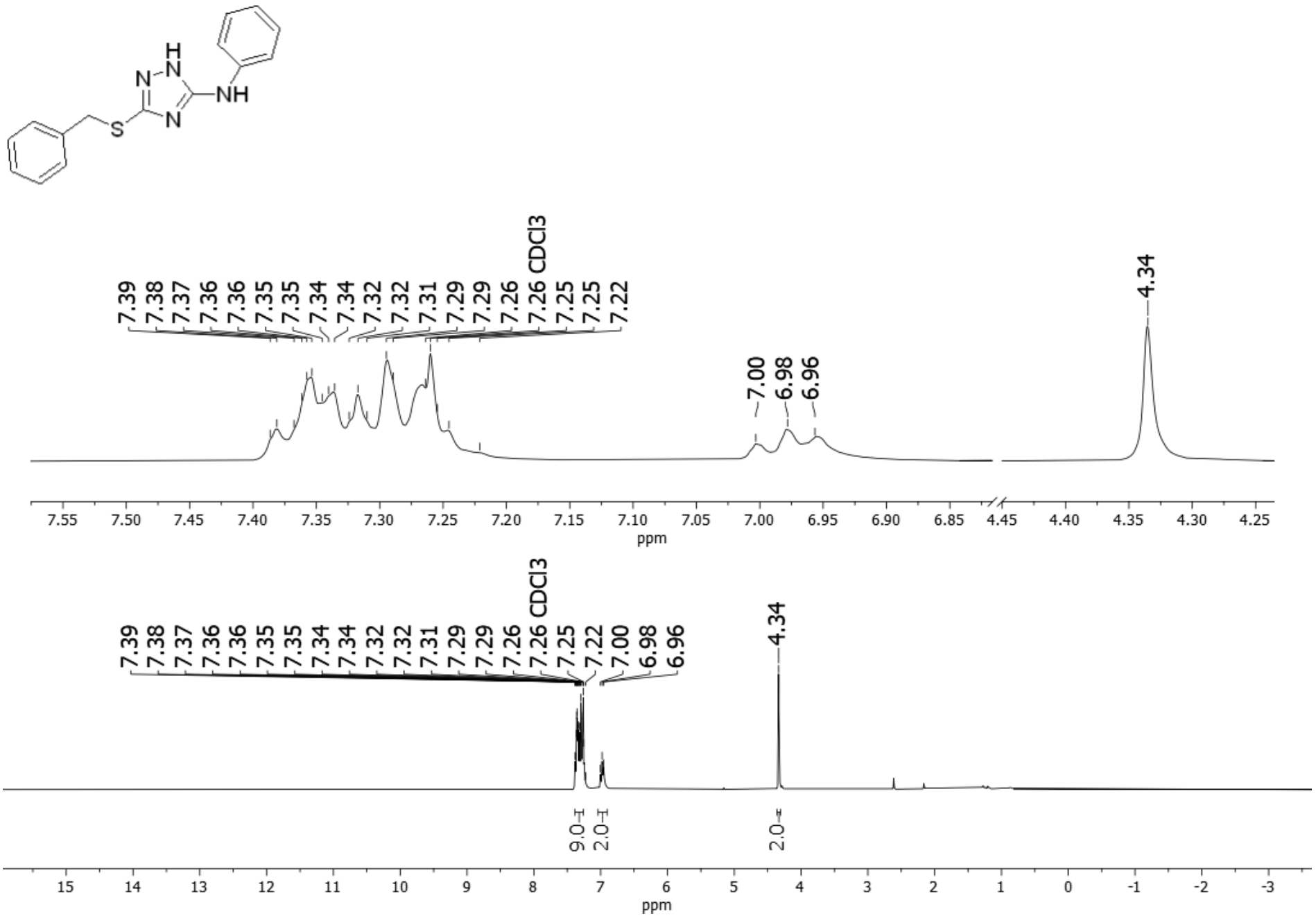

Figure S135. ^{1}H NMR spectrum of compound **8m** ($CDCl_3$, 300 MHz)

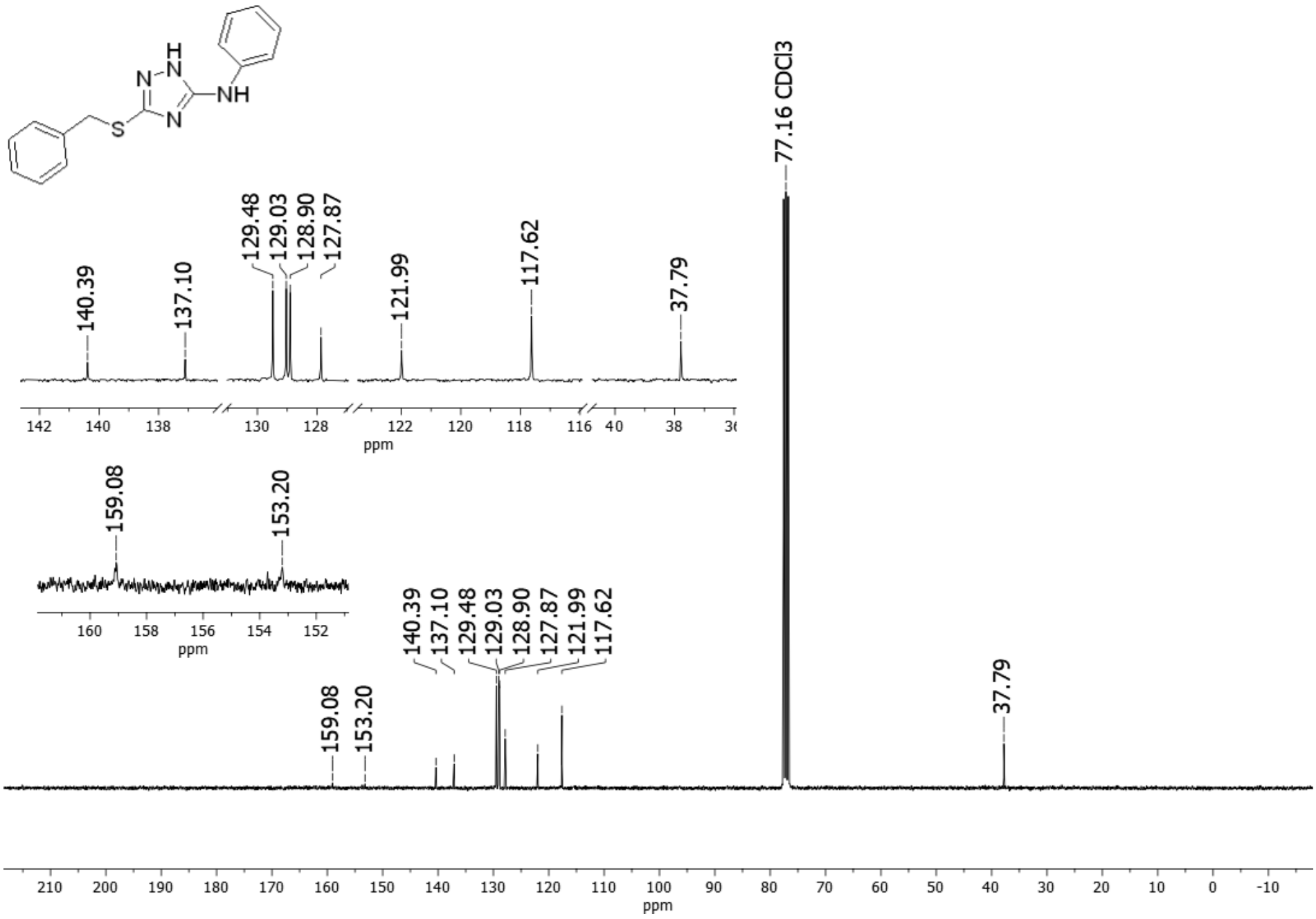

Figure S136. ^{13}C NMR spectrum of compound **8m** ($CDCl_3$, 75 MHz)

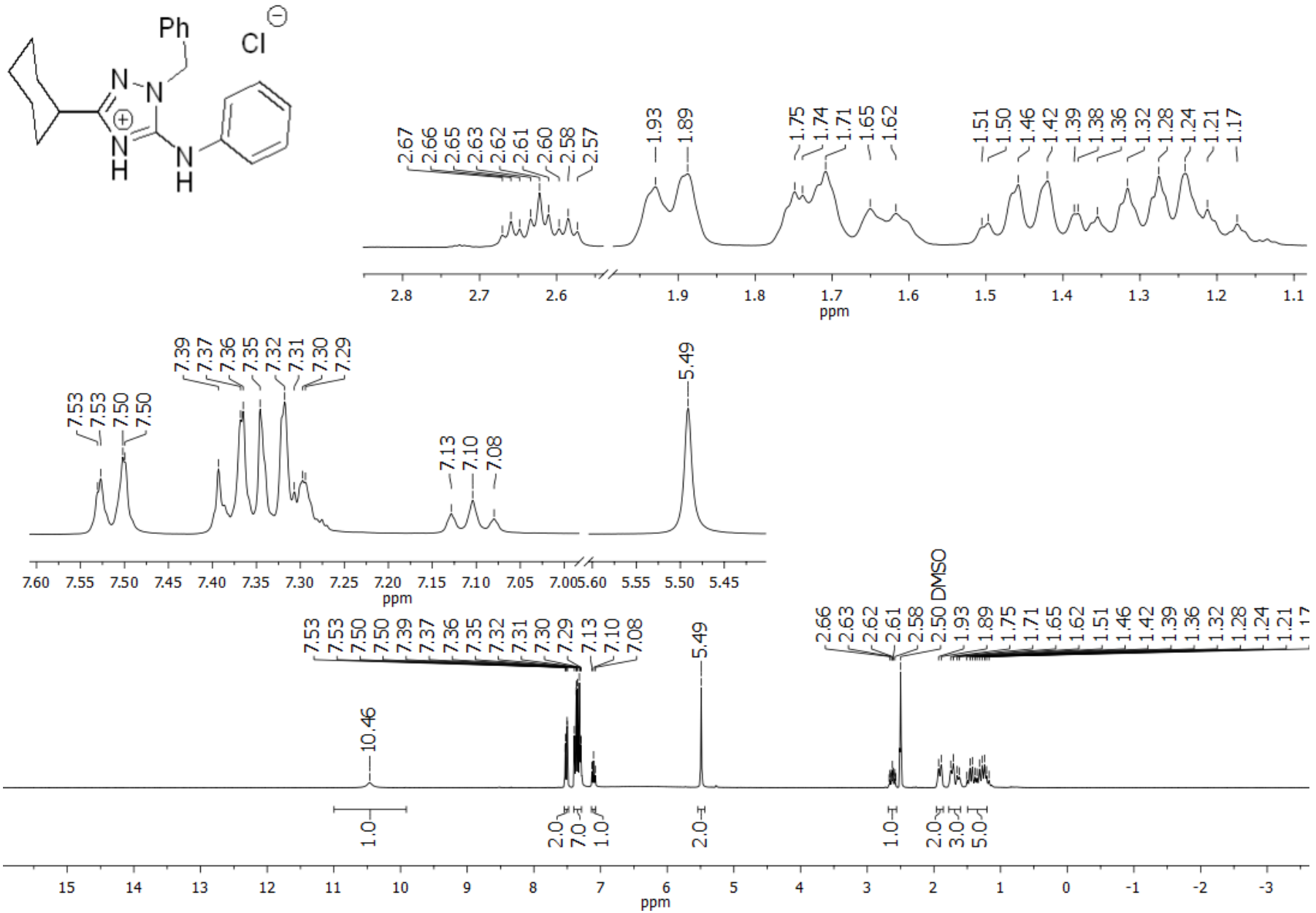

Figure S137. ^{1}H NMR spectrum of compound **9a** (DMSO-d_6, 300 MHz)

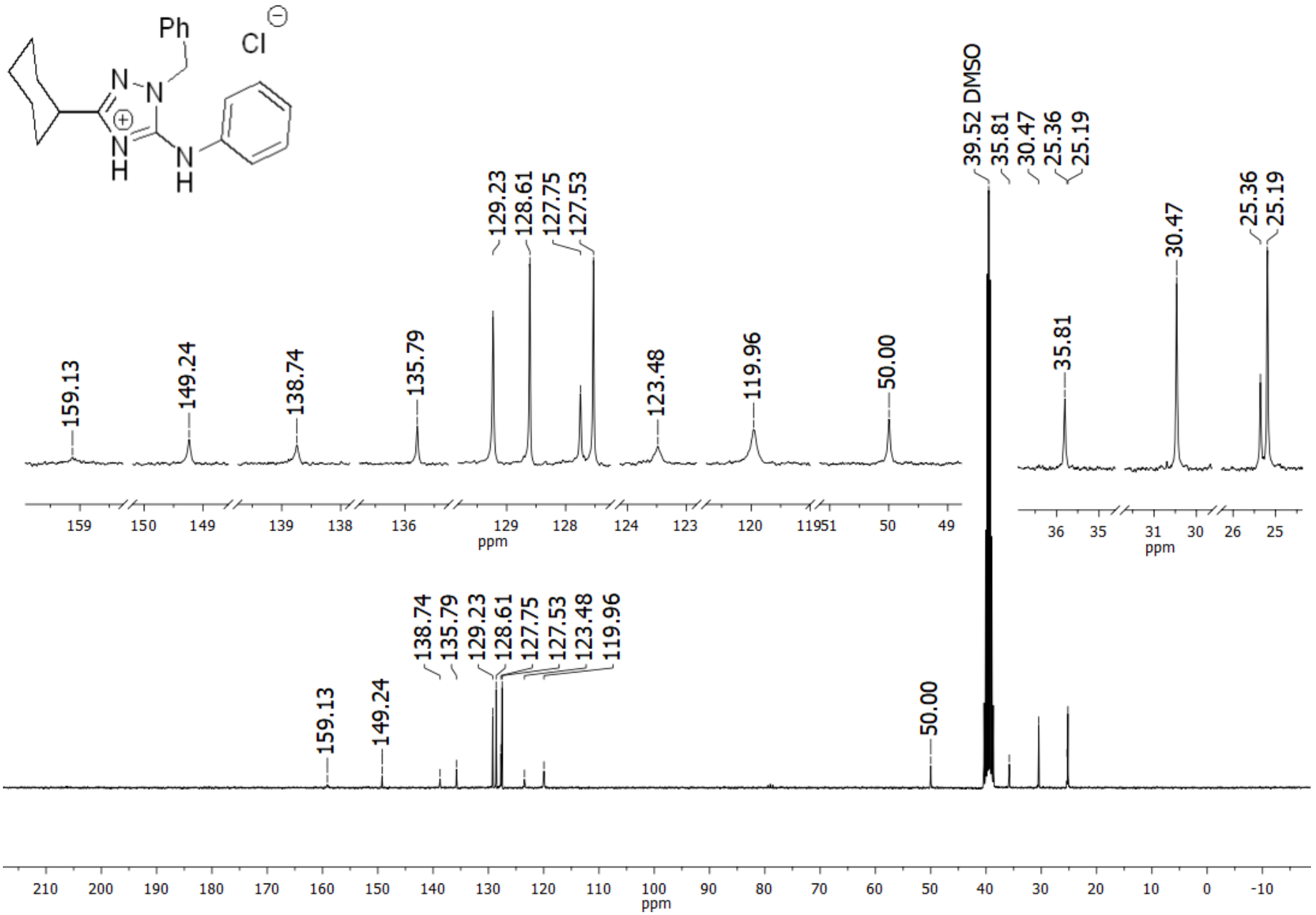

Figure S138. ^{13}C NMR spectrum of compound **9a** (DMSO-d_6, 75 MHz)

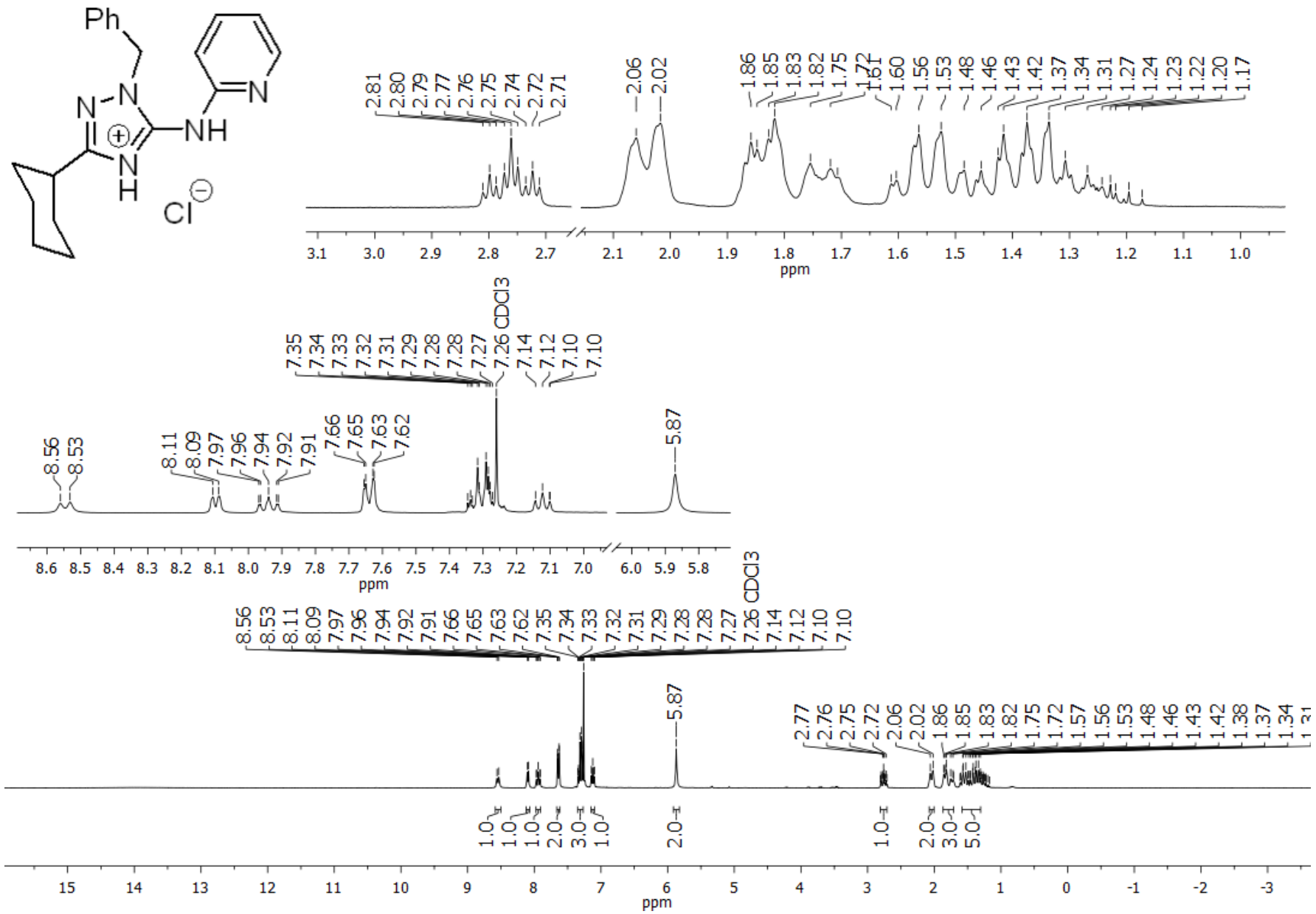

Figure S139. ^{1}H NMR spectrum of compound **9b** ($CDCl_3$, 300 MHz)

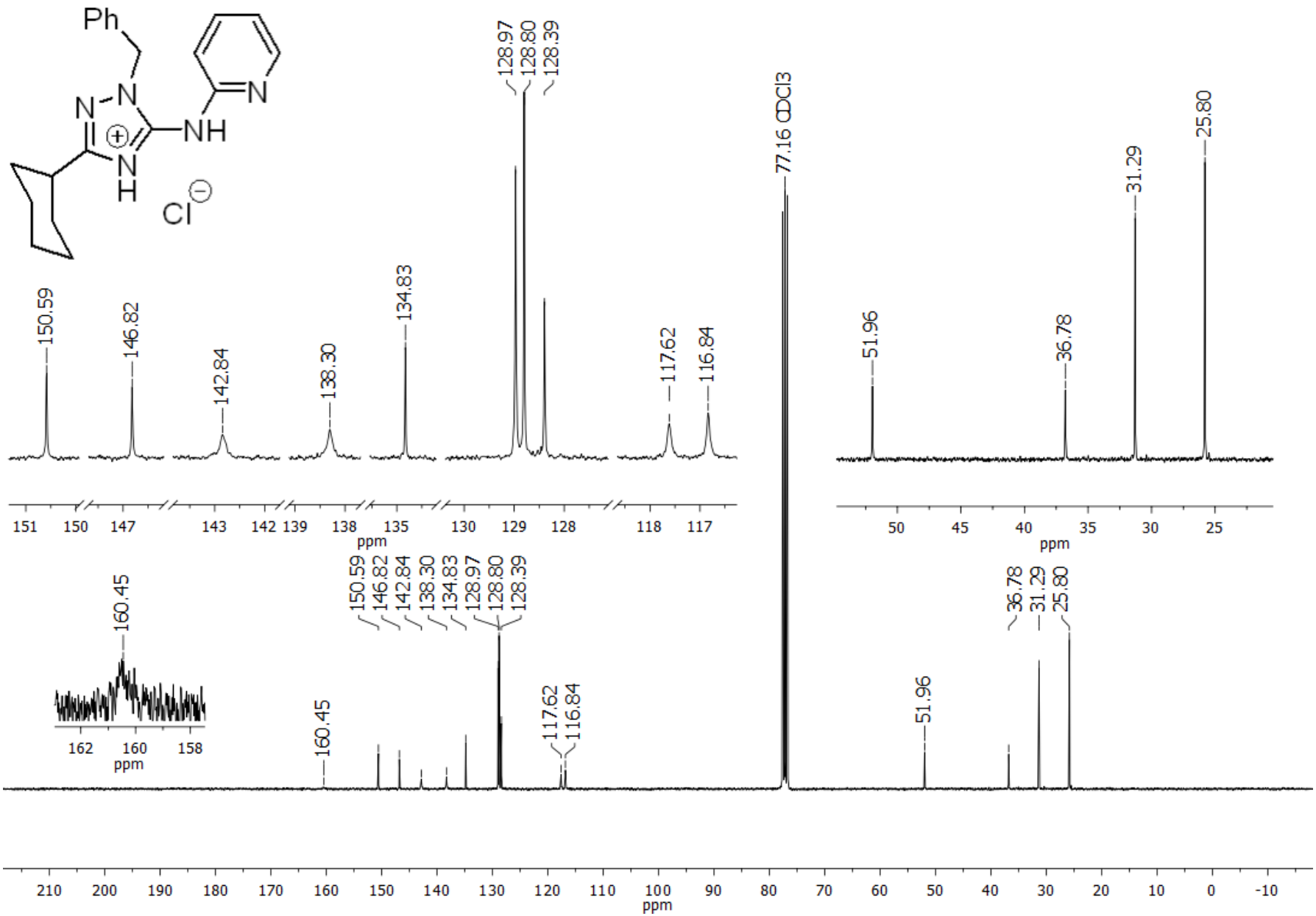

Figure S140. ^{13}C NMR spectrum of compound **9b** ($CDCl_3$, 75 MHz)

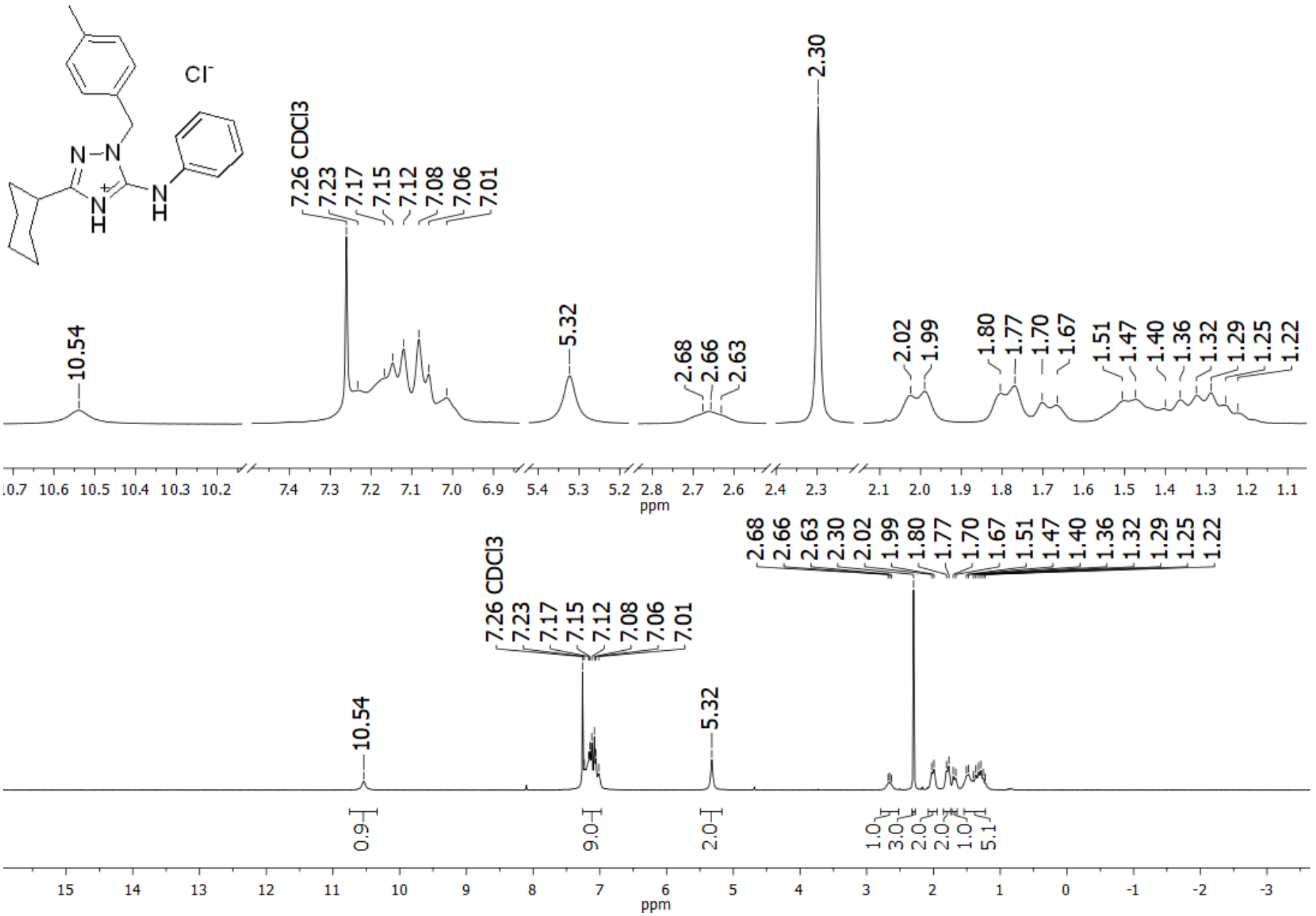

Figure S141. ^{1}H NMR spectrum of compound **9c** ($CDCl_3$, 300 MHz)

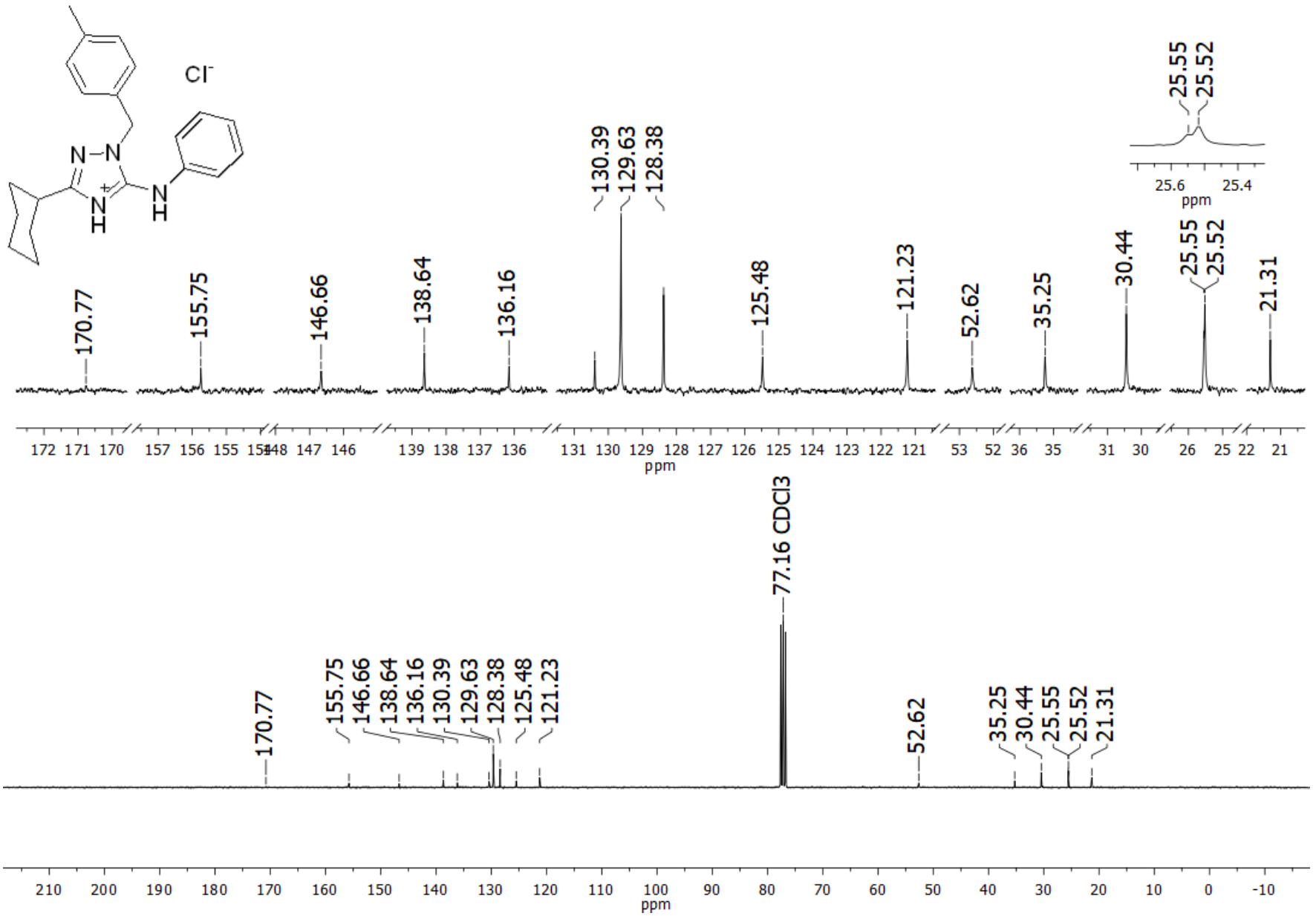

Figure S142. ^{13}C NMR spectrum of compound **9c** ($CDCl_3$, 75 MHz)

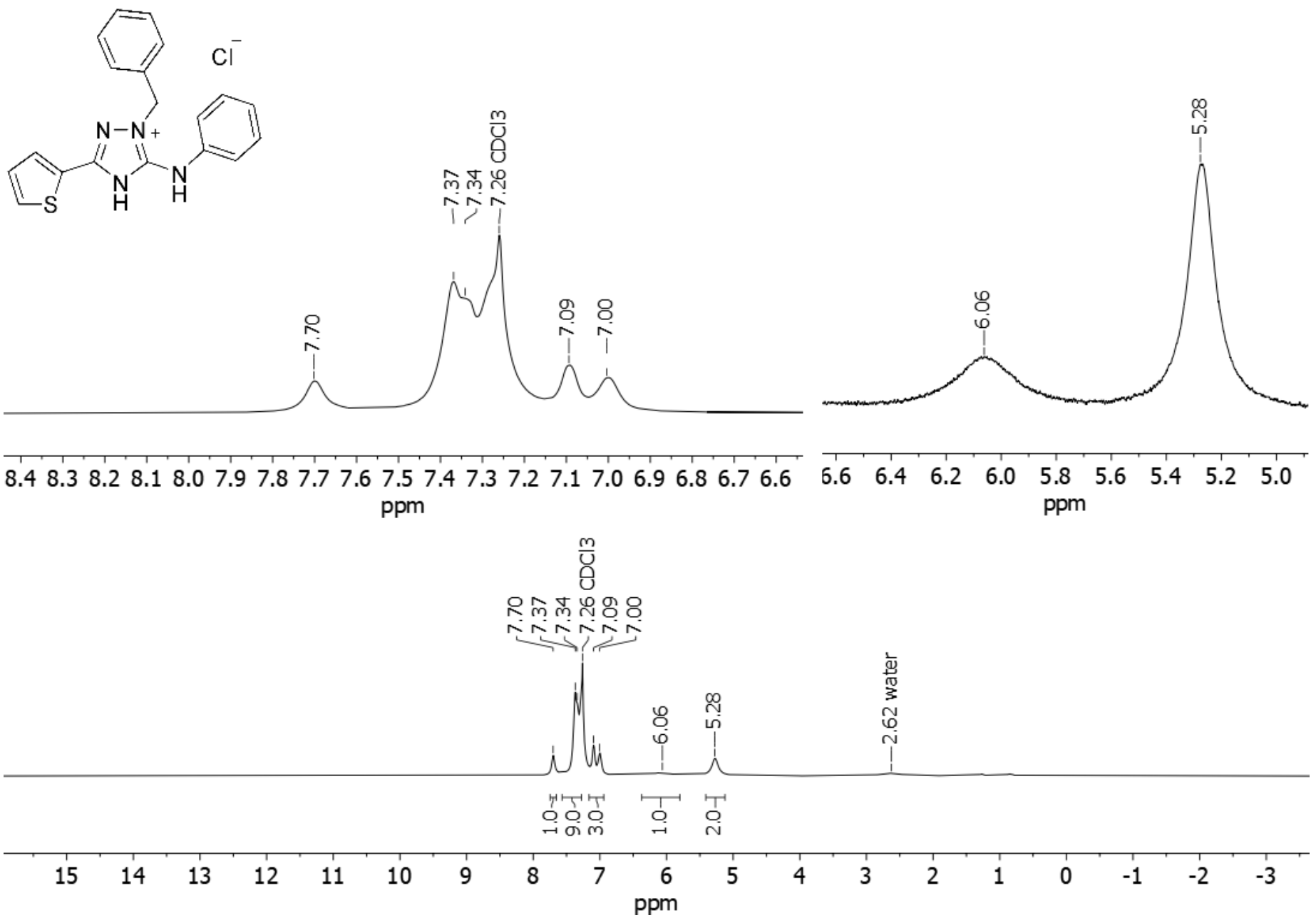

Figure S143. ^{1}H NMR spectrum of compound **9d** ($CDCl_3$, 300 MHz)

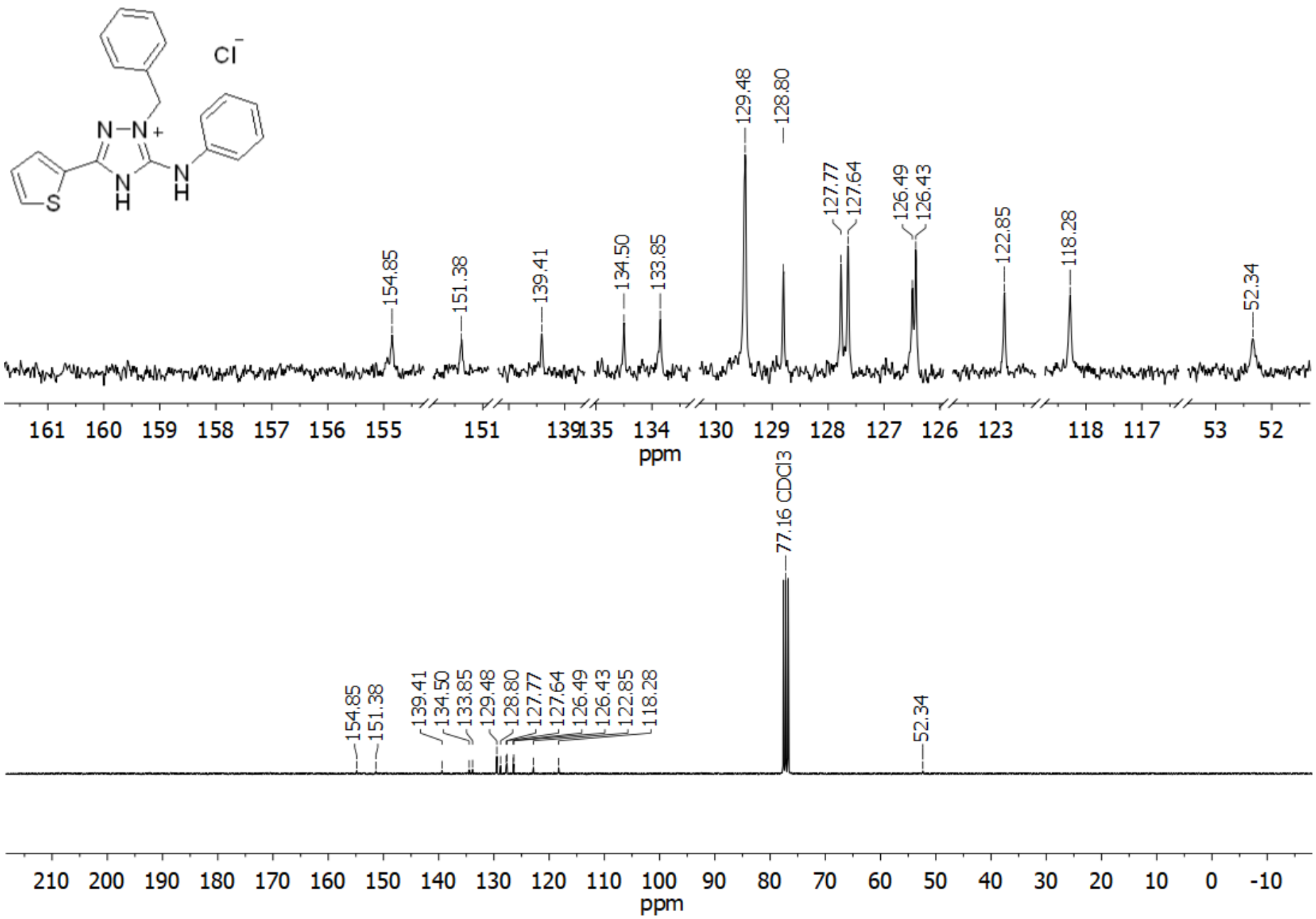

Figure S144. ^{13}C NMR spectrum of compound **9d** ($CDCl_3$, 75 MHz)

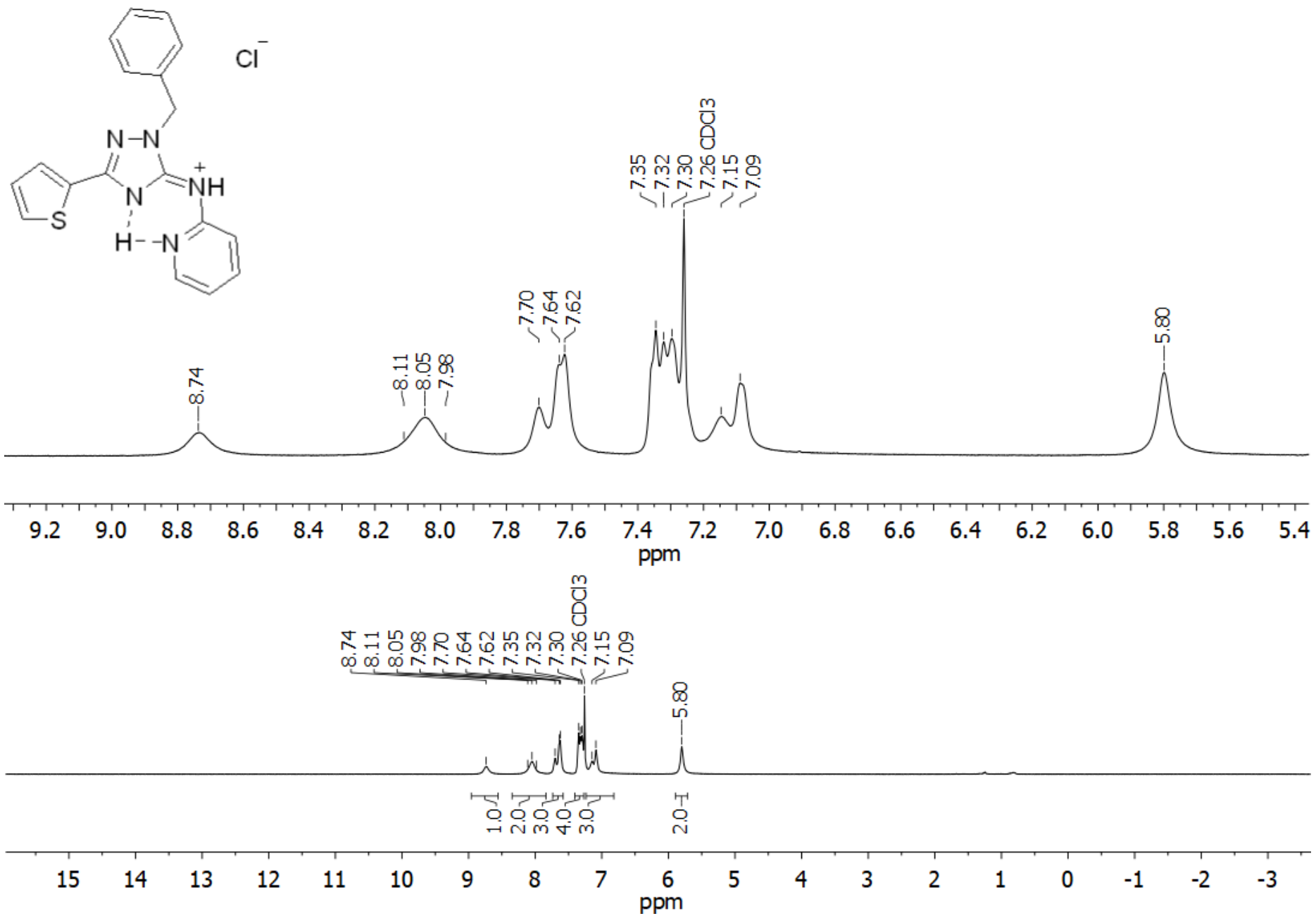

Figure S145. ^{1}H NMR spectrum of compound **9e** ($CDCl_3$, 300 MHz)

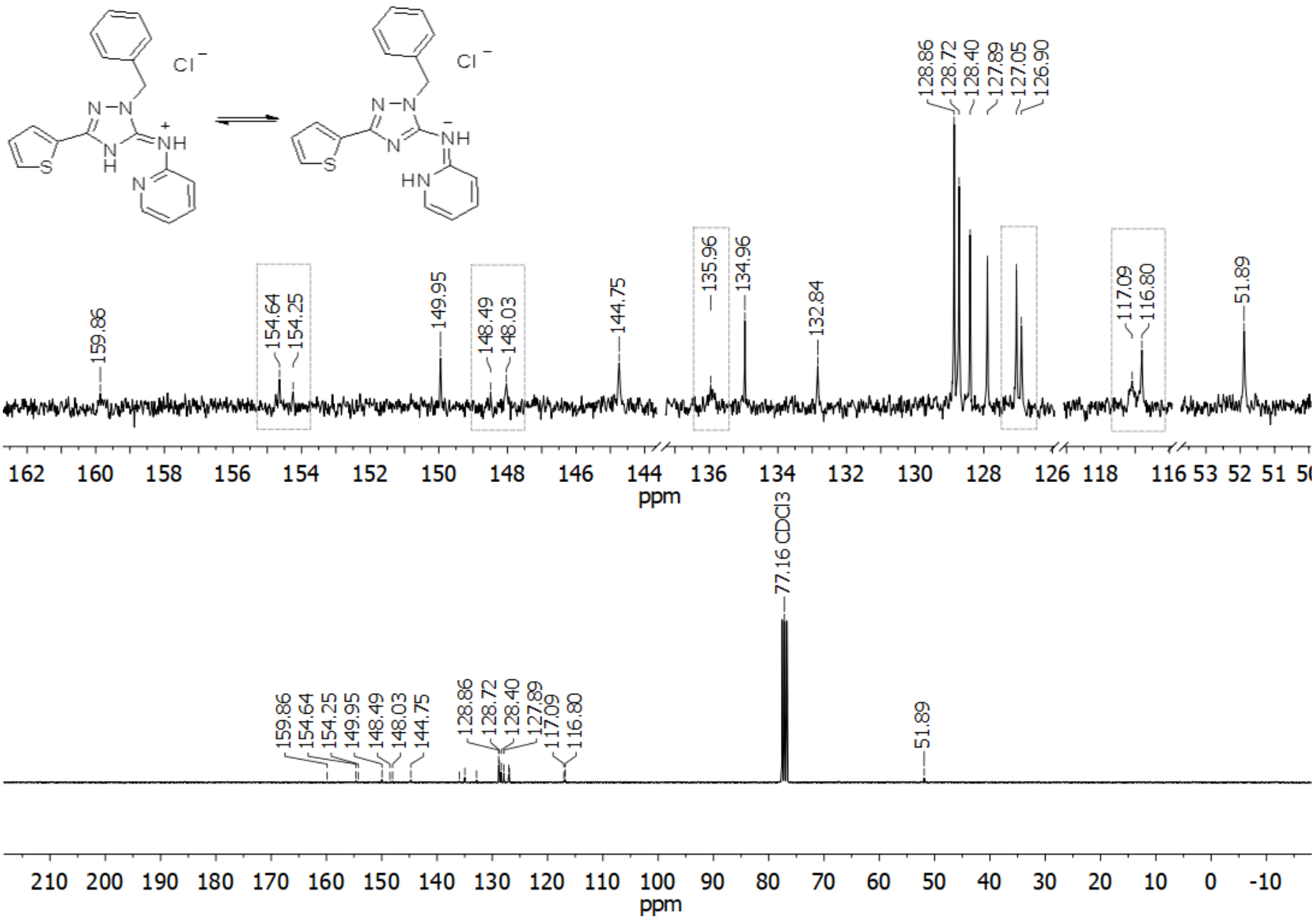

Figure S146. ^{13}C NMR spectrum of compound **9e** ($CDCl_3$, 75 MHz)

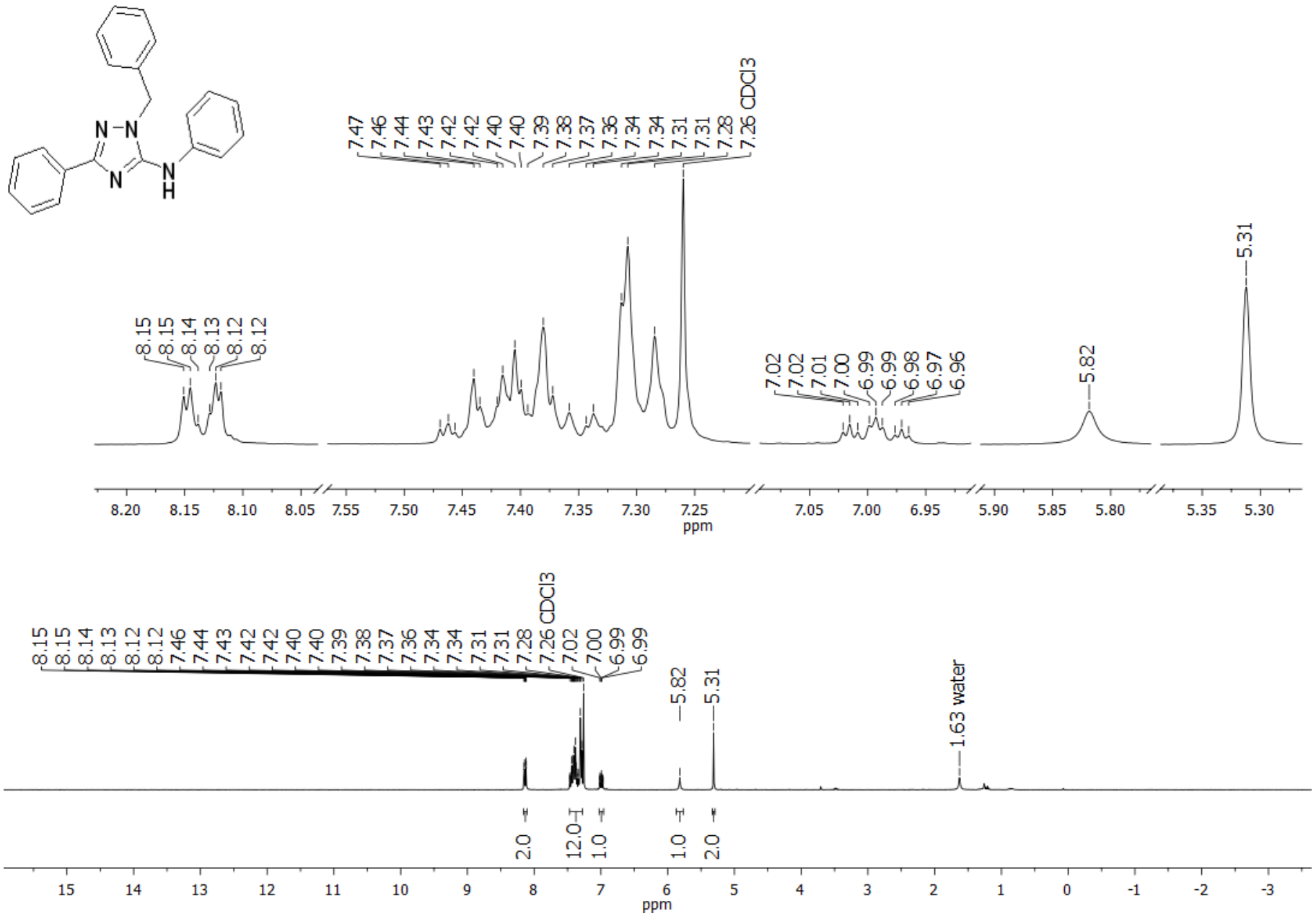

Figure S147. ^{1}H NMR spectrum of compound **9f** ($CDCl_3$, 300 MHz)

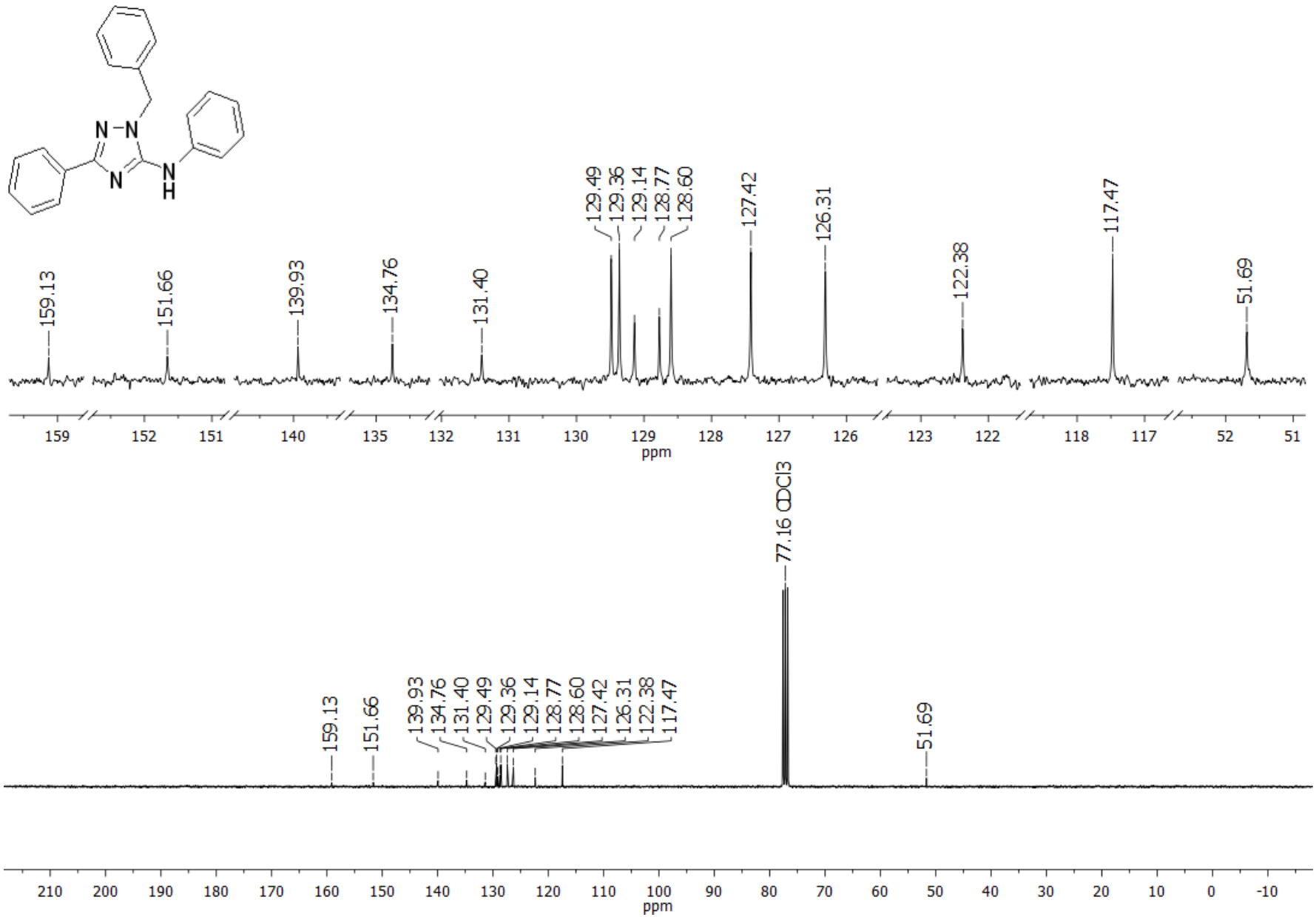

Figure S148. ^{13}C NMR spectrum of compound **9f** ($CDCl_3$, 75 MHz)

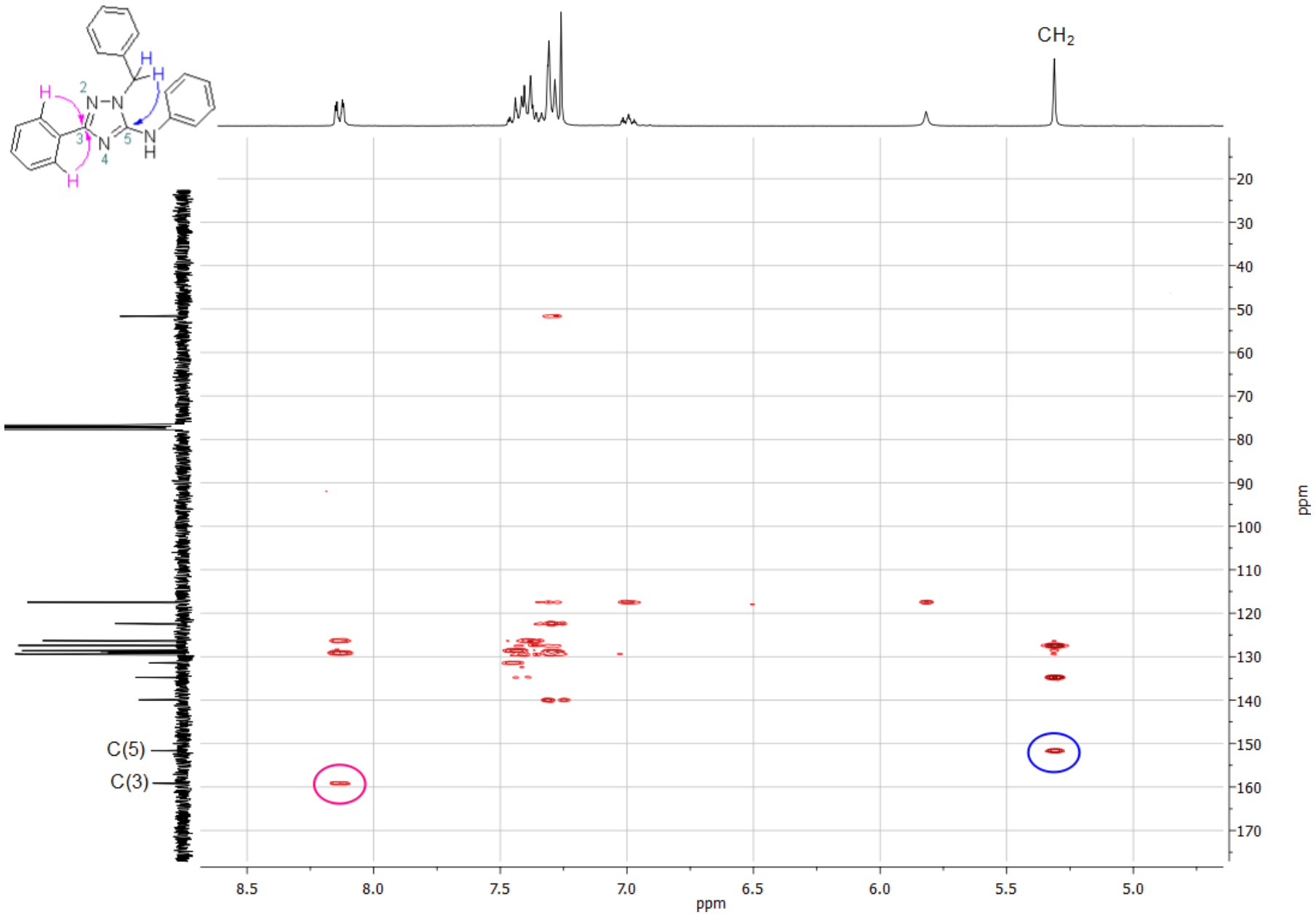

Figure S149. ^{1}H-^{13}C HMBC spectrum of compound **9f** ($CDCl_3$)

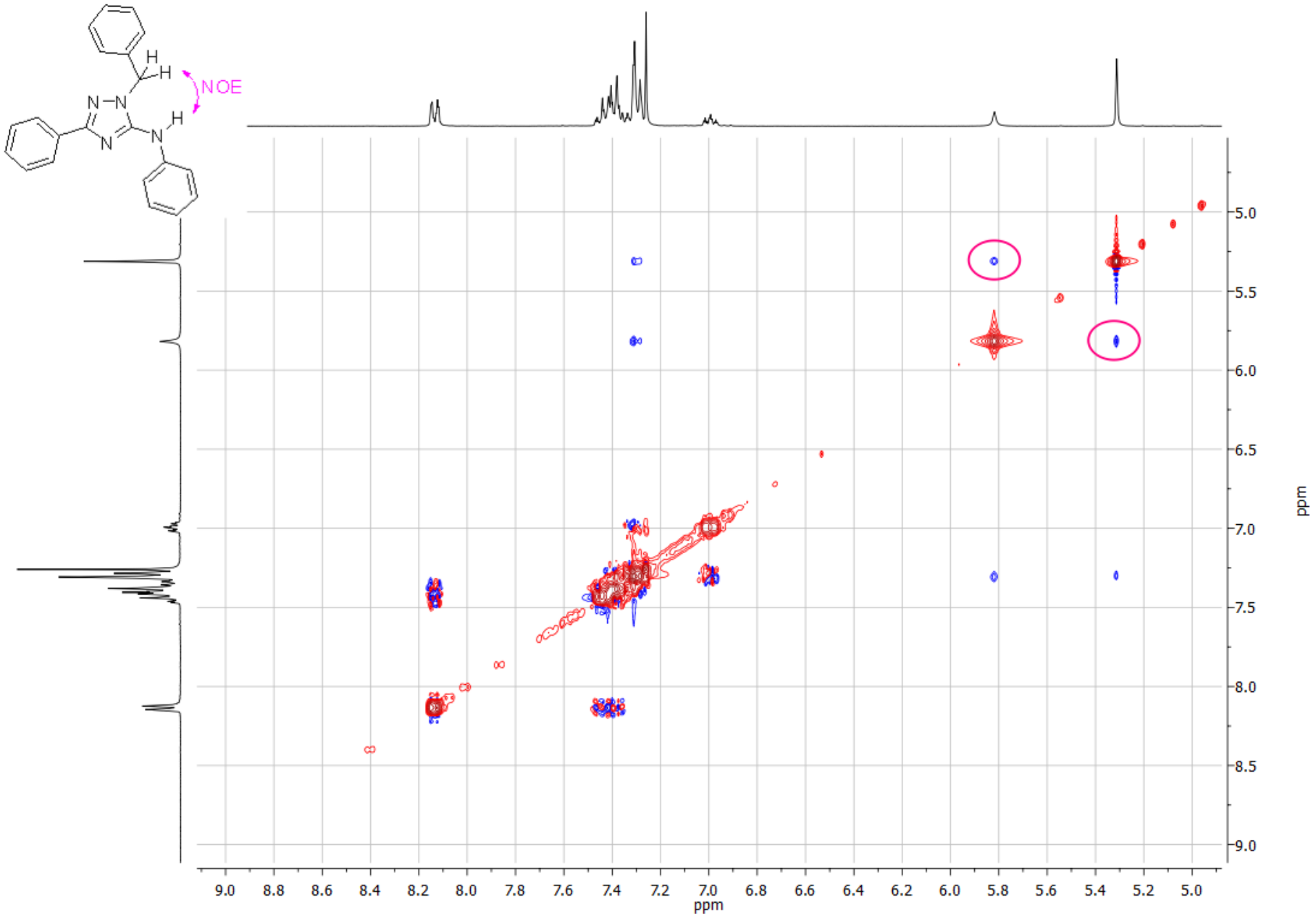

Figure S150. ^{1}H-^{1}H NOESY spectrum of compound **9f** ($CDCl_3$)

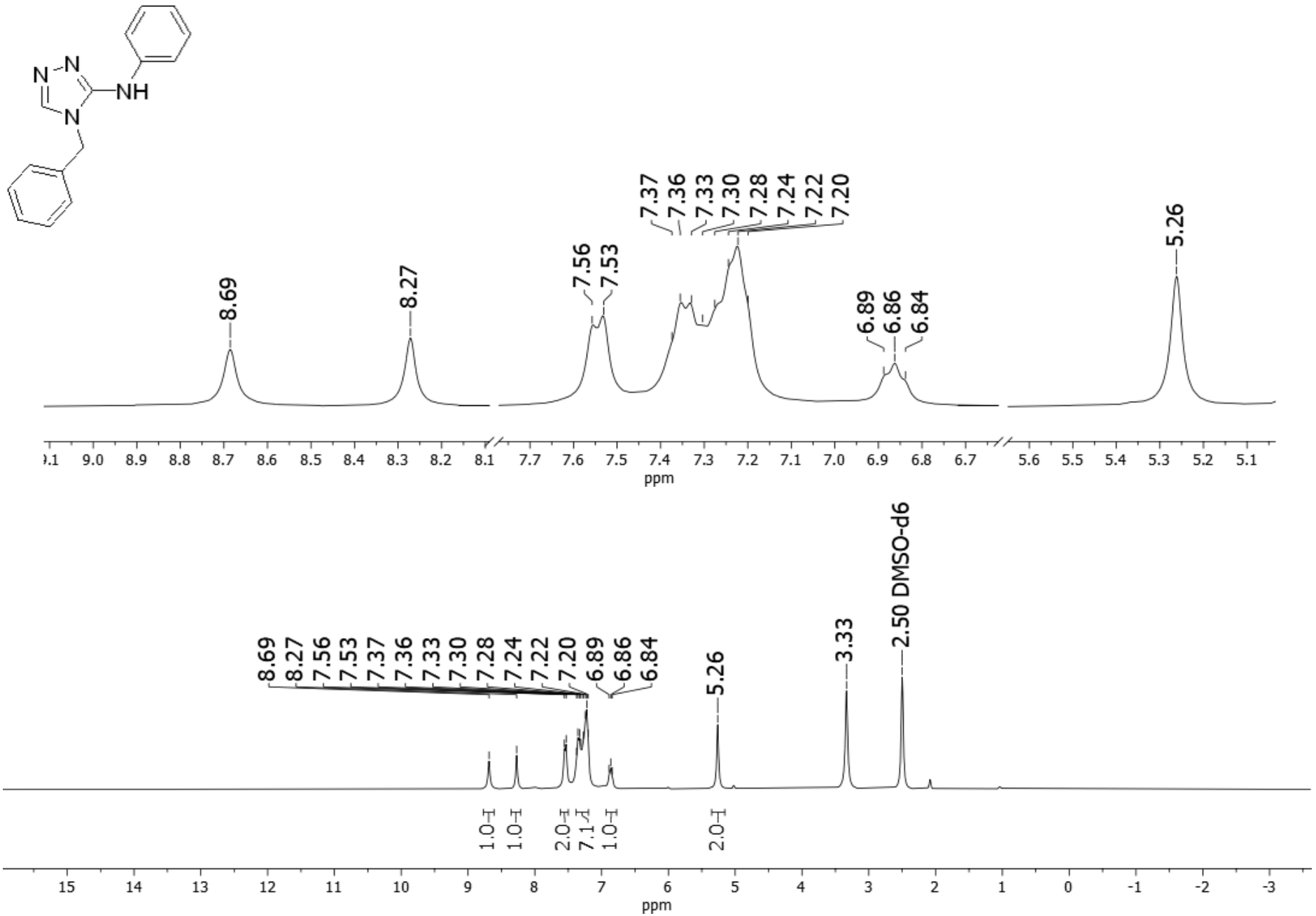

Figure S151. ^{1}H NMR spectrum of compound **10a** (DMSO-d_6, 300 MHz)

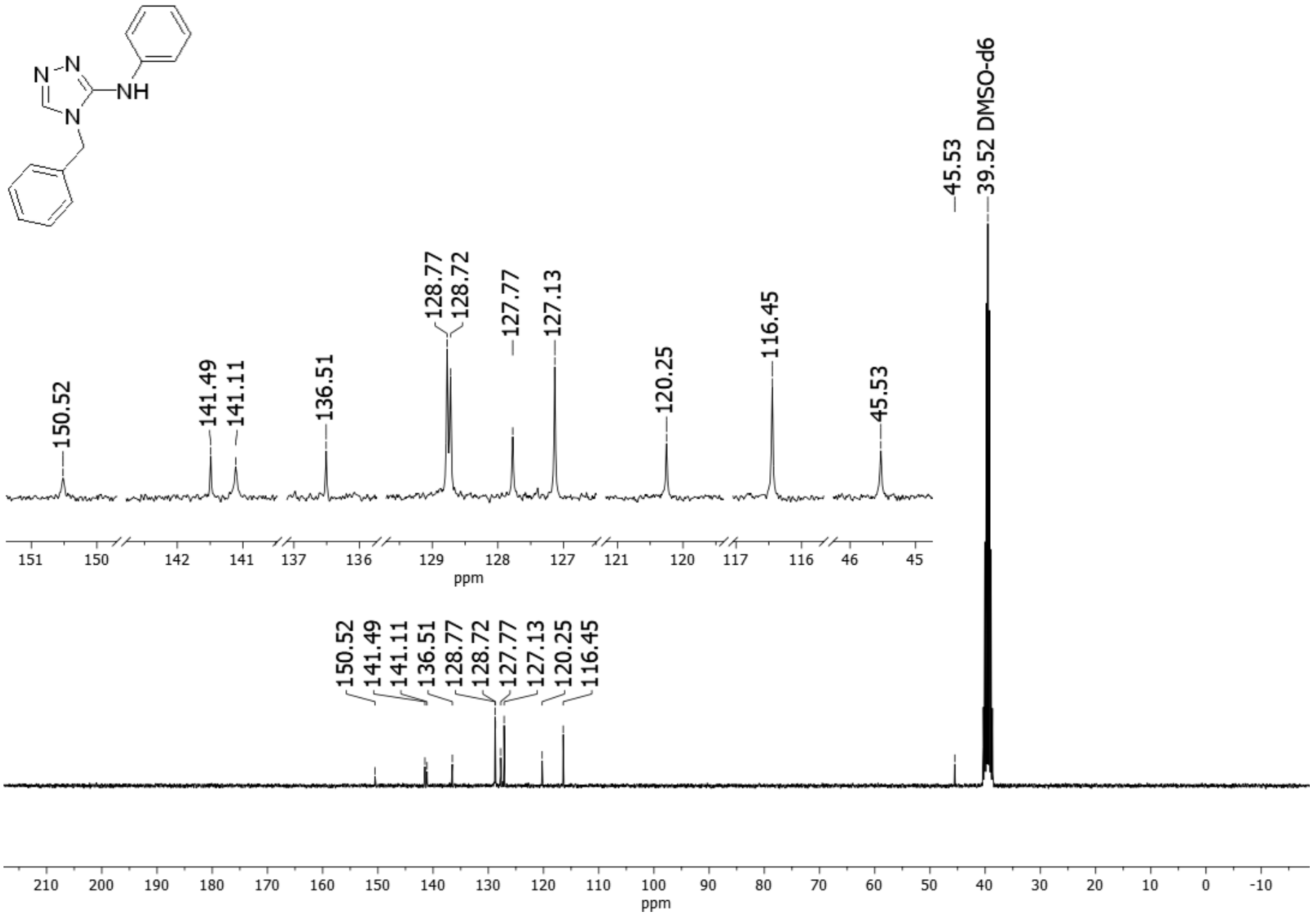

Figure S152. ^{13}C NMR spectrum of compound **10a** (DMSO-d_6, 75 MHz)

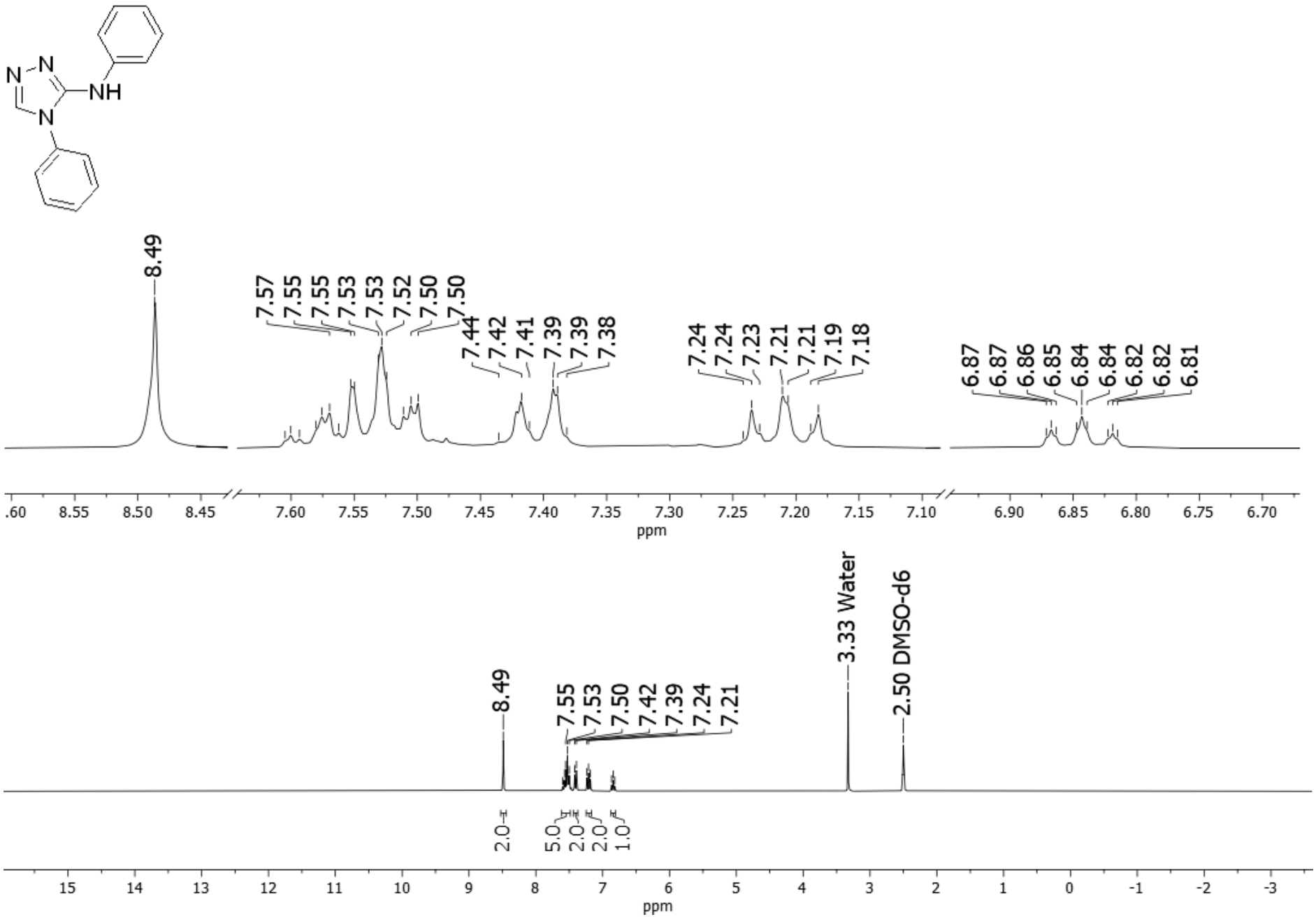

Figure S153. ^{1}H NMR spectrum of compound **10b** (DMSO-d_6, 300 MHz)

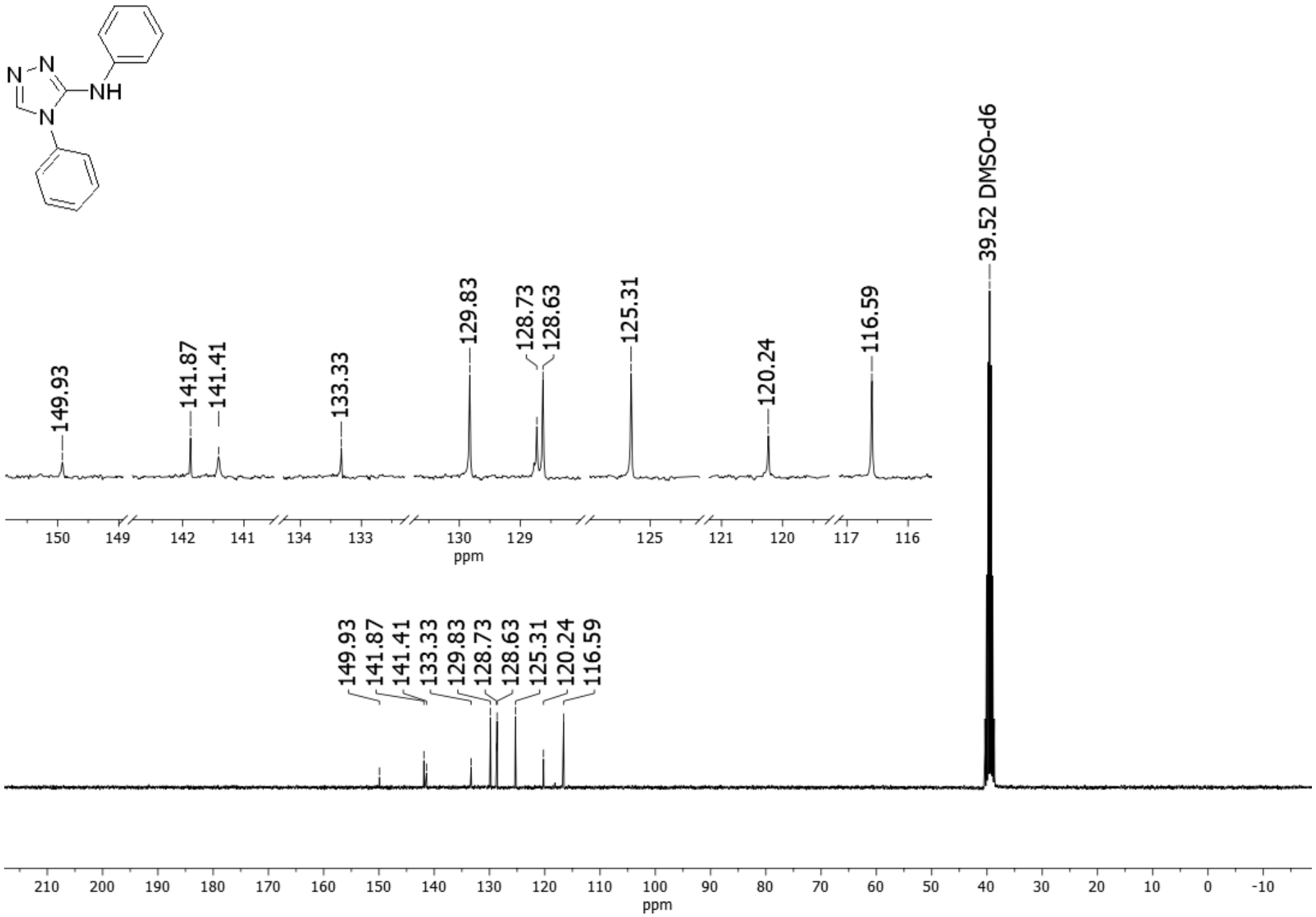

Figure S154. ^{13}C NMR spectrum of compound **10b** (DMSO-d_6, 75 MHz)

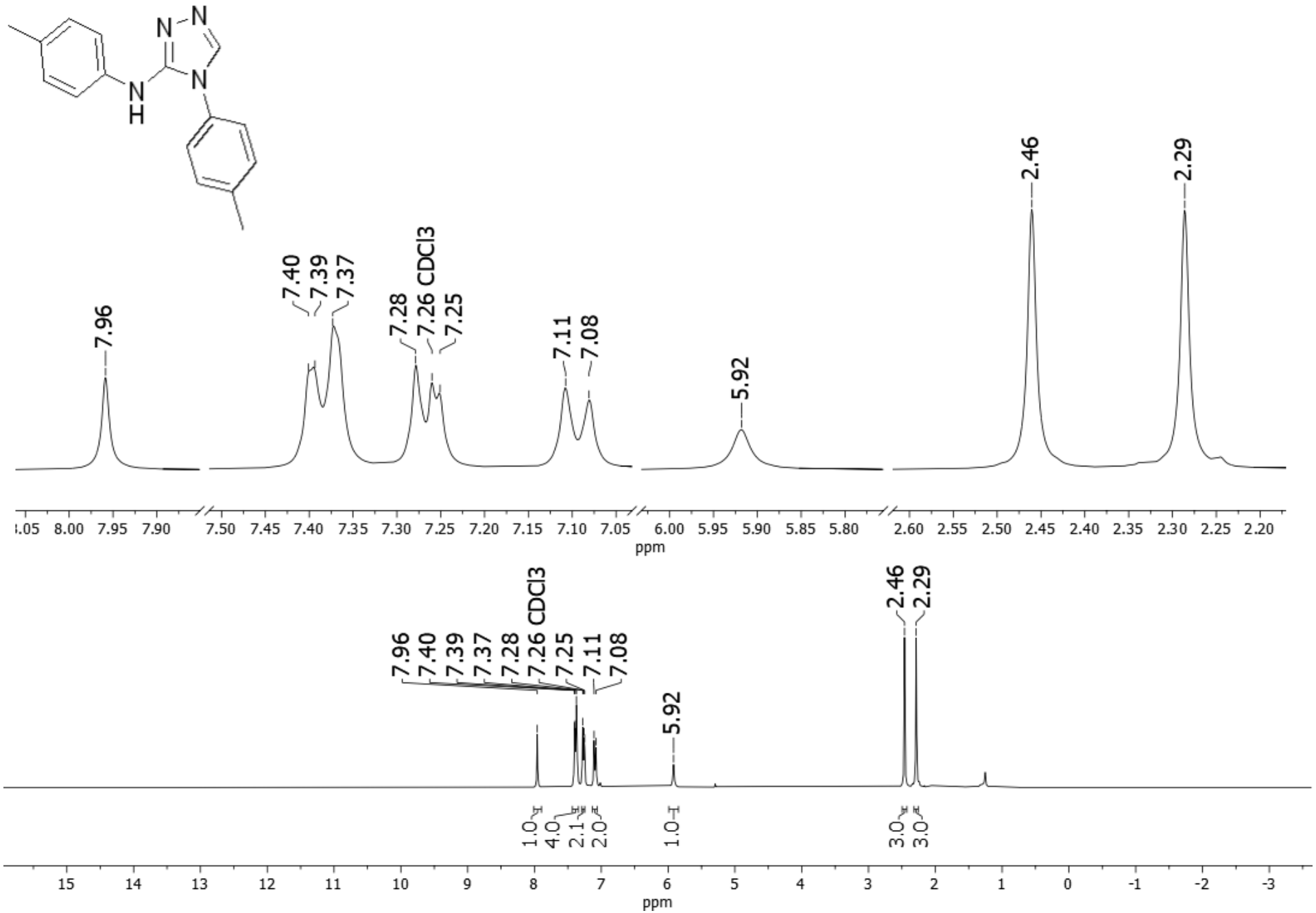

Figure S155. ^{1}H NMR spectrum of compound **10c** ($CDCl_3$, 300 MHz)

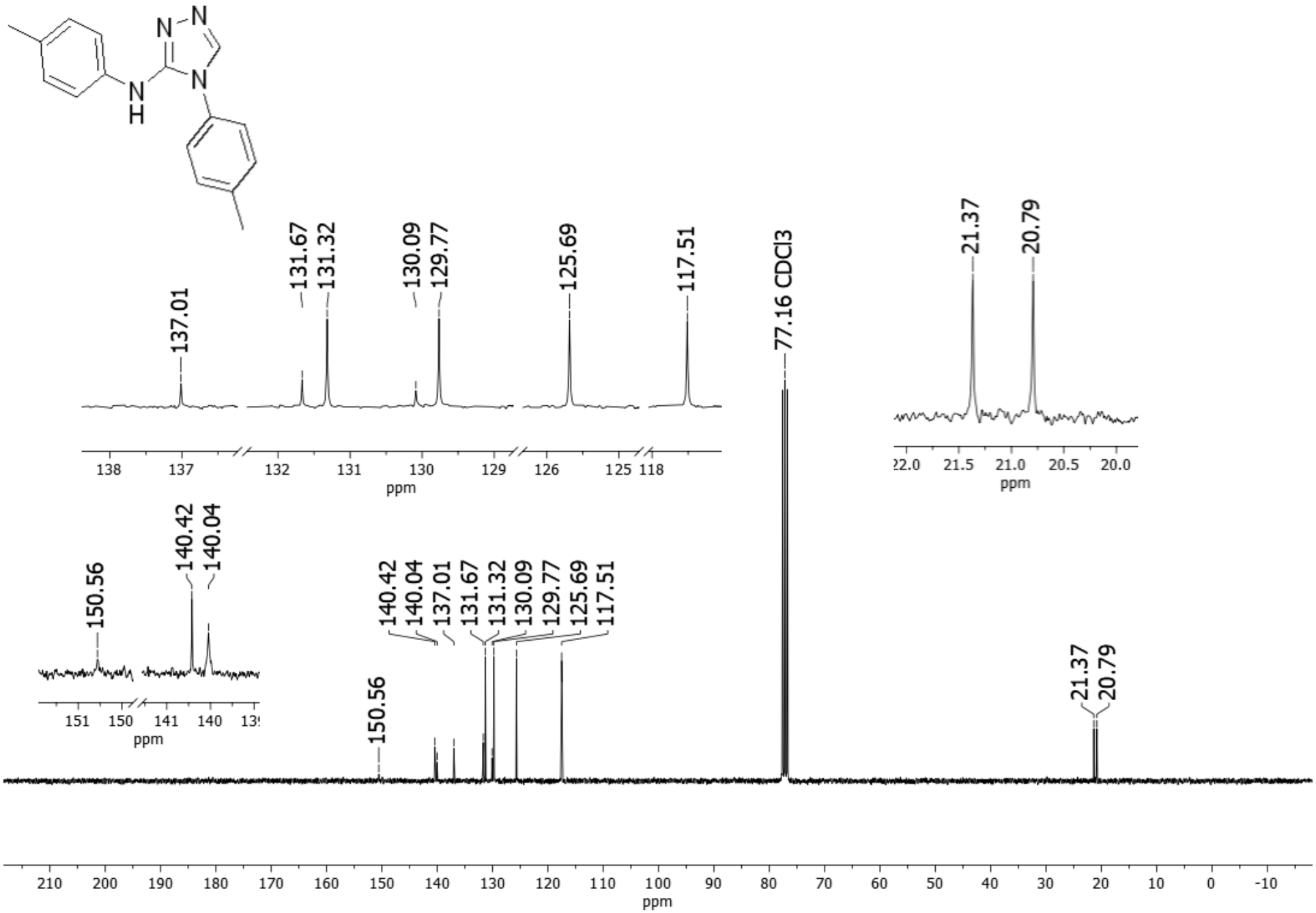

Figure S156. ^{13}C NMR spectrum of compound **10c** ($CDCl_3$, 75 MHz)

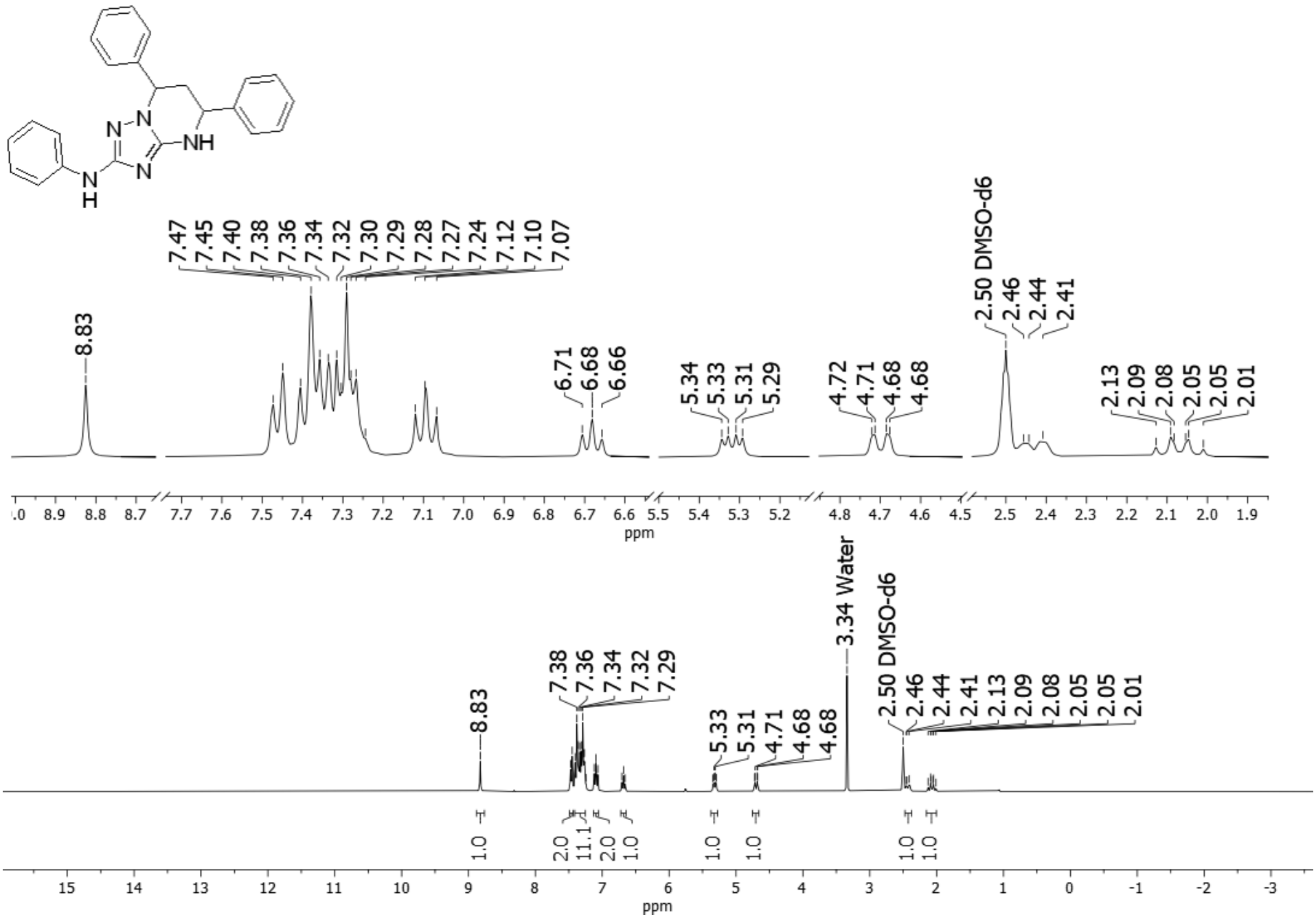

Figure S157. ^{1}H NMR spectrum of compound **12a** (DMSO-d_6, 300 MHz)

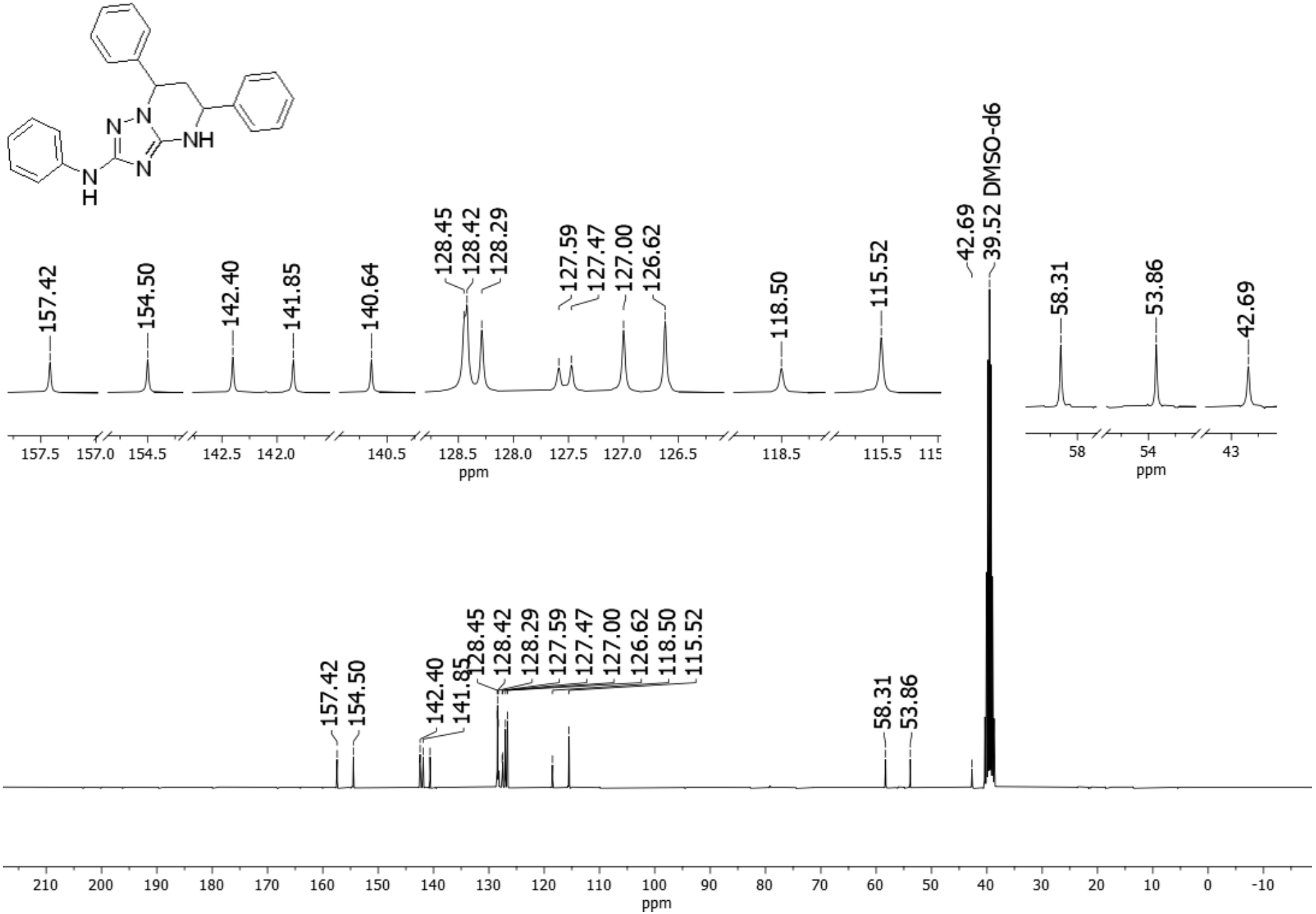

Figure S158. ^{13}C NMR spectrum of compound **12a** (DMSO-d_6, 75 MHz)

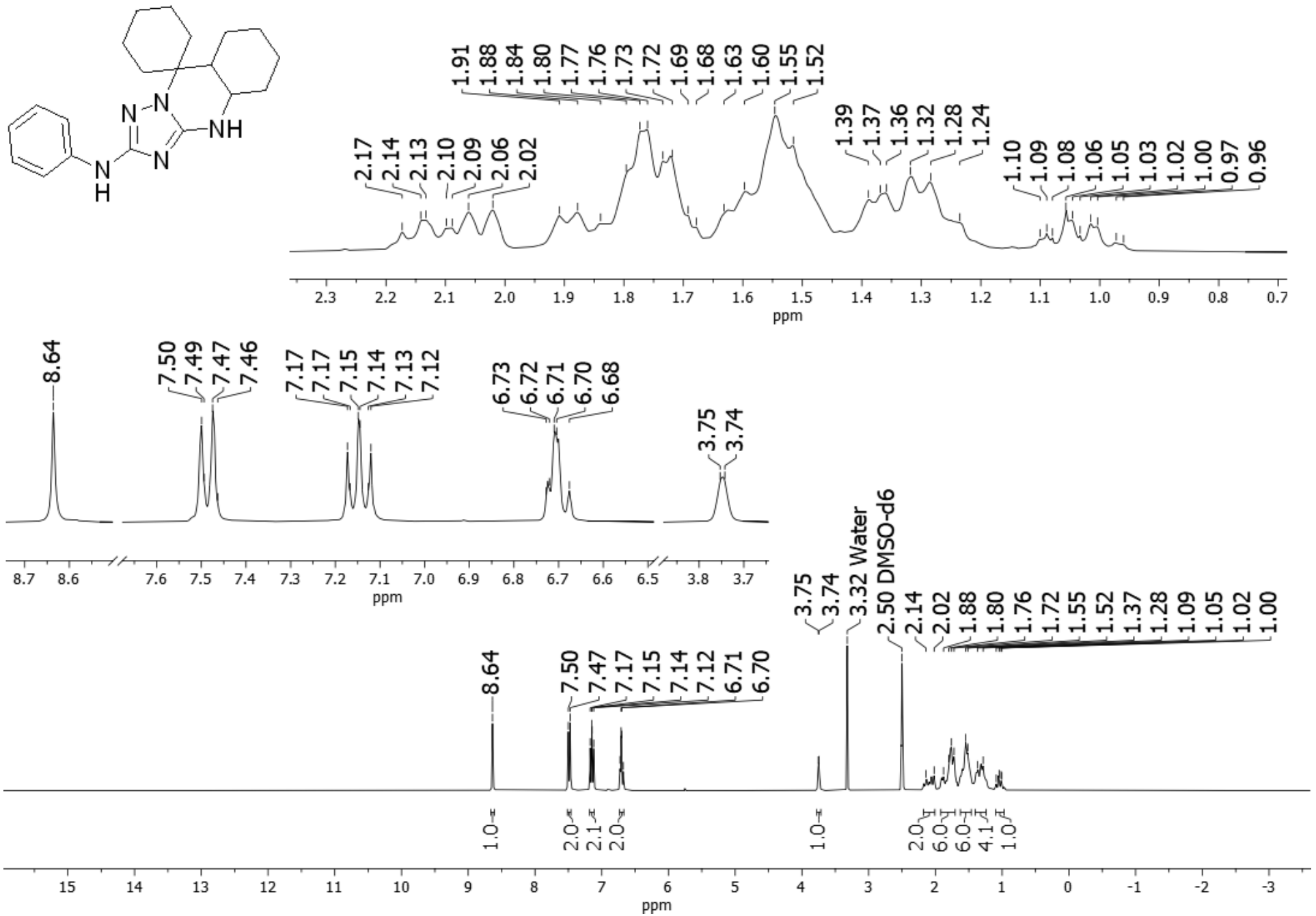

Figure S159. ^{1}H NMR spectrum of compound **12b** (DMSO-d_6, 300 MHz)

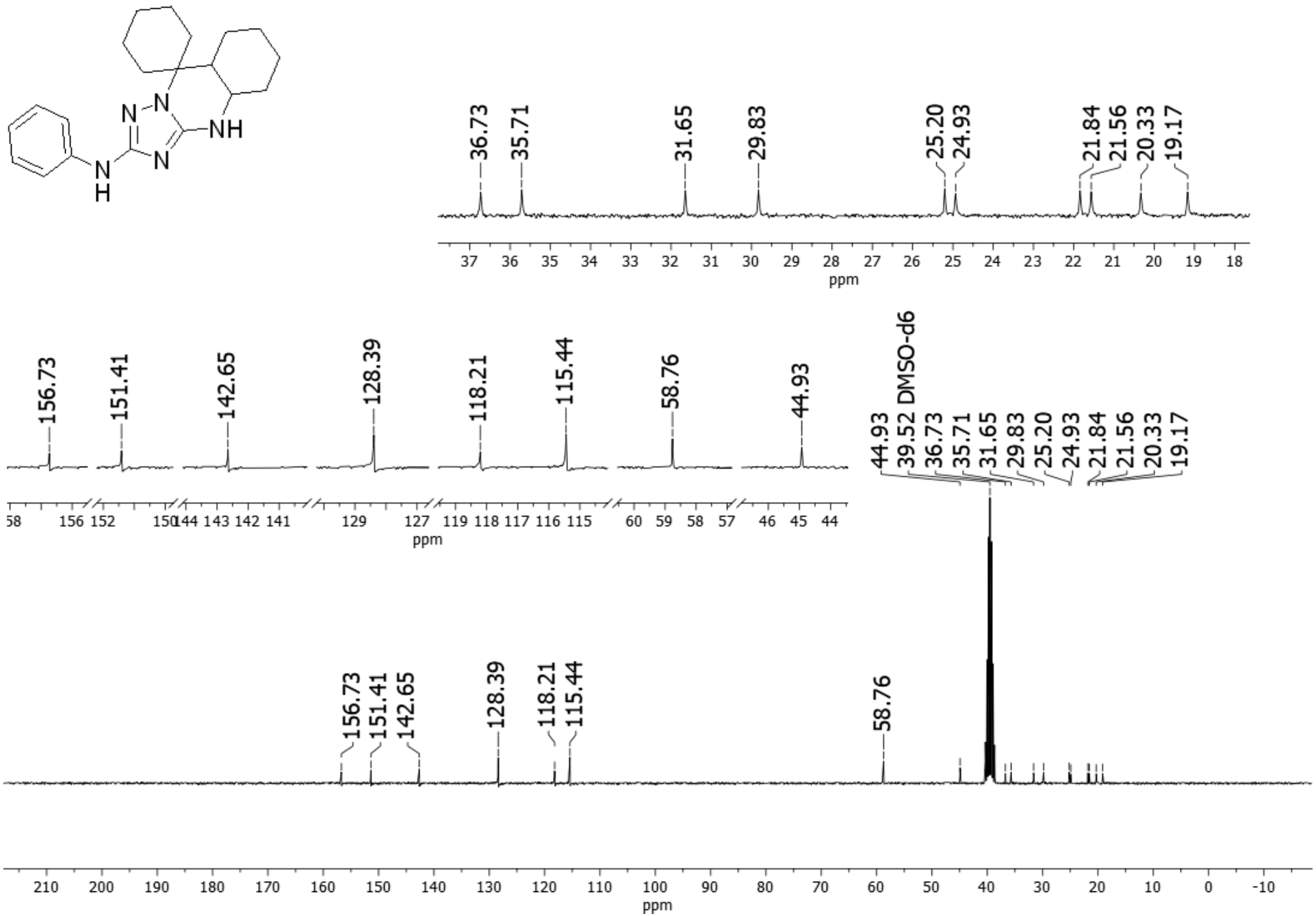

Figure S160. ^{13}C NMR spectrum of compound **12b** (DMSO-d_6, 75 MHz)

Figure S161. ^{1}H NMR spectrum of compound **12c** (DMSO-d_6, 300 MHz)

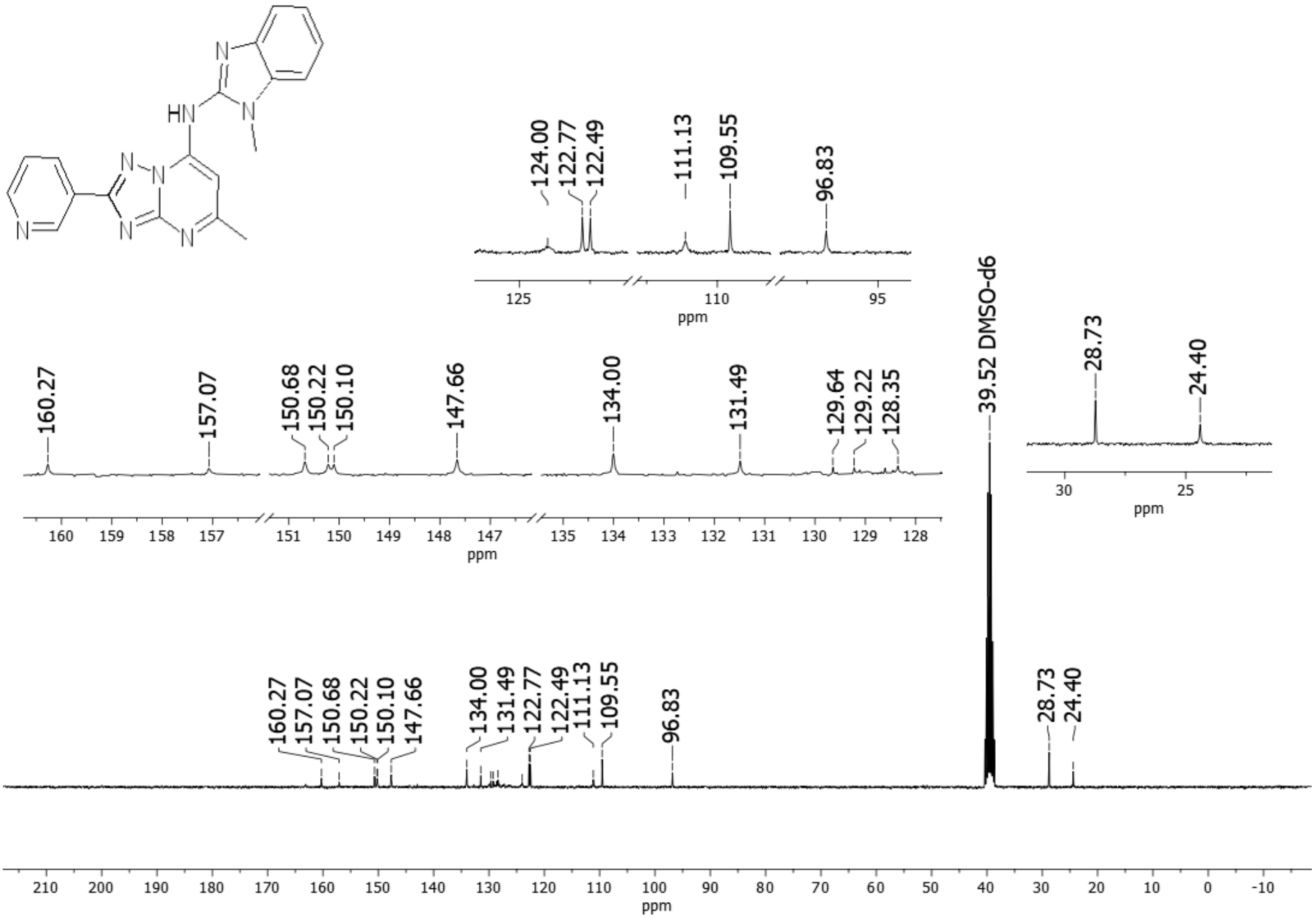

Figure S162. ^{13}C NMR spectrum of compound **12c** (DMSO-d_6, 75 MHz)

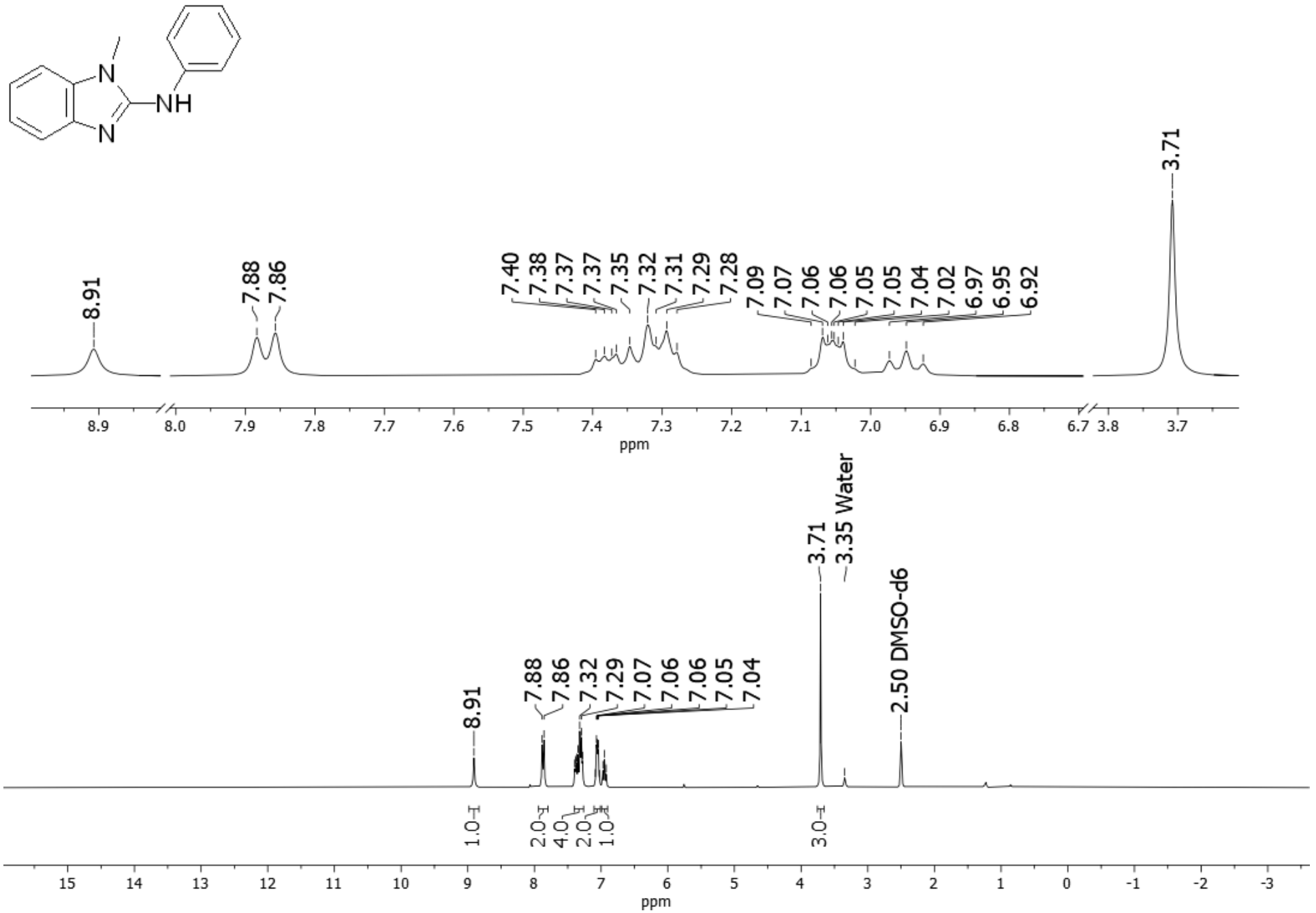

Figure S163. ^{1}H NMR spectrum of compound **12d** (DMSO-d_6, 300 MHz)

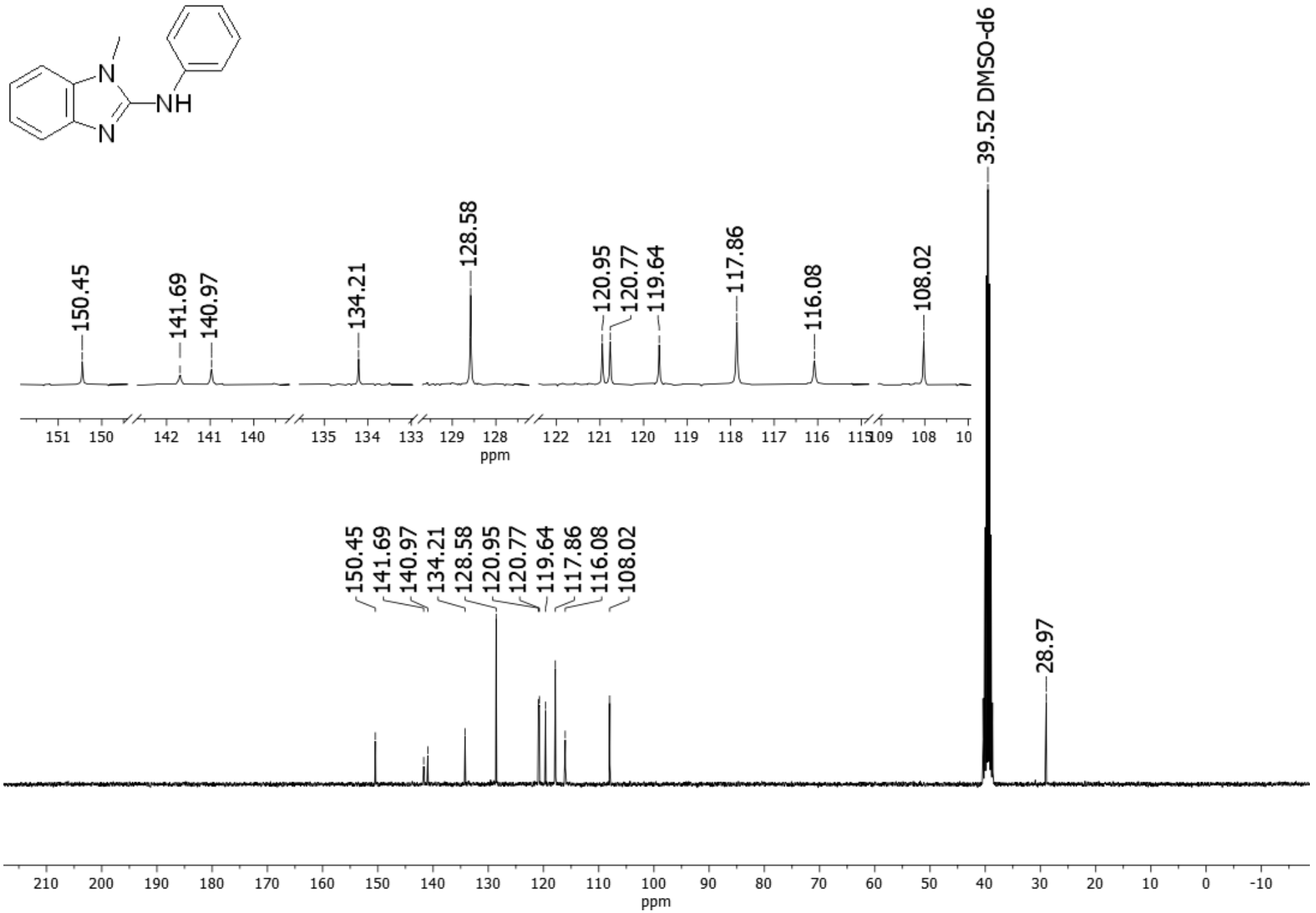

Figure S164. ^{13}C NMR spectrum of compound **12d** (DMSO-d_6, 75 MHz)

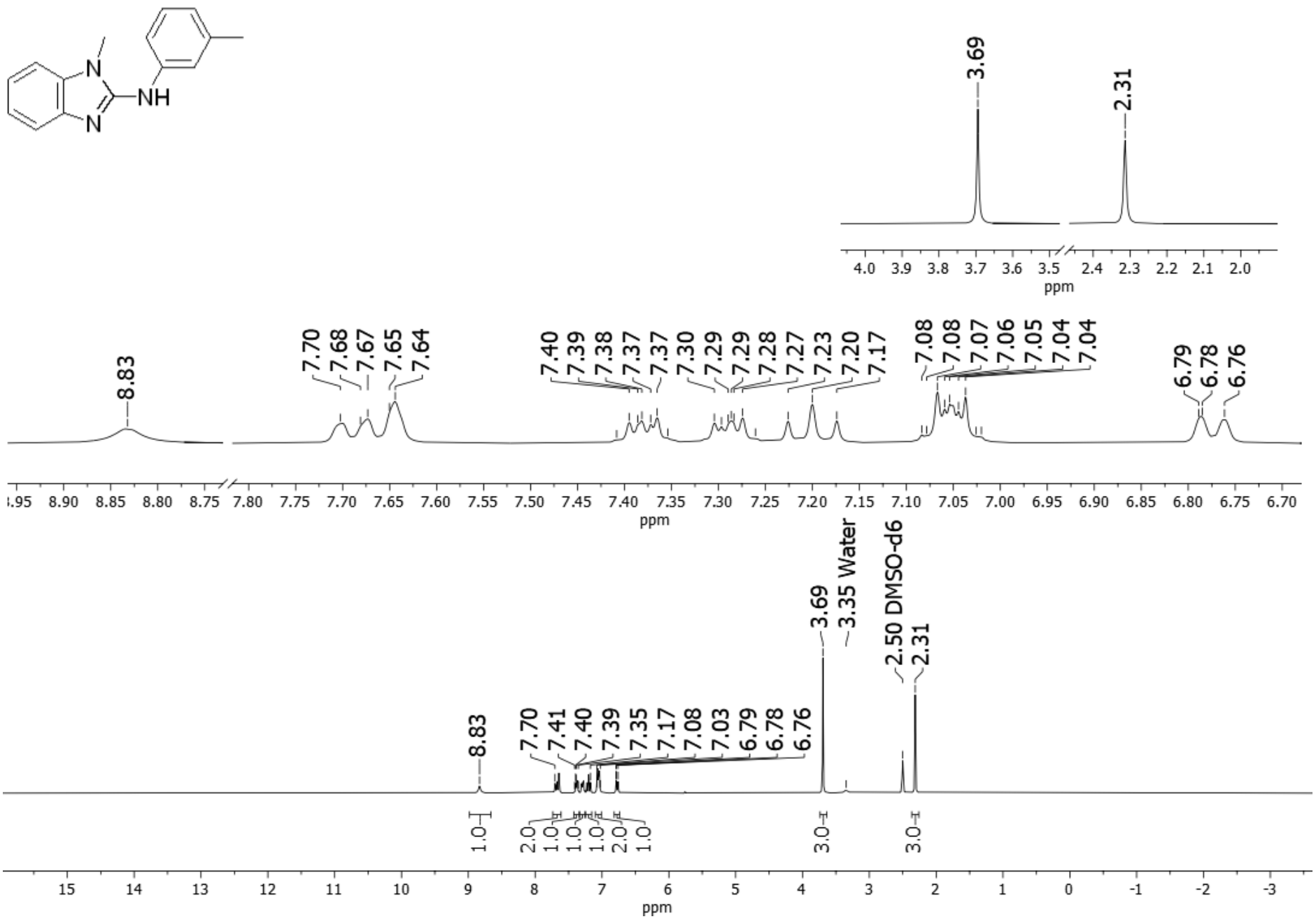

Figure S165. ^{1}H NMR spectrum of compound **12e** (DMSO-d_6, 300 MHz)

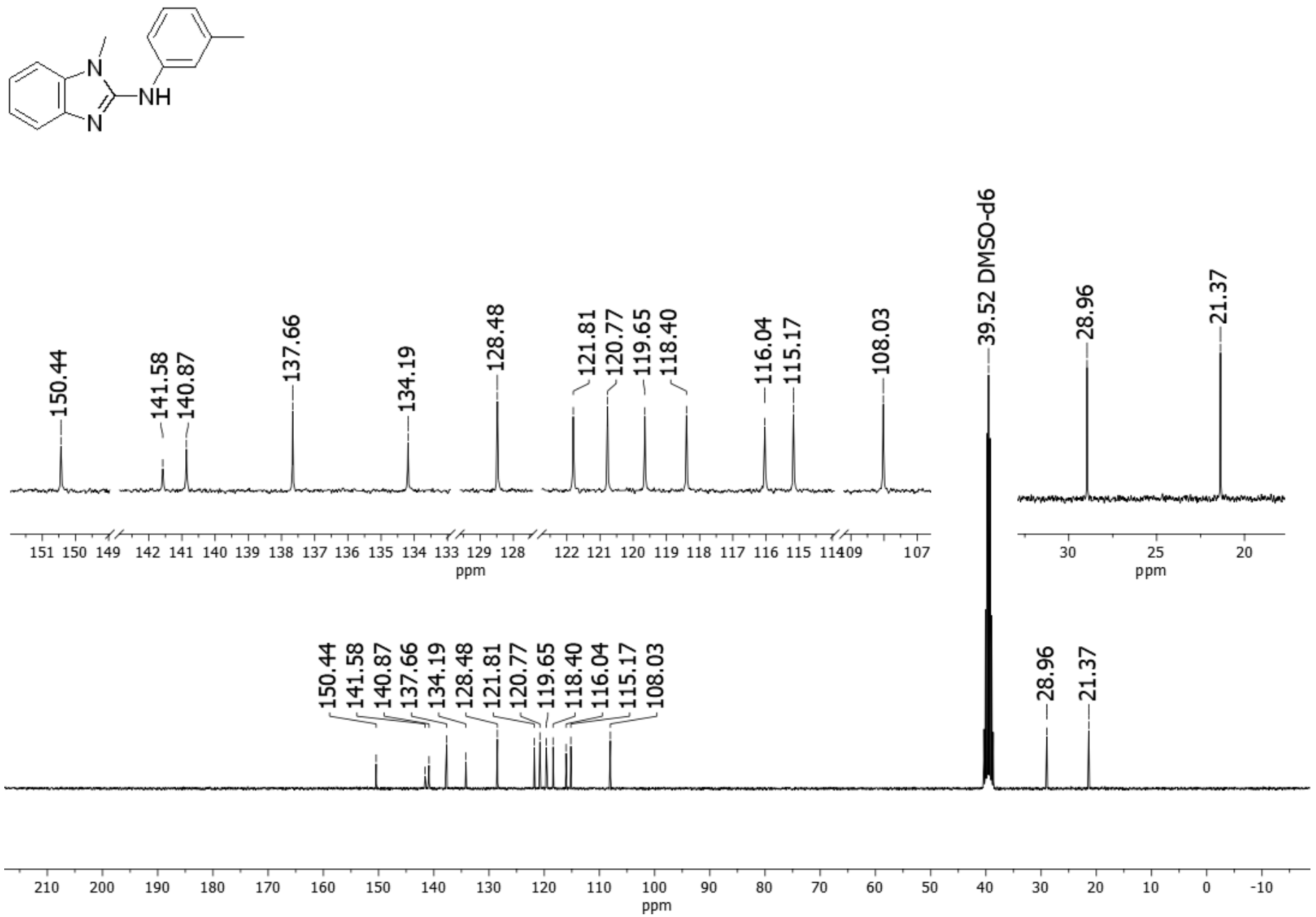

Figure S166. ^{13}C NMR spectrum of compound **12e** (DMSO-d_6, 75 MHz)

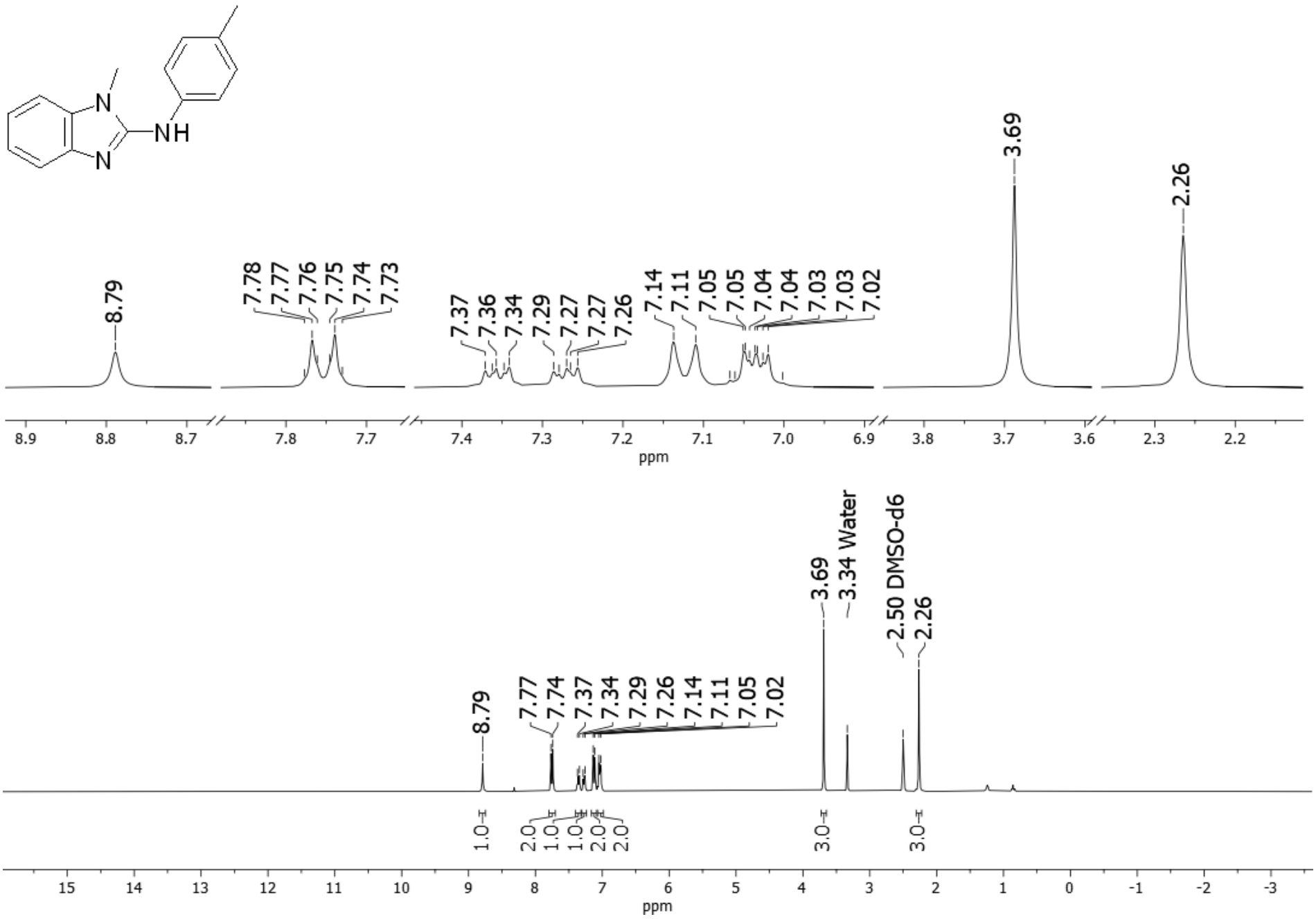

Figure S167. ^{1}H NMR spectrum of compound **12f** (DMSO-d_6, 300 MHz)

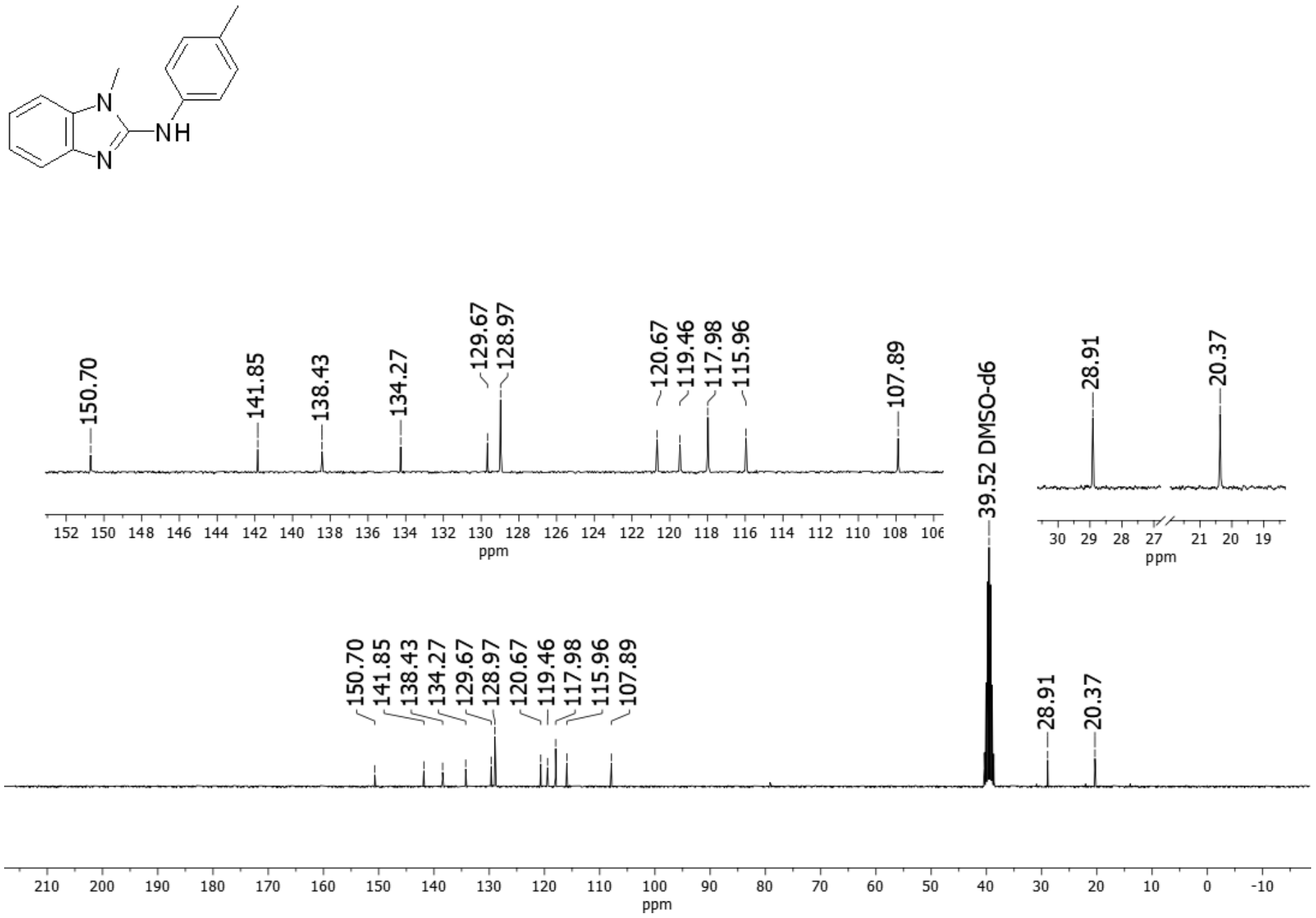

Figure S168. ^{13}C NMR spectrum of compound **12f** (DMSO-d_6, 75 MHz)

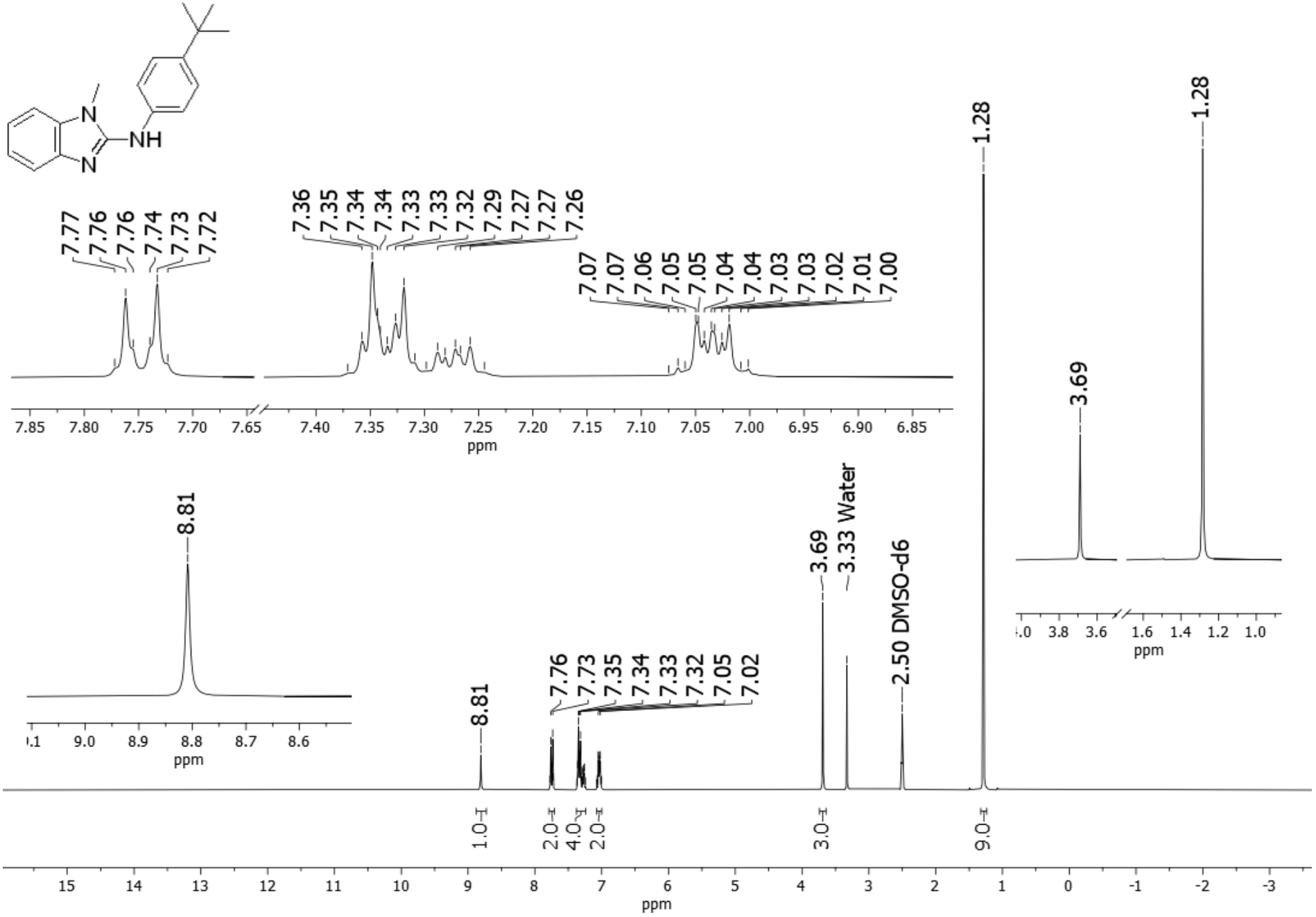

Figure S169. [1]H NMR spectrum of compound **12g** (DMSO-d_6, 300 MHz)

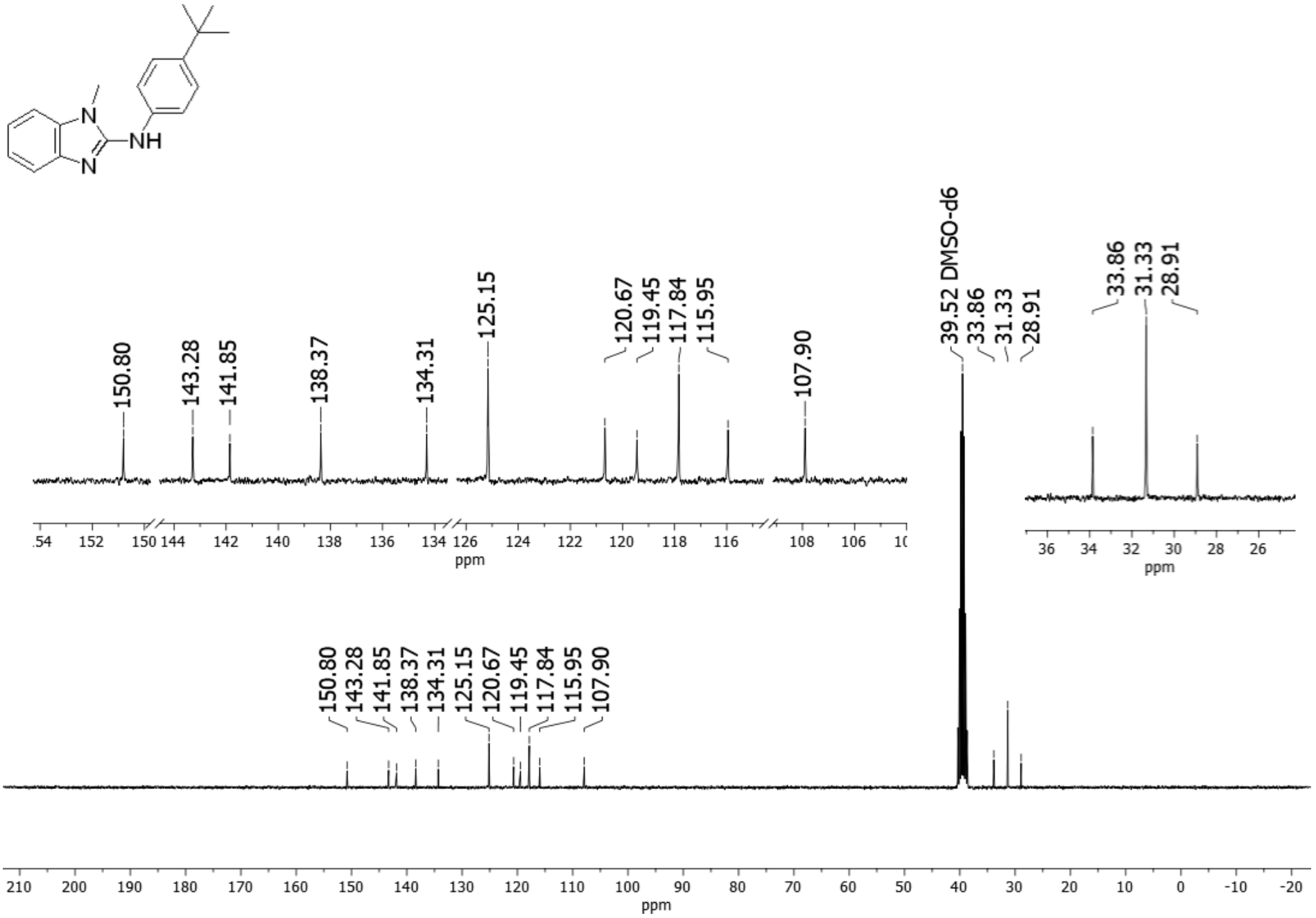

Figure S170. ^{13}C NMR spectrum of compound **12g** (DMSO-d_6, 75 MHz)

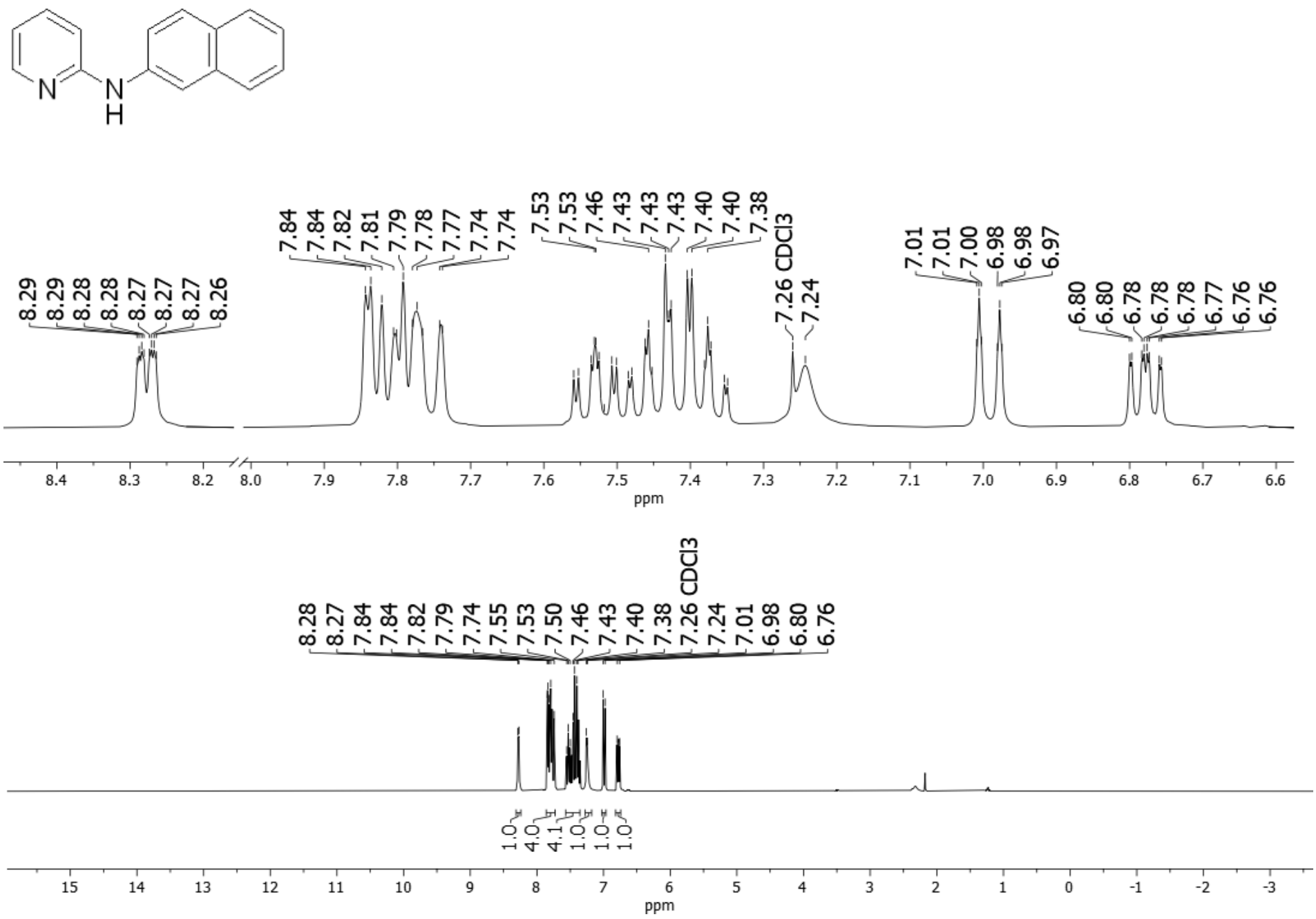

Figure S171. ^{1}H NMR spectrum of compound **12h** ($CDCl_3$, 300 MHz)

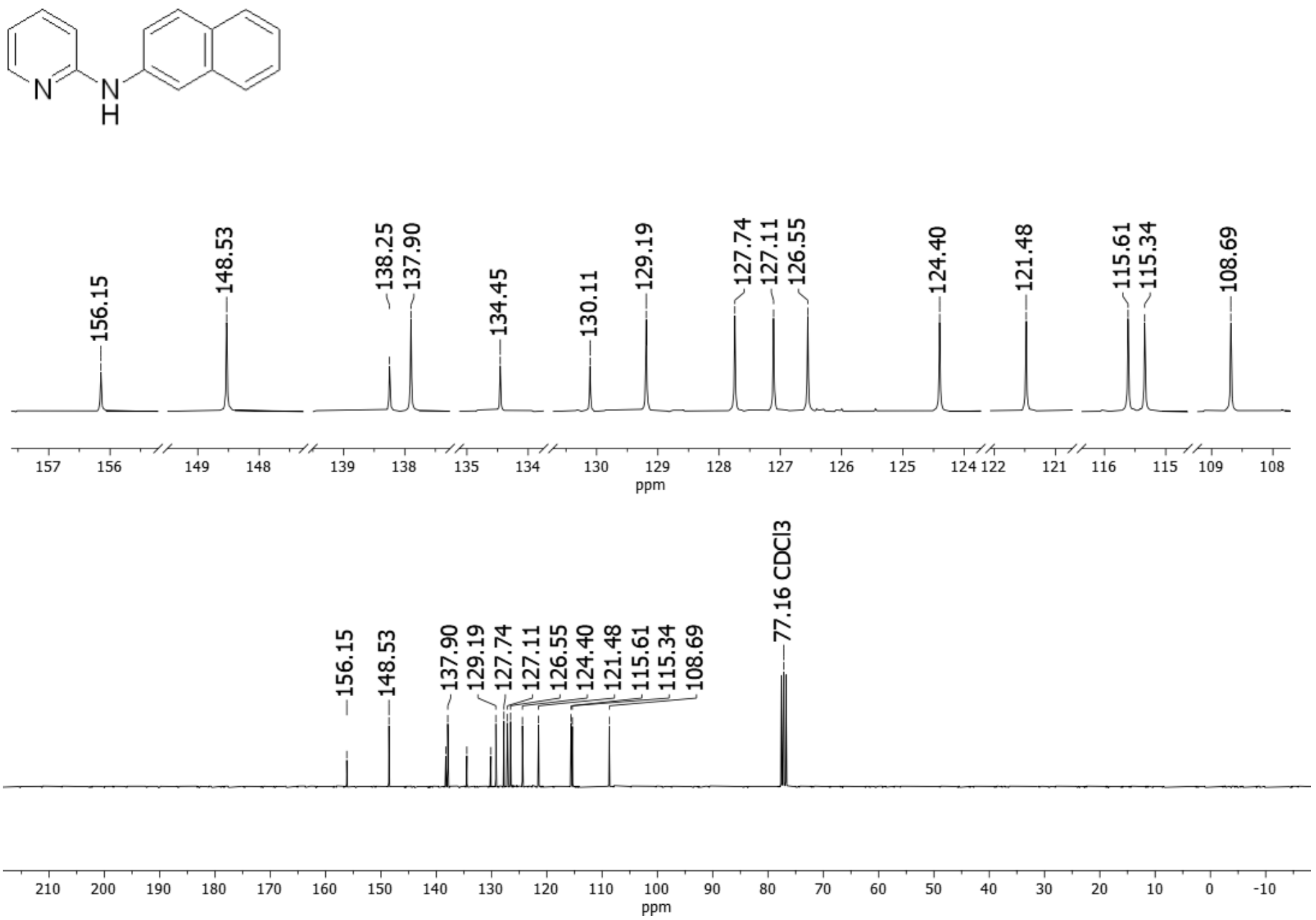

Figure S172. ^{13}C NMR spectrum of compound **12h** ($CDCl_3$, 75 MHz)

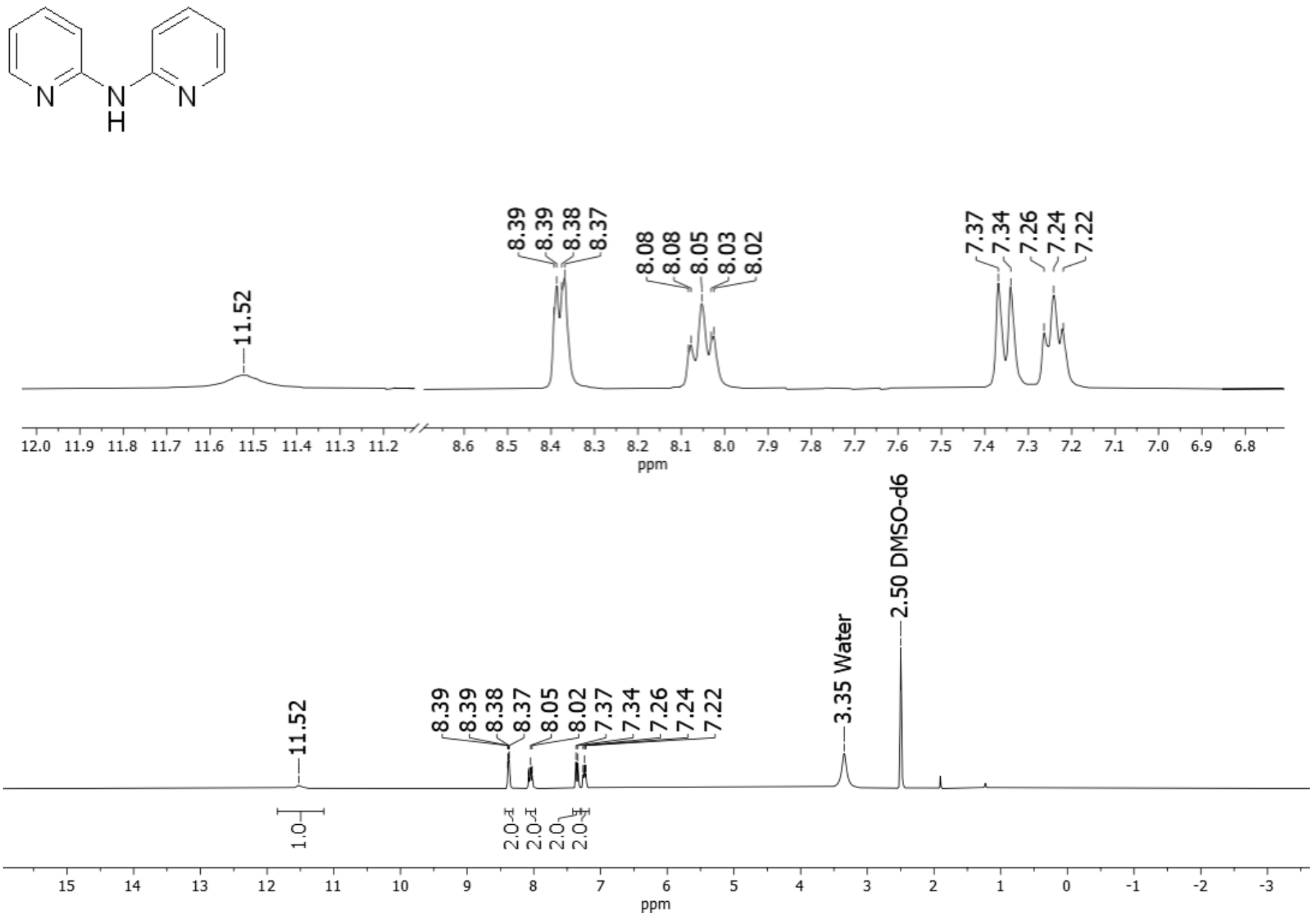

Figure S173. ^{1}H NMR spectrum of compound **12i** (DMSO-d_6, 300 MHz)

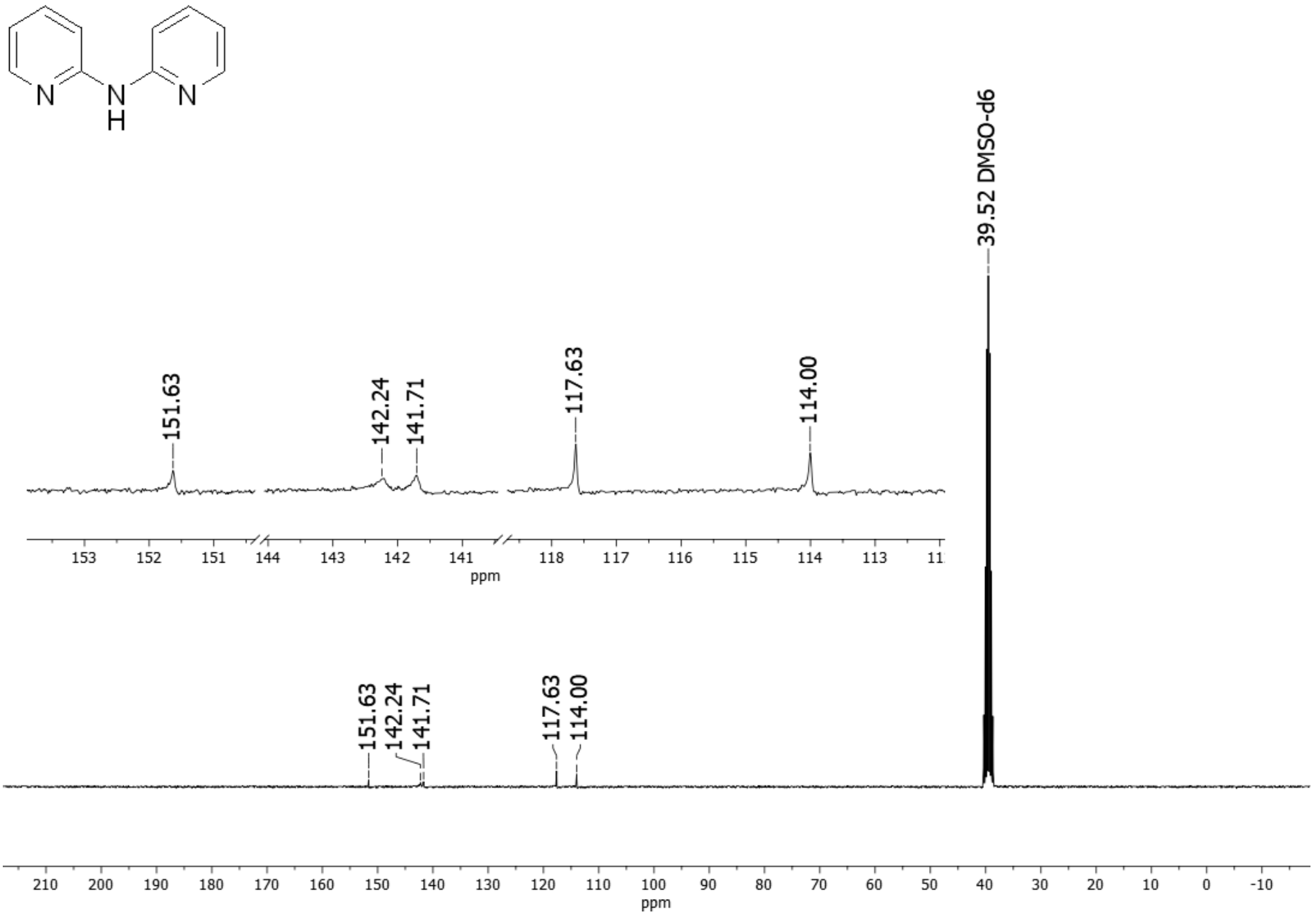

Figure S174. ^{13}C NMR spectrum of compound **12i** (DMSO-d_6, 75 MHz)

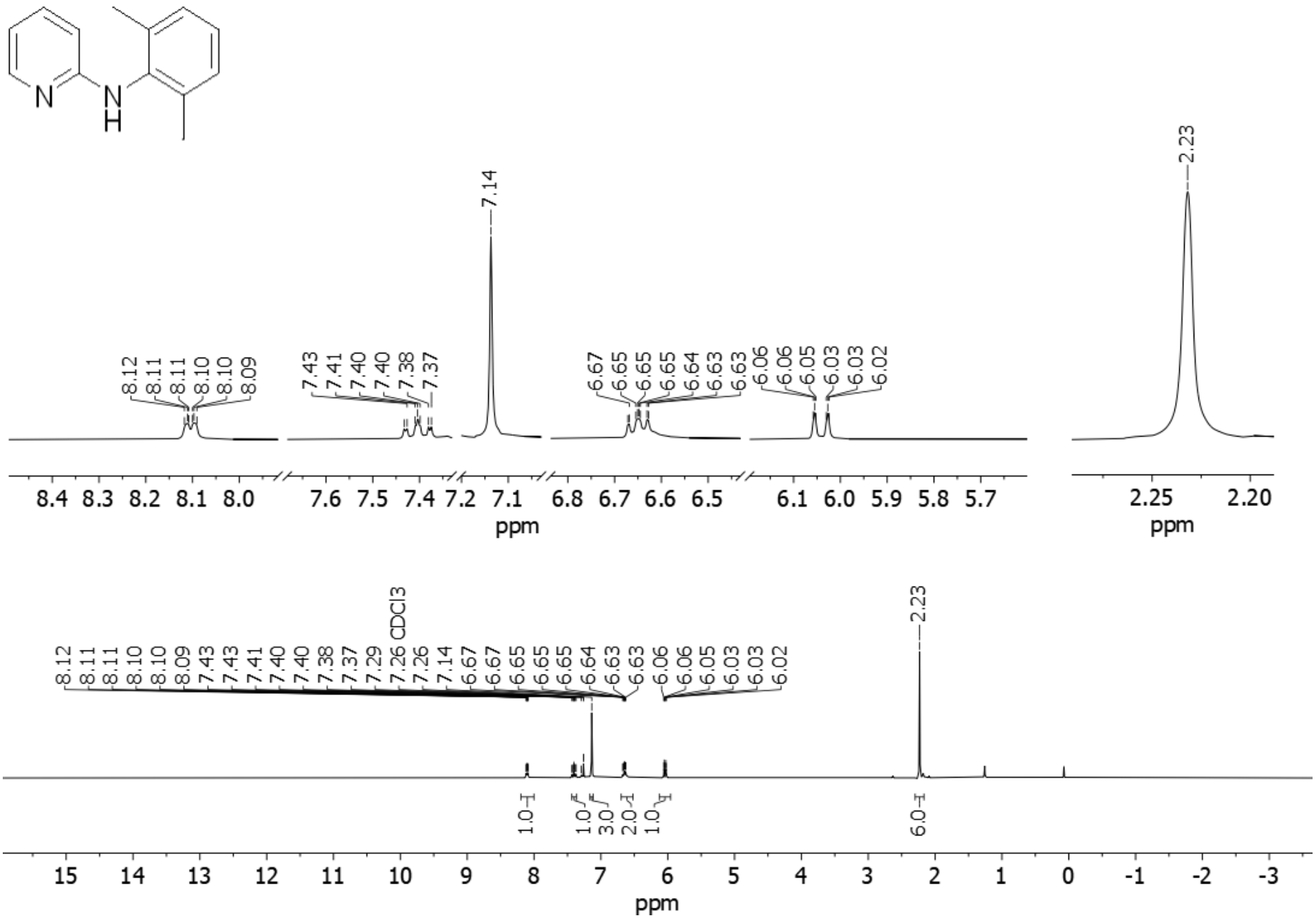

Figure S175. ^{1}H NMR spectrum of compound **12j** ($CDCl_3$, 300 MHz)

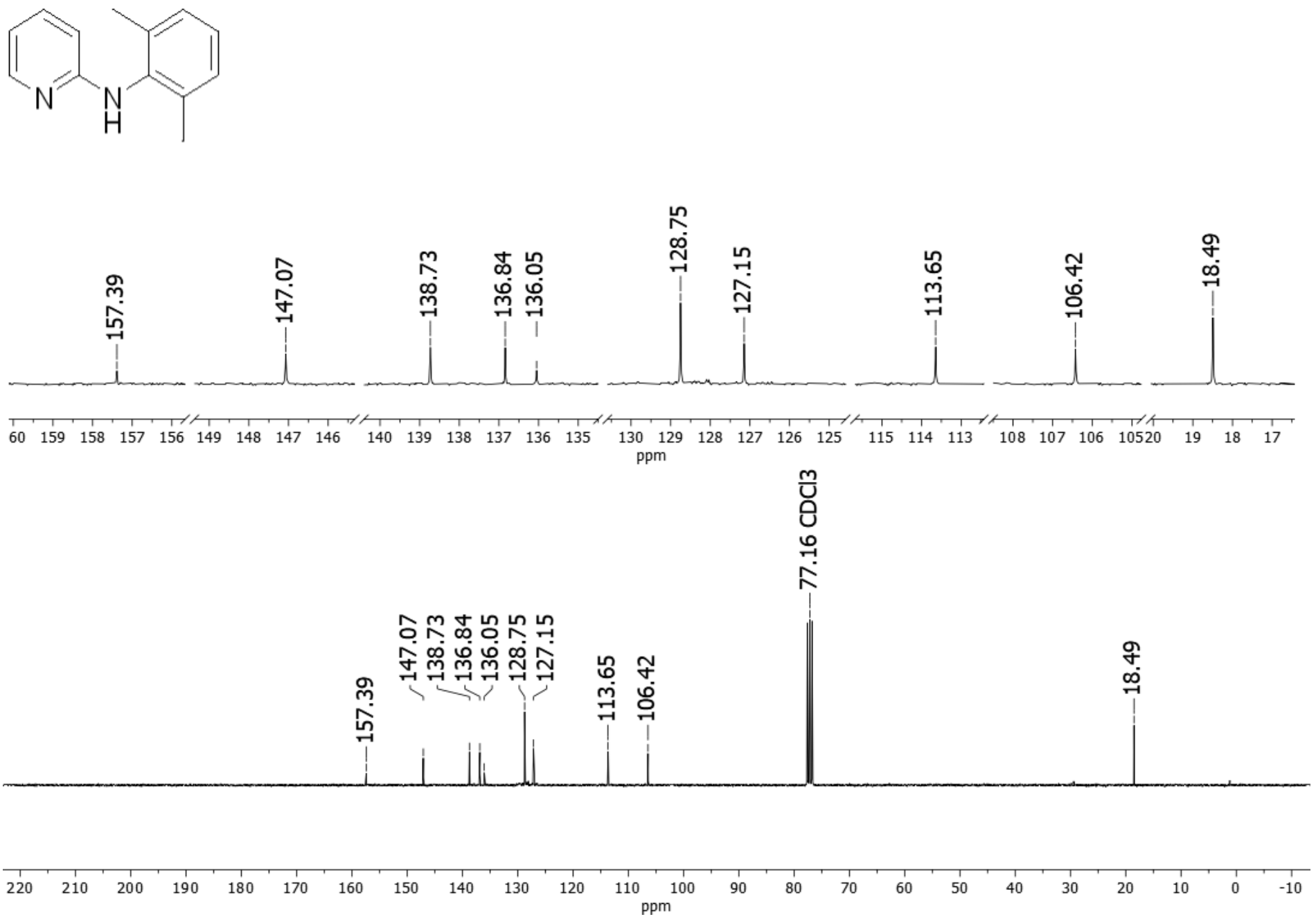

Figure S176. ^{13}C NMR spectrum of compound **12j** ($CDCl_3$, 75 MHz)

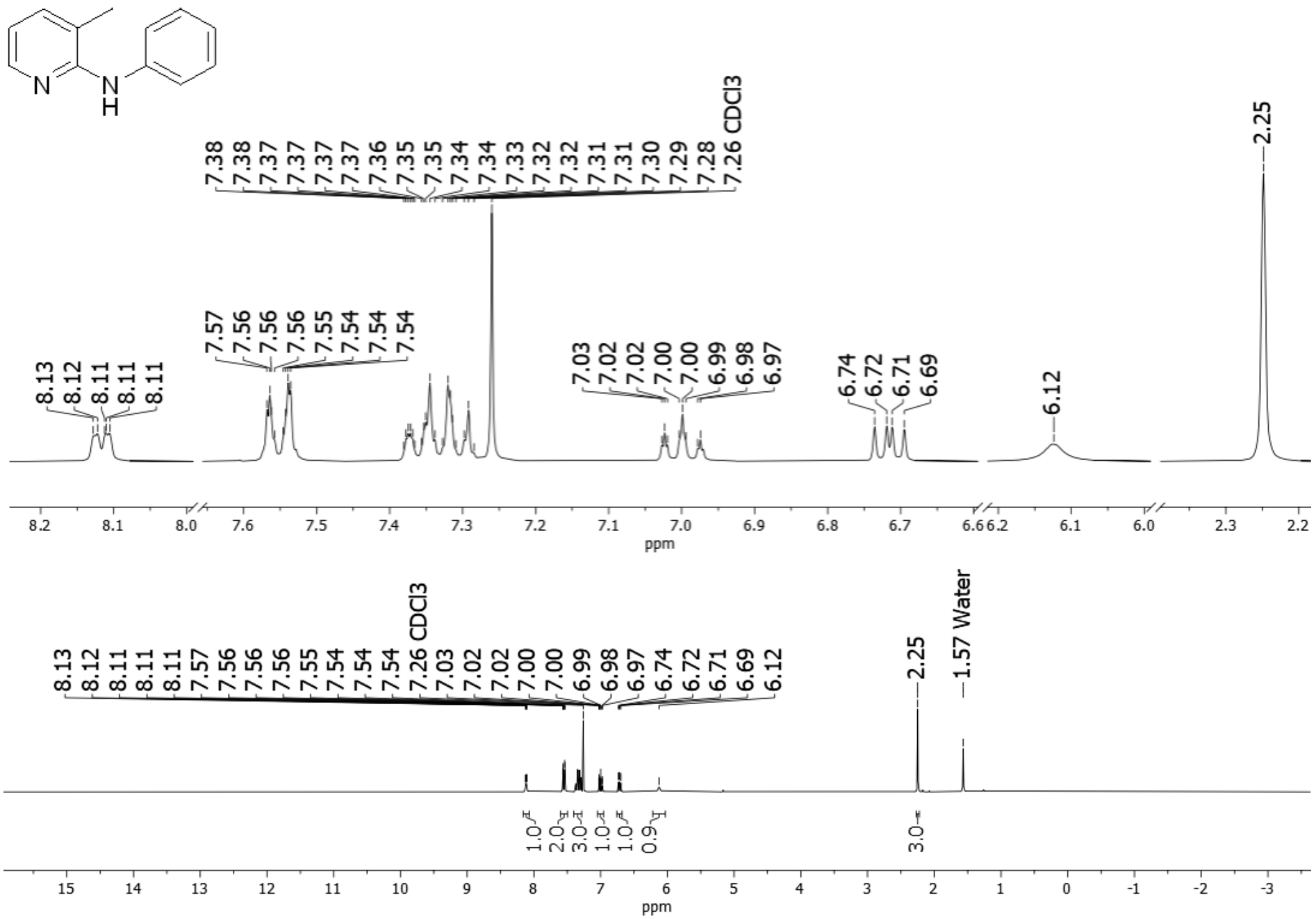

Figure S177. ^{1}H NMR spectrum of compound **12k** ($CDCl_3$, 300 MHz)

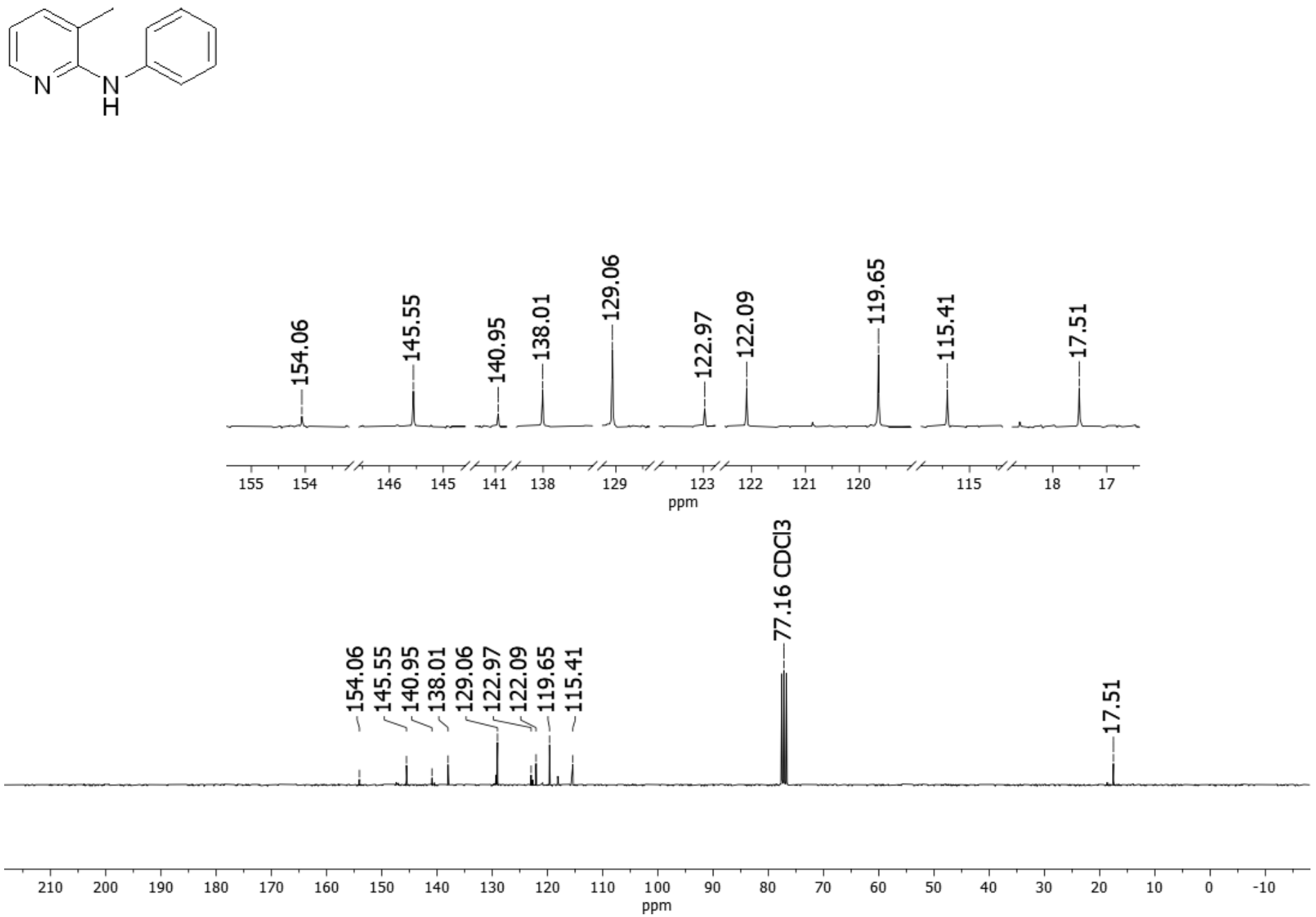

Figure S178. ^{13}C NMR spectrum of compound **12k** ($CDCl_3$, 75 MHz)

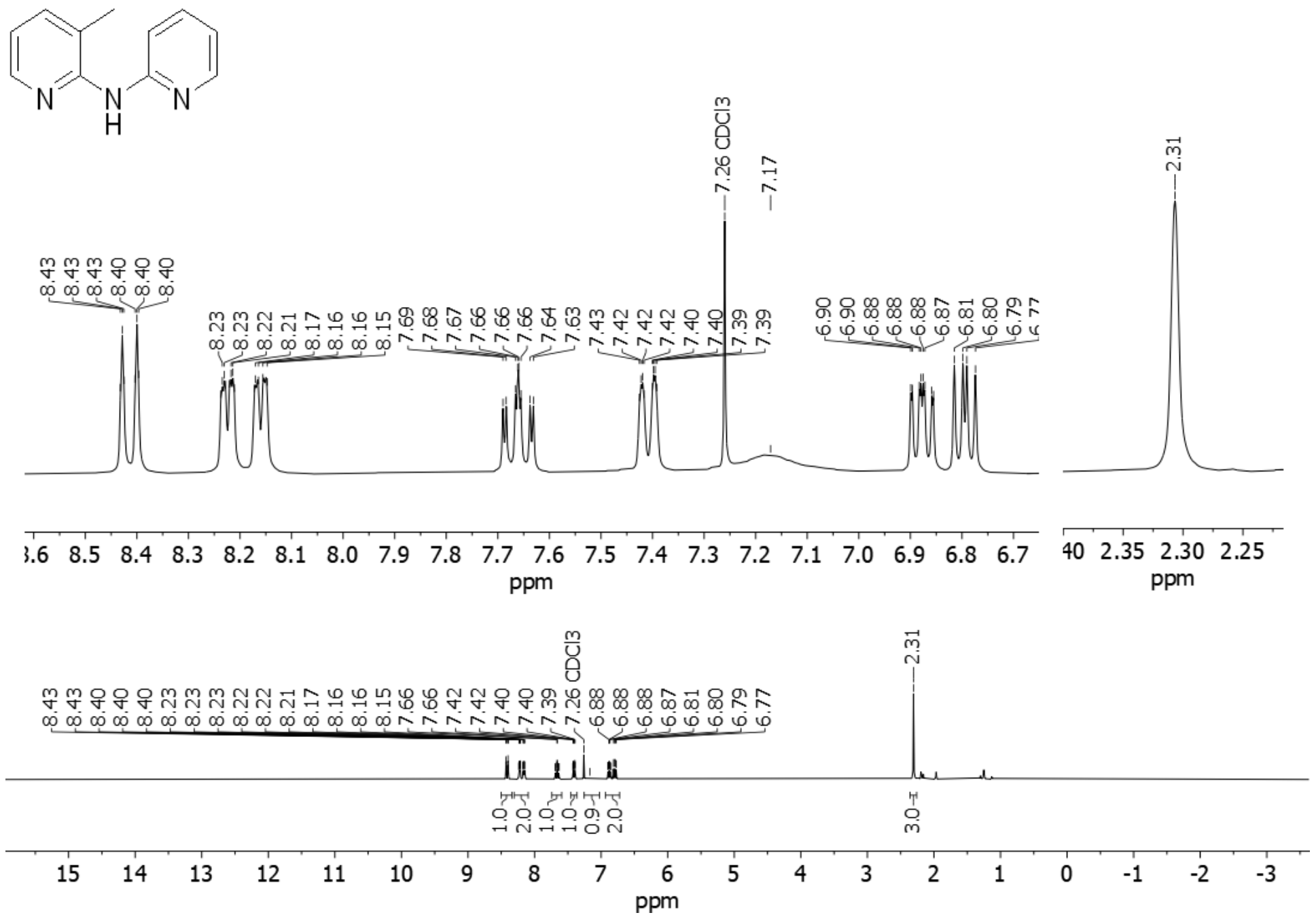

Figure S179. ^{1}H NMR spectrum of compound **12l** ($CDCl_3$, 300 MHz)

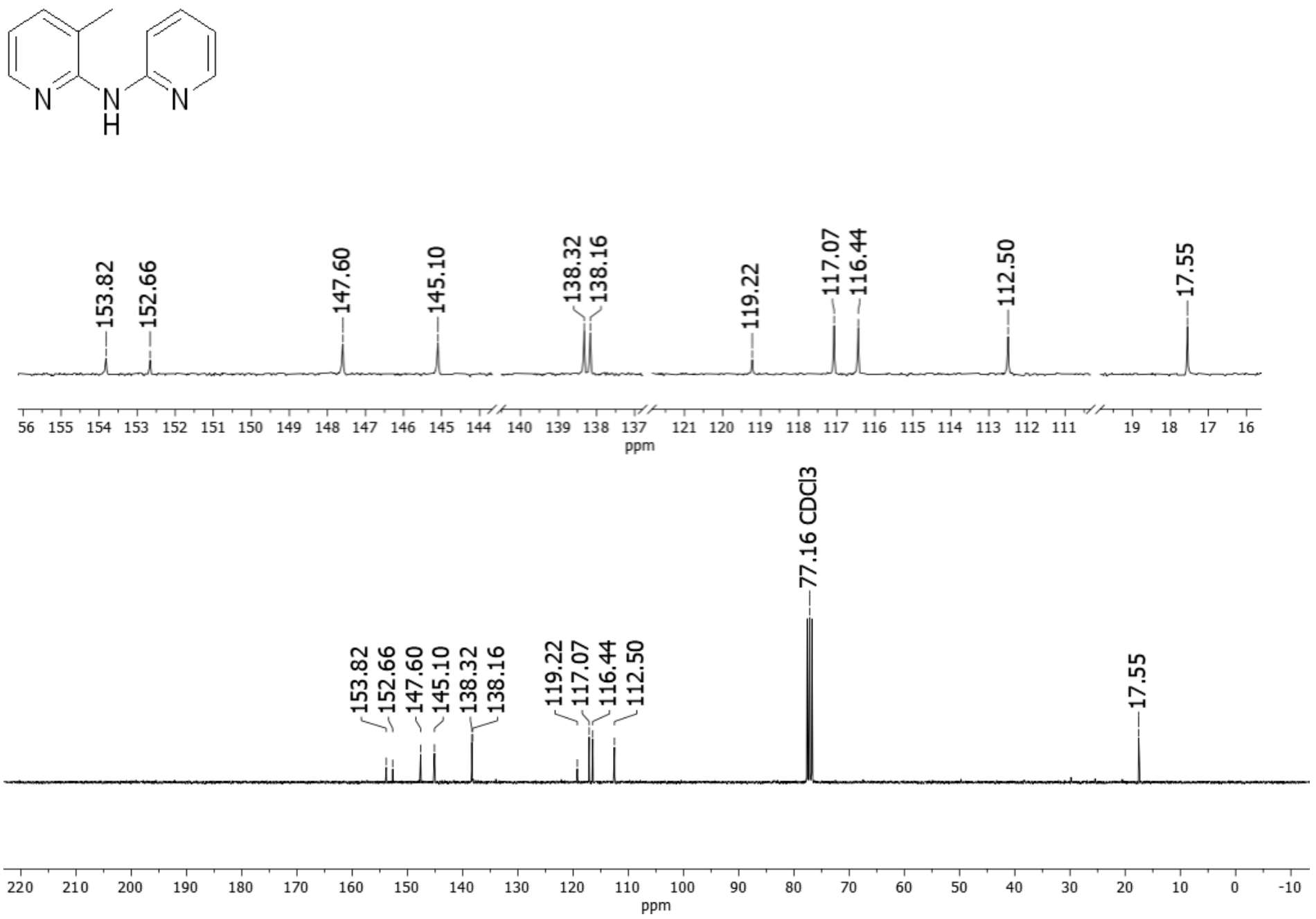

Figure S180. ^{13}C NMR spectrum of compound **12l** ($CDCl_3$, 75 MHz)

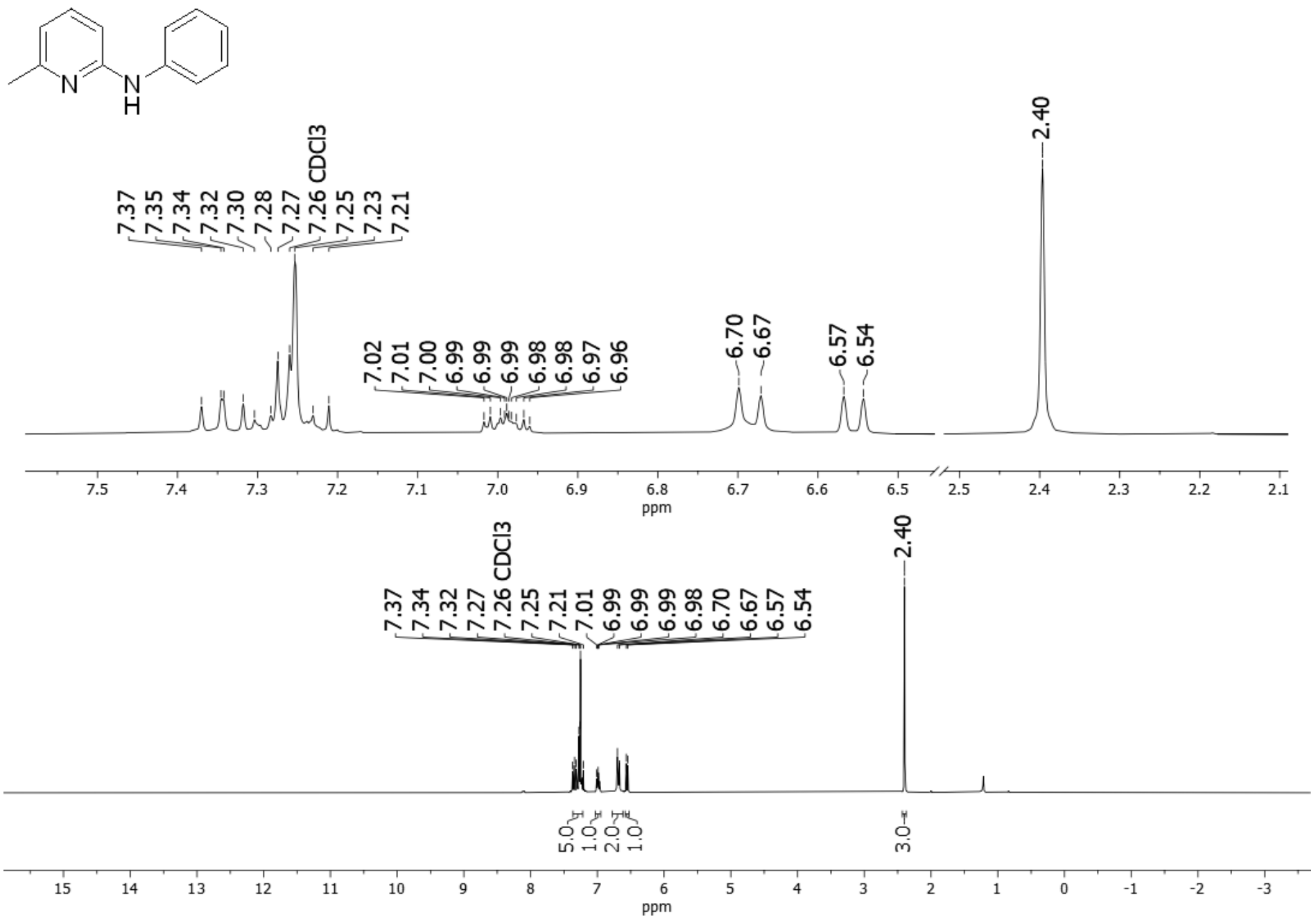

Figure S181. ^{1}H NMR spectrum of compound **12m** ($CDCl_3$, 300 MHz)

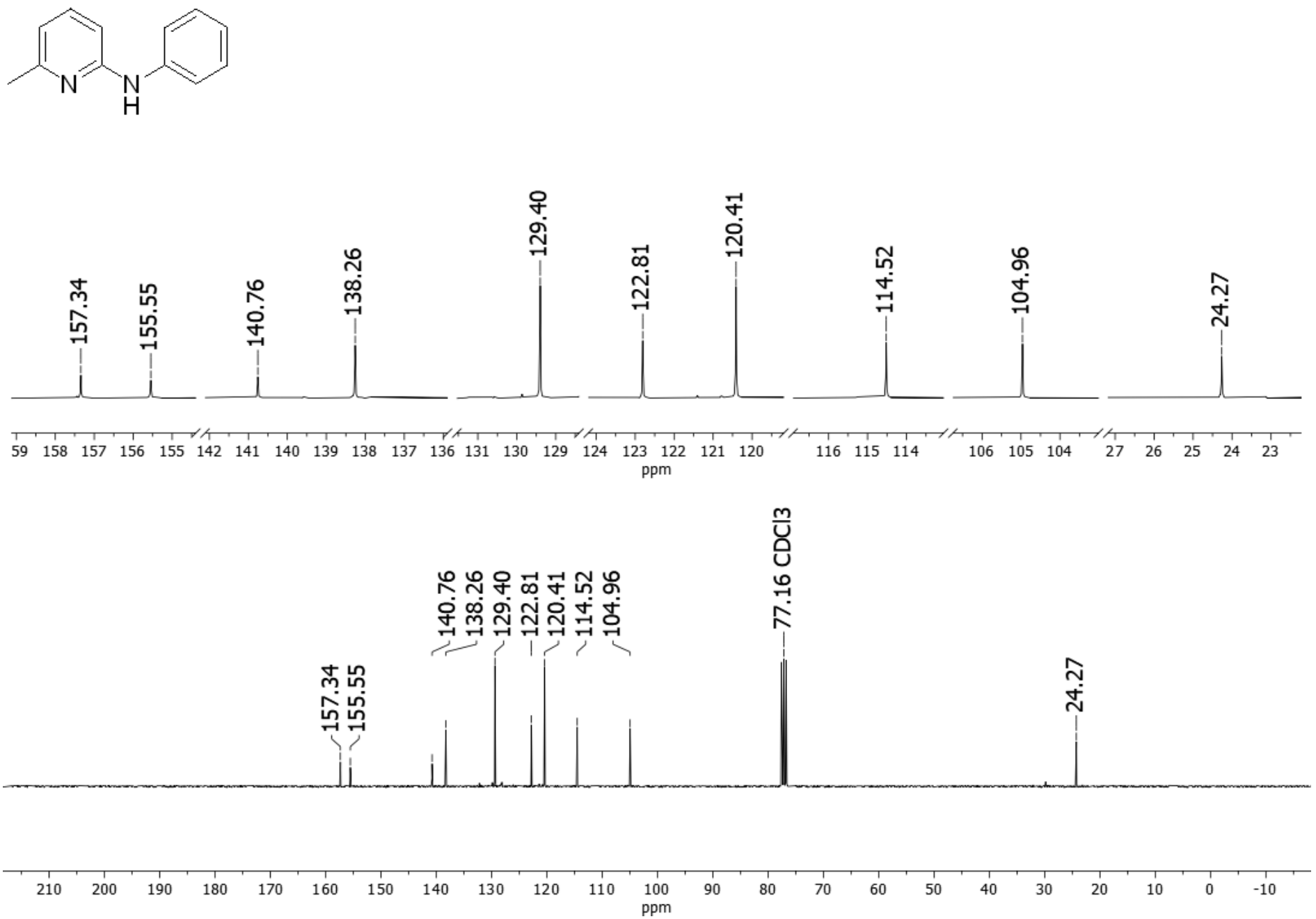

Figure S182. ^{13}C NMR spectrum of compound **12m** ($CDCl_3$, 75 MHz)

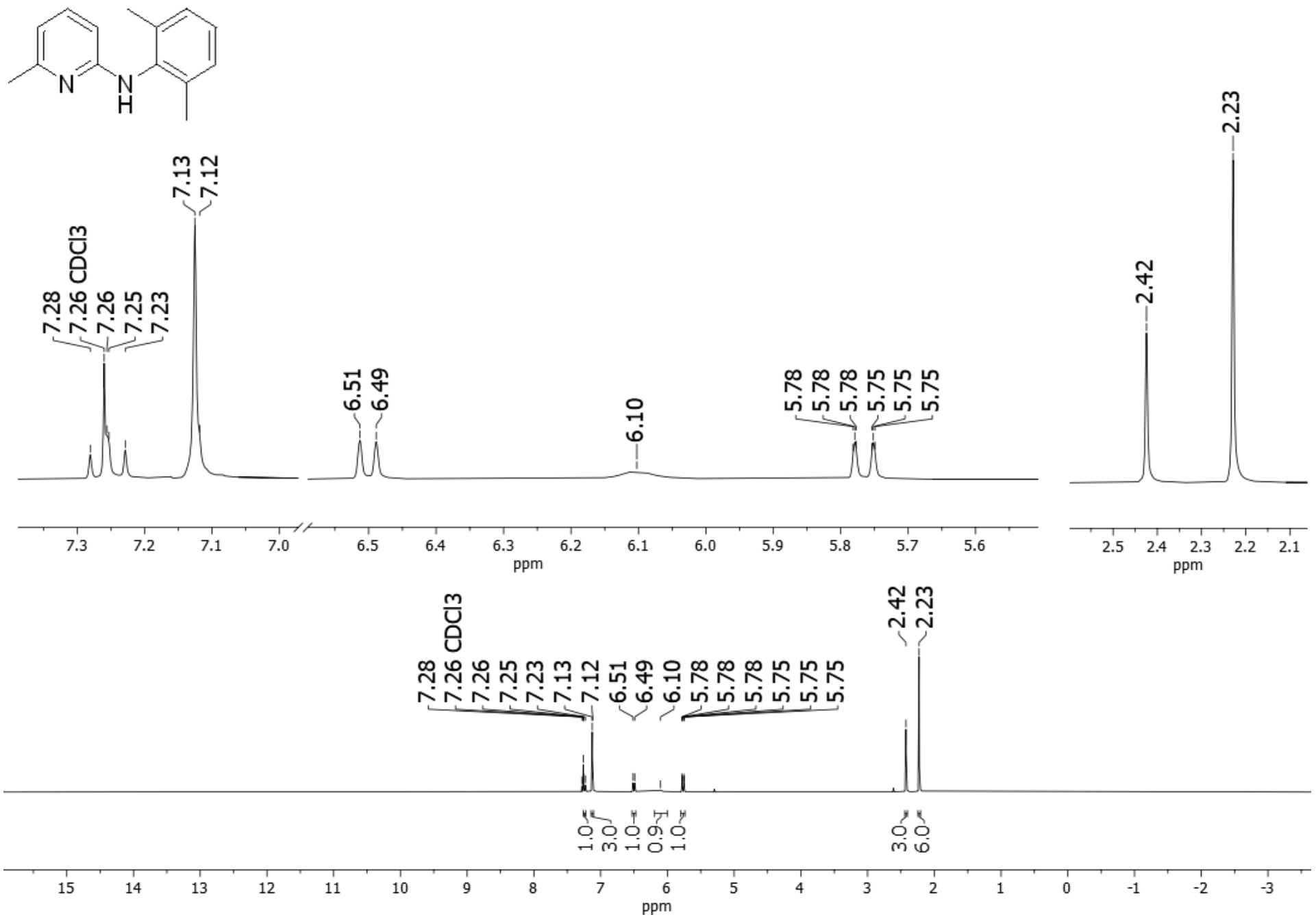

Figure S183. ^{1}H NMR spectrum of compound **12n** ($CDCl_3$, 300 MHz)

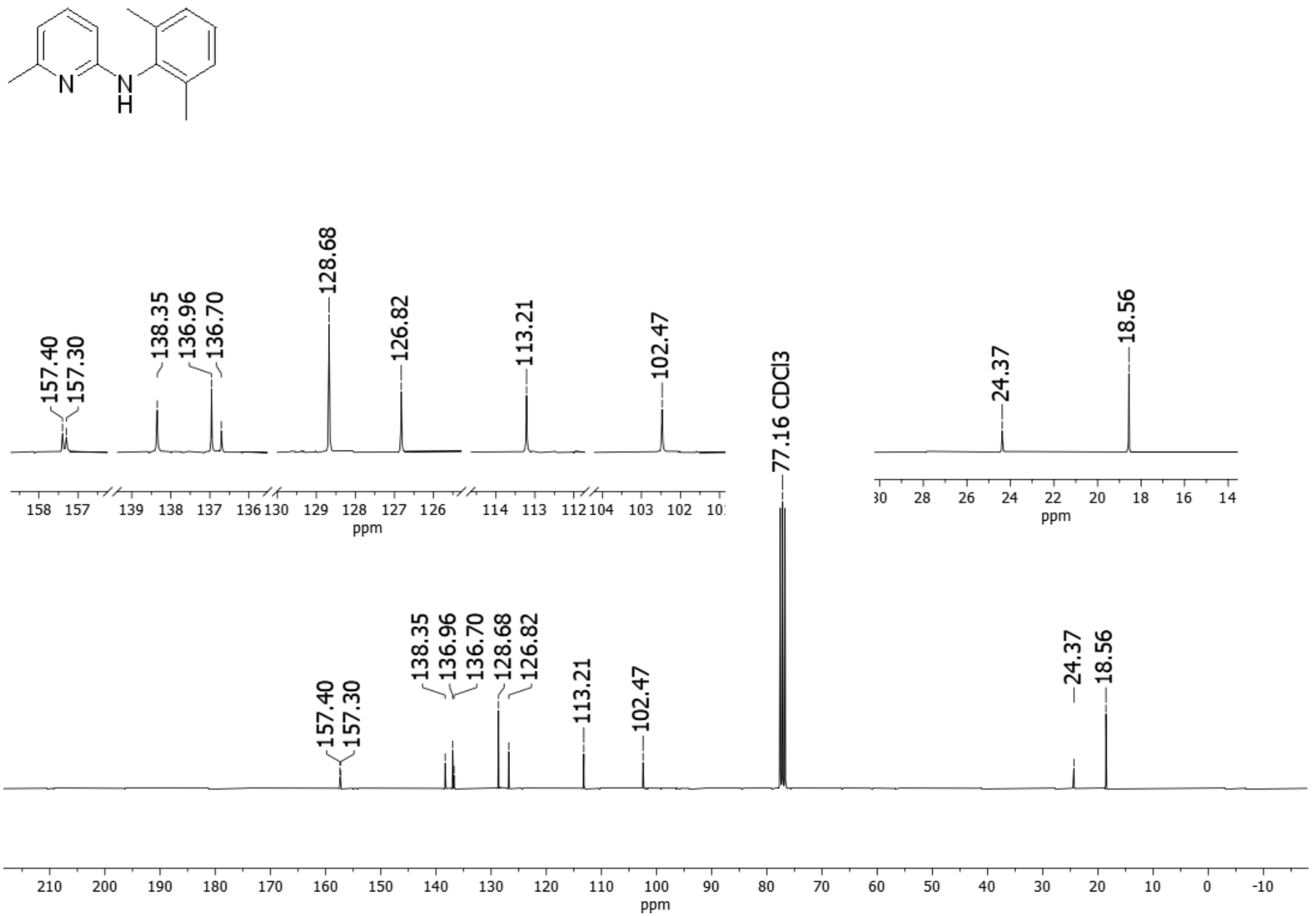

Figure S184. ^{13}C NMR spectrum of compound **12n** ($CDCl_3$, 75 MHz)

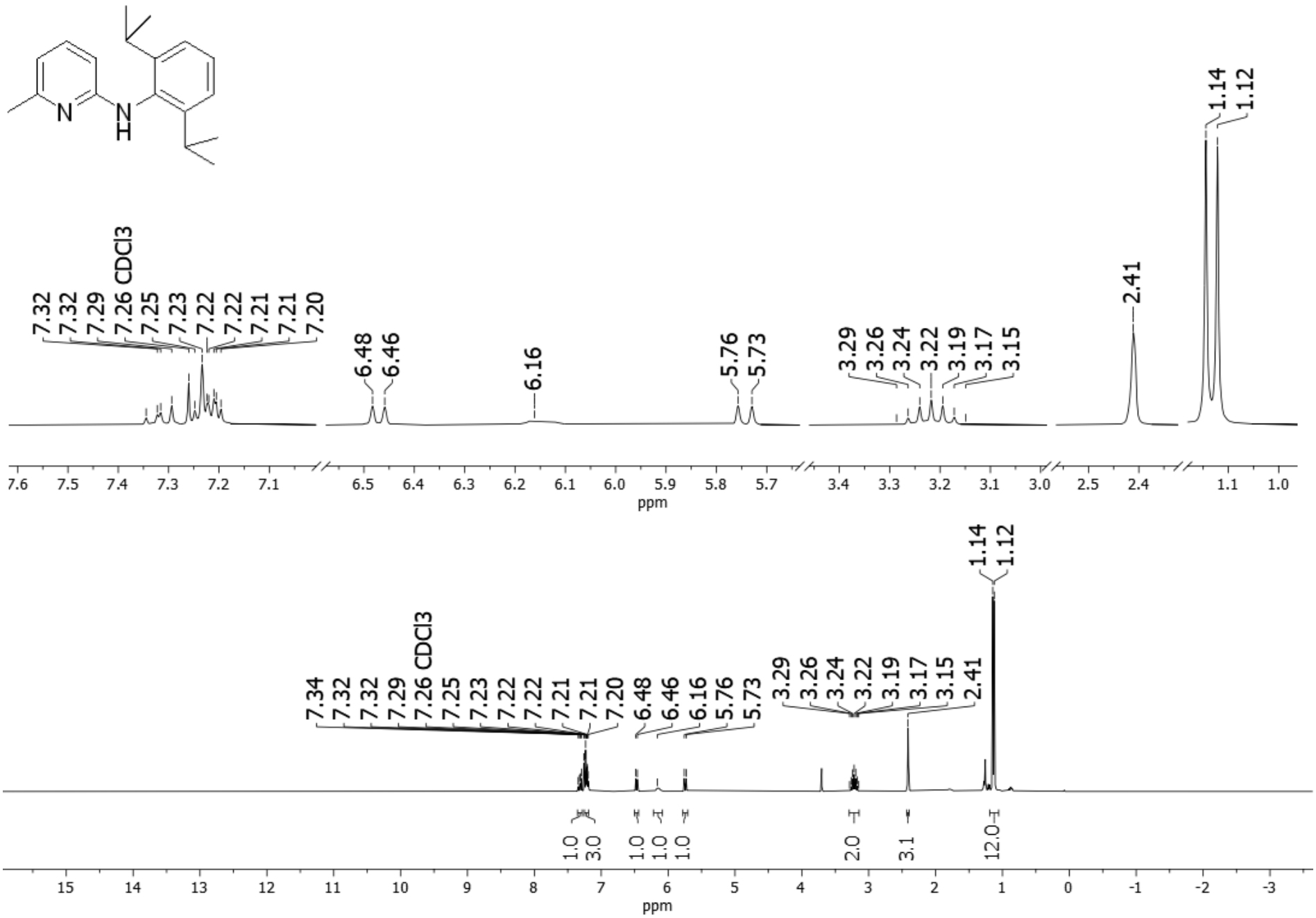

Figure S185. ^{1}H NMR spectrum of compound **12o** ($CDCl_3$, 300 MHz)

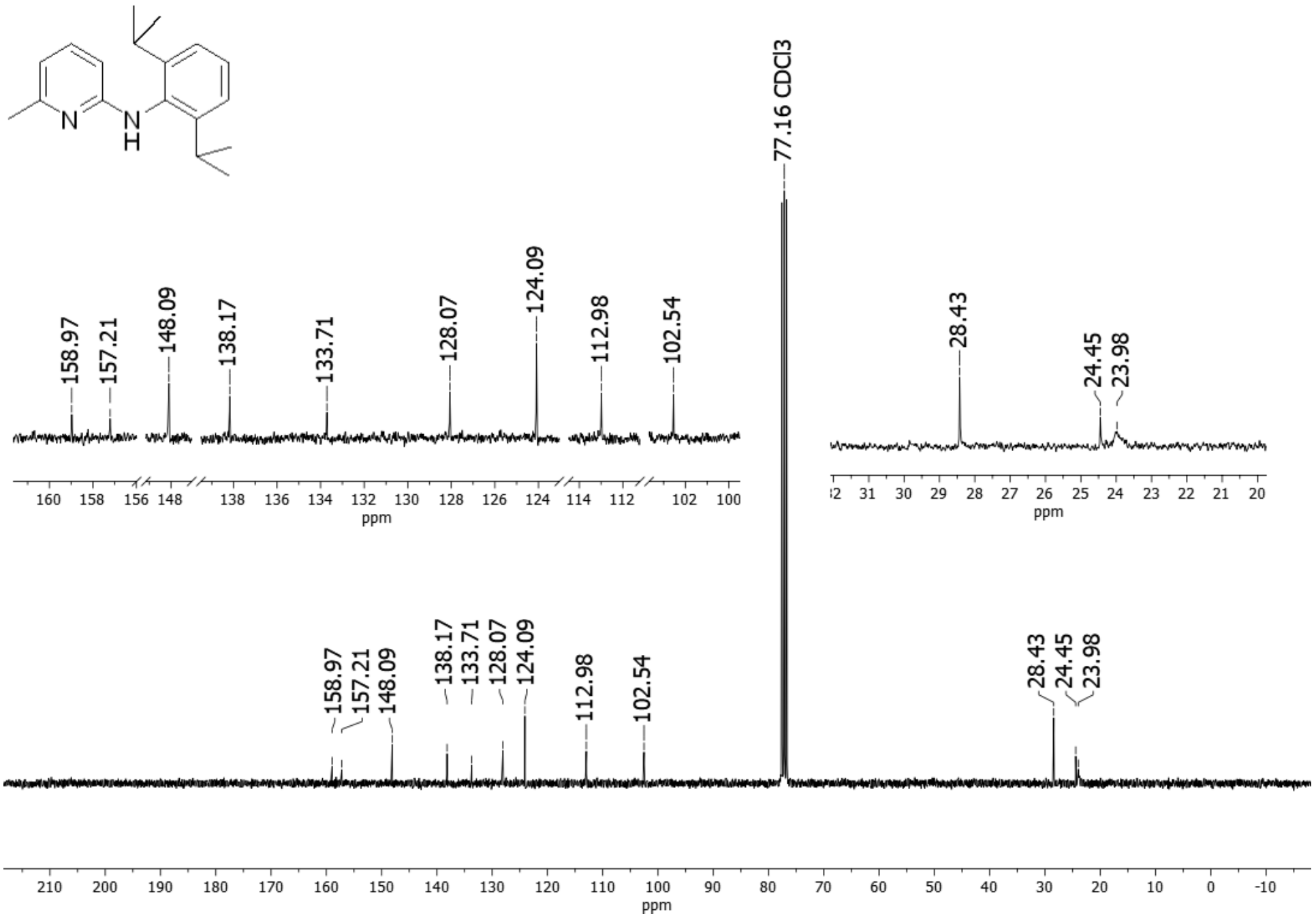

Figure S186. ^{13}C NMR spectrum of compound **12o** ($CDCl_3$, 75 MHz)

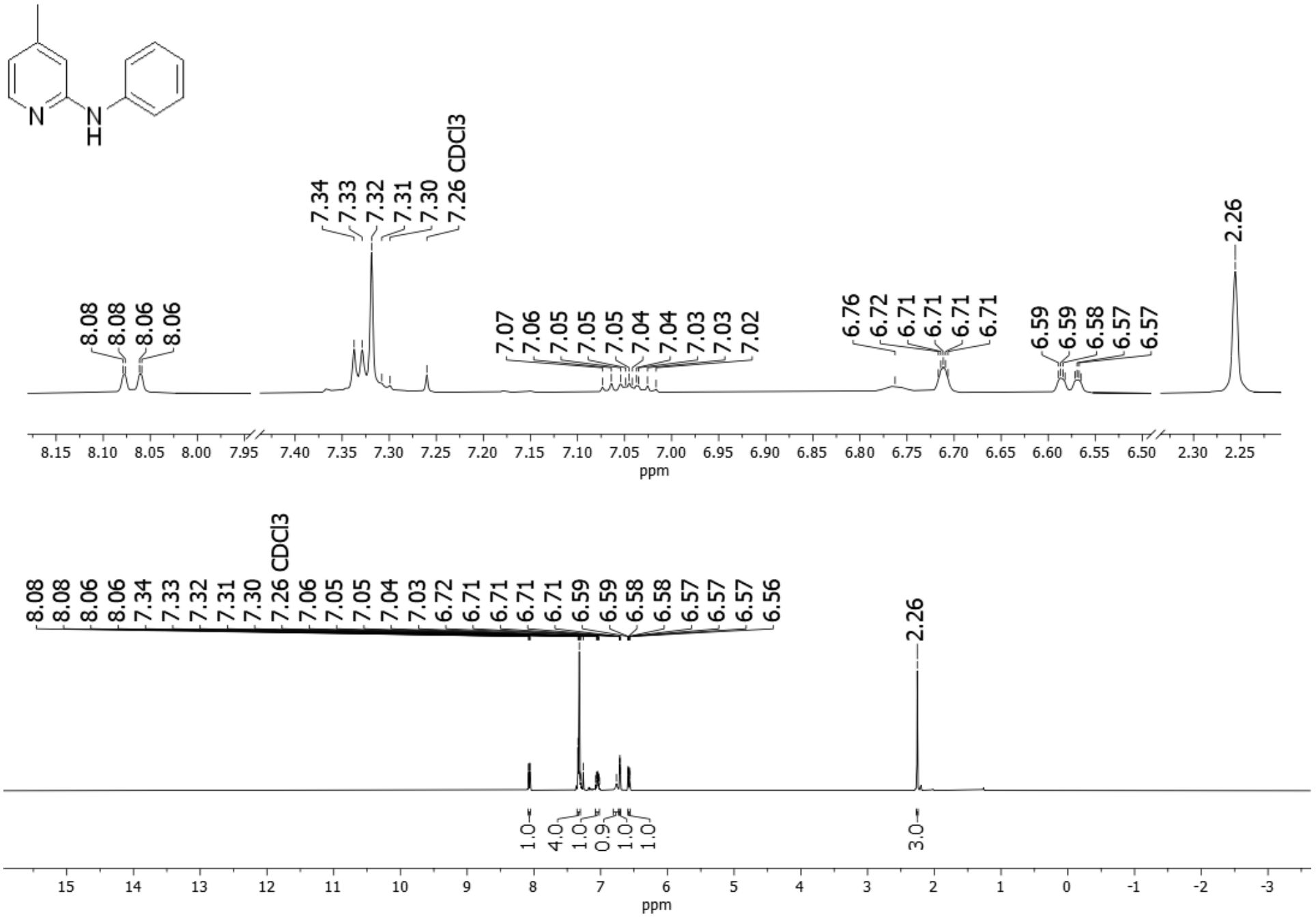

Figure S187. ^{1}H NMR spectrum of compound **12p** ($CDCl_3$, 300 MHz)

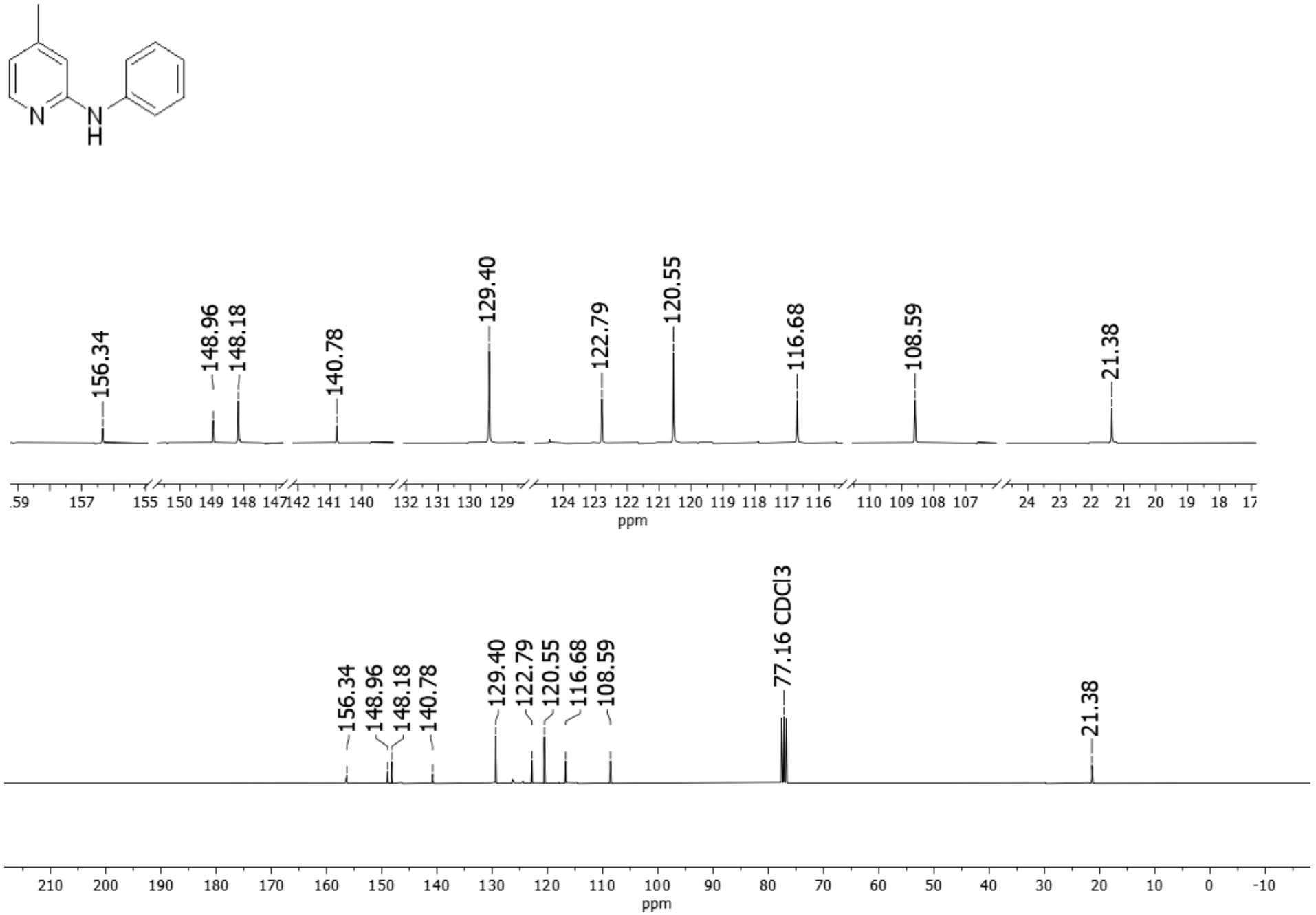

Figure S188. ^{13}C NMR spectrum of compound **12p** ($CDCl_3$, 75 MHz)

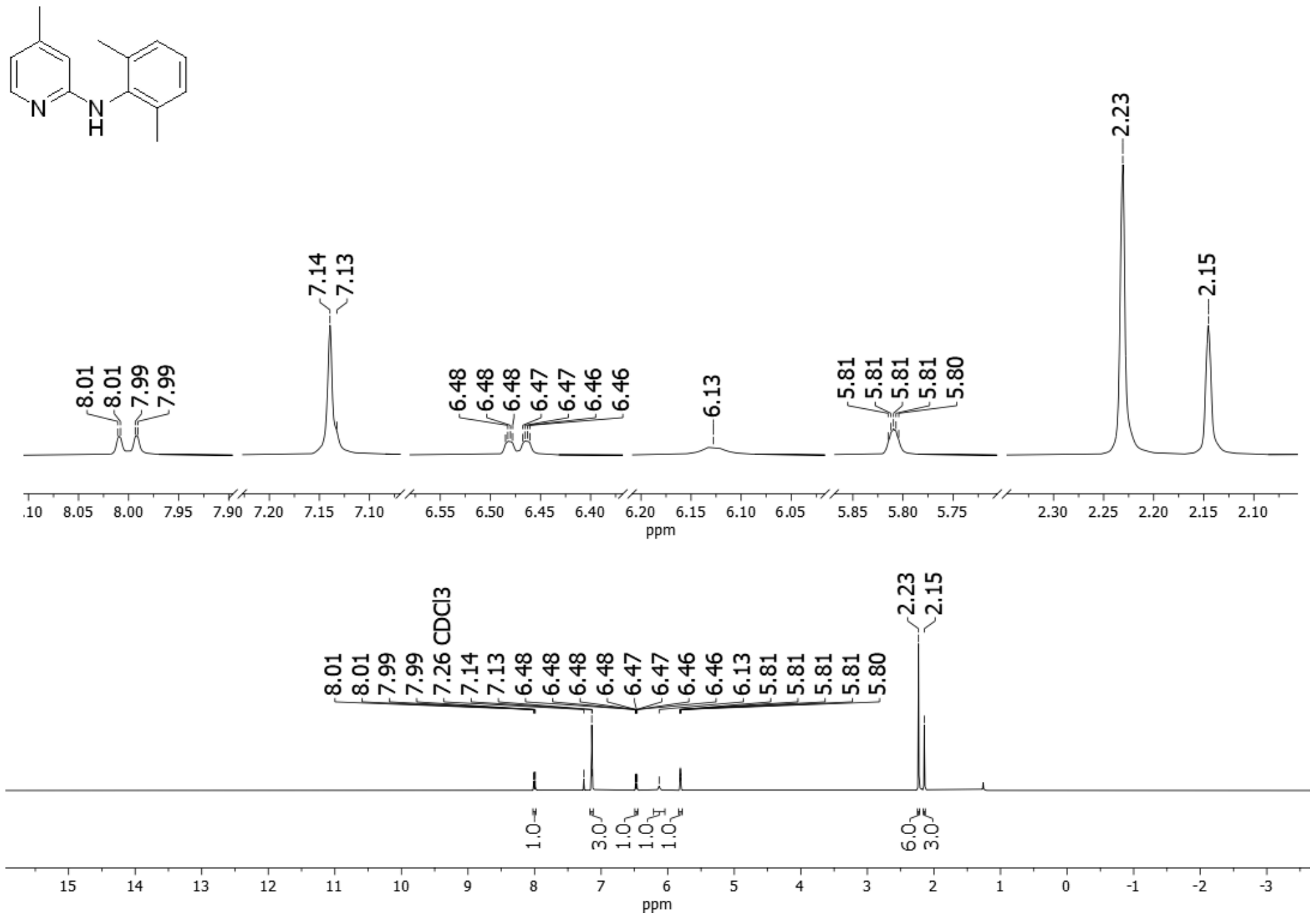

Figure S189. ^{1}H NMR spectrum of compound **12q** ($CDCl_3$, 300 MHz)

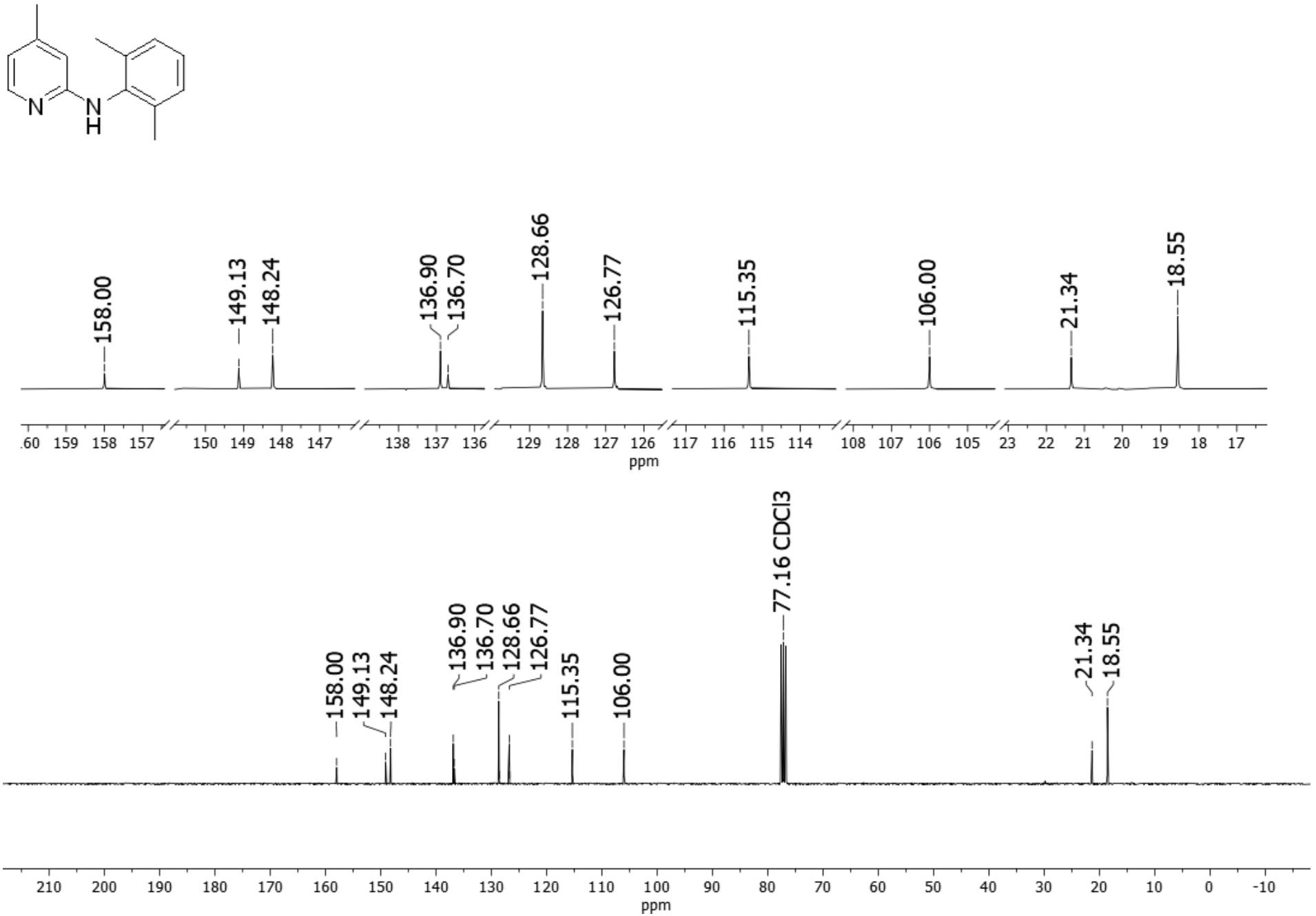

Figure S190. ^{13}C NMR spectrum of compound **12q** ($CDCl_3$, 75 MHz)